Immobilisation des catalyseurs sur supports textiles- cas du fer zérovalent et de l'enzyme glucose oxydase

(Immobilizing catalysts on textiles- case of zerovalent iron and glucose oxidase enzyme)

Thèse
Présentée à l'Université de Lille en vue de l'obtention du titre de docteur dans la spécialité
Mécanique des solides, des matériaux, des structures et des surfaces
par

Mohammad Neaz MORSHED

Dans le cadre du programme Erasmus Mundus Joint Doctorate SMDTEx : *Sustainable Management & Design for Textiles.* Cotutelle entre Université de Lille, University of Borås, Soochow University.

Soutenue le 23 Juin 2021 devant la commission d'examen

JURY		
Mme Nemeshwaree BEHARY	Associate Professor, HDR, ENSAIT, France	Directeur
M. Vincent NIERSTRASZ	Professor, University of Borås, Sweden	Directeur
M. Georg M. GUEBITZ	Professor, University of Natural Resources and Life Sciences, Austria	Président
M. Frank HOLLMANN	Professor, Delft University of Technology, The Netherlands	Rapporteur
Mme Deepti GUPTA	Professor, IIT New Delhi, India	Rapporteur
Mme Laurie BARTHE	Associate Professor, Université de Toulouse, France	Examiner
Mme Rozenn RAVALLEC	Professor, Université de Lille, France	Examiner
Mme Kerstin H.-JACOBSEN	Professor, Niederrhein University of Applied Sciences, Germany	Examiner
Jinping GUAN	Professor, Soochow University, China	Invite
Zhenhui KANG	Professor, Soochow University, China	Invite

European Commission
ERASMUS MUNDUS

Année 2021

"Read in the name of your Lord who created (everything)"
-     *Al-'Alaq 96:1*

Preface

This thesis has been comprehended under the framework of Erasmus Mundus joint-doctorate program about sustainable management and design for textiles (SMDTex). According to the structure and content of SMDTex, this thesis is a part of theme 4: Sustainable and innovative design processes and materials. The research works in this thesis has carried out in four institutions from three locations (divided into three-mobilities) .

First mobility (September 2017 - February 2019): Ecole nationale supérieure des arts et industries textiles (ENSAIT) – Génie et matériaux textiles (GEMTex) laboratory, and Université de Lille – Department of materials and mechanics in France . Second mobility (March 2019 - August 2020): University of Borås – Department of textile technology in Sweden. Third mobility (September 2020 - August 2021): Soochow University – Department of textile engineering in China. The thesis has been co-supervised by four supervisors- Dr. Hdr. Nemeshwaree BEHARY (ENSAIT), Prof. Dr. ir. Vincent A. NIERSTRASZ (University of Borås) and Prof. Guoqiang CHEN and Dr. Jinping GUAN (Soochow University).

This thesis contains experiment-based insight and proof of concept of innovative idea related to immobilizing catalysts on textiles as inexpensive and easily accessible support material. As an original approach, this thesis studied the case of zerovalent iron (inorganic catalyst), glucose oxidase enzyme (biocatalyst) and explored their application as heterogeneous catalysts in catalytic wastewater treatment systems. Catalysts immobilized textiles has shown potentiality in Fenton and Fenton-like removal system, catalytic reduction system, and/or pathogen inhibition system (antibacterial activities). The findings of the thesis addresses the scientists/researchers working within the field of catalysis, textile material science, surface chemistry, wastewater treatment, multifunctional textiles and textile biotechnology.

Abstract

Catalytic systems are one of the most effective technologies of modern chemical processes. The system uses a molecule called 'catalyst' that is capable of catalyzing a reaction without being produced or consumed during the process. A catalytic system requires the separation of catalysts from products after each cycle, which is an expensive and resource-intensive process. This brought to the relevance of immobilization of catalyst, where catalysts are bind to a solid support material that will ensure the easy separation of catalyst. Immobilized catalysts are reusable and usually show better stability than the free catalyst. However, immobilization of catalyst is challenging, as it requires exclusive support material involving a complex preparation process. In many instances, the preparation of support material is more resource-intensive and expensive than the catalyst themselves.

Therefore, this doctoral thesis focused on the innovative concept of using textile as reliable, widely accessible, and versatile support material for catalyst immobilization. Evidence from systematic experiments was gathered for the case of immobilization of an inorganic catalyst (zerovalent iron-Fe^0) and a biocatalyst (glucose oxidase -GOx) on textile support. The goal of this thesis is to establish the feasibility of textile as support material for immobilization of catalyst in the pursuit of fabrication of heterogeneous catalytic system (oxidative and reductive) for wastewater treatment. Polyester nonwoven fabric (PF) was chosen as textile support material for catalyst immobilization due to both qualitative (high strength, porosity, biocompatibility and resistance to most acids, oxidizing agents, and microorganisms) and commercial (availability, cheap and easily customizable) advantages. A combination of eco-friendly and resource-efficient processes (such as plasma treatment, hyperbranched dendrimer, bio-based polymers) has been used for tailoring the PF surface with favorable surface chemical properties in the view of high and stable immobilization yield of the catalyst.

The thesis has three distinct parts related to immobilizing catalyst on textiles- (a) immobilization of Fe^0 on PF and optimizing their feasibility in both oxidative and reductive catalytic system; (b) immobilization of GOx on PF and optimizing their use in a bio-catalytic system; (c) design of the complete heterogeneous bio-Fenton system using immobilized catalysts (Fe^0 and GOx). In all parts, the hydrophobic surface of PF was activated by plasma ecotechnology (either air atmospheric -AP or cold removal plasma-CRP) followed by chemical grafting of hyperbranched dendrimers (polyethylene glycol-OH or polyamidoamine ethylene-diamine core) or functional polymers (3-aminopropyl-triethoxysilane, polyethylenimine, chitosan, or 1-thioglycerol) before immobilizing either of two catalysts. The immobilization of Fe^0 was carried out through either the *in-situ* or *ex-situ* reduction-immobilization method, whereas GOx was immobilized through the physical adsorption method. Several approaches were explored in search of optimum conditions for catalyst immobilization as well as to improve the catalytic performance of immobilized catalysts.

Diverse analytical and instrumental techniques were used to monitor the surface modification of textiles, efficiency of immobilization of catalysts, Physico-chemical properties of immobilized catalysts, and their catalytic activities in the removal of dyes, phenols, or pathogenic pollutants from water. Results from plasma treatment showed that both AP and CRP successfully activated the PF surface through integrating polar functional groups (–COOH and –OH) by AP and carboxyl/hydroxyl (–COOH/–OH), amino (–NH_2) functional groups by CRP. Along with that, grafted hyperbranched dendrimers and functional polymers on plasma-activated PF provided a tailor-made surface with specific end functional groups. Regarding the immobilization of Fe^0 on PF, the results revealed that the reduction method (*in-situ* or *ex-situ*) of producing Fe^0 have synergistic effects on the morphology, stability, particle size, and distribution of the immobilized Fe^0. The surface chemical properties of PF also influenced the stability of immobilized Fe^0 and related properties as observed throughout various studies. Detailed results revealed that a PF surface rich in –COOH, –OH, and –SH functional groups favors the loading and stabilization of Fe^0 over surface rich in –NH_2 functional groups. To end with, all Fe^0-immobilized PF showed high catalytic activates in the removal of pollutants from water in both oxidative and reductive systems. In the case of GOx-immobilized PF, the success

of immobilization of enzyme on textile was found to be related to the type and extent of surface functional groups present on the PF surface. The results demonstrated that PF surface rich in $-COOH$, $- NH_2$ functional groups guaranteed higher loading and stability of GOx compared to $-COOH$, $-OH$ functional groups-rich surface. These results carry great importance as they provide evidence of textile:enzyme interactions and grounds for further robust immobilization of GOx on textile support through surface engineering. As a proof of concept, this thesis also reveals the first successful design of a complete heterogeneous bio-Fenton system for wastewater treatment using immobilized catalysts (Fe^0 and GOx).

The novelty of the research presented in this doctoral thesis is primarily attributed to the novelty of immobilizing two different types of catalysts (inorganic catalyst and biocatalysts) on synthetic textile support for wastewater treatment application. In general, this thesis contributes to general knowledge of the heterogeneous catalytic system, Fenton/Fenton-like system, and the bio-Fenton system as well as it opens promising prospects of the use of textile as support material for immobilizing different catalysts for a wide range of applications.

KEYWORDS: Biocatalysts; Catalyst immobilization; Catalytic reduction; Chitosan; Dye removal; Environmental remediation; Enzyme immobilization; Glucose oxidase; Hyperbranched dendrimers; Heterogeneous catalysis; Heterogeneous bio-Fenton; Heterogeneous Fenton; Inorganic catalysts; Phenol removal; Polyester nonwoven fabric; Pathogenic bacteria removal; Plasma ecotechnology; Polyethylenimine; Textile catalyst; Textile biotechnology; Textile surface modification; Wastewater treatment; Zerovalent iron;

Abstrakt

Katalytiska system är en av de effektivaste teknikerna för moderna kemiska processer. I processen används en molekyl, en "katalysator" som är kapabel att pådriva en kemisk reaktion utan att själv bli producerad eller förbrukad under processens gång. Katalytiska system kräver separation av katalysatorerna från andra produkter efter varje cykel, vilket är både kostsamt och resurskrävande. Därför är det relevant att immobilisera katalysatorerna genom att binda dem till ett solitt stödmaterial som möjliggör att katalysatorerna enkelt kan separeras. Immobiliserade katalysatorer kan återanvändas och visar ofta på bättre stabilitet än fria katalysatorer. Men det är en långdragen process att immobilisera katalysatorer då det kräver exklusiva stödmaterial och ett komplext förberedelseförlopp. I många fall är stödmaterialen mer kostsamma än katalysatorerna själva.

I denna doktorsavhandling arbetar jag därför med ett innovativt koncept, där jag använder textil som ett billigt och enkelt stödmaterial för immobilisering av katalysatorer. Genom systematiskt utförda experiment har underlag samlats in för att visa på immobilisering av en oorganisk katalysator (nollvalent järnpartikel-Fe^0) och ett biokatalysator (glukosoxidasenzym-GOx) på en textil stödstruktur. Syftet med denna avhandling är att fastställa möjligheten att använda textil som stödmaterial för immobilisering av katalysatorer i jakten på framställningen av ett heterogent katalytiskt system (oxiderande och reducerande) för rening av avloppsvatten. Ett nonwoventyg av polyester (PF) valdes som textilt stödmaterial för immobilisering av katalysatorer för dess kvalitativa (hög styrka, porositet, biokompatibilitet och resistans mot de flesta syror, oxiderande medel samt mikroorganismer) och kommersiella (tillgänglighet, låg kostnad och enkelhet att modifiera) fördelar. En kombination av miljövänliga och resurseffektiva processer (så som plasmabehandling, användning av hypergrenade dendrimerer, biobaserade polymerer) har använts för att modifiera PF ytan till fördelaktiga ytkemiska egenskaper gällande hög och stabil utdelning av immobiliserade katalysatorer.

Avhandlingen består av tre separata delar som handlar om immobilisering av katalysatorer på textiler: (a) immobilisering och stabilisering av oorganiskt Fe^0 på PF och optimering av dess möjligheter i oxiderande och/eller reducerande katalytiska system, (b) immobilisering av GOx på PF och optimering av dess användning i biokatalytiska system, (c) utformning av heterogena bio-Fentonsystem med hjälp av immobiliserade katalysatorer (Fe^0 och GOx). I alla delar aktiverades PF:s hydrofobiska fiberyta genom en plasmabehandling (antingen atmosfärisk plasma -AP eller kall fjärrplasma -CRP) efterföljt av kemisk ympning med hypergrenade dendrimerer (polyetylenglykol-OH/polyamidoamin-etylendiaminkärna) eller polymerer som innehåller den funktionella gruppen amin/tiol (3-aminopropyl-trietoxysilan/polyetylenimin, kitosan/1-tioglycerol) innan immobilisering av endera katalysatorerna. Immobiliseringen av Fe^0 genomfördes med *in-situ* eller *ex-situ* reduktions-immobiliseringsmetod, medan GOx immobiliserades genom en fysisk adsorptionsmetod. Ett antal tillvägagångssätt utforskades i sökandet efter optimala förhållanden för immobilisering av katalysatorer samt förbättringsmöjligheter av immobiliserade katalysatorers katalytiska förmåga.

Olika analytiska och instrument-tekniker användes för att kontrollera ytmodifieringen av textilier, effektiviteten av immobiliserade katalysatorer, fysiokemiska egenskaper av immobiliserade katalysatorer och deras katalytiska aktivitet för avlägsnandet av färgämnen, fenoler eller patogena föroreningar från vatten. Resultaten från plasmabehandlingen visade att både AP och CRP framgångsrikt aktiverat PF ytan genom integrering av polära funktionella grupper (–COOH och –OH) genom AP och karboxyl/hydroxyl-grupper (–COOH/–OH) och aminogrupper (–NH_2) genom CRP. Dessutom kunde ympade hypergrenade dendrimerer och funktionella polymerer på plasma-aktiverad PF ge en skräddarsydd yta med specifika funktionella ändgrupper. När det gäller immobiliseringen av Fe^0 på en PF-yta visade resultaten att reduktionsmetoderna (in-situ eller ex-situ) för framställning av Fe^0-partiklar hade synergieffekter på hur väl immobiliseringen lyckades när det gäller morfologi, stabilitet, partikelstorlek och spridning av immobiliserad Fe^0. Ytkemiska egenskaper av PF påverkade också

stabiliteten av immobiliserad Fe^0 och tillhörande egenskaper, något som observerats genom flertalet studier. Detaljerade resultat visade att en PF-yta som innehåller de funktionella grupperna –COOH, –OH, och –SH främjar belastning och stabiliseringen av Fe^0 mer än en yta rik på de funktionella grupperna – NH_2. Slutligen, alla Fe^0-immobiliserade PF prov visade hög katalytisk aktivitet i avlägsnandet av föroreningar i vatten i både oxiderande och reducerande system. När det gäller GOx-immobiliserade PF prov fanns det att lyckad immobilisering av enzym på textil var relaterad till typen och omfattningen av funktionella ytgrupper integrerade i PF-ytan. Resultaten visade vidare att en PF-yta med –COOH eller – NH_2-grupper garanterade högre belastning och stabilitet hos GOx jämfört med -COOH och -OH rika ytor. Dessa resultat är viktiga eftersom de styrker interaction mellan den textila ytan och enzymer, vilket utgör en grund för möjligheterna för starka immobiliseringar av GOx på textila stödmaterial. Som validering av konceptet så visar denna avhandling också den första lyckade framtagningen av ett komplett heterogent bio-Fenton system för rening av avloppsvatten med hjälp av immobiliserade katalysatorer (Fe^0 och GOx).

Denna avhandling om immobilisering av katalysatorer på textil och applicering av immobiliserade katalysatorer i rening av avloppsvatten (både oxiderande och reducerande system) bidrar inte bara till allmän kunskap om heterogena katalytiska system, Fenton/Fenton-system och bio-Fenton system, utan öppnar också upp för lovande möjligheter att använda textilier som stödmaterial för immobilisering av olika katalysatorer för ett brett spektrum av användningsområden.

NYCKELORD: Biokatalysatorer; Katalysatorimmobilisering; Katalytisk reduktion; Kitosan; Avlägsnande av färgämnen; Miljösanering; Enzymimmobilisering; Glukosoxidas; Hypergrenade dendrimerer; Heterogen katalys; Heterogen bio-Fenton; Heterogen Fenton; Oorganiska katalysatorer; Fenolavlägsnande; Polyester fiberduk; Avlägsnande av patogena bakterier; Plasmaekoteknik; Polyetylenimin; Textil katalysator; Textil bioteknik; Modifiering av textilytor; Avloppsrening; Zerovalent järn.

Résumé

Les systèmes catalytiques font partie des technologies les plus efficaces des procédés chimiques modernes. Le système utilise une molécule appelée « catalyseur » qui est capable de catalyser une réaction sans n'être produit ni consommé pendant le procédé. Le système catalytique requiert de séparer les catalyseurs des produits après chaque cycle, ce qui est un processus coûteux et gourmand en ressources. Cela montre la pertinence de l'immobilisation des catalyseurs, où les catalyseurs se lient à un matériau de support solide afin de garantir la séparation facile des catalyseurs. Cependant, l'immobilisation des catalyseurs n'est pas toujours facile, car elle nécessite un procédé de préparation complexe du matériau de support comprenant multiples étapes. Dans de nombreux cas, la préparation du matériau de support est plus énergivore et plus coûteuse que les catalyseurs.

Cette thèse de doctorat porte sur un concept innovant d'utilisation du textile comme matériau de support peu coûteux et robuste pour l'immobilisation de deux catalyseurs différents. Des preuves expérimentales ont été rassemblées pour le cas de l'immobilisation de particules de fer zéro-valent (catalyseur inorganique Fe^0) et l'enzyme glucose oxydase (GOx-biocatalyseur) sur support textile. Le but de cette thèse est de confirmer l'utilisation potentielle de ces catalyseurs supportés au textile, pour le traitement des eaux usées, par le biais d'un système catalytique robuste (oxydative ou réductive). Un tissu non tissé en polyester (PF) a été choisi comme matériau de support textile pour l'immobilisation des catalyseurs en raison des avantages à la fois qualitatifs (haute résistance, porosité, biocompatibilité et résistance à la plupart des acides, agents oxydants et micro-organismes) et commerciaux (disponibilité, bon marché et facilement personnalisable). Une combinaison de procédés et de matériaux plus écologiques et économes en ressources (traitements plasma, des dendrimères, des polymères biosourcés) a été utilisée pour la modification de surface des fibres de polyesters créant ainsi des groupements fonctionnels capables de mieux fixer les catalyseurs (Fe^0 et GOx), en termes de quantité et stabilité, tout en préservant les performances inhérentes des catalyseurs.

La thèse comporte trois parties distinctes liées à l'immobilisation des catalyseurs sur textiles : (a) l'immobilisation et la stabilisation de Fe^0 inorganique sur PF et l'optimisation de leur viabilité dans un système catalytique oxydant et / ou réducteur ; (b) l'immobilisation des GOx sur les PF et l'optimisation de leur utilisation dans les systèmes bio-catalytiques ; (c) la conception d'un système bio-Fenton hétérogène utilisant des catalyseurs immobilisés (Fe^0 et GOx) sur textile. Dans toutes les parties, la surface de la fibre hydrophobe de PF a d'abord été activée par un traitement plasma atmosphérique sous air (AP) ou par un plasma froid (CRP) suivi d'un greffage chimique de dendrimères hyper-ramifiés ou de polymères riches en groupements amine ou thiol. Les dendrimères utilisés sont à base de noyau polyéthylène glycol-OH ou de polyamidoamine éthylène diamine, tandis que les polymères riches en amine/thiol utilisés sont le 3-aminopropyl-triéthoxysilane, le polyéthylèneimine, le chitosane et le 1-thioglycérol. Cela a été suivi par l'immobilisation de catalyseurs Fe^0 via des méthodes de réduction in-situ / ex-situ ou par l'immobilisation d'enzymes GOx via l'adsorption physique. Un nombre d'approches a été exploré dans la recherche des conditions optimales pour l'immobilisation de catalyseurs ainsi que pour l'amélioration des performances catalytiques des catalyseurs immobilisés.

Diverses techniques analytiques et instrumentales ont été utilisées pour surveiller la modification de surfaces des textiles, l'efficacité de l'immobilisation des catalyseurs, les propriétés physico-chimiques des catalyseurs immobilisés et leur activité catalytique dans l'élimination des colorants, des phénols ou des contaminants pathogènes dans les eaux usées. Les résultats ont montré que, pour les deux types de traitement plasma, l'AP a activé avec succès la surface de la fibre PF avec l'intégration de groupes fonctionnels polaires (–COOH et –OH), tandis que la CRP avec un mélange O_2 / N_2 intègre à la fois des groupes carboxyle / hydroxyle (–COOH / –OH) et des groupes fonctionnels amines (–NH$_2$). Parallèlement, le greffage des dendrimères hyper-ramifiés ou des polymères ont conduit à des propriétés de surface faites sur-mesure avec des groupes fonctionnels spécifiques à

la surface de la fibre PF. En ce qui concerne l'immobilisation de Fe^0 sur une surface PF, les résultats ont révélé que les méthodes de réduction (in-situ ou ex-situ) pour la formation de particules Fe^0 avaient des effets synergiques sur le succès de l'immobilisation en termes de morphologie, de stabilité, de taille et de distribution des particules. Les propriétés chimiques de surface PF ont également influencé la stabilité du Fe^0 immobilisé et des propriétés associées, comme observé tout au long des études. Les résultats détaillés dans cette thèse ont révélé qu'une surface PF riche en groupes fonctionnels –COOH, –OH et –SH favorise la quantité et la stabilisation de Fe^0 en comparaison avec une surface riche en groupes fonctionnels $-NH_2$. Les catalyseurs Fe^0 immobilisés sur PF ont montré une propriété catalytique élevée dans les systèmes catalytiques pour l'élimination des polluants aquatiques par le biais d'un système hétérogène de type Fenton ou d'une réduction catalytique. Dans le cas des GOx immobilisés sur le polyester-PF, ce résultat est lié au type et à l'étendue des groupes fonctionnels de surface intégrés à la surface PF. Les résultats ont démontré qu'une surface PF riche en groupes fonctionnels –COOH, $–NH_2$ assurait une quantité et une stabilité plus élevées de GOx par rapport à une surface PF riche en groupes fonctionnels –COOH, –OH. Ces résultats portent grande importance car ils fournissent des preuves de l'interaction entre la surface textile et l'enzyme, posant les bases pour des possibilités d'immobilisation forte de GOx sur des matériaux textiles de support. En tant que preuve de concept, cette thèse révèle également la première conception fructueuse d'un système bio-Fenton complètement hétérogène pour le traitement des eaux usées utilisant des catalyseurs immobilisés (Fe^0 et GOx).

Le caractère innovant de la recherche présentée dans cette thèse de doctorat est tout d'abord attribuée à la nouveauté de l'immobilisation de deux types de catalyseurs (catalyseurs inorganiques et biocatalyseurs) sur non-tissé polyester pour l'application dans le traitement des eaux usées. De manière générale, cette thèse contribue à la connaissance générale du système catalytique hétérogène, des procédés de Fenton et de bio-Fenton, aussi bien qu'elle ouvre des perspectives prometteuses d'utilisation de textiles comme matériau de support pour l'immobilisation de divers catalyseurs pour un large éventail d'applications.

Mots-clés: Biocatalyseurs ; Immobilisation de catalyseurs ; Reduction de catalyseurs ; Chitosane ; Élimination de colorants ; Assainissement de l'environnement ; Immobilisation d'enzymes ; Glucose oxydase ; Dendrimères hyper-ramifiés ; Catalyse hétérogène ; Bio-Fenton hétérogène ; Fenton hétérogène; Catalyseurs inorganiques ; Élimination de phénols ; Non-tissé Polyester ; Élimination de bactéries pathogènes ; Écotechnologie plasma ; Polyéthylèneimine ; Catalyseur textile; Biotechnologie textile; Modification de surface textile; Traitement des eaux usées ; Fer zéro-valent.

摘要

催化系统是当代化学处理手段中最有效的技术之一。 这一项技术利用"催化剂"这种小分子去催化一个反应。 在这一过程中，"催化剂"既不会被消耗，也不是这一化学反应的产物。催化系统需要在每次反应后分离催化剂，催化剂的分离过程通常是昂贵且资源密集。过程中涉及到催化剂的固定化，即催化剂与固体载体材料结合，以确保催化剂易于分离。固定化催化剂可重复使用，通常比催化剂在溶液中表现出更好的稳定性。然而，催化剂的固定化具有挑战性，因为它需要多步骤复杂的制备过程，尤其是载体材料。在许多情况下，制备载体材料比制备催化剂更耗费资源和成本。

基于此，本论文提出了一个创新的概念，即使用纺织品作为廉价并且易于制备的载体材料来固定催化剂。本文收集了无机催化剂（Fe⁰-零价铁离子）和生物催化剂（GOx-葡萄糖氧化酶）在纺织品上固定化的实验证据。本论文的目的是建立纺织品作为催化剂固定化载体材料的可行性，以寻求制造异质催化系统（氧化反应和还原反应）用于废水处理。涤纶无纺布（PF）由于其质量上的（高强度、孔隙率、生物相容性和对大多数酸、氧化剂和微生物的耐受性）和商业上的（可用性、廉价和易于定制）的优点，被优选为催化剂固定化的纺织支撑材料。通过采用结合环保和资源高效的工艺（如等离子体处理、使用超支化树状大分子、生物基聚合物）可以对 PF 进行表面改性而使其具有良好的表面化学性质，从而可以获得催化剂的高固定化率和稳定固着。

本论文分为三部分：（a）无机 Fe⁰ 在 PF 上的固定，以及在氧化和/或还原催化体系中的活性优化；（b）将 GOx 固定在 PF 上并优化其在生物催化系统中的应用；（c）纺织品固定化催化剂（Fe⁰ 和 GOx）非均相生物-芬顿体系的设计。在所有体系中，首先通过空气常压（AP）或冷远程等离子体（CRP）处理活化 PF 的疏水纤维表面，然后在其上化学接枝超支化树状大分子（聚乙二醇 OH/聚酰胺胺-乙二胺核）或功能性聚合物（3-氨丙基三乙氧基硅烷/聚乙烯亚胺，壳聚糖/1-硫代甘油）去固定两种催化剂中的任意一种。然后用原位/非原位还原法固定 Fe⁰，或用物理吸附法固定 GOx。通过进行一系列的试验方法，以研究催化剂固定化的最佳条件，并且提升催化剂的催化固定性能。

两种等离子体处理的结果表明，AP 通过集成极性官能团（–COOH 和–OH）成功活化了 PF 纤维表面，而使用 O₂ / N₂ 气体的 CRP 则集成了羧基/羟基（–COOH / –OH ）和氨基（–NH₂）官能团。随之而来的是，接枝的超支化树枝状大分子或富含胺/硫醇官能团的聚合物为定制的表面提供了在 PF 纤维表面具有特定末端官能团的表面。多种仪器和分析技术验证了 PF 纤维表面的活化和官能团定制效果。纺织品的表面改性；催化剂的固定效率以及固定后催化剂的物理化学性能；对污水中染料，苯酚以及致病污染物的催化反应被一系列理论和仪器分析进行了监测。结果表明，还原法制备 Fe⁰ 粒子的方法（原位或非原位）在形貌、稳定性、粒径和分布等方面对 Fe⁰ 的成功固定具有协同效应。随着还原方法的采用，PF 的表面化学性质也影响了固定化 Fe⁰ 的稳定性及相关性质。本论文所考虑的多种方法的详细结果表明，富含-COOH、-OH 和-SH 官能团的 PF 表面比富含-NH₂ 官能团的 PF 表面更有利于 Fe⁰ 的负载和稳定。Fe⁰ 固定化 PF 催化剂在非均相芬顿/类芬顿体系、催化还原体系和病原体抑制体系中均表现出良好的催化性能。在固定化 GOx 的 PF 样品中，CRP 比 AP 更能保证固定化 GOx 的高负载和稳定性。这一结果与集成在 PF 表面的表面官能团的类型和程度有关。当 GOx 被固定在特制的 PF 表面（用交联聚合物）时，也观察到了类似的现象。结果进一步表明，与富含-COOH， - OH 这两种官能团的表面相比，含有-COOH 或-NH₂ 基团的 PF 表面确保了GOx 的较高负载量和稳定性，这反映在所得 GOx 固定化纺织品的催化性能上。这一结果的重要性在于它提供了酵素于纺织材料表面应用的证据并且为 GOx 强大的固化作用应用在纺织支撑材料上的可能性打下了基础。最后，本论文研究在纺织品上使用固定化催化剂的异质生物芬顿系统进行的实验， 提供了与概念证明有关的充分证据并且展示了利用固定化催化剂（Fe⁰ 和 GOx）设计的首个成功的为污水处理设计的异质生物芬顿系统。

本博士论文的创新之处首先在于将两种催化剂（无机催化剂和生物催化剂）固定在涤纶无纺布上用于废水处理的新颖性。总的来说，这一项论文研究有助于催化系统、芬顿和生物芬顿工艺的一般认识同时也有助于提高污水处理系统的效率和可持续性。

关键词：生物催化剂；涤纶无纺布；金属颗粒；铁固定化；超支化树状大分子；聚酰胺胺树状大分子(3-氨基丙基）；三乙氧基硅烷；1-硫代甘油；聚乙烯胺；壳聚糖；葡萄糖氧化酶；氧化还原酶；酶固定化，物理吸附；纤维催化剂；多相催化；抗菌纺织品；革兰氏阳性（G+ve）菌/革兰氏阴性（G-ve）菌；类芬顿；生物芬顿；染料去除；苯酚去除；生物催化；产业纺织品；纺织生物技术；纺织品表面改性；环境治理；废水处理；零价铁。

Acknowledgments

List of appended publications

The works included in this thesis were carried out at three different locations (ENSAIT –GEMTex Laboratory, University of Borås, and Soochow University) between September 2017 to August 2021. The findings of the thesis have been exposed through the publications below. Appended publications will be referred in the thesis by publication numbers written in roman numerals (I-XII).

Peer-reviewed journal publications

Publication I
M. N. Morshed*, N. Behary, N. Bouazizi, J. Guan and V. A. Nierstrasz (2021); An overview on biocatalysts immobilization on textiles: preparation, progress, and application in wastewater treatment ; *Chemosphere* (279), 130481; DOI: 10.1016/j.chemosphere.2021.130481.

Publication II
M. N. Morshed*, N. Bouazizi*, N. Behary, J. Guan and V. A. Nierstrasz (2019); Stabilization of zero-valent iron (Fe^0) on plasma/dendrimer functionalized polyester fabrics for Fenton-like removal of hazardous water pollutant ; *Chemical Engineering Journal* (374), 658-673. DOI: 10.1016/j.cej.2019.05.162.

Publication III
M. N. Morshed*, N. Behary, N. Bouazizi*, J. Vieillard, J. Guan, F. Le Derf, and V. Nierstrasz (2020); Modification of fibrous membrane for organic and pathogenic contaminants removal: from design to application ; *RSC Advances* 10(22), 13155-13173. DOI: 10.1039/D0RA01362E.

Publication IV
M. N. Morshed*, N. Bouazizi, N. Behary, J. Vieillard, O. Thoumire, V. A. Nierstrasz and, A. Azzouz (2019); Iron-loaded amine/thiol functionalized polyester fibers with high catalytic activities: Comparative study ; Dalton Transactions (48), 8384-8399. DOI: 10.1039/C9DT00937J.

Publication V
M. N. Morshed*, M. N. Pervez, N. Behary, N. Bouazizi, J. Guan, and V. Nierstrasz (2020); Statistical modeling and optimization of heterogeneous Fenton-like removal of organic pollutant using fibrous samples: a full factorial design ; *Nature: Scientific Reports* 10(1), 1-14. DOI: 10.1038/s41598-020-72401-z.

Publication VI
M. N. Morshed*, N. Behary, N. Bouazizi, J. Guan, G. Chen and V. A. Nierstrasz (2019); Surface modification of polyester fabric using plasma-dendrimer for robust immobilization of glucose oxidase enzyme ; *Nature: Scientific Reports* 9(1), 1-16. DOI: 10.1038/s41598-019-52087-8.

Publication VII
M. N. Morshed*, N. Behary, J. Guan and V. A. Nierstrasz; Immobilizing Redox Enzyme on Amino Functional Group-Integrated Tailor-Made Polyester Textile: High Loading, Stability, and Application in a Bio-Fenton System. *ACS Sustainable Chemistry & Engineering* 9(26):8879–8894. DOI: 10.1021/acssuschemeng.1c03775.

Publication VIII
M. N. Morshed*, N. Bouazizi, N. Behary, J. Guan and V. A. Nierstrasz; An innovative design of heterogeneous Bio-Fenton system using GOx and Fe^0 immobilized textiles: Proof of concept. *Manuscript submitted.*

Conference publications

Publication IX
M. N. Morshed*, N. Behary, N. Bouazizi, V. Nierstrasz; Dendrimer-mediated immobilization of zero-valent iron (Fe^0) on plasma-treated polyester nonwovens ; 18th AUTEX World Textile Conference, 20 – 22 June 2018, Istanbul – Turkey.

Publication X
M. N. Morshed*, N. Behary, N. Bouazizi, V. Nierstrasz; Zero-valent iron immobilized polyester nonwoven for Fenton degradation of methylene blue ; 12th European wastewater management conference, 17-18 July 2018, Manchester –The UK.

Publication XI
M. N. Morshed*, N. Behary, N. Bouazizi, V. Nierstrasz; Activity of glucose oxidase enzyme immobilized on polyester fabric mediated by hyper-branched dendrimers ; Journées des jeunes chercheurs UGéPE_Nord de France - GEPROC, 20-21 November 2018, Campus scientifique, Villeneuve d'Ascq, University of Lille – France.

Publication XII
M. N. Morshed*, N. Behary, N. Bouazizi, V. Nierstrasz; 3-Mercapto-1,2-propanediol modified robust polyester nonwoven for stabilization of zerovalent iron nanoparticles for multifunctional application ; 257th ACS National meeting, 31 March – 4 April 2019, Orlando – The USA.

∗ = Corresponding/presenting author

Above listed publications have not been included in this version of the thesis. However, electronic/print versions of these publications are available in the database of the respective publisher.

Contribution to appended publications

The author of this thesis designed the hypothesis, carried out the experimental works, and performed the data collection for all publications. Co-authors in each publication were involved in analyzing and interpreting data, as well as writing and revising the manuscript.

Common abbreviations

Name	Abbreviation	Name	Abbreviation
Iron	Fe	Glucose oxidase	GOx
Zero valent iron	Fe^0, ZVI	Potassium phosphate buffer saline	PBS
Iron nanoparticles	Fe-NPs	Enzyme commission	EC
Polyethylene terephthalate	PET	Milli-units	mU
Polyester nonwoven	PN	Liquor ratio	L/R
Polyester nonwoven fabric	PF	Dielectric barrier discharge	DBD
Hydroxyl group	-OH	Atmospheric pressure plasma	AP
Carboxyl group	-COOH	Cold remote plasma	CRP
Amine group	$-NH_2$	Plasma treatment power	TP
Thiol group	-SH	Atmospheric pressure glow discharge	APGD
Parts per million	ppm	Maximum velocity	V_{max}
Hour, Minute	h, min	Michaelis constant	K_m
Mole, millimole	M, mM	Velocity of reaction	V_0
Gram, milligrams	g, mg	Glass transition temperature	T_g
Concentration	C	*Escherichia coli*	*E. coli*
Temperature	T	*Staphylococcus epidermidis*	*S. epidermidis*
Chemical oxygen demand	COD	Horseradish peroxidase	POD
Total dissolved solids	TDS	Chitosan	CS
Electrical conductivity	EC	Polyethylenimine	PEI
Ferric ions	Fe^{3+}	3-(Aminopropyl)triethoxysilane	APTES
Ferus ions	Fe^{2+}	1-thioglycerol	1-TG
Emerging pollutants	EMPs	Poly-(ethylene-glycol)–OH	PEG-OH, PEG
Malachite green	MG	Polyamidoamine (PAMAM)	PAM
Methylene blue	MB	Advance oxidation processes	AOPs
Crystal violet	CV	Reactive oxygen species	ROS
4-Nitrophenol	4-NP	Metal-organic framework	MOFs
4-Aminophenol	4-AP	Bio-Fenton	BF
Potassium chloride	KCl	Hydroxyl radical	$^\bullet$OH
Iron(II) sulfate	$FeSO_4$	Equilibrium concentration	Qe
Iron(III) chloride	$FeCl_3$	Derivative thermogravimetric	DTG
Iron(III) nitrate	$Fe(NO_3)_3$	Optical microscope	OM
Hydrogen peroxide	H_2O_2	Scanning electron microscope	SEM
Sodium borohydride	$NaBH_4$	X-ray photoelectron spectroscopy	XPS
Ethanol	C_2H_6O	Fourier transform infrared	FTIR
Ultraviolet-Visible	UV-Vis	Thermogravimetric analysis	TGA
Water contact angle	θ_{H2O}	Differential scanning calorimetry	DSC
Weight %	wt.%	X-ray diffraction	XRD
Analysis of variance	ANOVA	Energy-dispersive spectroscopy	EDS
Design of experiments	DOE	Centre européen des nontissés	CENT
Melting temperature	T_m	Attenuated total reflection	ATR
Crystallization temperature	T_c	Standard cubic centimeters per min	sccm
Difference in absorption	ΔE	Persistent organic pollutants	POPs
Chemical vapor deposition	CVD	Phenolic endocrine-disrupting chemicals	PEDCs
Physical vapor deposition	PVD		

Table of contents

List of tables

List of figures

Chapter 1
Introduction

Chapter outline

The introductory chapter of this thesis presents the background for the immobilization of catalysts on textiles and catalytic wastewater treatment systems. Following the background, the chapter describes the framed research gaps that motivate the research questions of this thesis. In addition, the scope and limitations of this thesis have been briefly summarized. A detailed framework and outline of the thesis, along with its relevance to UN's SDGs-2030, are given at the end.

1.1. Background

In a typical catalytic system, additional efforts are necessary to separate the catalysts from the system, which is counterproductive, resource-intensive, and expensive. This has led to the concept of the immobilization of catalysts, which involves fixing catalysts to or within solid support materials for better reaction control and easier recovery/separation of the catalyst from the system. The characteristics and performance of the immobilized catalysts depend to a large extent on the choice of support material. A wide variety of materials from inorganic and organic sources have been introduced as support materials for the immobilization of catalysts, including mesoporous materials [1], nanotubes [2, 3], inorganic nanoparticles [4, 5], biopolymers [6, 7], and so on. The choice of material depends on the desired application—although there is no one ideal material that satisfies all applications. Yet, there are some common characteristics that all support materials must have; these include high flexibility, durability, versatility, broad accessibility, and affinity for the intended catalyst. Most support materials that have been introduced so far are exclusive and require a multi-step synthesizing process, which makes immobilized catalysts an expensive resource. This has led to the idea of using textiles as the simple and inexpensive support material for immobilizing catalysts.

Most textiles are resilient, available in various forms, and contain most of the desirable primary characteristics of support material for immobilization of catalysts. A comparison of textile materials from natural and synthetic sources has shown that synthetic fibers are more reliable for catalysts immobilization than natural fibers in a number of ways including greater strength, durability, resistance to most acids and alkalis, and so on. Thanks to advances in organic chemistry and polymer technology, the production of synthetic textiles are growing. Despite the above-mentioned leads, synthetic textiles such as polyester, polyamide, and nylon have rarely been used for chemical applications, mainly due to their inertness to further manipulation. However, over the last few decades, surface modification of textiles through different methods has allowed the surface chemical properties of the synthetic textiles to be altered without changing their primary properties while allowing further manipulation. Although surface modifications offer higher potentiality in terms of synthetic textile, but it also been used for natural textiles which opens up possibilities for creating a desirable property through integrating specific surface functional groups on the textile's surface. Specific functional groups possibly facilitate the immobilization of catalysts as well as, allowing for robust immobilization and their wider applications. A thorough literature search on catalyst immobilization on textiles was carried out at the beginning of this work (in December 2017) and

compared with the recent data (from December 2020). Four quadrants of keywords were identified; "immobilization, textile, enzyme, and zerovalent iron" were used to search in the Web of Science (all databases) in four combinations: (1) immobilization AND enzyme; (2) immobilization AND enzyme AND textile; (3) immobilization AND zerovalent iron; (4) zerovalent iron AND textile. The search results for combination 1 in December 2017 consisted of 29,182 published articles and reviews, which increased to 35,116 by December 2020. The earliest publication was from as early as 1940. For combination 2, the search results in December 2017 consisted of 290 published articles and reviews, which increased to 404 by December 2020. The earliest publication was from 1989. For combination 3, the results in December 2017 consisted of 116 published articles and reviews, and 181 by December 2020, with the earliest publication from 1998. For combination 4, the results in December 2017 consisted of only 10 published articles and reviews, and 25 by December 2020, with the earliest publication from 2006. These statistics reflect the growing interest, relevance, and novelty of using textiles as a support material for immobilization of various catalysts.

Water pollution monitoring and decontamination have become a major challenge worldwide. In the Global Risks 2015 report of the World Economic Forum, the water supply crisis has been identified as the single greatest high-impact risk for the 21st century [8]. Among the many existing water pollutants, the European Commission has identified a first watch list under the Environmental Quality Standards Directive 2015, which includes colorants, residues from personal care products, pesticides, pharmaceuticals/antibiotics, and bacterial pathogens, based on their suspected risk to the aquatic environment, biodiversity, and/or human health [9]. These pollutants are typically aromatic persistent organic pollutants (POPs) and are resistant to conventional physical, chemical, and biological wastewater treatments such as coagulation, flocculation, adsorption, filtration, aerobic/anaerobic biological systems, or a combination of physical and biological systems [10, 11]. Catalytic systems comprise both oxidation and reduction, where at least one catalyst generates hydroxyl radicals ($^{\bullet}OH$, highly reactive—$E_0 = 2.8$ V) and nonselective species are effective in the removal of those pollutants from the water [12]. Ozonation (O_3, O_3/ultraviolet (UV), O_3/H_2O_2, O_3/H_2O_2/UV), photolysis of H_2O_2 (photochemistry assisted, UV/H_2O_2), photocatalysis/ semiconductors (TiO_2/UV), and Fenton/Fenton-like processes (Fe^{2+}/H_2O_2, Fe^{2+}/H_2O_2/UV, Fe^{3+}/H_2O_2/UV, bio-Fenton) are some of the popular oxidation processes that use inorganic catalysts and efficiently remove a wide variety of pollutants. Nevertheless, Fenton or Fenton-like systems are among the most effective and reliable catalytic systems for wastewater treatment. The realm and efficiency of Fenton reaction in pollutants removal has been time tested through various approaches, yet this technology is not been widely implemented in industrial applications. Continuous advancement in this realm is in progress and new improvements are being introduced in regular basis. One of the most recent innovation based on Fenton chemistry is bio-Fenton system, which is a green and sustainable alternative to the traditional Fenton system where the energy consumption is lower and uses biomolecules for in-situ production of Fenton reagents. In bio-Fenton system, hydroxyl radicals are produced through the joint effort of an inorganic catalysts and biocatalysts. A number of reports have shown the potential of the bio-Fenton system in the removal of toxic contaminants (dyes, chlorinated organic contaminants) from water [13-16]. Although the bio-Fenton system for wastewater treatment is theoretically complacent, the technology is still far from large-scale implementation. Catalytic reduction system using solid metal catalysts and a reducing agent eventually also degrade the pollutants from water through either hydroxyl radical or electron-transfer reactions route. With appropriate attention, the catalytic system can effectively replace the conventional physical, chemical, and biological wastewater treatments providing a high standard of treated water while effectively mineralizing varieties of aromatic persistent organic pollutants.

1.2. Research gaps

Despite the attractive properties of catalytic systems in terms of activity and selectivity, they suffer from difficulties associated with recycling, removal, and reuse of the catalysts. Immobilizing catalysts on solid supports substantially eliminates those difficulties. Immobilized catalysts are popular for easy separation and removal of the catalysts from the products and subsequent reuse of the catalysts. These features propagate the catalytic system using immobilized catalysts as greener and sustainable alternatives to conventional (homogeneous) catalytic systems. However, the use of exclusive support material and complex preparation processes causes many low-turnover industries to be relatively reluctant to use them for large-scale applications. Thus, the gap related to simple support material is a significant concern that is limiting the application of this technology to a wider extend.

There has been a growing interest in the innovative idea of using textiles as support materials for immobilization of organic catalysts (including biocatalysts) and inorganic catalysts, this technology is just in the early stages of development, and many questions remain to be answered. One of them is related to the surface chemical property of textile in terms of efficiency in catalysts immobilization. Textile surfaces are the boundaries between the textile and the external environment in which it works and behaves; the importance of surface chemical property is fundamental for interaction with the catalysts during immobilization. Tailoring the surface of textile with specific functional groups before immobilization of predetermined catalysts might improve the efficiency of catalysts immobilization on textiles. There has been great progress in surface modification of textile various smart and functional applications, but an in-depth study on textile materials for catalysts immobilization has not made enough progress and indeed a vital gap to address.

In the case of the application of Fenton, Fenton-like, and catalytic reduction system (using Iron particles) in wastewater treatment, the technology is struggling to make progress towards large-scale application as the widely used homogenous system produces secondary pollutants (iron sludge) on the process. This secondary pollutant along with the process for catalyst separation requires additional attention, which is costly and counterproductive. A solution to recover the catalysts and no production of sludge is a crucial gap for the future of this technology and catalysts immobilized on textile can provide a solution.

In the direction of catalytic wastewater treatment, bio-Fenton is the most recent innovation in Fenton chemistry, but due to the use of multiple expensive catalysts in the system, a homogeneous bio-Fenton system is economically undesirable. Since it had introduced, little research has been done to bring this technology to a mature stage. Few attempts have been found where only the biocatalyst (enzyme) used in the system has been immobilized, which solves half of the problem [13, 16-18]. Therefore, it is necessary to immobilize both catalysts (biocatalysts and iron) on robust and inexpensive support material (textile being the best candidate) to achieve total heterogeneity of the system and advance this resource-efficient and sustainable water and wastewater treatment technology.

1.3. Research purposes

Driven by the research gaps identified and explained above, the general purpose of the thesis is to explore the concept of catalyst immobilization on textiles using a simpler, eco-friendlier, and resource-efficient preparation process. In addition, the thesis is also testing the hypothesis of a heterogeneous Fenton, bio-Fenton, and catalytic reduction system for wastewater treatment using immobilized catalysts.

Catalyst immobilization

The purpose of catalyst immobilization is to ensure easy separation of the catalysts from the system and provide subsequent reusability. In the context of this thesis, catalysts immobilization was aimed for application in the heterogeneous catalytic wastewater treatment system for effective removal of dyes, phenols, and pathogens. A catalytic system is a reliable method for wastewater treatment. As discussed as gaps, some inherent drawbacks of this system related to operation sensitivity (to the surrounding environment), use of expensive reagents, and production of secondary pollutants hinder its large-scale application. The immobilization of catalysts can provide the solution to those drawbacks while contributing to the scaling up of this technology. This hypothesis has predominantly stimulated the purpose of this thesis.

Catalyst immobilization on textiles

There have been several exclusive support materials for the immobilization of catalysts, but as industries are seeking a simple and inexpensive support material, within our best knowledge, there are no better option than textiles to match those requirements. Besides, in the context of this thesis, the support material for immobilized catalysts for wastewater treatment needs to be strong, inexpensive, resistant to the surrounding chemicals/environment, and textile came out as the most favorable candidate. Nevertheless, when the work of this thesis started, there were few if any reports on the use of textiles as a support material for the immobilization of catalysts in wastewater treatment, particularly for Fenton or Fenton-like systems. The idea of using textiles as the support material for catalyst immobilization is the central hypothesis of this thesis.

Proof of concept of complete heterogeneous bio-Fenton system

The bio-Fenton system is a green alternative to the conventional Fenton system, as it uses biocatalysts and performs in milder conditions. However, this system is very resource-intensive due to the use of costly catalysts. The challenges around the bio-Fenton system can be greatly reduced through immobilizing all catalysts (inorganic and bio) necessary for the complete operation to achieve total heterogeneity of the system. In this direction, this thesis is not only the first of using textile as robust and inexpensive support for the immobilization of two catalysts (inorganic catalyst- zerovalent iron and a biocatalyst -glucose oxidase) but also the proof of concept of a complete heterogeneous bio-Fenton system for pollutant removal from water using immobilized catalysts (enzyme and iron) on textile.

The purpose of this thesis is also to promote the use of resource-efficient processes (plasma eco-technologies) and the use of milder but more eco-friendly chemical alternatives for catalysts immobilization.

1.4. Research questions

This thesis aims to contribute to the field of catalyst immobilization and its application in heterogeneous systems (particularly for wastewater treatment). Four (4) research questions (RQs) have been identified to broadly address the research gap and the research purpose of this thesis. RQ1 investigates the suitability of textile materials as a support for immobilizing different catalysts. Since the selection of support material for catalyst immobilization is directly related to the anticipated application, this question will look at the requirements specifically for a textile-based system in wastewater treatment. RQ2 and RQ3 investigate the immobilization of zerovalent iron (Fe^0) particles and glucose oxidase (GOx) on textiles, with a focus on improving the loading and stability of catalysts. Finally, RQ4 validates the proof of concept of the heterogeneous bio-Fenton system using immobilized catalysts to remove pollutants from water. Figure 1.1 schematically presents the relationships between the research questions and their role in this thesis. The specific research questions that will be answered in this thesis are the following:

Research Question 1 (RQ 1): How feasible is the use of textile as a support material for catalyst immobilization?

Research Question 2 (RQ 2): Can we immobilize inorganic catalyst (Fe^0) on textile without compromising its inherent catalytic performance?

(a)   How does the method of immobilization influence the yield and stability of the immobilized Fe^0 on textile?
(b)   Can a tailor-made textile surface increase the yield and stability of the immobilized Fe^0?
(c)   How effective are Fe^0-immobilized textile as catalysts in oxidative/reductive wastewater treatment?

Research Question 3 (RQ 3): Can we immobilize biocatalysts (GOx) on textile without compromising their inherent catalytic performance?

(a)   To what extent do the surface properties of textile fibers affect the yield and stability of immobilized GOx?
(b)   Can a tailor-made surface provide favorable conditions for robust GOx immobilization on textiles?
(c)   Can GOx-immobilized textiles be used in a heterogeneous bio-Fenton system for wastewater treatment?

Research Question 4 (RQ 4): Can we develop a heterogeneous bio-Fenton system for wastewater treatment using immobilized catalysts (Fe^0 and GOx)?

By answering these research questions, this thesis will contribute to the general knowledge on catalytic systems, immobilization of catalyst on textiles, and heterogeneous Fenton/Fenton-like systems, and will contribute to the advancement of resource-efficient and sustainable technologies.
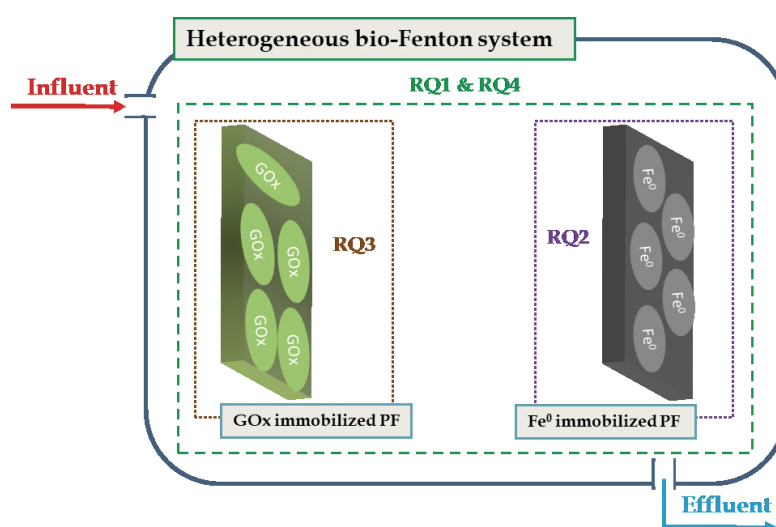
Figure 1. 1: Main research questions of this study placed on the schematic heterogeneous bio-Fenton system.

Through presenting new approaches for modifying the textile surface to obtain high yield and stability of the chosen catalysts, this thesis contains the knowledge related to:

(a)   The use of resource-efficient and sustainable processes for modification of the textile surface.
(b)   The idea of immobilizing inorganic catalysts and/or biocatalysts on textile support matrix.
(c)   The role of the tailor-made surface chemical properties of textiles in immobilization of catalysts.

1.5. Scope and limitations of the thesis

The immobilization of catalysts falls under the scope of a multidisciplinary field, requiring technical competencies in material sciences, surface chemistry, and, biotechnology in the case of biocatalysts. The context of this thesis is on the scope of material sciences and surface chemistry, with applications in environmental remediation. The research perspectives and conclusions are based on laboratory-based experimental data and their respective analysis. The necessary interpretations about the scope and limitation of this thesis emphasize the following matters; (a) The study related to the immobilization of inorganic zerovalent iron particles on textiles falls under the scope of material science, inorganic chemistry to some extent, and surface chemistry. (b) The study on the

immobilization of enzymes on textile has been done under the scope of surface chemistry. The enzymes were used as received, without any further modification; therefore, the biotechnological study of enzymatic properties was out of scope. (c) The section on the surface modification of textiles (in order to provide a favorable surface for catalyst immobilization) also falls under the scope of surface chemistry. This part of the work is not in the scope of textile engineering. (d)The integration of functional materials into the textile surface to alter the functional properties of the textile surface falls under the scope of both material science and surface chemistry. T The related field of multifunctional or smart textiles is outside the scope of this thesis. (e) All the results presented here have been collected in laboratory-scale trials. Large-scale industrial trials are outside the scope of the thesis. They are subject to further development and optimization.

1.6. Thesis framework and outline

This doctoral thesis investigates the potential use of textile as an inexpensive and robust support material for the immobilization of inorganic catalysts (Fe^0) and biocatalysts (GOx) to create a novel fibrous oxidative and reductive heterogeneous catalytic system for wastewater treatment. The framework of the research work has been divided into three parts: (a) immobilization of Fe^0 on synthetic textile (polyester nonwoven fabric) and optimizing its viability in oxidative and/or reductive catalytic systems; (b) immobilization of GOx on synthetic textile and optimizing their use in bio-catalytic systems; (c) proof of concept of the complete heterogeneous bio-Fenton system using immobilized catalysts (Fe^0 and GOx).

In each part, one or more hypotheses have been tested through laboratory-based trials and experiments. In all studies, the hydrophobic surface of the synthetic textile was activated through a plasma eco-technology treatment, followed by chemical grafting of either hyperbranched dendrimers or functional polymers rich in amine/thiol functional groups before immobilizing either of the two catalysts. A series of systematic experiments were conducted to find the optimum conditions for catalyst immobilization, as well as to test the usefulness and performance of the resultant catalysts in a model catalytic system designed to remove dyes, phenols, or pathogenic contaminants from water.

The thesis has been presented in seven (7) chapters termed as Chapter 1-7;

Chapter 1_ of the thesis presents the introductory background of context related to the immobilization of catalysts on textile. Following the background, the chapter comprehends the framed research gaps that motivate the purpose and research questions of this thesis. In addition, the scope and limitations of this thesis have been briefly summarized. A detailed framework and outline of the thesis along with the relevance of this thesis to UN's SDGs-2030 have been provided in the end.

Chapter 2_ of the thesis presents a comprehensive overview of the literature related to catalysts, catalytic system, immobilization of inorganic catalyst on textile, immobilization of biocatalyst on textile, surface functionalization of textile for catalyst immobilization as well as catalytic pollutant removal from water. The chapter further discusses – selection of catalysts studied in this thesis and the textile used as support material for immobilization of catalysts. In the end, approaches and strategies identified for this thesis based on the state of art have also been provided in detail.

Chapter 3_ presents materials and methods used in this thesis to achieve research objectives. A detailed description of instruments and parameters used for surface modification of polyester nonwoven fabric (PF) before and after immobilization of zerovalent iron (Fe^0) or glucose oxidase (GOx) enzyme has been presented. In the end, the description of analytical, instrumental, and mathematical characterization tools used to assess the preparation of immobilized catalysts and their performances in catalytic activities has also been provided.

Chapter 4_ discusses the results and analysis of immobilization of zerovalent iron (Fe^0) particles (an inorganic catalyst) on polyester nonwoven fabric (PF). The chapter further comprehends an overall discussion of the main findings based on the success of the Fe^0 immobilization on textile and its use as a catalyst in heterogeneous

oxidative/reductive removal of pollutants from water. The outcome of this chapter paves the way to fabricate robust Fe^0 immobilized PF designed for heterogeneous bio-Fenton systems (discussed in chapter 6).

Chapter 5_ deals with the results obtained in the context of immobilizing biocatalyst (glucose oxidase-GOx enzyme) on textile (polyester nonwoven fabric-PF). Results obtained through various surface functionalization approaches of PF to improve the stability of immobilized GOx have been discussed in detail. The overall findings of this chapter will provide grounds for designing robust enzyme-immobilized textile for the heterogeneous bio-Fenton system.

Chapter 6_ presents the proof of concept related to fabrication of complete heterogeneous bio-Fenton system for removal of pollutants from water using immobilized catalysts. The functionality of the system in the batch system has been studied and summarized.

Chapter 7_ refers to the summary and overall finding from the thesis based on the results obtained from all the experiments and countless observations. An insight into the limitation and potential future directions on the domain has also been described in the later part of the chapter.

The sequence of experimental approaches and strategies on this thesis has been schematically presented in Figure 1.2;
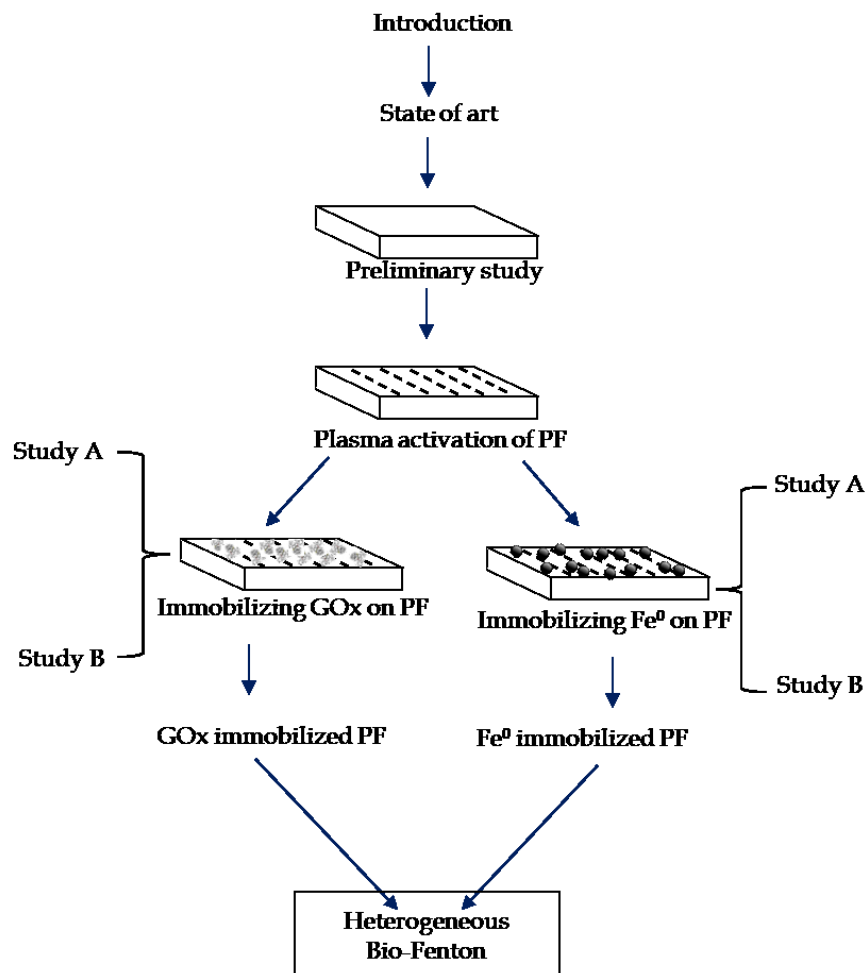
Figure 1. 2: Schematic illustration of the framework and the sequence of the project work carried out in this thesis.

1.7. Relevance of this thesis to UN's SDGs - 2030

This thesis is relevant to more than one goal of the UN's global sustainable development goals (SDGs) in agenda 2030. Particularly, the overall thesis is related to Goal 6: clean water and sanitation. Besides that, the innovative approach introduced in this thesis for a robust water treatment system is related to Goal 9: Industry, innovation, and infrastructure. Finally, the choice of eco-friendly and resource-efficient methods to minimize material demand, energy consumption, environmental footprint, and an overall reduction in the cost of operations during immobilization of catalysts is related to Goal 13: climate action.

Chapter 2

State of art

Chapter outline

This chapter presents a comprehensive overview of the literature related to catalysts, catalyst immobilization on textiles, and catalytic wastewater treatment systems. The chapter further discusses the catalysts selected for this thesis and the textile used as support material for immobilization of catalysts. The chapter ends with a detailed description of the approaches and strategies chosen for this thesis based on the current state of the art.

2.1. State of art on catalysts and catalyst immobilization

2.1.1. Catalysts

Catalysts are additional molecules other than the reactants that increase the rate of a reaction. They do not affect the thermodynamics of a reaction and are not formed or consumed in the process [19]. More than 90% of commercially produced chemical products are now processed using a method that requires at least one catalytic stage [20-22]. Inorganic and organic catalysts are the two main types of catalysts. Inorganic catalysts are simple inorganic molecules that are not normally found in biological systems. They usually consist of a metal center with some bound ligands. These metal complexes vary widely and are chosen based on the desired chemical reaction. Metals have some interesting electronic properties that allow them to facilitate chemical reactions by lowering the activation energy. Inorganic catalysts are less sensitive to temperature and pH than organic catalysts [23, 24]. Organic catalysts are low-molecular-weight organic molecules derived from nature that catalyze a chemical reaction in sub-stoichiometric quantities [25, 26]. Organic catalysts are also known as organocatalysts. They are composed of nonmetal elements such as carbon, hydrogen, and sulfur [27]. Biocatalysts, such as proteins and enzymes, are a type of organic catalysts involved in biochemical processes [28].

Inorganic catalysts are being used extensively, both in laboratory research and in industrial/manufacturing processes. It is hard to find a complex synthetic reaction or an industrial process that does not, at some stage, require an inorganic catalyst [29]. Transition metals (iron, titanium, copper, nickel, etc.) are the metals of choice for use as inorganic catalysts in organic, organometallic, and electrochemical reactions due to their ability to exist in multiple oxidation states, to change oxidation states, to form complexes with organic ligands, to act as a good source of electrons, and to adsorb other substances onto their surface, activating them in the process [30-32].

Biocatalysts are catalysts of natural origins, which activate or speed up biochemical reactions [33]. An ideal biocatalyst has strong selectivity, wide availability, and low cost. Enzymes are the most abundant and well-known natural biocatalysts (found in plants, animals, and microorganisms), and are at the core of all biological processes in all living beings [28]. Enzymes are natural non-living entities, generally composed of complex proteins. They resemble a long chain of amino acids and can be reorganized into a variety of forms using different types of amino acids [33]. There are seven classes of enzymes, based on the types of reactions they catalyze: oxidoreductases (EC

1), transferases (EC 2), hydrolases (EC 3), lyases (EC 4), isomerases (EC 5), ligases (EC 6), and translocases (EC 7). EC 7 is a new class of enzymes, added to the enzyme database website in August 2018 [34]. Each enzyme is assigned a name and an enzyme code (EC) by the International Union of Biochemistry and Molecular Biology. The EC is a number consisting of four digits: the 1st indicates the enzyme's class; the 2nd is the subclass; the 3rd is the sub-subclass; and the 4th is the enzyme's serial number in its sub-subclass [35].

Homogeneous and heterogeneous catalysis

There are two major types of catalytic systems: homogeneous and heterogeneous catalytic systems (catalysis). Homogeneous catalysis is those where catalysts exist in the same phase (gas or liquid) as the reactants, in while heterogeneous catalysis, catalysts are in a different phase from the reactants. In most cases, heterogeneous catalysis entails the use of solid catalysts in a liquid reaction mixture [36]. Homogeneous catalysis is much more effective and selective than standard heterogeneous catalysis. Most homogeneous catalysis reactions occur in a liquid state, whereas heterogeneous catalysis can happen in either a liquid or a gaseous phase [37]. Heterogeneous catalysts are faster and cheaper to recover and reuse than homogeneous ones since they are in a separate phase from the reaction medium. The difficulty of recovering homogeneous catalysts from the reaction medium is a significant disadvantage. To reuse homogeneous catalysts, they must be precipitated, with subsequent recovery, which is an energy-intensive operation. The catalysts are often deactivated after the process in homogeneous catalysis.

These shortcomings in homogeneous catalysis encouraged research on the immobilization of homogeneous catalysts. The aim is to combine the benefits of homogeneous catalysts (high activity and selectivity) with the ease of reuse in heterogeneous systems [38]. When homogeneous catalysts are converted into heterogeneous catalysts through an additional mechanism (binding or grafting to a support material), the results are referred to as heterogenized homogeneous catalysts. Catalysis with heterogenized homogeneous catalysts is known as heterogenized homogeneous catalysis [39]. It should not be confused with hybrid catalysis, which is the use of a combination of homogeneous and heterogeneous catalysts, either from organic and inorganic sources, in the same framework.

Sustainability of catalysis

Sustainability consists of three components: societal, ecological, and economic. They are also referred to as the three Ps (people, planet, and profit). Since catalysis is at the heart of chemical synthesis, it is obviously a central theme in sustainable chemistry [40]. Catalysts are used in both synthesis and degradation/breakdown of molecules. Catalysis can play a role in finding new routes for fuels, base chemicals, and fine chemicals, and plays a role in both pollution prevention and remediation [41, 42]. A catalytic process can be considered sustainable and resource-efficient, as catalysts increase the reaction rate by a factor of up to a million by lowering the activation energy (see Figure 2.1.), which saves a considerable amount of time and energy. A catalytic process also releases less CO_2, uses fewer resources, and produces purer products at a lower cost than a corresponding non-catalytic process [43, 44].
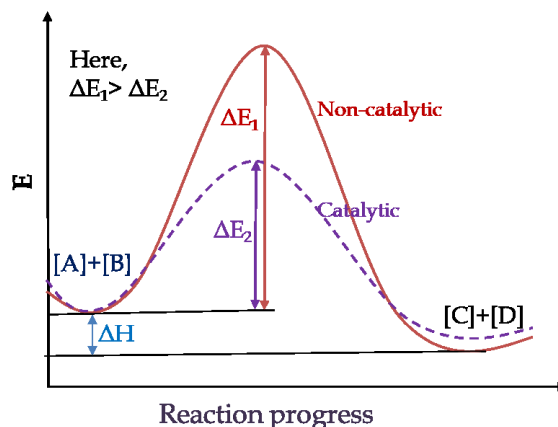
Figure 2. 1: Energy diagram for a generic catalytic (solid line) and non-catalytic (dotted line) reaction. The differences in energies indicated (ΔE_1 and ΔE_2) for the forward reaction and enthalpy of the reaction (ΔH). Note: [A] [B] = reactants, [C] [D] = products.

2.1.2. Catalyst immobilization

The immobilization of catalysts can be described as "physically confining or localizing catalysts in a defined region where they can maintain their catalytic activities and can be used repeatedly and continuously" [45, 46]. It is much simpler to isolate immobilized catalysts (by filtration, centrifuge, magnetic isolation, etc.) than it is to separate homogeneous catalysts, so this process is more practical in terms of reusing the catalysts. It is often also more effective for product separation and purification, as well as for the elimination of catalyst residues, which is particularly important for toxic catalytic systems. The immobilization of homogeneous metal-ligand catalysts may also help separate the surface-active microbes, preventing catalyst agglomeration and extending catalyst activity [47]. Supports can sometimes associate with immobilized functional groups, contributing to the overall catalytic reaction. Immobilized catalysts can be used in a variety of reactors, including fixed bed and membrane reactors, making them easier to integrate into industrial processes [48].

Techniques of catalyst immobilization

Catalysts can be immobilized using a variety of techniques, such as chemisorption of the catalyst, physisorption on the support, encapsulation of the catalyst within the configuration of the support, physical entrapment of the catalyst, and so on. The following is a brief description of the common techniques for catalyst immobilization.

Chemisorption of catalysts on the support: Chemisorption involves the chemical forces that allow the catalyst to interact with the support material, such as covalent/ionic bonding, crosslinking, etc. (see Figure 2.2) [49, 50]. Many well-known catalysts can be immobilized through this technique by impregnating inorganic supports, such as alumina, silica, or zeolites, with metal salts. These catalysts can operate in heterogeneous environments, but their activity is often different from that of homogeneous catalysts.

Physisorption of catalysts on the support: Physical adsorption immobilization of catalysts involves attaching catalysts to the surface of the support matrix through weak forces, such as van der Waals force, electrostatic force, hydrophobic interaction, and hydrogen bonds (see Figure 2.2) [51]. The benefits of physical adsorption methods for catalyst immobilization include simplicity and high catalyst yield, with a minimal effect on the catalytic properties of the immobilized catalysts. The drawbacks of this process include the leaching of catalysts due to the

weak interaction with the support material. Furthermore, often the pH, ionic strength, and temperature of the solution influence the efficiency of immobilization of the catalysts.
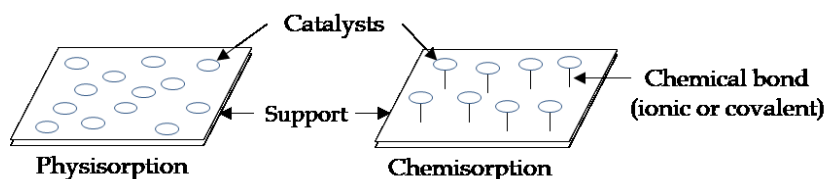
Figure 2. 2: Depiction of physisorption and chemisorption interaction between the support and catalysts.

Physical entrapment of catalysts on the support: Entrapment immobilization is the capture of catalysts inside a network in the support matrix, which allows the substrate and products to pass through while holding the catalyst in place [52, 53]. Although the catalysts cannot leave the network due to steric restrictions, they can move around inside the pore, and therefore may be assumed to behave very similarly to their homogeneous equivalents. The key limitations of this approach are the high cost and the steric hindrance caused by small pore size, which has so far precluded this category of catalysts from being used in industry. However, the catalysts produced in this manner are more robust than the catalysts immobilized through chemisorption and physisorption.

Encapsulated of catalysts within the structure of the support: Co-casting of catalysts with the support polymer is the basis of the encapsulation technique. Since this approach does not use crosslinking, the catalysts are immobilized while retaining their primary structure. Nevertheless, the polymer slows the transport of the substrate to the catalyst, resulting in a lower relative catalytic performance than with free catalysts. Both metal complexes and enzymes are commonly immobilized using this technique [54].

Support materials for catalysts immobilization

Since the beginning of the research about immobilization of catalysts, there has been a need to define a group of materials to which catalysts may be attached. In general, materials have been sought which offer high stability, availability, relatively low price, and high affinity to the bound catalysts. A wide variety of materials of both inorganic and organic origin (inorganic oxides, silica materials, mineral materials, magnetic nanoparticles, polymers, textiles, and various new support materials) have been evaluated as effective support for catalysts immobilization.

Organic materials: It is well known that there is no universal support material suitable for all catalysts for all of their applications. Inorganic carriers have certain limitations, such as limited biocompatibility, lower affinity to catalysts, and reduced possibilities to create various geometrical shapes [55, 56]. Often it requires the use of a cross-linking agent to create a covalent bond between the catalysts and inorganic support [55]. Due to these reasons, some materials of organic origin are also used for the immobilization of various catalysts under different immobilization protocols. In general, organic support materials can be divided into two groups: (i) synthetic materials (mainly polymers) and (ii) renewable materials obtained from natural sources (biopolymers). Both groups have been widely used for the immobilization of both organic and inorganic catalysts.

Inorganic oxides: Inorganic oxides are known for their high stability, mechanical resistance, and good sorption capacity. Moreover, they are inert under various reaction conditions, which facilitates their application as support material for immobilization of various types of catalysts from both organic and inorganic sources [55]. Due to the presence of many hydroxyl groups on their surface, these materials are highly hydrophilic; this enhances catalysts

immobilization and surface modification modified that favors the formation of relatively stable catalysts–matrix interactions.

Silica materials: Silica is one of the most frequently used inorganic support materials for catalysts immobilization. Its high thermal and chemical resistance and good mechanical properties make it a suitable material for many practical applications [57]. Silica offers good sorption properties due to its high surface area and porous structure. These properties allow effective catalyst attachment and reduce diffusional limitations [58, 59]. Both organic and inorganic catalysts have been immobilized on silica materials. Zuo *et al.* (2014) [60] reported the lipases immobilized on silica gel matrix, which retained 91% of the activity of the free enzyme.

Mineral materials: Minerals are abundant in nature, are easily available, offer high biocompatibility, and can be used as obtained without further advanced treatment and purification, which makes them relatively cheap. Moreover, the presence of many functional groups (such as –OH, COOH, C=O, –SH, –NH_2) on the surface of the minerals allows the formation even of covalent bonds between the catalysts and the support and facilitates modification of the minerals. Biocatalysts immobilized on minerals are used mainly in environmental engineering for waste and wastewater treatment as well as in biosensors to improve linear range and detection limit. For example, according to Chrisnasari *et al.* (2015) glucose oxidase immobilized on bentonite modified by tetramethylammonium hydroxide retains over 50% of its initial activity after five repeated catalytic cycles [61].

Magnetic nanoparticles: Magnetic nanoparticles are another fascinating substance to consider for catalyst immobilization. Magnetic nanoparticles are very appealing for a wide variety of uses, including catalysis, because of their unusual properties. The use of magnetic nanoparticles as catalyst immobilization has many benefits, including fast catalyst recovery from an external magnetic field, which is a more energy-effective catalyst separation process than conventional filtration and centrifugation methods. Magnetic nanoparticles often have a large exterior surface region, which allows them to immobilize a large number of catalysts [62, 63]. Since the active sites are located on the outer surface of the magnetic nanoparticles, internal diffusion issues are minimized. Despite this, magnetic nanoparticles are extremely dispersible in solvents due to their limited particle size, allowing active locations to be easily accessed [64].

Polymers and textiles: Over the last few decades, there has been growing concern about using polymeric materials and textiles (such as polyamide, polyvinyl alcohol, polylactic acid, and polyethylene terephthalate) as supports for immobilization of catalysts due to their good mechanical strength and easily adjustable properties [65-67]. An alternative to the use of synthetic polymers as support material for catalysts immobilization is the use of biopolymers—polymers of natural origin. Biopolymers include carbohydrates but also proteins such as albumin and gelatin. Furthermore, a great many works have been done to improve the activity retention and stabilities of immobilized catalysts on tailor-made surfaces of polymeric materials and textiles. An overview of catalysts immobilization on textiles will be provided in the following section.

New support materials for catalysts immobilization: Possibilities for practical applications of immobilized catalysts are growing. Therefore, the discovery and use of new materials with desired properties for immobilization of catalysts have recently become extremely important. Materials from both organic and inorganic origin characterized by exceptional thermal and chemical stability and good mechanical properties have been introduced as new materials for catalyst immobilization. They include, ceramic materials (alumina, zirconia, titania, iron oxide, and calcium phosphate) [56], mesoporous materials (zeolites, carbons, and sol-gel matrices, as well as precipitated and ordered mesoporous oxides) [68], nanoparticles (nano-gold, nanorod) [69] carbon nanotubes [70], graphene and graphene oxide [71], Electrospun materials (nanofibrous mat), polymeric membranes (polyvinyl alcohol, polyurethane, polyvinyl fluoride, chitosan, and cellulose), hybrid and composite materials (organic-organic; inorganic-inorganic, or organic-inorganic) [72]. These carriers are characterized by good stability under harsh reaction conditions, high availability or relatively simple synthesis, and consequently low price.

2.2. State of art in textile supports for catalyst immobilization

Textile technologies provide robust, inexpensive solutions for many different scientific and social challenges other than clothing. Recently, interest has been growing in using textiles as the support material for the immobilization of organic (including biocatalysts) materials and inorganic materials for various applications [73]. The use of textile support materials offers several advantages. Textiles are much cheaper than other commercially available inorganic and organic carrier materials (aluminum silicates, porous glass, or various hydrophilic polymers). Textiles accommodate a wide variety of dimensions, shapes, and orientations, allowing many different designs for different reactors [74]. Furthermore, textiles allow the immobilized catalysts to be separated quickly and completely, without leaving any waste in the reactor. The open, active, and porous surface structure of textiles often provides a low-pressure drop, allowing the mixture, the mass transfer, and the optimum turnover of suspensions to be diffused easily [75]. Figure 2.3 lists the benefits of textiles as a support material for the immobilization of catalysts.
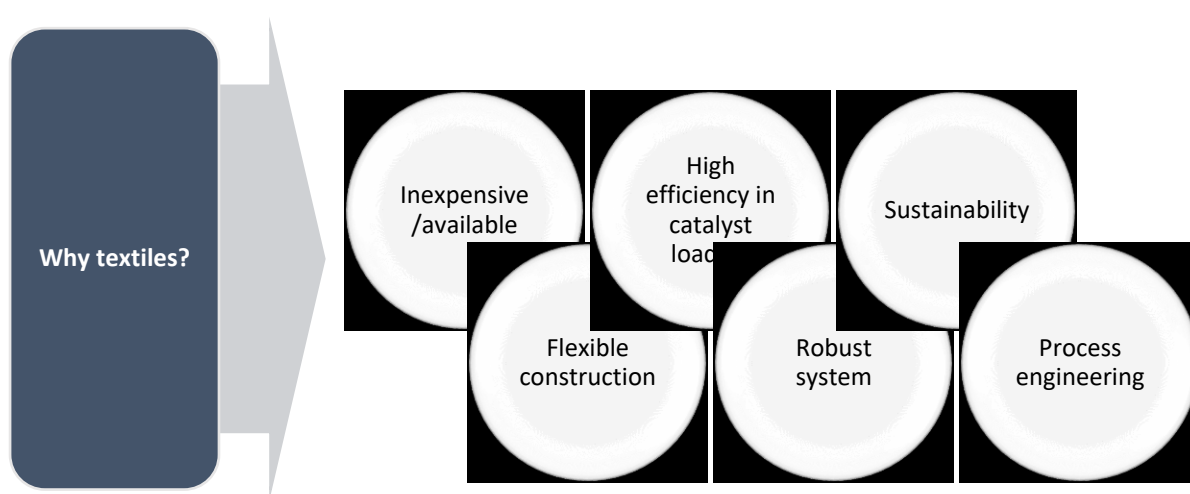
Figure 2. 3: Benefits of the textile as support material for catalyst immobilization (adopted from publication I).

Textiles can be derived from natural or synthetic fibers. Natural fibers (cotton, jute, wool, silk, etc.) come from plants and animals, while synthetic fibers (polyester, nylon, polyamide, etc.) are made from chemical compounds. Synthetic fibers appear to be more reliable than natural fibers for catalyst immobilization on a number of criteria, such as strength, durability, resistance to most acids and alkalis, and so on [75, 76]. Thanks to advancements in organic chemistry and polymer technology, the production of synthetic textiles are on the rise. Nonetheless, in the past, synthetic textiles were rarely been used in chemical applications, mainly due to their surface inertness and limitations towards further manipulation [66]. However, over the last 20 years, various methods of textile surface modification have allowed altering the surface chemical properties of the material without changing its primary properties. This opens numerous possibilities for creating a desirable property by adding specific surface functional groups to the textile surface. This can facilitate the long-lasting immobilization of a catalyst, allowing a powerful catalytic system to be designed.

For more than 2,000 years, chemical finishing has been used to modify the surface of textiles by integrating functional materials on the surface through adhesive forces to yield various functionalities, creating, for example, hydrophobic/hydrophilic, antibacterial, or fireproof textiles. According to many researchers, this principle of surface modification of textiles by integrating favorable surface functional groups is a promising solution for robust immobilization of organic and inorganic catalysts [74].

2.2.1. Preparation of textile surface for catalyst immobilization

The textile surface provides an important medium for practical modifications in a variety of applications in order to satisfy specific requirements. Surface modification of textile is a vastly interdisciplinary field, which involves polymer chemistry, surface science, fiber science as well textile engineering. Several surface modification techniques have been developed to improve wetting, adhesion, and other properties of textile surfaces by introducing a variety of reactive groups that will facilitate the immobilization of catalysts. The techniques used to modify textiles can generally be grouped into two major categories: chemical and physical. Chemical techniques usually involve careful control of the surface chemical environment or the addition of specific chemical species to modify the textile surfaces. Physical methods, however, generally tend to use non-chemical forces to control the etching or deposition of material. Physical forces – such as gas plasma, vaporization, and irradiation may apply to modify textiles by adding or removing excess material from bulk assemblies.

Wet chemical surface modification of textiles: Treatment of textiles with wet reagents to produce reactive functional groups on the surface is known as a wet chemical surface modification. The chemical agent reacts with the fiber surface of the textile as a part of this procedure to alter the orientation of the polymers and integrate tailored surface features. The use of chromic acid, sodium hydroxide, or potassium permanganate to introduce oxygen-containing moieties on polyester fibers is a typical example of textile surface modification. Besides, traditional textile coloration and finishing processes also fall under the domain of wet chemical modification of textiles, which involves considerable economic and ecological considerations. The degree of surface modification through wet chemical processes is not repeatable between polymers of different molecular weights and crystallinity. This method will also result in the formation of dangerous chemical waste [77, 78].

Modification by chemical vapor deposition: Chemical vapor deposition (CVD) is a process of surface modification of textile where gaseous precursors react to the textile surface to form a solid coating of heated substrates. Treatment of the textile surface by means of a vapor-phase chemical reaction allows the production of a conformal coating that can provide additional functions to the textile material, ranging from improved mechanical or chemical resistance to electrical conductivity or biochemical activity [79, 80]. An apparatus of chemical vapor deposition consists of a heating system mounted on both sides of a cylinder, a sample holder, gas inlet and outlet, and a quartz tube. In this method, deposition of material is achievable in a single layer, multilayer, composite, nanostructured, and functionally graded coating materials with well-controlled dimension and unique structure at low processing temperatures.

Modification by physical vapor deposition: Physical vapor deposition (PVD) is a physical process for the modification of the textile surface. Of all these physical techniques, physical vapor deposition stands out as a promising technique for the functionalization of textiles. PVD is a vaporization coating method that involves transferring content from the solid phase to the vapor phase atom by atom or molecule by molecule and then depositing it on textile surfaces [79, 81]. There are various processes considered as PVD technologies, such as evaporation, ion implantation, and sputtering. Among them, sputtering technology has been regarded as an environmentally friendly technique for the functionalization of textile materials. Magnetron sputtering techniques are widely used to deposit different kinds of coatings, such as metallic coatings, oxide coatings, polymer coatings, and composite coatings on textile materials.

Modification through nanomaterial grafting: Nanotechnology deals with materials having at least one dimension in the nanometer scale, and includes nanoparticles, nanorod, nanowires, thin films, and bulk materials made of nanoscale building structures [82, 83]. Several new functionalities can be added to the base textile as a result of the integration of nanomaterials on the fiber surface. Those functional properties are of the highest importance, giving noticeable improvements in the end-use. For example, deposition of silver nanoparticles on the textile surface will impart antibacterial properties, while titanium dioxide nanoparticles will make the textile surface ultraviolet ray resistant. Platinum and palladium nanoparticles incorporation on the textile surface will impart catalytic properties that can be used in the decomposition of harmful gases or toxic industrial chemicals. These nanomaterials are often impregnated into textile fabrics, with little or no impact on their structure or comfort. The existence of surface plasmons is another advantage of using metal nanoparticles. The optical extinction of these plasmons is solid, and they can be adjusted to different colors by changing their size and shape. Silver nanoparticles

may be used to offer textiles a gleaming metallic yellow to dark pink color while still imparting antibacterial properties.

Enzymatic surface modification of textile: Enzymatic surface modification of textiles involves the processing of fibers to increase hydrophilicity or to remove components from the surface through hydrolysis, oxidation, or eliminative cleavage as well as the (targeted) introduction of functional groups on the surface. Vertommen *et al.* (2005) [84] reported the hydrolysis of synthetic polymer poly(ethylene terephthalate), the most important synthetic fiber in the textile industry using *cutinase* enzyme (see Figure 2.4). Another attempt of enzymatic surface modification of textiles involves immobilization of enzymes on the textile surface to adhere to biocatalysis properties in textiles [85]. Several examples of such approaches have been broadly described in previous sections. Desizing of cotton, de-pilling of cotton, enzymatic aging of denim fabrics, enzymatic scouring of greige cotton fabrics, shrink-resistant treatment of yarn, and enzymatic degumming of silk have all been researched thoroughly during the last two decades. These results suggest that utilizing enzymes to alter the surface of textile polymers can substitute typical chemical processes. Progress in biochemistry, biocatalysis, genetics, and largescale production of enzymes makes industrial processes using enzymes more attractive and competitive [86].
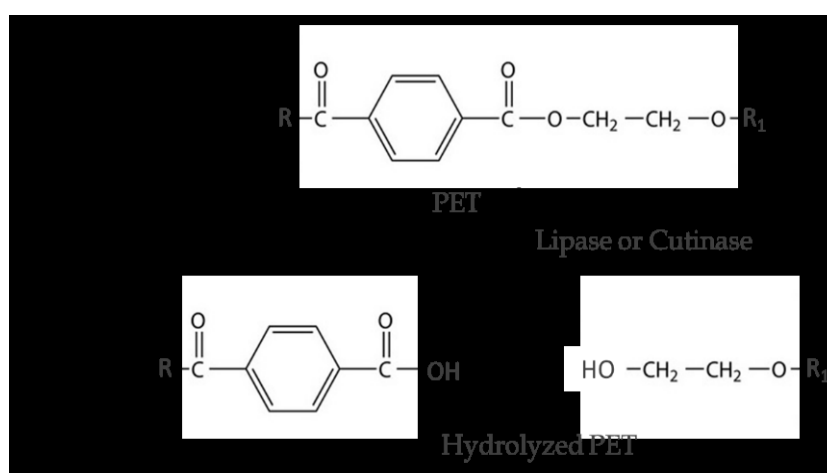
Figure 2. 4: Enzymatic hydrolysis of polyethylene terephthalate.

Plasma surface modification of textiles: Plasma treatment is called eco-technology since it can functionalize a variety of products in a dry state without the use of chemicals and in a limited amount of time. Plasma does not involve the use of solvents or water, and it is a nondestructive technology in general, unlike wet and chemical manufacturing [87]. Different functionalities may be achieved by integrating numerous elements and gases. Several forms of plasma have been used to treat textile fabrics, including conductive fibers, throughout the last decade, with a number of gases to improve or decrease the wettability of PET, cotton, linen, silk, aramid, acrylic, and polyamide. Plasma treatments of textiles alter their surface character without affecting their bulk properties. The depth of the surface treatment is < 100 nm. Plasma treatment changes the topography of the textile's surface where in some cases chemical properties can change as well. Various reports confirm the changes of surface chemical property of textile through plasma treatment [88, 89]. A detailed overview related to the application of plasma technology in textile modifications can be found in Höcker (2002) [90], Abd Jelil (2015) [91], and Rino *et al.* (2008) [92]. Varieties of plasma treatment of textiles were reported in the literature [92]. The gas used in these plasma treatments varies based on the purpose that must be accomplished. In the literature, gases like nitrogen, helium, oxygen, and argon were mostly used to increase wettability, while gases like CF_4, C_3F_6, $C_6H_{18}OSi_2$, and SF_6 were mostly used to decrease wettability.

2.2.2. Immobilization of inorganic catalyst on textiles

The concept of immobilizing inorganic catalysts is long-established and well documented. It was thought that in this way, the catalysts could be not only separated more easily from the product but also reused several times, reducing their cost. In 1966, Anderson and his coworker prepared a variety of inorganic catalysts by immobilizing different metals, such as platinum, palladium, nickel, tungsten, and cobalt, on carbon [93]. Since then, the field has grown considerably. The thermodynamic instability of inorganic catalysts, especially metal particles, and their tendency to agglomerate during synthesis and successive applications is a serious drawback [94]. Furthermore, the environmental concerns related to a homogeneous catalytic system, involving corrosion, toxicity, difficulty in catalyst handling and separation, high cost, and solid waste have encouraged the research on the immobilization of catalysts.

Various support materials have been proposed for inorganic catalyst immobilization, including organic and inorganic sources (such as minerals, silica gel, and zeolites). Designing and preparing a support matrix in a conventional catalyst immobilization phase is could be more expensive than the catalysts themselves. From an economic point of view, a low-cost, reliable, and widely accessible support material for catalyst immobilization is highly desirable. Therefore, the immobilization of inorganic catalysts on textile support materials was explored, both on the surface and inside the layers and microspores of the textiles (See Figure 2.5). Zhang *et al.* (2012) [95] immobilized Fe-doped TiO_2 nanoparticles on polyamide fabric. The common methods for immobilizing inorganic catalysts are discussed in the following section, along with a brief analysis of the key influencing factors. The general application of inorganic catalysts on textiles is also discussed in the context of recent literature.
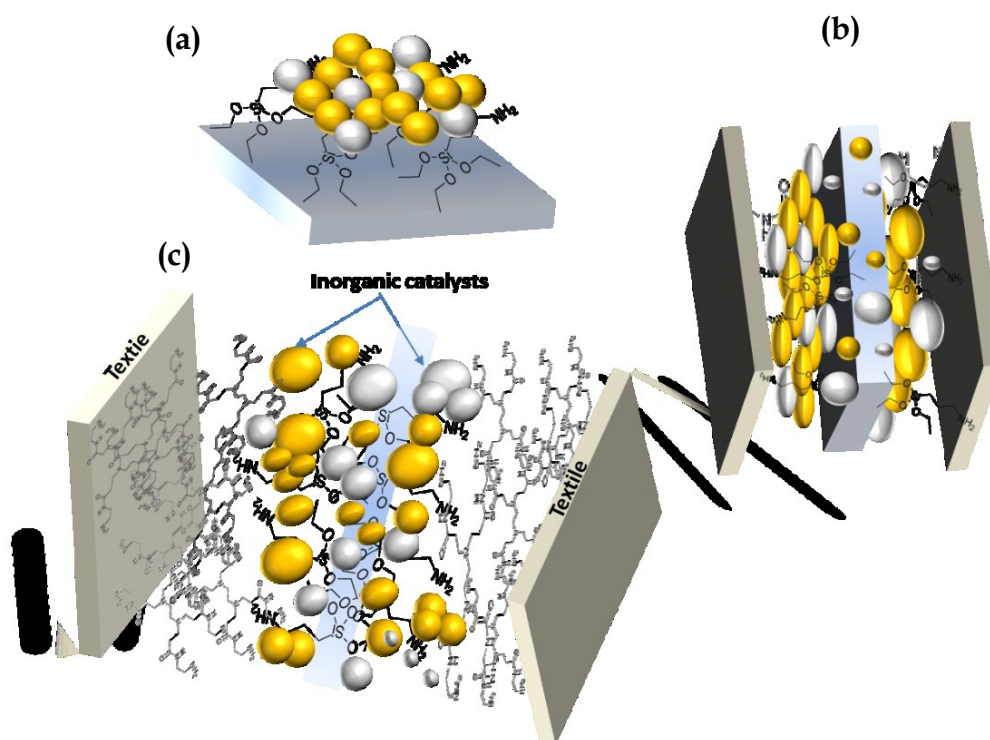
Figure 2. 5: Immobilization of inorganic catalyst on the textile surface; (a) inorganic catalyst immobilized on the surface of the textile, (b) inorganic catalyst immobilized between the layers of fibers (c) postulated interaction between inorganic catalyst and textiles during immobilization (adopted from additional publication III).

2.2.2.1. Methods for immobilization of inorganic catalyst on textiles

There are four common methods for the immobilization of inorganic catalysts on textiles, based on the interaction between the catalyst and the textile support material: covalent binding, electrostatic interaction, adsorption, and entrapment (encapsulation) [52, 96]. There are some other preparation methods for the immobilization of inorganic catalysts on other, non-textile support materials (such as silica gel, minerals, or nanostars/nanotubes); these include impregnation, ion exchange, and deposition precipitation. The process involving the methods of immobilization comprises two common immobilization strategies: (a) the chemical-based or solvent-based approach (dipping) and (b) the physical approach (padding, printing, or entrapment). The solvent-based chemical approach uses an aqueous solution to transport the inorganic catalysts to the surface of the textile; they are later immobilized on the textile via the interaction between the catalyst and the textile (see Figure 2.6). In the physical approach, inorganic catalysts are subjected to a physical force to confine them inside the textile support material. Most chemical processes involve the simultaneous synthesis and immobilization of the inorganic catalysts on textiles [97, 98]. Notably, chemical methods consume more energy, chemicals, time, and catalyst than physical methods.

Out of the basic interactions between inorganic catalysts and textiles, the covalent interaction is by far the most frequently used method for immobilization. For this method, the textile support material must provide reactive sites for the functionalization of catalysts and offer tunable surface properties where the position and density of the immobilized catalyst can be precisely controlled. The covalent binding method is relatively complex, involving several preparative steps, currently making it unsuitable for large-scale preparations. Therefore, immobilization via ionic interaction between the catalyst and textile has been used instead for many years. Immobilization via electrostatic ionic interaction is conceptually simple and is easy method for immobilizing inorganic catalysts under milder immobilization conditions. For this method, the surface chemical properties of the textile support material play a significant role in the efficiency of the inorganic immobilization.

Another common simple method for inorganic catalyst immobilization is adsorption. This method relies mainly on weak van der Waals interactions. This means that the catalyst can readily leach into the reaction medium during use. The stability of the immobilized catalyst can be improved by modifying the surface of the textile to enable hydrogen bonding [52]. Encapsulation is the only catalyst immobilization method that does not require any interaction between the inorganic catalyst and the textile. The only requirement is that the pore openings in the support must be smaller than the kinetic size of the immobilized catalyst.
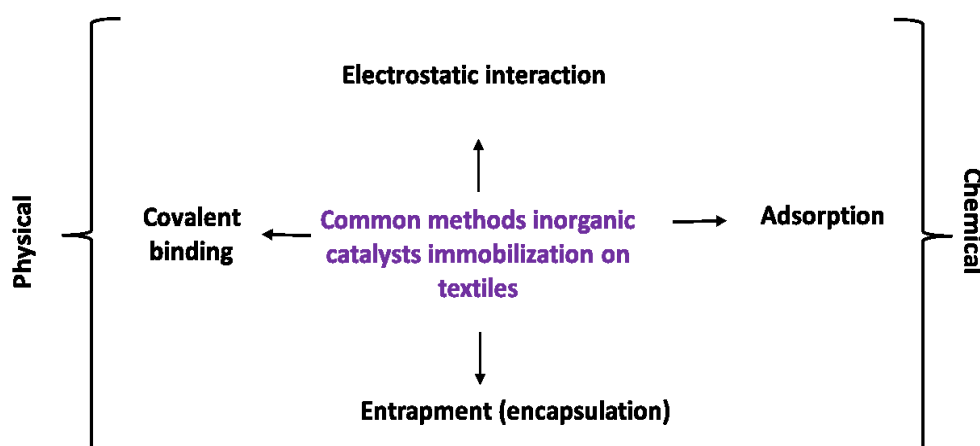
Figure 2. 6: Illustration of common methods of immobilization of inorganic catalysts on textile.

2.2.2.2. Influencing factors of inorganic catalyst immobilization on textiles

Immobilization of inorganic catalysts on textiles falls under the multidisciplinary effort that involves a number of key influencing factors. Apart from the condition of the environment of immobilization, such as pH, temperature, the concentration of inorganic catalyst, immobilization of inorganic catalyst on textiles greatly influences by the three major factors; (a) diffusion of inorganic catalyst on the textile support material, (b) interaction between the catalysts and textile material towards loading and stability and, (c) the method of immobilization. Diffusion limitation during immobilizing catalysts causes poor loading of the immobilized catalysts. However, the open, active and porous structure of the textile surface offers a low-pressure drop, which enables easy diffusion of the catalyst to the textile surface and ensures optimal loading. The end functional groups present on the surface of the textile have to have the ability to bind the inorganic catalysts. Many approaches adopted the surface modification of textile to have a favorable condition for robust immobilization of catalyst. Methods of immobilization such as physical sorption, ion exchange, crosslinking, covalent binding, or entrapment affect the performance of immobilization of catalysts. However, covalent binding and crosslinking have been reported as the most effective method for catalyst immobilization in terms of loading, stability, and leaching of the catalyst.

2.2.2.3. Applications of inorganic catalyst immobilized textiles

Starting from chemical synthesis, food technology, and pharmaceutical preparation to environmental remediation, inorganic catalysts in general covers the most of the application that uses any catalysts [99, 100]. Most of the applications used free inorganic catalysts, instead, very few approaches were found on industrial use of immobilized inorganic catalysts. The general application of inorganic catalysts immobilized textile is still on the laboratory scale. Wilkanowicz *et al.* (2020) [101] used immobilized calcium oxide onto polyacrylonitrile (PAN) fibers for biodiesel production to present an alternative method of biodiesel production that uses electrohydrodynamic processing combined with catalyst immobilization onto a textile. Immobilized catalyst on textiles did not require to be removed from the biodiesel after reaction and ensured satisfactory reusability. Zhang *et al.* (2020) [102] reported the immobilization of $CoSe_2$-CoO on N-doped carbon fibers for application in water electrolysis. The multiple features of different components of the catalyst immobilized textile lead to desired kinetics and remarkable catalytic performance. Zhand *et al.* (2019) [103] immobilized $ZnBr_2$ catalyst on simplest and most common heterogeneous material carbon fibers for chemical fixing CO_2 into the fine chemicals. Hosseini *et al.* (2020) [104] fabricated novel bulk inorganic catalyst (TiO_2) based carbon felt for oxidation of benzene under mild conditions. They have mentioned that the inorganic catalyst immobilized in textiles continued to operate after a period of eight cycles while offering direct conversion of benzene to phenol under mild conditions. Apart from the above-discussed application, a majority of literature that has been reported the application of inorganic catalysts immobilized textile were in environmental remediation, particularly in wastewater treatment. They have shown the effectiveness in both oxidative and reductive catalytic system such as photocatalysis, Fenton/Fenton-Like (advance oxidation processes) and catalytic reduction removal of pollutants from water. A wide range of pollutants such as colorant, heavy metals, micropollutants, phenol endocrine-disrupting chemicals, pharmaceutical residue, functional materials, and personal care products as well as pathogenic toxins has been reported to be removed by using inorganic catalysts immobilized textile while maintaining satisfactory reusability of the heterogeneous catalysts [105-111]. A detailed overview on the topic of application of inorganic catalysts immobilized textiles in wastewater treatment has been provided in section 2.3.2.

Several other studies also reported the functionalization of textile support material for various technical and protective applications such as antibacterial textiles, UV blocking textile, Fire-retardant textile, self-cleaning and artistic textiles. The as-mentioned applications immobilized inorganic catalysts are not entirely addressed the mechanism of catalysis; they remain in the domain of smart and multifunctional textiles.

2.2.3. Immobilization of biocatalysts on textiles

Biocatalyst or enzyme immobilization is defined as the physical or chemical confinement of enzyme molecules onto/within a support matrix in such a way that they maintain their full or nearly full activity. Enzyme immobilization is one of the most significant new industrial biotechnologies. Since immobilized enzymes were first used in industry in the 1960s, enzyme immobilization methods, hypotheses, and products, as well as immobilization chemistry, have advanced rapidly. A timeline of the progress in biocatalyst immobilization on various forms of textiles is shown in Figure 2.7 [75]. Today, the production of immobilized enzymes for various practical applications is no longer done by trial and error and has progressively transitioned to logical design. which is marked by the fact that enzyme immobilization technology is now used not only to realize the reuse of expensive enzymes but also to better control the process. The main goal of enzyme immobilization is to allow continuous operation of biocatalysis processes while avoiding contamination of the product with free enzymes and retaining the biological activity of native enzymes, easy process control, and a wide range of compatible reactor configurations. The interest in enzyme immobilization techniques is growing [112] as they become more sophisticated, improving the properties of the immobilized enzymes, such as function, selectivity, and stability through merging the two characteristics of the enzyme with heterogeneity. The presence of a robust immobilized enzyme in the early stages of process growth is increasingly recognized as providing early insight into process development and saving costs, not only during process development but also during production.

1833	**1966**	**1979**	**1984**	**1988**	**2002**
Anselme Payen was the 1st to discover an enzyme.	1st industrial use of immobilized enzyme was reported by Chibata *et al.*	Shemer *et al.* 1st reported biocatalysts immobilization on nonwoven textiles.	1st approach of biocatalysts immobilization on woven textiles was reported by Yamazaki *et al.*	Vlasov *et al.* 1st reported biocatalysts immobilization on knitted textiles.	Jia *et al.* 1st reported nanofibrous biocatalysts immobilization on textiles.

Figure 2. 7: Timeline of progress in biocatalysts immobilization on various forms of textiles (adopted from publication I).

Designing and preparing an exclusive support matrix in conventional biocatalyst immobilization methods holds true for various enantioselective and noble organic and inorganic catalysts [25]. In response, researchers are seeking low-cost, reliable, widely accessible, and versatile support materials for catalyst immobilization. Several studies have established textile as an important support material, which outperforms resins, silicone, carbon nanotubes, gold nanostars, and cellulose crystals. This gave rise to the idea of immobilizing biocatalysts on textiles, which is a new concept in the field of both heterogeneous biocatalysis and technical textiles.

2.2.3.1. Methods for biocatalysts immobilization on textiles

Immobilization methods have a significant impact on the properties and characteristics of the biocatalysts immobilized textile. Physical adsorption, covalent binding, cross-linking, and encapsulation are the most common methods of biocatalyst immobilization used in the design and development of biocatalyst immobilized textiles (see Figure 2.9). These methods have been applied to two separate immobilization protocols; (a) dipping/solution-based immobilization and (b) printing-based immobilization (see Figure 2.8). During the dipping phase, bio-catalysts and textiles are placed in a solution to create a complex with each other, whereas during the printing process, bio-catalyst are mixed with the solvent for the preparation of printing ink. Screen, ink-jet, and valve-jet printing of biocatalyst immobilization of textile have so far been introduced as resource-efficient and environmentally friendly processes. Due to the open exposure of all sites of the fibrous textile in the solution at

once, dipping allows for a comparatively higher amount of biocatalyst loading than printing. However, the dipping method requires higher energy, chemicals, time, and biocatalyst consumptions than printing.
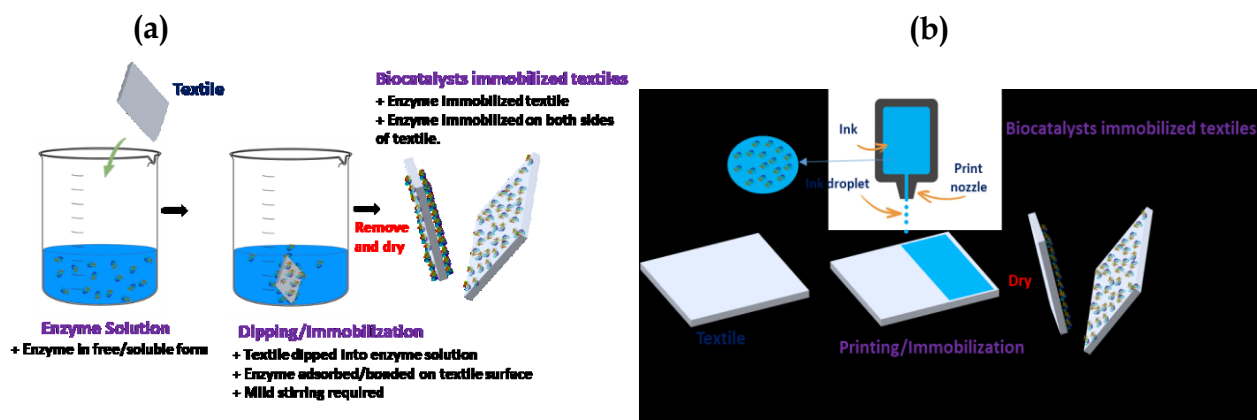
Figure 2. 8: (a) Dipping and (b) printing method for immobilizing biocatalysts on textiles (adopted from publication I).

Physical adsorption: Physical adsorption is the easiest way to produce biocatalysts or enzyme immobilized textiles where, by weak forces such as van der Waals, Ionic, Hydrophilic and hydrophobic interactions, the adsorbed enzyme molecules bind to the textile surface. The immobilization procedure involves the activation of the textile fiber surface in a suitable condition before exposure to the enzyme solution or ink [112]. This procedure enables a greater loading of the enzyme while the active site of the enzyme is not affected, thus ensuring a good bio-catalytic activity [45]. However, this method of immobilization of enzymes suffers from high leaching of immobilized enzymes on any support material because of its weak physical forces (for binding the enzyme to support matrix), which requires pre-treatment to ensures better carriers: enzyme interactions. Researchers have taken into account several sustainable processes and products, including plasma ecotechnology-based surface treatment or hyperbranched dendrimer functionalized textile surface before immobilizing enzymes by physical adsorption method [34].

Covalent binding: The covalent binding process, in which enzyme molecules form a stable covalent bond with the textile fiber surface, is a widely used method for the preparation of biocatalysts immobilized textile. Because of the covalent interaction between the enzyme and the textile, leaching of immobilized enzymes is minimal. The presence of favorable functional groups on the surface of the textile fiber is required by this immobilization method. In many cases, it is necessary to incorporate strong electrophile functional groups that will react with the enzyme's strong nucleophile groups. Free amino, carboxyl, hydroxyl, and sulfhydryl groups rich support material can be used for better efficiency in the immobilization process [113]. Covalent binding between enzyme and textile can occur in three ways: binding with enzyme via the side chains of lysine (-amino group) or binding with the thiol group in cysteine, or the third and most common binding with carboxylic group of aspartic and glutamic acids. It should be noted that functional groups necessary for the activity of enzyme shouldn't participate in the covalent interactions with the textile support, especially those that are close to the active site of the enzyme. In that case this enzyme:textile interaction may distort the orientation and can lead to denaturation of the enzyme. Besides, the additional molecule might be needed between the enzyme and the surface, not necessarily leading to crosslinking between the enzyme molecules. As a result of these sensible precautions in covalent binding immobilization of enzyme on textile; it be high loading of the immobilized enzyme, but the activity is usually relatively poor while the process is resource-intense and expensive [114].

Crosslinking: Cross-linking of enzymes is another popular method for preparing biocatalysts immobilized textile. This is an irreversible process where cross-connections between the enzyme molecules via covalent bands occur on the surface of the textile [76]. This approach involves binding the nonessential functional group in an enzyme (e.g., an amino group of Lysine residues) to one end of the cross-linker molecule while binding to another end in the textile surface with functional groups. Glutaraldehyde, hydroxylamine, hexamethylenediamine, etc. are the

21

usually used crosslinkers in the immobilization of enzymes in the textile industry. Most of them are poisonous, resulting in serious changes to enzymes, which can lead to alteration in enzyme formulation and activity loss [34, 115]. The cross-linking technique of enzyme immobilization, however, also obstructs the efficiency of biocatalyst immobilized textiles because the active site of immobilized enzymes is less accessible to the substrates [75].
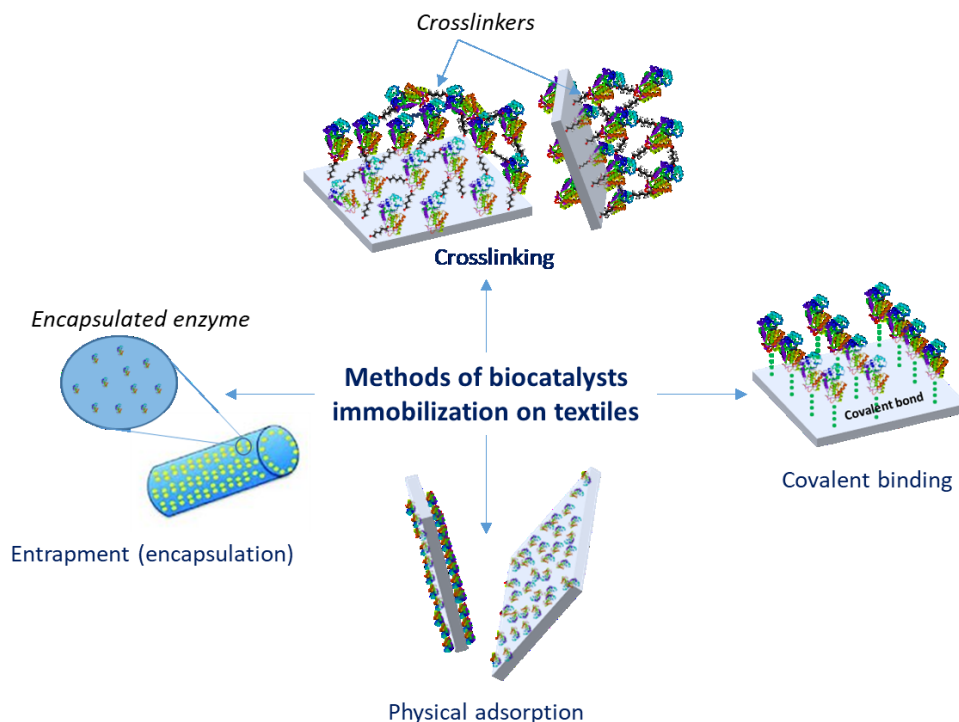
Figure 2. 9: Common methods of biocatalysts immobilization on textiles (adopted from publication I).

Entrapment (encapsulation): Encapsulation of enzymes into textile materials refers to the mechanism by which either textile material itself or semi-permeable membrane physically or chemically embed enzymes within textile structures [116]. The encapsulation techniques permit several enzymes to be simultaneously immobilized, and the conditions are milder compared to other enzyme-immobilizing methods. The encapsulated immobilized enzyme does not move through the membrane pore when the substrates are free to pass. Therefore, the membrane pores must be less than the enzyme molecules and larger than those of the molecules in the substrate. This fundamental requirement of this process made it more difficult to be regarded as a carrier material for common textile fibers. Due to that, the majority of enzyme encapsulation attempts in textiles have been made on nanofibrous textiles, which retain a predetermined surface and pores size. Nevertheless, there are some limitations of this process as well, such as the diffusion limitations between enzymes and substrates, which emerged as an uncompromising issue compared to other methods. [117].

Innovations in biocatalysts immobilization on textiles: A variety of innovative techniques for immobilizing biocatalysts on textile includes digital printing (ink-jet or valve-jet), electrostatic binding (layer-by-layer deposition, electrochemical doping/polymerization), etc. have been developed. Houshyar *et al.* (2014) [118] reported the immobilization of oxidoreductase enzymes on flexible textiles by a new generation resource-efficient method in personalized outlines (digital inkjet printing). Biswas *et al.* (2021) [119] investigated the efficacy of various factors in the immobilization of enzymes on synthetic polyethylene terephthalate textile surfaces through inkjet technology. In addition to printing, a new approach to improving the loading and stability of immobilized enzymes on the textile surface through electrostatic bindings on textile surfaces has also been introduced as innovative methods for biocatalysts immobilization on textiles. Karimpil *et al.* (2012) [120] reported the lipase immobilization on a cotton cloth treated with polyethylenimine by layer by layer self-assembly technique. They have found high loading of textile immobilized enzymes, although the apparent activity of the immobilized enzyme may reduce

after a limit of layers. Recently, Zhang *et al.* (2020) [121] found that layer by layer assembles controllable enzyme layers through electrostatic loading providing a high density of immobilized enzyme on textile surface.

2.2.3.2. Influencing factors of biocatalysts immobilization on textiles

The success of immobilization of biocatalysts on textiles can be influenced by various factors. Since the surface of the textile is not entirely neutral, therefore it interacts with the physicochemical properties of the immobilized enzyme and hence influencing the performance of the biocatalysts. There are a number of key factors that might affect the performance of biocatalysts immobilization on textiles are as follow;

Structure of textile support matrix: The features of the textile structure are crucial in immobilizing enzymes. The immobilization mechanism will be affected by the structure selected since the properties of both the enzyme and the support material can determine the properties of the assisted enzyme preparation. Fiber type, fabric formation structure, surface functional groups of the textile support will determine the protein affinity, mechanical flexibility, rigidity, recovery viability, non-toxicity, and biodegradability of textile material, which is essential for the success of biocatalysts immobilization on textiles [75].

Nature of crosslinkers: The most commonly used technique for immobilizing enzymes was the direct anchoring of enzymes at the textile fiber surface. Nevertheless, several reports indicate that raw surface fabrics do not provide the best surface condition for the immobilization of enzymes, particularly in the case of compatibility in terms of surface charge on the specific type of fibers used. In some reports, the interaction of the enzyme with the raw surface could lead to the enzyme unfolding once after immobilization [122]. To solve the problem, crosslinking of enzyme on the textile surface have been proposed where the interaction of the enzyme with the support material is restricted which improves the stability of the enzyme. An appropriate set of crosslinkers based on a particular enzyme and supporting matrix is a prerequisite for a stable, robust bio-catalytic system with higher loading of active enzymes.

Extend of enzyme loading: Bio-catalytic activity and output of enzyme-immobilized textiles are affected by the amount of active enzymes loaded on the textile surface. Most research on this fresh domain focused on the research for improving the loading efficiency of enzyme on the textile support matrix, which echoes the importance of this factor [123-125]. Through various surface modifications of textile surface, the loading was increased which is still not well matured. However, the excess loading of enzymes on textile surfaces can lead to negative impacts, which can result in enzyme structure deformation, compression, and blocking the solvation and fast accessibility of the active site of the enzyme by substrates [126]. The imbalance between the diffusion rate and the immobilization rate can categorize the limit of enzyme loading on a support matrix.

Multipoint attachments on the textile surface: Enzymes that are immobilized may be connected by one and several points to the surface of textiles (see Figure 2.10). The covalent binding method of enzyme immobilization makes this form of phenomenon more apparent. Multipoint enzyme attachments to the textile supports may increase the enzyme stability during the wash and successive use [75]. Since the formation of multiple linkages between enzyme and surface can potentially result in enzyme structure distortion if the linkages are not well aligned, multipoint attachments on textile surfaces are relatively difficult to achieve. The method therefore requires the modification of the textile surface into favorable conditions while preserving optimal reaction conditions [127]. A limitation of this strategy is the need to maintain protein dynamics and large-scale protein motions that are essential in many enzymes for substrate binding, product release, and chemical catalysis.

Enzyme orientation on the textile surface: The three-dimensional structure and orientation of immobilized enzymes are critical for ensuring high enzyme stability and activity. Since the orientation of the enzymes cannot be actively controlled by the immobilization methods, this might result in unexpected but unavoidable burying, which further causes the inaccessibility of active site of the immobilized enzymes [75]. Therefore, the orientation of enzyme on textile fiber surface after being immobilized is an important factor that influences the performance of the biocatalysts immobilized textile. Proper orientation of enzyme on the textile surface will provide a number of benefits, namely; activity of all immobilized enzyme, improved enzyme-substrate interaction, reduce the effect

of surrounding stimuli in the activity of the enzyme, limit use of essential functional groups during covalent or multipoint attachment and finally, the active site of enzyme will be less exposed to deformation or rigidification.
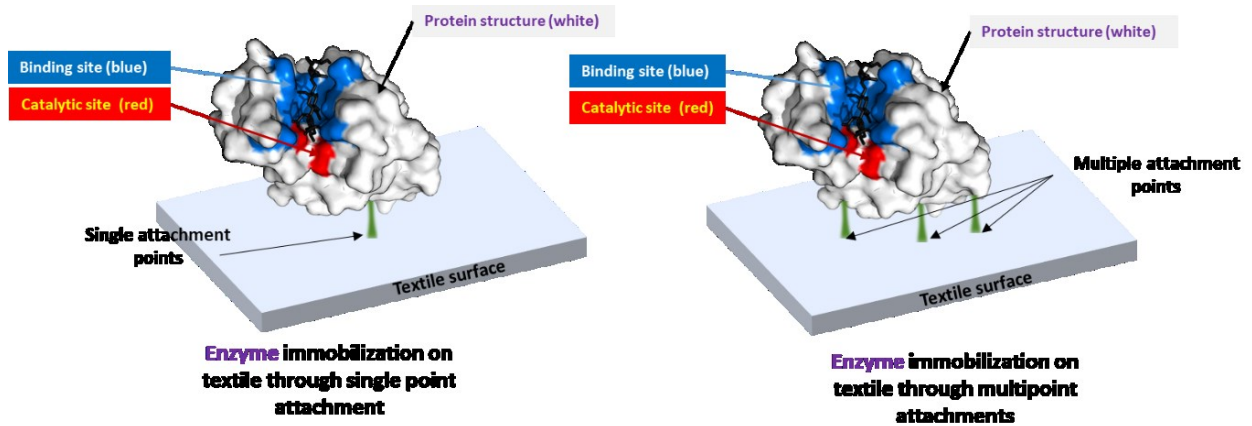
Figure 2. 10: Schematic illustration of single and multipoint attachment of enzyme on support matrix during immobilization (adopted from publication I).

Mass transfer and diffusion limitations: The effect of mass transfer and diffusion of substrate and product on the activity of immobilized enzymes is critical for catalytic activities [128]. Immobilization of enzymes on textiles typically raises resistance to mass transfer. For determining the kinetics of biocatalysts immobilized textile, internal mass transfer and diffusion limitation of the enzyme, substrates, and products need to be taken into consideration before designing a system using biocatalyst-immobilized textile. Optimal enzyme loading on the textile support matrix during immobilization was not possible due to poor diffusion, which prevented enzyme molecules from reaching many areas of the textile (correlated differences in flow on the intra- yarn and inter-yarn pores), see Figure 2.11.
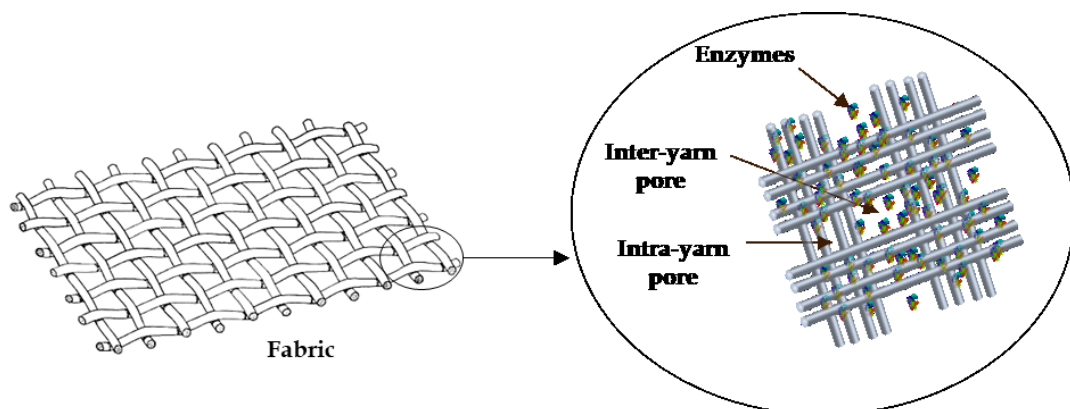
Figure 2. 11: Structure of fabric with intra-yarn & inter-yarn pores (adopted from Nierstrasz and Warmorskerken, [128]).

However, when it comes to the factors that influence the behavior of immobilized biocatalysts: pH, temperature, and substrate concentration are all important to remember. The behavior of an immobilized enzyme can greatly be influenced by the pH of the reaction medium, as the interactions between amino acids change as the pH

24

changes. The change in the interactions among amino acids may alter the structure and shape of the enzyme, which later on fails to bind with the specific substrates, meaning deactivation of the enzyme [129]. In most catalytic reactions, the temperature usually accelerates the rate of reaction, but in biocatalysis using immobilized enzyme, the temperature may increase the rate of reaction for a certain limit, but after the limit its offers the opposite phenomenon. The concentration of substrate also influences the rate of reaction, until all the enzymes in the reaction system are bind with corresponding substrates, the reaction rate increases with the increased substrate concentration. After that, a plateau effect occurs, where the rate of the catalytic reaction is no longer affected by the addition of substrate. It should be noted that an excessive amount of substrate would cause an enzyme's active site to become blocked. For enzymatic kinetics, most enzymes use the Michaelis-Menten model [34].

2.2.3.3. Applications biocatalysts immobilized textiles

Immobilized biocatalysts on textiles have a number of advantages over free biocatalysts, including reusability, separation ease, and higher stabilities (pH, thermal, storage) [130, 131]. As summarized in Table 2.1, biocatalyst immobilized textile (immobilized enzymes on textile support matrix) is useful in various applications ranging from food preparation and preservation, pharmaceuticals and medical devices, fine chemical synthesis, biodegradation, bioremediation, wastewater treatment application, and so on . Enzymes that have been immobilized can be reused and processed at a lower cost. In comparison to other similar systems, they are more cost-effective, environmentally friendly, and simple to use.

Table 2. 1: A brief overview on the application of biocatalyst immobilized textiles (adopted from publication I).

Biocatalysts immobilized textile	Most targeted Enzyme class	Immobilization method	The primary focus of the application
Nanofibrous textile	+ Oxidoreductase	+ Encapsulation> + Crosslinking > + Physical adsorption	+ Biodegradation, bioremediation and environmental application. + Oxyfunctionalization of organic substrates. + Diagnostic and biosensors.
Woven textile	+ Hydrolases + Oxidoreductase	+ Covalent binding > + Crosslinking	+ Pharmaceuticals and Fine Chemical synthesis. + Food preparation and preservation. + Biodegradation, bioremediation, and environmental application.
Non-woven textile	+ Oxidoreductase + Hydrolases	+ Physical adsorption> + Crosslinking > + Covalent binding	+ Biodegradation, bioremediation and environmental application. + Oxyfunctionalization of organic substrates. + Pharmaceuticals & fine chemical synthesis. + Food preparation and preservation.
Knitted textile	+ Oxidoreductase + Hydrolases	+ Covalent binding > + Crosslinking > + Physical adsorption	+ Food preparation and preservation + Pharmaceuticals and medical devices. + Fine Chemical synthesis + Biodegradation, bioremediation, and environmental application.

> = more frequent than.

2.2.4. Challenges of inorganic catalyst and biocatalyst immobilization on textiles

Catalytic technologies are becoming increasingly important in the fields of sustainability and green technology. In mild conditions, catalysts readily catalyze different complex reactions. As discussed previously, recyclability and reusability are part of the immobilization process, ensuring high stability and improving process control. The process minimizes the use of chemical substances, energy, and time, which reduces costs.

Despite all the advantages of organic and inorganic catalyst immobilization, the catalytic immobilization on textiles faces great challenges until it becomes more and more scalable. Sometimes a complete or partial loss of catalytic activity in immobilized catalysts may occur. Here are a few examples of the challenges.

(a) Waste of catalysts during immobilization was reported in almost all the studies, since not all catalysts are adsorbed on the textile, and some cease to be active after being adsorbed.
(b) Catalyst leaching to media: while catalysts are bound to textile fiber surfaces through various bonds, reports show that a large quantity of catalysts is leached away during use. Excessive leaching may require the removal of the catalyst from the products, which would defeat the purpose of catalyst immobilization.
(c) Blocking of catalyst active sites: an inconvenient confrontation of catalysts on the textile surface may cause disorientation of the catalysts, which is undesirable for commercial applications.
(d) Interaction of the textile surface with immobilized catalysts: the surface of the textile is not inherently neutral and is likely to interact with the immobilized catalyst and change its physicochemical properties, leading to a reduced affinity for the substrates.
(e) Harsh conditions during immobilization: usually, immobilization requires specific conditions, such as a specific pH and temperature. Although most approaches have considered the ranges of optimum conditions for catalysts, unintentional changes can lead to the loss of active sites and activity of the catalyst as a whole.
(f) Storage: catalyst activity decreases over time even under optimal conditions, which limits the possibilities for large-scale production and long-term use of catalyst-immobilized textiles.

There are other challenges, involving textile structure, modifications of the textile surface, integration of favorable surface functional groups, and so on. These challenges have been addressed in the literature, and considerable improvements have been made, but more remains to be done.

2.3. State of art in wastewater treatment

Water is essential for life and an important element of the world's ecosystem. Even though water covers 71% of the Earth's surface, just 1% is suitable for human use. Due to the rapid industrialization different contaminants such as heavy metal ions, pathogenic bacteria, other organic toxicants are released into water streams which pose serious threats to biodiversity as well as human health due to their high toxicity, chemical stability, bioaccumulation, and resistance to conventional treatment methods [132]. Among the variety of water pollutants, colorants, the residue of personal care products, pesticides, pharmaceuticals/antibiotics, and bacterial pathogens poses serious risks to the aquatic environment for human health and biodiversity [9].

Colorants that are widely using in industrial, printing, food, cosmetic and clinical purposes are highly toxic in nature [133]. In a release to the water, they increase biochemical and chemical oxygen demand (BOD and COD), impair photosynthesis, inhibit plant growth, enter the food chain, provide recalcitrance and bioaccumulation, and may promote mutagenicity and carcinogenicity. Along with colorants, the complex chemical structure of pharmaceuticals made it very difficult to remove them from wastewater, even with the most advanced treatment technologies. Painkillers, vaccines, antidiabetics, beta-blockers, condoms, lipid inhibitors, hormones, and impotence medications are among the nearly 3000 substances used as medicinal ingredients. Phenol is widely

used in a variety of sectors, including petroleum refineries, gas and coke ovens, pharmaceuticals, explosives, phenol-formaldehyde resin production, and plastic and varnish production. Because of its toxicity to living things, phenol-containing wastewater must be properly treated before being released into the environment. For industrial effluents released into inland surface waters, the allowable limit of phenol is 1.0 mg.L.$^{-1}$ (IS: 2490-1974), and for discharge into municipal sewers, it is 5.0 mg.L.$^{-1}$ (IS: 3306-1974).

Biocides and pesticides are also been found in water streams. They are mostly of complex chemicals with aromatic structures and multiple branches. The growth of bacterial tolerance after the introduction of biocides and pesticides into the atmosphere is one of the main concerns [134, 135] along with the negative impact on plant biodegradation, which disrupts the primary food chain in marine environments [136]. Personal care products are the newest but most alarming pollutants in wastewater. Breast cancer, diabetes, autism, fertility disorders, and other health problems have also been related to elevated exposure to toxic residues of personal care products [137-139]. Last but not least, contamination of water supply by pathogens (bacteria, protozoa, and viruses) has gained attention to local and international audiences. The main risk factor correlated with wastewater is infection by pathogenic microorganisms, which is also a serious issue in terms of wastewater reuse.

These pollutants are typically termed emerging contaminants (ECs) and are resistant to conventional physical, chemical, and biological wastewater treatments such as coagulation, flocculation, adsorption, filtration, aerobic/anaerobic biological system, or combination of a physical and biological system [10, 11]. Different new generation treatment methods based on catalytic systems as well as advanced oxidation processes (AOPs) have been introduced as an expedient process for the removal of pollutants in water systems [140]. AOPs are technologies defined by the generation of hydroxyl radicals (•OH), [highly reactive (E_0 = 2.8 V) and nonselective species] to remove pollutants present in a medium (water, air, and soil) [12]. The •OH is the second strongest oxidant preceded by the fluorine, which attacks the most organic molecules with rate constants of 10^6–10^9 L.mol^{-1}.s^{-1} [141]. Glaze *et al.* (1987) [142] first reported the generation of •OH in sufficient quantity to affect water pollutants. Since then, various researchers have contributed to the classification and development of AOPs. Over time, several new methods have been included to produce •OH and other reactive oxygen species (ROS) such as superoxide anion radical, hydrogen peroxide (H_2O_2), and singlet oxygen. AOPs are classified in a variety of types based on the method of •OH generation -namely; ozonation (O_3, O_3/ultraviolet (UV), O_3/H_2O_2, O_3/H_2O_2/UV), photolysis of H_2O_2 (photochemistry assisted, UV/H_2O_2), semiconductors (TiO_2/UV), ultrasound, Fenton reaction (Fe^{2+}/H_2O_2, Fe^{2+}/H_2O_2/UV, Fe^{3+}/H_2O_2/UV), electrochemistry (anodic oxidation), supercritical water oxidation and electron beams [143, 144]. AOPs can also be classified as homogeneous and heterogeneous according to the reactive phase. Expecting a higher performance in pollutants removal, the combination of AOPs systems (such as UV radiation with ozone) has also been suggested by many researchers [145, 146].

2.3.1. Catalytic systems for wastewater treatment

Advanced efficient technology was needed to replace the conventional flocculation, coagulation, and separation process for the removal of pollutants from wastewater. A number of new technologies based on catalytic and non-catalytic systems have been introduced for the sustainable removal of hazardous and complex pollutants from water. These technologies include photocatalytic degradation using various types of photocatalyst [147], supercritical water oxidation above the mixture's thermodynamic critical point [148], the Fenton and Fenton-like processes using various sources of iron ions and hydrogen peroxides [149], ozonation by infusion of ozone into water [150], microwave degradation using electromagnetic irradiation [151], sonochemical degradation based on an acoustic cavitation process [152], wet air oxidation [153], hydrodehalogenation [154], catalytic reduction [155], and enzymatic systems [156, 157]. In particular, Fenton and Fenton-like processes, catalytic reduction, and enzymatic systems are considered the most promising for tackling a wide range of pollutants in an eco-friendly and resource-efficient way.

2.3.1.1. Enzymatic systems

Enzymatic systems are an emerging and sustainable wastewater treatment method involving the transformation or degradation of wastewater contaminants into nonhazardous or less hazardous substances using enzymes. Compared with traditional Physico-chemical methods, an enzymatic system is safer, less disruptive, and more cost-effective [158]. The most common class of enzymes used in enzymatic systems for wastewater treatment or bioremediation is oxidoreductase (EC 1). Many studies report the sustainable removal of colorants [159], pharmaceuticals [160], phenolic endocrine-disrupting chemicals [161], and pathogenic toxins [162] with common oxidoreductases such as laccase, glucose oxidase, horseradish peroxidases, etc. The electron transfer oxidation can be considered the main mechanism of oxidative enzyme transformation or degradation of pollutants. Generally, the efficiency of the process is related to the oxidative-reductive potential of the compounds compared to that of the enzyme. Some compounds, such as most phenolic compounds, more easily accept to transfer a single electron to the enzyme. However, compounds with strong electron-withdrawing functional groups, such as non-phenolic compounds with amide, carboxyl, halogen, or nitro groups, have a higher oxidative-reductive potential than the enzyme [163]. In these cases, mediators can help transfer electrons between the enzyme and the compounds, enhancing the degradation efficiency. Nevertheless, regardless of the class or type of enzyme used, enzymatic systems are limited by factors such as mass transfer (low contaminant bio-availability), aeration, the nutrient level at the contaminant sites, and problems with the thermal conditions [130, 164]. All of these challenges should be addressed on a case-by-case basis to reach the maximum pollutant removal efficiency.

2.3.1.2. Fenton and Fenton-like systems

The Fenton reaction, defined as the mixing of H_2O_2 and ferrous iron (Fe^{2+}) to produce $^\bullet OH$, is currently considered one of the most effective and reliable methods for removing pollutants from water (see Reactions 2.1–2.3). H. J. Fenton first introduced the Fenton reaction in 1894, reporting the oxidation of tartaric acid by hydrogen peroxide in the presence of ferrous ions [165]. However, only in the 1960s was the Fenton reaction first applied to the degradation of complex pollutants [166, 167]. Due to the faster reaction rate, lower usage of chemicals, easy generation of hydroxyl radicals, and overall cost-effectiveness, this method of AOPs were studied extensively, leading to various improvements [168]. There have been various modifications to the Fenton reaction method for pollutant removal [169], including electro-Fenton (electrochemical), photo-Fenton (photochemical), sono-Fenton (sonochemical), and bio-Fenton (biochemical) reactions. These new methods have enabled a wide range of reactors based on the Fenton reaction. In all methods, the primary focus is on *in-situ* generation of either H_2O_2 or $^\bullet OH$. There have also been attempts to combine two Fenton processes (e.g., photo-electro-Fenton, bio-electro-Fenton, etc.) for additional pollutant removal efficiency [169].

$$Fe^{2+} + H_2O_2 \quad \rightarrow \quad Fe^{3+} + {}^\bullet HO + OH- \qquad (2.1)$$

$$Fe^{3+} + H_2O_2 \quad \rightarrow \quad Fe^{2+} + {}^\bullet HOO + H+ \qquad (2.2)$$

$$2H_2O_2 \quad \rightarrow \quad {}^\bullet HO + {}^\bullet HOO + H_2O \qquad (2.3)$$
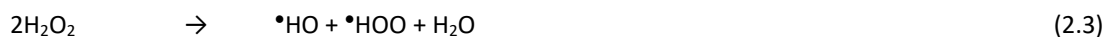
As reported in various literature, specific conditions must be met to achieve optimal efficiency in the removal of pollutants by the Fenton reaction [170]. Fenton reactions are highly pH-sensitive due to the iron chemistry. The ferric salts used in the Fenton reaction as precursors of Fe^{2+} precipitate as hydroxides at pH ≤ 4. Therefore, the Fenton reaction must be carried out in acidic conditions (pH < 4). A higher temperature during the reaction favors the generation of ROS; however, it may also cause H_2O_2 to dissociate into O_2 and H_2O. The most important factor of all may be the concentration of the reagents because it affects not only the overall efficiency of the process but also its cost. Since the reaction of H_2O_2 with Fe^{3+} is significantly slower than that with Fe^{2+}, the catalyst regeneration phase is considered the most critical stage of the process, as it reduces the radical production rate and could deplete the iron available for the reaction. Despite its many advantages, the Fenton reaction has some serious

drawbacks: the need for acidic conditions, the generation of iron sludge, the need for after-treatment to remove reagents, and problems related to the handling and storage of dangerous chemicals such as H_2O_2 [171, 172].

The Fenton/bio-Fenton reaction can be either homogeneous or heterogeneous. The homogeneous Fenton reaction takes place in the same phase as the reactants (such as the dissolved Fe^{2+} precursor and H_2O_2). The homogeneous Fenton reaction ensures high selectivity, good diffusivity, and well-defined active sites on the catalyst, with a well-understood reaction mechanism. However, the reagents can only be used once, and the reaction releases a large amount of iron into the environment and generates a huge amount of sludge in the post-treatment process. These disadvantages can be mitigated through a heterogeneous process. Heterogeneous catalysts can be defined as consisting, in most cases, of catalytically active material on the surface of the solid support (normally a porous solid to increase reaction rate). Therefore, the reactants are not in the same phase (e.g., the Fe^{2+} precursor in the solid phase with H_2O_2 in the aqueous phase). Although this is highly application-dependent, heterogeneous systems are usually considered superior to homogeneous systems. In a typical heterogeneous Fenton reaction, the physio-chemical changes to the reagents and the generation of $^\bullet OH$ take place at the active sites on the surface of the heterogeneous catalyst. At the end of the reaction, both the residue of the second reagent and the products leave the active sites and leaving them available for a new set of reagent molecules to repeat the process. The use of metallic iron or zerovalent iron particles (Fe^0) instead of iron salts is a popular option for heterogeneous Fenton catalysts.

In the mid-1990s, researchers started to develop heterogeneous catalysts for the Fenton reaction, using solid iron to degrade a wide range of organics at a lower operational cost [173-175]. Fe^0 is stable to oxidation at higher pH than other iron salts. Xu *et al.* [176] reported that a Fe^0-based heterogeneous Fenton-like system provides better degradability of phenolic compounds, even at a neutral pH. Several other reports suggest that the use of solid metal iron or Fe^0 requires less iron, reduces the precipitation of oxides, increases the rate of the reaction, and generates nontoxic final products [177-179]. This process also accelerates the recycling of Fe^{3+} into Fe^{2+} through the so-called pseudo-catalytic zerovalent iron (Fe^0/Fe^{2+}) system [180, 181]. Nevertheless, to the best of our knowledge, Fe^0 had never been used in a bio-Fenton system.

Although Fe^0 enhances the system reactivity, the treatment does use iron powder, which would still need to be separated in a post-treatment process. Furthermore, while Fe^0 acts as a catalyst and is reusable if recovered, the separation/recovery of Fe^0 from treated water requires additional time and energy, which is costly and counterproductive. The immobilization of Fe^0 in a solid support material seems like a promising alternative, allowing Fe^0 to be used under neutral pH conditions with satisfactory results while avoiding neutralization and separation [182]. It has also been reported that immobilizing Fe^0 on solid supports further improves the stability of the Fe^0 particles, allowing easy recovery, reusability, and other advantages of immobilized catalysts [183, 184].

The bio-Fenton system

The bio-Fenton system is considered a green and sustainable alternative due to lower energy consumption and the use of bio-sourced materials. The bio-Fenton system involves the *in-situ* generation of H_2O_2 by using redox enzymes (as catalysts) and the subsequent formation of $^\bullet OH$ in the presence of Fe^{2+} (see Reactions 2.4-2.5). The enzymes used in the bio-Fenton system are natural catalysts that perform under milder conditions to oxidize specific substrates without being consumed in the process. The bio-Fenton system was initially proposed by Chun-Hua *et al.* (2010) [185] and was later used by Afzal *et al.* (2012) [17] to remove malachite green dye from water. In a typical bio-Fenton system, the redox enzymes (either glucose oxidase or alcohol oxidase) catalyze a reaction producing H_2O_2 as the main product or byproduct, supplying it as Fenton's reagent. A number of reports have shown the potential of the bio-Fenton system to remove toxic contaminants (dyes, chlorinated organic contaminants) from water [13-16]. Although the bio-Fenton system was proposed as a sustainable method, the use of expensive enzymes and their subsequent denaturation require additional energy, making the process expensive and hindering its large-scale application.

$$C_6H_{12}O_6 + O_2 \xrightarrow{\text{GOx}} C_6H_{12}O_7 + H_2O_2 \tag{2.4}$$

$$H_2O_2 + Fe^{2+} \rightarrow Fe^{3+} + {}^\bullet HO + OH^- \tag{2.5}$$
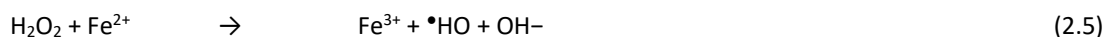
Furthermore, the denaturation process (also termed as catalysts separation) after the cycle use is counter-productive, since active enzymes that could have been reused are lost. This is a common drawback not only of the enzymatic bio-Fenton system, but also of classical enzymatic processes in other domains (food, cosmetics, and pharmaceuticals industries) [186]. Many studies in various fields report that binding or immobilizing the enzymes to a solid material facilitates enzyme recovery/separation and ensures their continuous reusability [187-189]. Enzyme immobilization can be defined as the confinement of enzyme molecules on or inside a support matrix, physically or chemically or both while allowing the enzyme to retain its full activity or most of its activity [190]. Immobilization also ensures high enzyme stability, enhances reactivity, increases the operational half-life, and offers better reaction control. The immobilization of enzymes is considered a key modern industrial biotechnology, which has gradually helped replace the traditional trial-and-error approach with rational design [191]. Although few studies address the necessity of enzyme immobilization for the bio-Fenton system [18, 34], all studied so far used free iron salt as a source of iron ions to catalyze a bio-Fenton reaction. No study was found where both enzyme and iron were immobilized for such application.

Influencing factors of Fenton-like systems

The degradation of organic pollutants by the conventional Fenton process is very sensitive to the wastewater pH. At low pH values, the scavenging effect of radical ${}^\bullet OH$ by H+ becomes stronger, resulting in a decrease in oxidation capacity of the Fenton process. At high pH values, the hydrolysis and precipitation of Fe^{3+} in the solution become stronger, resulting in a decrease in catalytic capacity of Fe^{3+}. Therefore, organic pollutants in wastewater can not be treated effectively by the conventional Fenton process at both low and high pH. In other words, there is always an optimum pH range for the degradation of organic pollutants.

The different Fenton optimization processes are found to follow a similar oxidation mechanism: Fe^{2+} catalyzes the decomposition of H_2O_2 to produce the highly oxidative radical ${}^\bullet OH$ which can degrade most stubborn organic pollutants. Therefore, Fe^{2+} as a catalyst is a highly important parameter affecting the degradation efficiency of organic pollutants. Usually, the degradation efficiency of organic pollutants increases with the increase of Fe^{2+} concentration. However, Fe^{2+} can not be added without any limitation. The excessive Fe^{2+} not only increases the operational costs and iron sludge production but also enhances the scavenging effect of radical ${}^\bullet OH$ by Fe^{2+}, which has a negative effect on the degradation of organic pollutants. In order to obtain the maximum removal of organic pollutants, the study on the optimum Fe^{2+} concentration can be a complicated but significant issue, which can be determined experimentally.

According to the reaction of Fe^{2+} and H_2O_2 for radical ${}^\bullet OH$ generation, the effect of H_2O_2 concentration on the degradation of organic pollutants by various Fenton optimization processes is similar to that of Fe^{2+} concentration. Therefore, H_2O_2 is also a highly important parameter affecting the degradation efficiency of organic pollutants. Usually, the degradation efficiency of organic pollutants increases with the increase of H_2O_2 concentration. However, H_2O_2 can not be added without any limitation. The excessive H_2O_2 not only increases the operational costs but also enhances the scavenging effect of radical ${}^\bullet OH$ by H_2O_2, which has a negative effect on the degradation of organic pollutants. In order to obtain the maximum removal of organic pollutants, the optimal H_2O_2 concentration should be examined. The stubborn pollutants can be degraded by highly oxidative radical ${}^\bullet OH$ formed from the reaction of H_2O_2 with Fe^{2+}. Researches show that a significant difference in degradation of wastewater with different organic loads is observed. Therefore, the concentration of organic pollutants is an important parameter affecting the degradation efficiency of organic pollutants. Most of the Fenton optimization processes can obtain high degradation efficiency with low concentration organic pollutants. Besides, the increase in initial organic pollutants concentration always leads to lower degradation and long degradation time.

2.3.1.3. Catalytic reduction systems

Catalytic reduction refers to heterogeneously catalyzed reduction, which involves the use of a solid catalyst and a reducing agent to degrade the pollutants from water through electron-transfer reactions [192]. Various metallic nanoparticles, including silver, nickel, gold, copper, and cobalt, have been used for the catalytic breakdown of various pollutants in water including colorants [193], phenols [194, 195], pharmaceuticals [196], pathogenic bacteria [82] and so on [197, 198] owing to their remarkable surface properties [199]. Essentially, the mechanism of a catalytic reduction system can be described as catalysts collecting electrons from nucleophilic sources (the reducing agents) and delivering them to electrophilic pollutants, which changes the structure of the pollutants and degrades them.

Recent studies show that most of these metal particles were immobilized on solid supports before being used in the catalytic reduction of pollutants. Immobilization of catalysts ensures easy recovery and better stability of the catalysts. Catalytic reduction is an emerging new and promising water treatment strategy, which has been extensively studied at the bench scale. Its trials in the field have also yielded exciting results on both industrial wastewater and groundwater. It exhibits good activity and is more selective than conventional technology, and yields products that are either non-toxic or substantially less toxic and more readily biodegradable than those derived by other methods. This method has also been criticized for its stringent condition requirements and toxic reducing agents; although its catalytic activity is better than that of other methods. A number of factors influence the performance of a catalytic reduction system, including the stability of the catalysts in the reaction system. Most monometallic catalysts are prone to oxidation in humid environments, which greatly reduces the speed and efficiency of the system. The concentration of catalysts, reducing agents, and pollutants are interrelated; a rapid increase in one would have little effect on the rate of the removal reaction, although a gradual increase up to a certain point has been reported by Gupta *et al.* (2014) [200]. However, the temperature of the system positively influences the rate of the removal reaction in the catalytic system. The reaction rate constants increase with increasing temperature for the catalytic reduction processes [200, 201]. Catalytic reduction systems are pH-sensitive. As reported by Liu *et al.* (2019) [202], no reactions occurred in an alkaline medium, while the catalytic reduction performance was significantly higher under acidic conditions.

2.3.1.4. Hybrid catalytic systems

By combining the strengths of two different catalytic systems, a new system can be developed. This new system is known as a hybrid catalytic system, and it can use a combination of biocatalysis with photocatalysis [203]; Fenton with biocatalysis [204]; Fenton with photocatalysis [205]; and many more. Abdi *et al.* (2017) [204] designed a photo-biocatalyst reactor coupled with the Fenton process for the decolorization of malachite green dye from water. Shoabargh *et al.* (2014) [203] described a hybrid photocatalytic and enzymatic process using glucose oxidase immobilized on TiO$_2$/polyurethane and reported that it was very efficient for the removal of a dye. Apart from hybrid catalytic systems, a number of approaches have been described where a catalytic system was supplemented with a non-catalytic system; examples include a photocatalysis-membrane distillation system [206], a photocatalysis-ultrafiltration process [207], and others [208]. Hybrid catalytic systems often offer better catalytic performance, but require complex catalyst preparation processes. The mechanism of the catalytic reaction in hybrid systems is also challenging to postulate. Therefore, despite the potential of hybrid systems to increase reaction selectivity, there are significant challenges to the rational design of such systems, which must be addressed before large-scale implementation in wastewater treatment.

2.3.2. Application of inorganic catalyst immobilized textiles in wastewater treatment

An ideal wastewater treatment process should be able to mineralize all the toxic species present in the stream without leaving behind any hazardous residues and should also be cost-effective. Catalytic removal of pollutants through inorganic catalysts appeared as a promising system that addresses a wide range of pollutants (see Table 2.2) including colorants, heavy metals, micropollutants, phenol endocrine-disrupting chemicals, pharmaceuticals, functional materials, and personal care products as well as pathogenic toxins.

In addition to being toxic, colorants in wastewater are carcinogenic, mutagenic, or teratogenic to various organisms. Removal of colorants from water can be done by inorganic catalysts (such as titanium, copper, silver, iron, nickel) through various approaches includes; photocatalysis, Fenton-like system, chemisorption, or catalytic reduction system [209, 210]. A numbers of example was found in the literature where inorganic catalyst (either free or mostly immobilized on ceramic material, polymeric membranes or metal complex] has been used for removal of colorants from wastewater, however, few studies were found related to immobilized inorganic catalysts on textiles. Liu *et al.* (2009) [211] reported the removal of malachite green dye through Fe(III)-loaded collagen fiber in a photocatalytic system. Similar studies with other inorganic catalysts (such as titanium, copper) for removal of colorants have been reported elsewhere [212]. Zhang *et al.* (2012) [95] immobilized Fe-doped TiO_2 nanoparticles on polyamide fabric for photocatalytic removal of dyes from water. Although the removal of colorants was addressed briefly, but studies related to heavy metal removal using inorganic catalysts immobilized textiles are even less. Exposure to heavy metals, even at trace level is believed to be a risk for human life. Effective removal of metals from wastewater is a very important and challenging task for environmental engineers. According to Hua *et al.* (2011) [213] nanosized inorganic catalysts, including ferric oxides, manganese oxides, aluminum oxides, titanium oxides, magnesium oxides, and cerium oxides, are promising catalyst for heavy metals removal from water [214]. Xiao *et al.* (2011) [215] reported the copper(II) removal using zero-valent iron - immobilized Electrospun nanofibrous mat.

Table 2. 2: A summary of removal of pollutants from wastewater using inorganic catalysts immobilized textiles.

Pollutant category	Inorganic catalysts	Catalytic system	References
Colorants	Fe-doped TiO_2	Photocatalysis	[95]
	Ag/Cu_2O	Photocatalysis	[105]
	$CuO/BiVO_4$	Photocatalysis	[106]
	Fe particles	Fenton-like	[107-109]
	PAN-Fe complex	Photo-Fenton	[110]
Pathogenic toxins	Modified $Ag/CuFe_2O_4$	Disc diffusion	[111]
	$CuO/BiVO_4$	Disc diffusion	[106]
Phenol	Titanate nanofibers with crystalline ZnS and Ag_2S	Photocatalysis	[216]
	$CuO-Si-N(OH)_2$	Catalytic reduction	[82, 194]
	Fe particles	Fenton/Fenton-like	[217]
Antibiotics	$Cu_2S/Ag_2S/BiVO_4$	Photocatalysis	[218]
	Fe particles	Hybrid	[219]
	Iron trinitro phthalocyanine	Fenton-Like	[220]
	TiO_2 particles	Photocatalysis	[221]
Heavy metals	Fe particles	Chemisorption	[215]

Another serious group of pollutants is emerging micropollutants (EMPs). EMPs can be defined as synthetic or natural compounds released from known and unknown resources that ended up in wastewater at low concentrations. EMPs are not commonly monitored and measured, and therefore they impose adverse effects on human health and aquatic life. Fenton-like, photocatalysis as well catalytic reduction system using inorganic catalysts immobilized textile was used in the removal of micropollutants from water [222, 223]. Inorganic catalysts immobilized textiles have shown the potential to remove phenol endocrine-disrupting chemicals.

Phenolic compounds are priority pollutants with high toxicity even at low concentrations. Barrocas *et al.* (2017) [216] reported removal of phenol from water using novel inorganic catalyst prepared by photoactive titanate nanofibers with crystalline ZnS and Ag_2S nanoparticles in a photocatalytic system. Studies related to the removal of pharmaceuticals, functional materials (UV-blocking/anti-bacterial, fire retardant material), personal care products, and pathogenic toxins reveal that the inorganic catalyst is capable of removal of these pollutants from water through an advanced oxidation process or electron transfer process [224, 225]. There is no shortage of literature on this domain, however, in most cases, it involves the use of free inorganic catalysts or complex support material for catalysts immobilization out of reports used of inorganic catalysts immobilized textiles, nanofibrous textiles were mostly used followed by polymeric membranes.

2.3.3. Application of biocatalyst immobilized textiles in wastewater treatment

Wastewater treatment is of utmost importance as industries are increasing at a fast pace and so their effluents in the environment. Bioremediation using enzymes appears as a promising technique; moreover, recent studies indicate that the use of enzymes for rapid degradation and removal of various toxic pollutants, such as dyes, pharmaceutical, and phenolic pollutants is an alternative to the traditional methods (see Table 2.3).

Colorants removal: Dyes or colorants are being extensively used in many industries such as textile, plastic, tannery, paper, pulp, electroplating, petroleum products, pharmaceutical, and cosmetic industries [109, 226]. Many of these dyes that we are using on daily basis and releasing into surface water are made of complex aromatic compounds and often pose serious life-threatening consequences to living organisms if they came in contact [227]. They are resistant to conventional physical, chemical, and biological wastewater treatments such as coagulation, flocculation, adsorption, filtration, aerobic/anaerobic biological system, or a combination of a physical and biological system [10, 11]. Therefore, special attention has been given to this avenue to explore new generation treatment methods. A number of reports have shown the potential of the heterogeneous enzymatic system using immobilized enzymes as green and resource-efficient process in the removal of toxic dyes and other contaminants from water [13-16].

Pharmaceuticals removal: Pharmaceuticals are among the group of chemicals that are continually released to nature which ends in wastewater. The chemicals are complex in nature and pose serious concern for both aquatic and human life. It is highly important to remove pharmaceutical residues from the wastewater. Removal of pharmaceuticals from wastewater by enzymes is being explored by many researchers, namely a few- Taheran *et al.* (2017) [228] used covalently immobilized *laccase* onto Electrospun nanofibrous textile. They have reported the mineralization of commonly available pharmaceuticals (such as chlortetracycline, carbamazepine, and diclofenac) in wastewater. Results from their study demonstrated a successful 72.7%, 63.3%, and 48.6% degradation efficiency for chlortetracycline, carbamazepine, and diclofenac, respectively in 8h of reaction. The nonlinear fitting results demonstrated that the kinetics of paracetamol removal followed the first-order reaction. Given an optimal condition during the batch removal reaction, resultant biocatalysts immobilized textile is capable of removing 90% of both pharmaceuticals (having concentration as high as 1 mg.L^{-1}).

Phenolic endocrine-disrupting chemicals removal: Phenolic endocrine-disrupting chemicals (PEDCs) have received extensive attention in recent decades in terms of their detections in environmental indicators, potential threats on human life and nature, and prospective removal from soil or water [130]. Several researchers have also reported the application of biocatalysts immobilized textile for the removal of PEDCs from wastewater. Based on the studies of kinetics and mechanisms of pollutant removal they proposed that the high removal efficiency might be attributed to the combined effect of adsorption by fibrous textile and enzymatic catalysis. In another attempt [229], they immobilized *laccase* on polyacrylonitrile/polyvinylidene fluoride nanofibrous textile for removal of 2,4,6-trichlorophenol (95.4% removal after 270 min) having appreciable reusability of during removal of 65.9% of 2,4,6-trichlorophenol for up to 7-cycles. Xu *et al.* (2014) [230] further used *laccase* immobilized on mesoporous nanofibers textile for removal of triclosan. Wang *et al.* (2014) [231] reported the removal of catechol from wastewater through the combined effect of biocatalysis and adsorption using commercial *laccase* immobilized on polyacrylonitrile/montmorillonite/graphene oxide composite nanofibers textile. Nevertheless, through remote

analysis, various other pollutants including pesticides, pathogenic toxins were effectively removed through catalytic system involving biocatalyst-immobilized textiles, which requires further scrutiny in terms of efficiency of pollutant removal as well as required retention time for the treatment.

Table 2. 3: A summary of removal of pollutants from wastewater using biocatalysts immobilized textiles.

Pollutants category	Biocatalysts	References
Pharmaceuticals	Laccase	[228, 232, 233]
	Horseradish peroxidase	[234]
Colorants	Laccase	[235]
	Glucose oxidase	[34]
	Horseradish peroxidase	[236]
Phenolic endocrine-disrupting chemicals	Laccase	[116, 229-231, 237, 238]
	Horseradish peroxidase	[117, 189]
	Tyrosinase	[239]
Pesticides	Organophosphate hydrolase	[76]
Pathogenic toxins	Glucose oxidase	[124]

2.4. State of art in the design and strategies chosen for this thesis

Based on the state of the art, research gaps, and potential research perspectives, design and strategies were chosen for this thesis. The purpose of the study is to immobilize zerovalent iron particles as inorganic catalysts, and the enzyme glucose oxidase as a biocatalyst, on the textile support material. The reason behind choosing these two particular catalysts lies in the intended application in wastewater treatment. Zerovalent iron particles were chosen because they are very efficient in catalyzing heterogeneous Fenton/Fenton-like reactions, as well as in catalytic reduction systems. They are also equally effective as catalysts in heterogeneous bio-Fenton systems (proof of concept for this is one of the main goals of this thesis). On the other hand, glucose oxidase was chosen because of its capacity for *in-situ* generation of hydrogen peroxide, which is an integral reagent in Fenton-like systems. The overall purpose of the study was unfolded into three main objectives;

(a) Immobilization of zerovalent iron particles on polyester nonwoven fabric.
(b) Immobilization of glucose oxidase enzyme on polyester nonwoven fabric.
(c) Implementation of a heterogeneous bio-Fenton system using catalysts immobilized textiles.

The detailed descriptions of materials and methods used in this thesis have provided in chapter 3. All the results from the studies have been presented in Chapter 4, 5, and 6.

2.4.1. Catalysts chosen in this thesis

This section briefly describes the characteristics of zerovalent iron particles (the metal catalyst) and of the glucose oxidase enzyme (the biocatalyst) that will be studied in this thesis.

Inorganic catalyst- Zerovalent iron particles (Fe^0)

Iron is the fourth most common element in the Earth's crust (6.3%) and the most common element by mass in the earth as a whole [240]. It is a common and cost-effective transition metal. Zerovalent iron (Fe^0) particles are sub-micrometer particles of iron metal [241]. Fe^0 can be obtained by both physical and chemical methods. Physical methods include grinding, abrasion, lithography, and so on [242]. The most popular chemical method for obtaining Fe^0 involves the reduction of an iron precursor using sodium borohydride (NaBH$_4$) as a reducing agent, as shown in Reaction 2.6. Another chemical method of obtaining Fe^0 is the reduction of goethite (α-FeOOH) or hematite (α-Fe$_2$O$_3$) at an elevated temperature [243].

$$Fe(H_2O)^{3+}_6 + 3BH_4^- + 3H_2O \quad \rightarrow \quad Fe^0 \downarrow + 3B(OH)_3 + 10.5H_2 \tag{2.6}$$
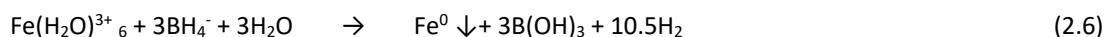
Fe^0 has a negative reductive potential (E_v^0 = −0.44 V) and tends to donate electrons (i.e., to act as a reductant and in turn be oxidized) in the presence of species with more positive reduction potentials [244, 245]. In the presence of oxygen and water, Fe^0 rapidly oxidizes to form free iron ions, as shown in Reactions 2.7–2.8 [246].

$$Fe^0 + 2H_2O \quad \rightarrow \quad Fe^{2+} + H_2 + 2OH^- \tag{2.7}$$

$$2Fe^0 + O_2 + 2H_2O \quad \rightarrow \quad 2Fe^{2+} + 4OH^- \tag{2.8}$$

Fe^0 exhibits typical core-shell structure and ferromagnetic properties, as shown in Figure 2.12. The core consists of mainly zerovalent iron and provides the reducing power for reactions. The shell is largely iron oxides/hydroxides formed in the oxidation of the zerovalent iron. The shell provides sites for chemical complex formation (e.g., chemisorption) [247, 248].
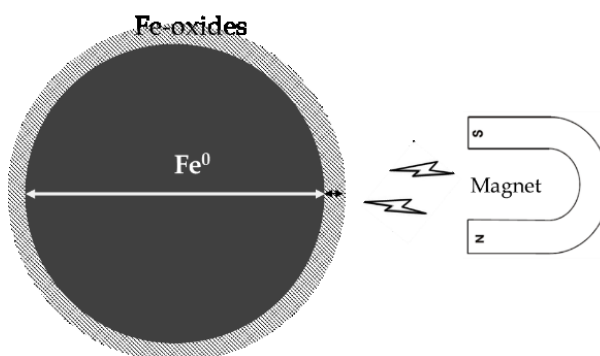
Figure 2. 12: Schematic illustration of typical core-shell structure of zerovalent iron particles and their magnetic attraction.

Fe^0 can produce reactive radicals, such as hydroxyl and sulfate radicals, by efficiently catalyzing common oxidants such as hydrogen peroxide, oxygen, and persulfate [168]. These radicals have a high redox potential and can non-selectively oxidize a wide range of recalcitrant organic pollutants. Taking advantage of the continuous supply of Fe^{2+} during the recycling of ferric ions at the surface, Fe^0 appears to be an appropriate alternative for iron salts in the Fenton reaction, which furthermore ensures the effective removal of recalcitrant pollutants [249].

Biocatalyst- Glucose oxidase (GOx) enzyme

Glucose oxidase (β-D-glucose, oxygen-1-oxidoreductase, EC 1.1.3.4) is a flavin adenine dinucleotide (FAD) enzyme, which is a dimeric protein consisting of two equal subunits with a molecular mass of 80 kDa each, with one FAD cofactor and one iron per monomer (see Figure 2.13) [250]. Glucose oxidase has been purified from various fungal sources, mainly *Aspergillus niger*, and *Penicillium genera* [251, 252].

Glucose oxidase specifically oxidizes β-D-glucose at its first hydroxyl group, utilizing molecular oxygen as the electron acceptor to produce D-gluconolactone and hydrogen peroxide (H_2O_2), as shown in Reaction 2.4 [253]. Under standard conditions, оne unit of GOx can oxidize 1.0 µmol of β-D-glucose per min at a pH of 5.1 and 35 °C. The optimal pH for glucose oxidase is 5.1, but it has a broad activity pH range of 3.6–7. Glucose oxidase does not require any activators, but it can be inhibited by Ag^+, Hg^{2+}, Cu^{2+}, p-chloromercuribenzoate, or phenylmercuric acetate [253-255].

GOx is widely used in the food and pharmaceutical industries and is a major component of glucose biosensors [256, 257]. In the food industry, GOx is mainly used in the following five areas: deoxidation, improving flour, glucose, glucose content, and sterilization. GOx is also a new type of enzyme feed additive, which can improve the intestinal environment of animals, regulate their digestion, and promote growth. A mixed feed additive containing glucose oxidase, lactic acid peroxide, and lactoferrin can be used to prevent gastrointestinal infections and diarrhea in livestock [258, 259].

Since glucose oxidase can catalyze the production of gluconic acid and H_2O_2 from intestinal glucose, the growth and reproduction of *Escherichia coli, Salmonella, Pasteurella, Staphylococcus*, and *Vibrio* are directly inhibited when H_2O_2 accumulates to a certain concentration [260]. Furthermore, the resultant H_2O_2 has recently been used as a reagent in the bio-Fenton reaction to produce reactive radicals to remove recalcitrant organic pollutants [13, 17].
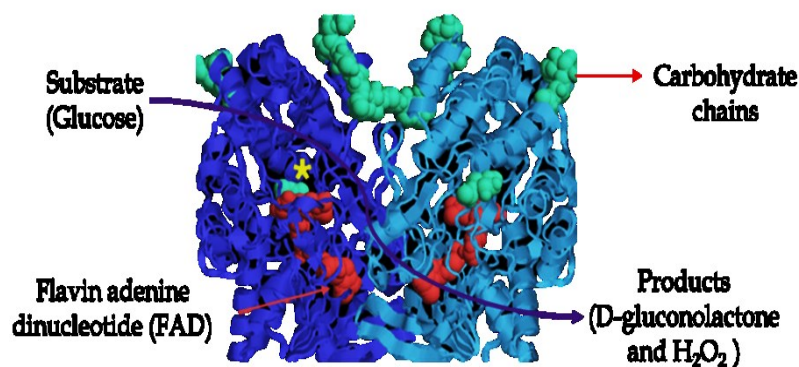
Figure 2. 13: Three-dimensional (3D) structure of Glucose oxidase enzyme (adopted from Bankar *et al.* [254]). [FAD cofactors bound deep inside the enzyme, shown in red. The active site is in a deep pocket shown with a yellow star. The enzyme has a cover of carbohydrate chains, shown in green.]

2.4.2. Choice of textile support for catalyst immobilization

In this study, the polyester nonwoven fabric was chosen as the textile support material for the immobilization of both the inorganic catalyst and the biocatalyst. Polyester fibers, specifically poly(ethylene terephthalate) (PET) fibers, are the most abundantly available fibers in the world, with over 50 million tons produced in 2016, and with production still growing [261]. The easy recyclability, high strength, low cost, high flexibility, durability, versatility,

and broad accessibility of polyester fibers make them a sustainable alternative for many fields, from apparel manufacturing to smart and multifunctional textile devices [262, 263].

In general, polyester fibers are resistant to weak acids, weak alkalis, bleach, and most organic solvents. However, they degrade in strong alkalis, strong acids, and cresol. The cross-sections of semi-crystalline polyester fibers are mostly circular, trilobal, or polygonal, with a fairly smooth hydrophobic surface (corresponding to fewer polar interactions on the surface). The moisture regains of polyester fibers is 0.1–0.4%. The density of polyester fibers is typically 1.23–1.38 gcm^{-3}, with a tenacity of 2.2–9.5 g/denier and 10–50% elongation. The glass transition temperature of standard polyester fibers is between 75 and 80 °C; the crystallization point is around 130 °C; the melting point is around 260 °C [261].

Polyester fibers can be made into woven, knitted, or nonwoven fabrics through various manufacturing processes. In particular, polyester nonwoven fabric (PF) is a new type of polyester fabric, which possesses a number of advantages over woven and knitted fabrics in terms of thickness, fiber density, permeability, porosity, elasticity, and flexibility. It is also somewhat shorter, faster, and more economical to construct than other fabrics [264, 265]. According to ISO 9092:1988, a nonwoven fabric is a manufactured sheet, web, or batt of directionally or randomly oriented fibers, bonded by friction, and/or cohesion and/or adhesion, excluding paper and products which are woven, knitted, tufted, stitch-bonded incorporating binding yarns or filaments, or felted by wet-milling, whether or not additionally needled [266, 267]. There is a considerable amount of literature discussing in detail nonwoven processes and products, such as Albrecht *et al.* (2003) [268]; Jirsa'k and Wadsworth (1999) [269]; Krcma (1971) [270]; Russell (2007) [271]; Turbak and Vigo (1989) [272]; and Karthik and Rathinamoorthy (2017) [273].

2.4.3.   Sustainable and resource-efficient technologies in this thesis

In general, the idea of wastewater treatment using immobilized catalysts is a sustainable initiative. However, to ensure the sustainability of the entire project, sustainable and resource-efficient technology such as plasma eco-technology was used to activate the support material (polyester nonwoven fabric). In addition, hyperbranched dendrimers and biopolymers were used in some cases to tailor the surface of the polyester nonwoven fabric.

Plasma eco-technology for the activation of polyester

In this thesis, the toxic chemical process of alkaline hydrolysis has been replaced with plasma eco-technology for the activation of the polyester nonwoven fabric (used as the textile support material for catalyst immobilization). Plasma is the fourth state of matter; it is composed of ionized gas and contains an equal amount of negatively and positively charged particles. It consists of ions, free electrons, radicals, and ultraviolet radiation. Generally, plasma can be created by subjecting a gas or gas mixture to energy, such as heat or an electric/electromagnetic field, leading to the formation of the ionized gas state, which can conduct electrical currents.

Plasmas are either thermal (hot) or non-thermal (cold). In a hot plasma, all the component species are in thermodynamic equilibrium. Temperatures on the order of 1,000 K are attained, so hot plasmas are unsuitable for treating textiles—or most other materials, for that matter! Cold plasmas, on the other hand, are maintained at around room temperature, or slightly above it, and so can be successfully applied to textile materials. The electrons in a plasma acquire energies in the range of 0.1–10 eV, much higher than the energies of ions and molecules, so equilibrium between all the species is far from established.

Plasmas can also be divided into low-pressure and atmospheric pressure plasmas, depending on how they were generated. Low-pressure systems generally operate at pressures between 0.01 and 1.0 mbar (1–100 Pa), and a flow of gas is fed continuously into the plasma chamber. To generate the plasma, electrical power of up to 5 kW may be necessary, depending on the treatment to be applied and the size of the chamber. The power is generated with a high voltage applied between positive and grounded electrodes, often in the radio frequency range, or from

a microwave source. Nowadays, fabrics wider than 1 m can be successfully treated on a commercial scale with low-pressure plasmas, often with the use of roll-to-roll web treatment equipment. The technology is often thought to be confined to batch processing, but this perception has been vigorously challenged. A detailed account of low-pressure plasma processing technology is available elsewhere [274, 275].

Atmospheric-pressure plasmas for treating textiles fall into three distinct categories: corona discharge, dielectric barrier discharge (DBD), and atmospheric-pressure glow discharge (APGD). Corona discharge is the oldest type of plasma treatment. Systems generating corona discharges consist of two oppositely charged electrodes connected to a power source that can provide up to 10 kV and separated by a small gap, often 1 mm. In the gap is the gas plasma. The geometries of the two electrodes are very different: one is steeply curved, like a thin wire or the point of a needle, while the other is planar or nearly planar. The gas plasma generated discharges in a spray away from the curved electrode.

The dielectric barrier discharge method uses an arrangement of two parallel plate electrodes, separated by 1 cm, and with a potential difference of up to 20 kV between them. To prevent arcs between the electrodes, one or both plates are covered with a suitable dielectric, such as a ceramic or glass. The DBD is powered by an alternating current with a frequency of 1–20 kHz. Atmospheric-pressure glow discharge is generated applying a low voltage, about 200 V, across parallel plate electrodes separated from each other by a few millimeters. The frequencies used are generally in the MHz range, i.e., radio frequencies, and so are much higher than those used for the other atmospheric discharges. In addition, the operating voltage is much lower. An APGD is uniform across the fabric being treated and is also relatively stable.

Plasma treatment technology offers a clean, dry alternative to many conventional chemical technologies. Plasma treatments are highly surface-specific: they do not affect the bulk properties of the textile fibers. Since no wet chemistry is involved, water consumption is negligible. Furthermore, the consumption of energy and chemicals is relatively low, and there is very little waste to treat, so plasma technology is environmentally friendly. However, it has been pointed out that the correct application of plasma treatments requires a thorough knowledge of the chemical and physical nature of plasmas, especially if treating a variety of different types of textiles. The durability of the treatment is also a serious concern that requires further research.

Biopolymer for surface modification of textiles

Chitosan (CS), a bio-sourced polymer, was used for the surface modification of plasma-activated polyester nonwoven fabric before the immobilization of the selected biocatalyst. We used it as the cross-linking agent. Chitosan is a linear polysaccharide composed of β-(1-4)-linked d-glucosamine (deacetylated unit) and N-acetyl-d-glucosamine (acetylated unit). It is a nontoxic, antibacterial, biodegradable, and biocompatible biopolymer widely used in biomedicine for the development of drug delivery devices, tissue engineering scaffolds, wound dressings, and antibacterial coatings. It is also a low-cost, abundant natural biomaterial with good biocompatibility and eco-friendliness [17]. It contains both amino and hydroxyl groups, which can interact with catalysts through strong electrostatic interactions and hydrogen bonding. CS was expected to provide the newly designed composite with a three-dimensional structure, increased surface area, good stability, eco-friendliness, and excellent catalyst adsorption capability during the immobilization on the textiles.

Hyperbranched dendrimers for the surface modification of textiles

The process of preparing polyester nonwoven fabric for immobilization of catalysts involves activation and surface modification. In this study, the activated surface of the polyester nonwoven fabric was further modified with different dendrimers before the immobilization of either zerovalent iron particles or the glucose oxidase enzyme. Dendrimers are radially symmetric nanoscale molecules with a well-defined, homogeneous, and monodisperse structure that includes a symmetric nucleus, an inner shell, and an outer shell. Their three traditional

macromolecular architectural groups are well known for producing polydisperse materials of varying molecular weight. Polyvalency, self-assembling, electrostatic interactions, chemical stability, low cytotoxicity, and solubility are some of the biological properties of dendrimers. A selection of terminal-group-based hyperbranched polymers (dendrimers) was chosen in this thesis to provide further favorable functional groups. They were chosen for their eco-friendliness and ability to form complexes via molecular encapsulation and covalent and non-covalent interactions [276]. Several studies have already reported the effectiveness of hyperbranched dendrimers in the immobilization of various catalysts [277-282]. The dendrimers used in this thesis are hyperbranched poly-(ethylene glycol)-pseudo-generation-5 dendrimer with a hydroxyl end group functionality, and polyamidoamine ethylenediamine core dendrimer, also known as PAMAM dendrimer, which consists of an alkyl-diamine core and tertiary amine branches.

2.4.4. Experimental approaches and strategies

The experimental work of this thesis was conducted in three phases. The plasma-activated and surface-modified polyester nonwoven fabric was used as the support material for catalyst immobilization. A summary of the three phases and the relevant experimental approaches and strategies can be found below. The materials and methods used in all experimental studies are given in Chapter 3.

(a)   1st phase: Immobilizing inorganic catalyst on textiles (Chapter 4)

This phase investigated the immobilizing of the inorganic catalyst on the polyester nonwoven fabric. The experimental work was done in the form of two studies, A and B. Study A investigated the effect of the reduction method (*in-situ* vs. *ex-situ*) on the loading, stability, and catalytic activity of Fe^0-immobilized PF. Study B explored the effects of the tailor-made PF surface on loading, stability, and catalytic activity of Fe^0-immobilized PF. In both studies, the resultant Fe^0-immobilized PF catalysts were assessed for their effectiveness in removing pollutants (organic and pathogenic) from water. The outcome of this investigation addresses research questions 1 and 2.

(b)   2nd phase: Immobilizing biocatalyst on textiles (Chapter 5)

This part of the experimental work investigated immobilizing the biocatalyst on polyester nonwoven fabric. The investigation was conducted as two interrelated studies, A and B. Study A assessed the competitive advantages of using plasma eco-technology (either atmospheric-pressure or cold remote plasma) and hyperbranched dendrimers (with either -OH or $-NH_2$ end terminal groups) for the efficient immobilization of GOx on the PF surface. Informed by the results of Study A, Study B investigated tailoring the surface of the PF with cationic amine-based polymers (either chitosan or polyethylenimine). Catalytic loading, activity, and stability (leaching, washing, and temperature) of the immobilized GOx were compared to find the best method for robust immobilization GOx on textiles. The catalytic behaviors of the resultant GOx-immobilized PF were assessed in terms of their antibacterial properties (Study A) and catalytic performance in a heterogeneous bio-Fenton system for water pollutant removal (Study B). The outcome of this investigation addresses research questions 1 and 3.

(c)   3rd phase: Heterogeneous bio-Fenton system using immobilized catalyst: proof of concept (Chapter 6)

The final phase of the experimental work was dedicated to the proof of concept of a heterogeneous bio-Fenton system for pollutant removal from water using immobilized inorganic and organic catalysts (on textile). This step used both zerovalent-iron- and glucose-oxidase-immobilized textiles from phases 1 and 2. The outcome of this investigation answers research question 4 and provides supporting evidence for research questions 1, 2, and 3.

Chapter 3
Materials and methods

Chapter outline

This chapter presents the materials and methods used in this thesis to achieve research objectives. A detailed description of materials, preparation processes, and instruments can be found here. The chapter has been divided into three sections. The first section describes the materials used in this thesis. The second section describes the general material preparation methods (with parameters) for all the studies. The third section discusses the details of the characterization tools and their parameters.

3.1. Materials

The materials used in this thesis were subdivided into two subsections. The first subsection describes the specifications of all chemicals used in this thesis; the second subsection describes the characteristics of the polyester nonwoven fabric. Materials were selected based on a number of factors, including availability, cost-effectiveness, and eco-friendliness.

3.1.1. Chemicals

Table 3.1. Summarizes the information of all chemicals. All chemical used in this thesis has been used as received (from the supplier) without any further purifications.

<div align="center">Table 3. 1: List of chemicals used in this thesis.</div>

Section name	Chemical name	CAS Number	Supplier
Pre-treatment of PF	Petroleum ether	8032-32-4	Sigma-Aldrich Inc.
	Ethanol	64-17-5	Sigma-Aldrich Inc.
	Sodium hydroxide	1310-73-2	Sigma-Aldrich Inc.
	Acetic acid	64-19-7	Sigma-Aldrich Inc.
Activation and modification of PF	Hyperbranched PEG-OH dendrimer	-	Sigma-Aldrich Inc.
	3-(Aminopropyl) triethoxysilane	919-30-2	Sigma-Aldrich Inc.
	1-Thioglycerol	96-27-5	Sigma-Aldrich Inc.
	PAMAM ethylenediamine core dendrimer	93376-66-0	Sigma-Aldrich Inc.
	Chitosan	9012-76-4	Sigma-Aldrich Inc.
	Polyethyleneimine	9002-98-6	Sigma-Aldrich Inc.
Fe^0 immobilization	Iron(III) chloride hexahydrate	10025-77-1	Sigma-Aldrich Inc.
	Iron(III) nitrate nonahydrate	7782-61-8	Sigma-Aldrich Inc.

Section name	Chemical name	CAS Number	Supplier
	Iron(II) sulfate heptahydrate	7782-63-0	Sigma-Aldrich Inc.
	Sodium borohydride	16940-66-2	Sigma-Aldrich Inc.
GOx immobilization	Glucose oxidase from *Aspergillus niger* X-S G7141 (E.C. 1.1.3.4)	9001-37-0	Sigma-Aldrich Inc
	Phosphate-buffered saline	-	Sigma-Aldrich Inc
	Potassium dihydrogen orthophosphate	7778-77-0	Sigma-Aldrich Inc
	β-D-Glucose	50-99-7	Sigma-Aldrich Inc
Pollutants	4-Nitrophenol (λ=400nm)	100-02-7	Sigma-Aldrich Inc
	Malachite green (λ=618nm)	569-64-2	Sigma-Aldrich Inc
	Methylene blue (λ=663nm)	61-73-4	Sigma-Aldrich Inc
	Crystal violet (λ=590nm)	548-62-9	Sigma-Aldrich Inc
	Staphylococcus epidermidis (ATCC 12228)	-	Sigma-Aldrich Inc
	Escherichia coli (ATCC 25922)	-	Sigma-Aldrich Inc
Other chemicals	Potassium chloride	7447-40-7	Sigma-Aldrich Inc
	Hydrochloric acid	7647-01-0	Sigma-Aldrich Inc
	Hydrogen peroxide 30%	7722-84-1	Sigma-Aldrich Inc

3.1.2. Polyester nonwoven fabric

In this thesis, polyester nonwoven fabric (PF) was used as the textile support material for the immobilization of inorganic catalyst (Fe^0) and biocatalyst (GOx). The polyester nonwoven fabric was produced at the nonwoven prototyping platform of the Centre Européen des Non-Tissés (CENT; Institut Français de la Mode, du Textile et de l'Habillement or IFTH). It was made using a carding process, followed by a hydroentanglement process using fine water jets under high pressure to consolidate for fiber web consolidation. The characteristics of the PF are given in Table 3.2 below.

Table 3. 2: Characteristics of polyester nonwoven fabric used in this thesis.

Characteristics	Values
Mass per unit area (g/m^2)	98.00
Thicknesses (mm)	0.94
Fiber density	0.80
Porosity (%)	99.91
Air permeability (mm/s)	854.20

3.2. Methods of material preparation

The methods of material preparation for this thesis have been divided into three different categories: methods of pretreatment and activation of the polyester nonwoven fabric (3.2.1), methods of modifying the polyester nonwoven fabric before catalyst immobilization (3.2.2), and methods of catalyst immobilization (3.2.3). The first category contains pretreatments and methods used to activate the PF. The second presents the methods used to further modify the PF to ensure favorable surface properties for catalyst immobilization. The last category contains the methods of immobilizing the metal and biocatalyst.

3.2.1. Pretreatment and activation of polyester nonwoven fabric

To activate the hydrophobic surface of PF, surface activation based on plasma eco-technology (atmospheric air plasma, cold-remote plasma) and alkaline hydrolysis was considered in this thesis. The choice of activation methods was dictated by the necessity of the surface chemical property necessary for the proceeding step. Before surface activation, spinning oil and any other contaminations were removed from polyester nonwoven fabric through a standard cleaning process.

Cleaning of the polyester nonwoven fabric

The cleaning of the PF was done following the Soxhlet extraction method using solvent vaporization and condensation process. Typically, the polyester nonwoven fabrics were placed in the extractor and cleaned with petroleum ether as the refluxing solvent. The apparatus consisted of a heating mantle with a thermostatic controller, a boiling flask, an extraction chamber, and a condenser (see Figure 3.1). Petroleum ether, the solvent in this closed system, was constantly heated by the heating mantle and vaporized continuously (for 5 h at 60 °C) in the boiling flask. The vaporized petroleum ether flowed through the polyester nonwoven fabric in the extraction tube and condensed in the condenser at the top of the assembly. The condensate fell back into the extraction tube. When the tube was full, the dirty solvent was returned to the boiling flask via a siphoning reflux sidearm located at the base of the extraction tube. Due to the difference in boiling point temperatures, only the solvent evaporated, while the oil remained trapped in the boiling flask.
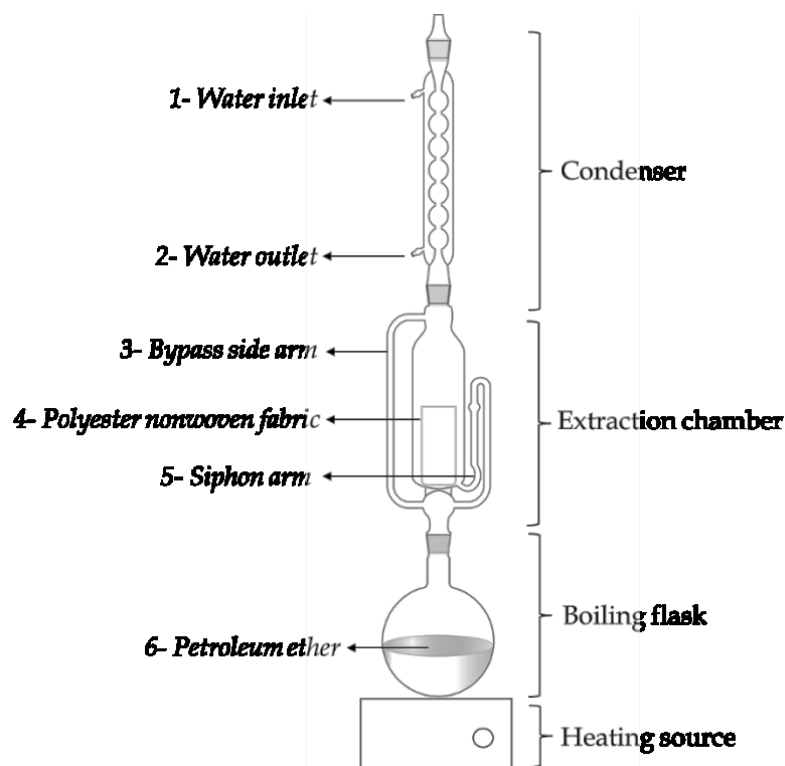
Figure 3. 1: Schematic illustration of Soxhlet extraction of cleaning of polyester nonwoven fabric by virtue of a solvent vaporization and condensation process.

After the removal of the spinning oil and other contaminants through Soxhlet extraction, the PF was washed in ethanol three times, each time for 20 min at 37 °C, in an ultrasonic benchtop bath. The PF was then dried at room temperature. The cleanliness of the PF was then assessed by measuring the surface tension of the residual water after rinsing the PF. The PF was considered clean if the surface tension of the residual water was close to 72.6 mN·m^{-1} (the surface tension of pure water).

Atmospheric pressure (air) plasma treatment of polyester nonwoven fabric

The plasma treatment was carried out using a Coating Star atmospheric-pressure plasma treatment machine manufactured by Ahlbrandt System (Germany) (see Figure 3.2). Atmospheric plasma operates at ambient conditions. The device is equipped with pair of feed rollers, an aerosol inlet, pair of electrodes, a roll-shaped counter electrode, and delivery rollers. The outer layer surfaces of both electrodes were ceramic (a dielectric material) so that when these electrodes were subjected to a potential difference, a glow discharge was created, called the dielectric barrier discharge (DBD). The cleaned polyester nonwoven fabrics were activated by this plasma treatment. The optimal parameters for the plasma treatment of polyester fabric have been established by Leroux et al. (2009) [283], and these parameters were used without modification. The width of the polyester nonwoven fabric was determined by the size of the electrodes and the glow area in the machine. Typically, PF samples were passed through the feed rollers into the glow area at a speed of 2 m per minute. The machine parameters summarized in Table 3.3 were kept constant throughout the project. After the treatment, the activated PF samples were separated, wrapped in aluminum foil, and placed into a sealed container before characterization and further use.
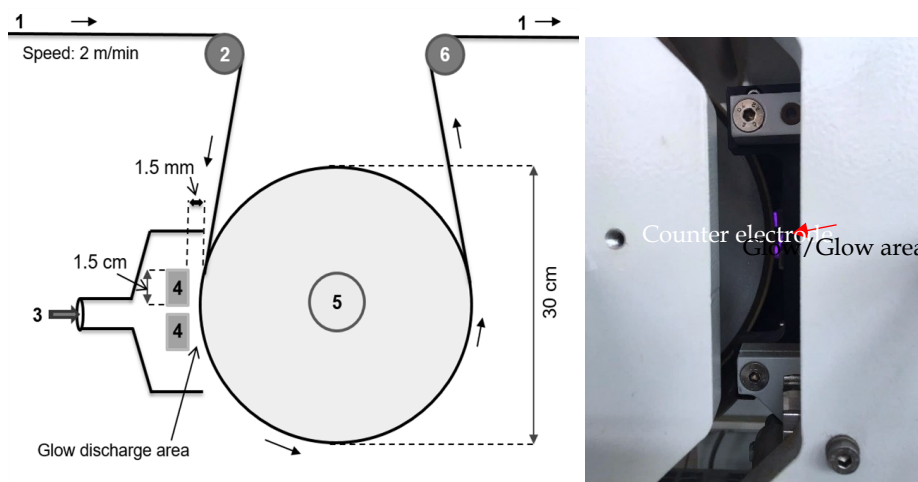
Figure 3. 2: (Left) Schematic flow diagram of air atmospheric plasma treatment of polyester nonwoven fabric; [1- Polyester nonwoven fabric, 2- Feed roller, 3- Aerosol inlet, 4- Electrodes, 5- Roll shaped counter electrode, and 6- Delivery roller]. (Right) image showing counter electrode and glow area in plasma treatment machine.

Table 3. 3: Machine parameters during plasma treatment.

Parameters	Values
Frequency (kHz)	26
Electrode length (cm)	1.5
Radius of counter electrode cylinder (cm)	30
Inter-electrode distance (mm)	1.5
Electrical power (W)	750
Plasma treatment power (kJ/m^2)	60

Cold remote plasma treatment of the polyester nonwoven fabric

The cold remote plasma (CRP) treatment of the polyester nonwoven fabric was carried out using the setup available at the Université de Lille (France). The setup consists of a coupling device, a microwave generator, a Pirani gauge, a treatment chamber with a sample holder, and a pump (see Figure 3.3). The flow of gas (N_2 or $N_2 + O_2$), created by continuous pumping, was excited by an electrodeless discharge through a microwave generator (2.450 *GHz*), which could deliver an incident power (P) of up to 1.5 kW. The discharge was produced in a quartz tube (32-mm diameter) connected to the fluidized bed reactor through a 90° elbow. This reactor consisted of a vertical cylindrical Pyrex glass tube (length: 1 m; inner diameter: 0.15 m) with a porous plate at the bottom to support the PF samples during treatment. The principal reactive species were atomic nitrogen, atomic oxygen, and vibrational electronically excited nitrogen molecules. Each of the cleaned PF samples was positioned on the porous sample plate in the CRP reactor. Here, the mixture of oxygen and nitrogen gases was used, instead of the air used in atmospheric-pressure plasma, to engineer the surface with tailor-made functional groups. The nitrogen gas flow was 1230 sccm, and oxygen flow was 89 sccm at 3.8 mbar. The PF samples were treated with the plasma flow at 4.0 mbar for 15 min. Due to the presence of N_2 and O_2 gases, amino, imide, and carboxyl groups formed extensively on the surface of the PF. After the plasma treatment, the PF samples were wrapped in aluminum foil and placed into a sealed container to avoid deterioration before characterization and further use.
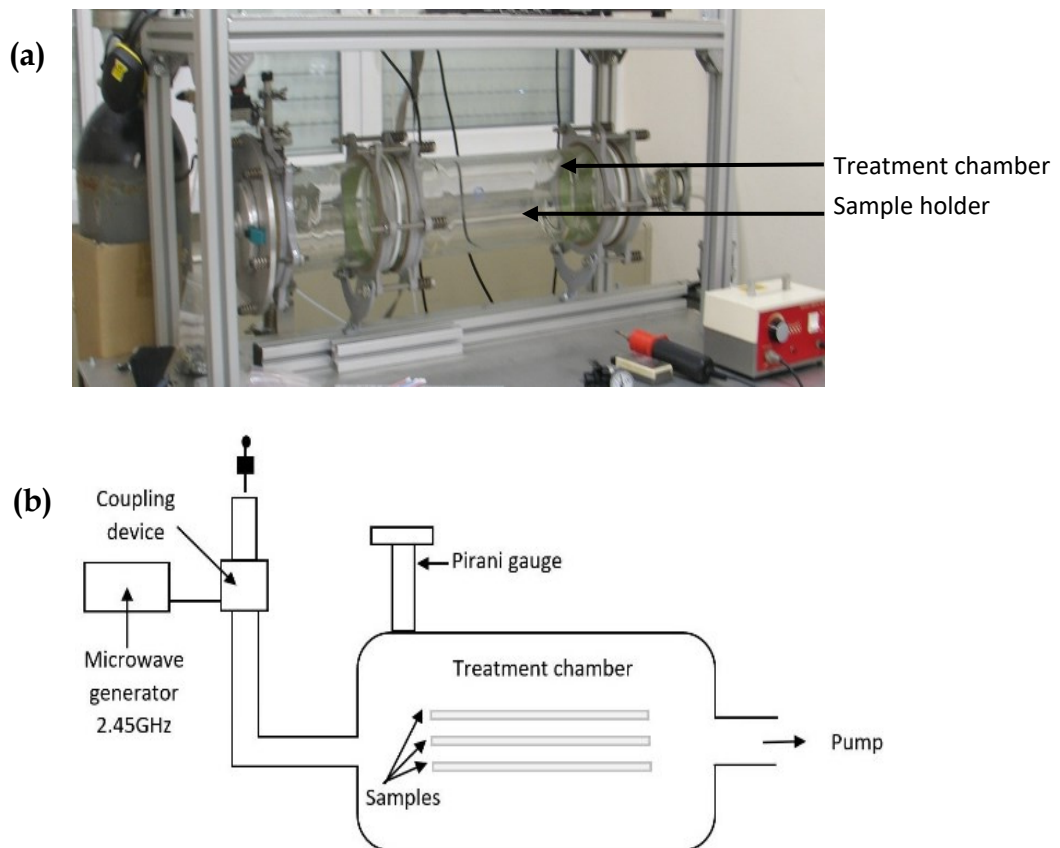
Figure 3. 3: (a) Image and (b) schematic flow diagram of cold remote plasma treatment set-up available at Université de Lille (France).

3.2.2. Methods of grafting of functional polymers on polyester nonwoven fabric

After the plasma activation, the surface of the polyester nonwoven fabric was further modified by chemical grafting of various amine/hydroxyl/thiol-rich polymers, such as polyamidoamine (PAMAM) ethylenediamine core dendrimer, poly-(ethylene glycol)-pseudo-generation-5 dendrimer, 3-(Aminopropyl) triethoxysilane (APTES), 1-thioglycerol (SH), chitosan (CS), and polyethylenimine (PEI), to facilitate the catalyst loading and stability during immobilization.

Grafting of polyamidoamine (ethylenediamine core) dendrimer on polyester nonwoven fabric

The most common class of dendrimers is polyamidoamine ethylenediamine core dendrimer (PAMAM dendrimer), which consists of an alkyl-diamine core and tertiary amine branches (see Figure 3.4) and is suitable for many materials science and biotechnology applications [284, 285]. "In this thesis, the activated polyester nonwoven fabric was further engineered with chemical grafting of PAMAM dendrimer. Typically, PAMAM (0.3 wt.%) was grafted on PF using a mixture of ethanol/water (9:1 v/v) as a solvent at 70 °C for 24 h under N_2 medium. The resulting materials were filtered, washed and dried overnight".
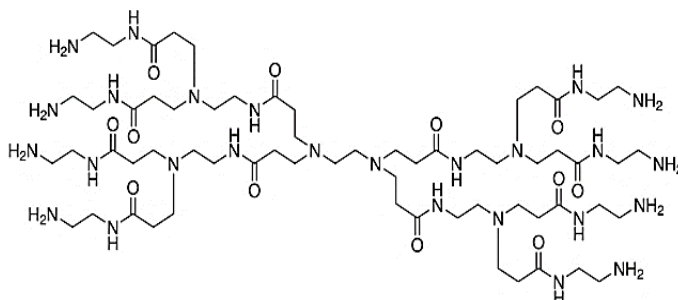
Figure 3. 4: Chemical structure of polyamidoamine ethylenediamine core dendrimer.

Grafting of poly-(ethylene glycol)-pseudo-generation-5 dendrimer on polyester nonwoven fabric

Hyperbranched poly-(ethylene glycol)-pseudo-generation-5 dendrimer having hydroxyl end group functionality (see Figure 3.5) was grafted on activated polyester nonwoven fabrics through chemical sorption as per the method described elsewhere [286]. Typically, plasma-treated nonwoven was impregnated in 1:3 (vol.) water-ethanol mixtures containing (0.3 wt.%) of dendrimer at 75 °C for 5 h. The resulting poly-(ethylene glycol)-pseudo-generation-5 dendrimer grafted PF was filtered, washed, and dried overnight at room temperature.
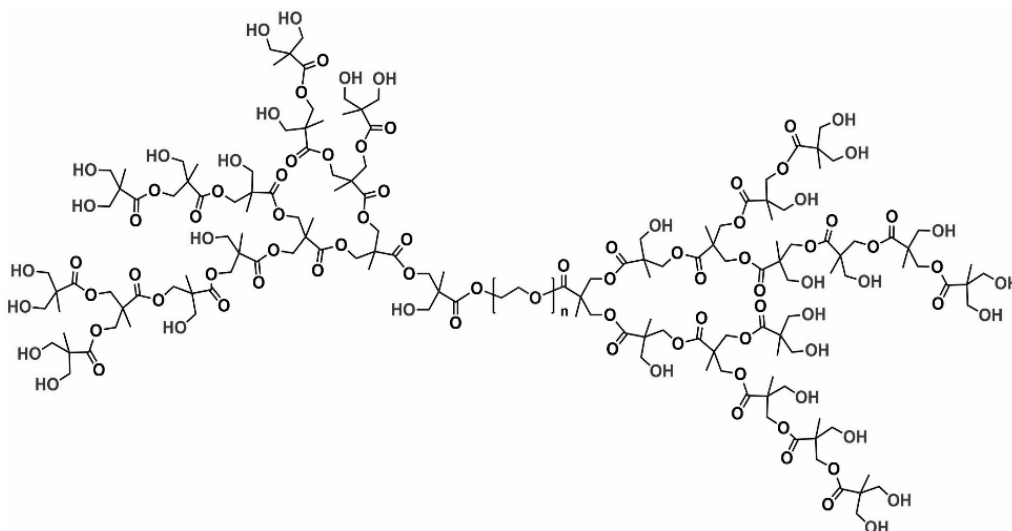
Figure 3. 5: Chemical structure of hyperbranched poly-(ethylene glycol)-pseudo-generation-5 dendrimer.

Grafting of 3-(Aminopropyl) triethoxysilane on polyester nonwoven fabric

(3-Aminopropyl) triethoxysilane (APTES) is a versatile amino-functional coupling agent used over a broad range of applications to provide superior bonds between inorganic substrates and organic polymers. The silicon-containing portion of the molecule provides strong bonding to substrates. The primary amine function reacts with a wide array of thermoset, thermoplastic, and elastomeric materials. The chemical structure of APTES has been provided in Figure 3.6. In this thesis, APTES (0.3 wt.%) was chemically grafted on activated polyester nonwoven fabric using a mixture of ethanol/water (75:25 v/v) as a solvent at 70 °C for 4 h under nitrogen gas and vigorous stirring. The resulting APTES grafted PF were washed, filtrated, and dried overnight.
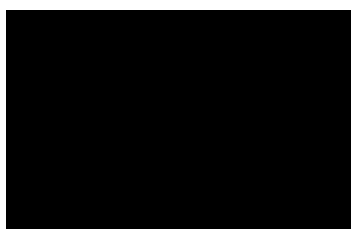
Figure 3. 6: Chemical structure of 3-(aminopropyl) triethoxysilane.

Grafting of 1-thioglycerol on polyester nonwoven fabric

3-Mercaptopropane-1,2-diol, also known as 1-thioglycerol (SH) is a sulfur-containing analog of glycerol. The chemical structure of 1-thioglycerol has been provided in Figure 3.7. In this thesis, SH has been used to modify the surface of activated polyester nonwoven fabric. Typically, SH (0.3 wt.%) was chemically grafted on activated polyester nonwoven fabric using a mixture of ethanol/water (75:25 v/v) as a solvent at 60 °C for 12 h under nitrogen gas and vigorous stirring. The resulting materials were washed, filtrated, and dried overnight.
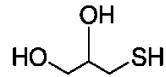
Figure 3. 7: Chemical structure of 1-thioglycerol.

Grafting of chitosan on polyester nonwoven fabric

Chitosan (CS) is an amino-polysaccharide obtained by alkali-induced de-N-acetylation of chitin (see Figure 3.8). This is a nontoxic, antibacterial, biodegradable, and biocompatible biopolymer widely applicable in biomedicine and material sciences [287]. Chemical grafting of CS on freshly activated polyester nonwoven fabric has been carried out to engineer the surface of the PF with additional favorable functional groups. Typically, the polyester nonwoven fabric was soaked in a CS solution (4.0 g.L-1, 1 M acetic acid, pH-4) under mild magnetic stirring. CS solutions were prepared earlier, stirred for 24 h, and balanced for 2 h before chemical grafting onto polyester fabrics. Resultant catalysts were rinsed with warm ultrapure water, dried at 60 °C, and stored in a desiccator before further use.
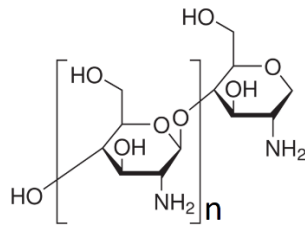
Figure 3. 8: Chemical structure of chitosan.

Grafting of polyethylenimine on polyester nonwoven fabric

Polyethylenimine (PEI) or polyaziridine is a polymer with a repeating unit composed of the amine group and two-carbon aliphatic ethylene spacer (see chemical structure of PEI in Figure 3.9). Linear polyethylenimine contains all secondary amines, in contrast to branched PEIs that contain primary, secondary, and tertiary amino groups. Here, chemical grafting of polyethylenimine was used to further modify the activated polyester nonwoven fabric with additional favorable functional groups. Typically, the polyester nonwoven fabric was soaked in a PEI solution (4.0 g.L-1, pH-5) for 1 h at 60 °C under mild magnetic stirring. PEI solutions were prepared earlier, stirred for 24 h, and balanced for 2h before chemical grafting onto polyester fabrics. Resultant catalysts were rinsed with warm ultrapure water, dried at 60 °C, and stored in a desiccator before further use.
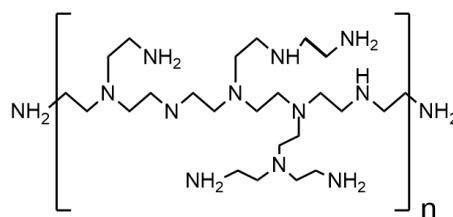
Figure 3. 9: Chemical structure of polyethylenimine.

3.2.3. Methods of catalysts immobilization

In this thesis, inorganic catalyst (zerovalent iron, Fe^0) and biocatalyst (glucose oxidase, GOx) was immobilized on polyester nonwoven fabric. In this section, methods used to immobilize both catalysts on polyester nonwoven fabric have been explained in detail.

Immobilization of zerovalent iron on polyester nonwoven fabric

Two pathways, *in-situ* and *ex-situ* methods were used for immobilization of zerovalent iron on polyester nonwoven fabric as illustrated in Figure 3.10.
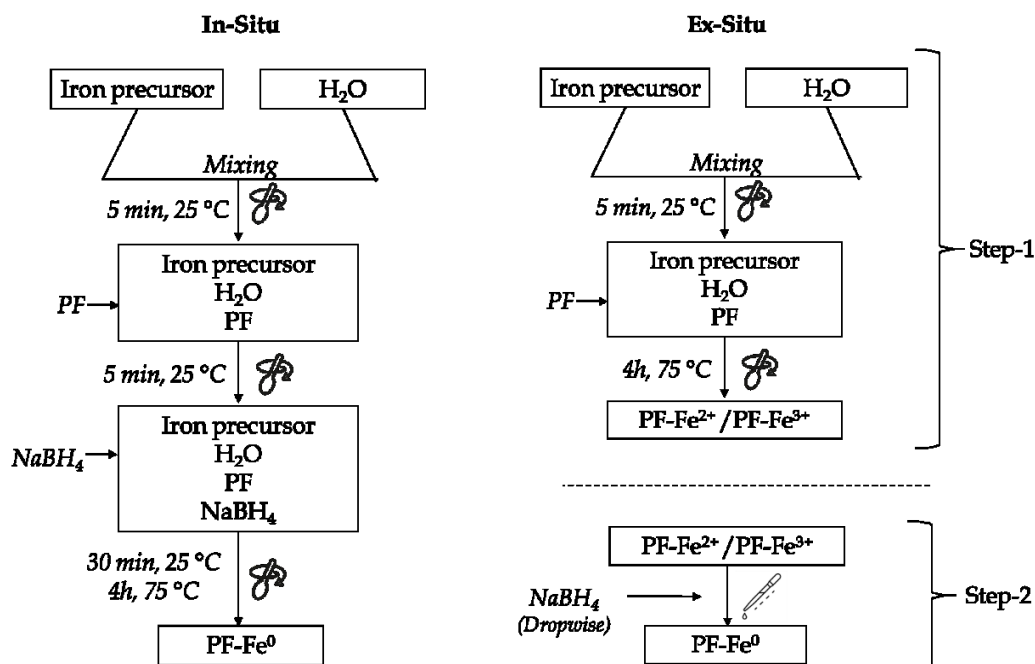
Figure 3. 10: Schematic illustration of in-situ and ex-situ synthesis and immobilization of zerovalent iron (Fe0) on polyester nonwoven fabric.

In-situ method: In situ is a single-step method for simultaneous synthesis and immobilization of Fe^0 on PF. For that, an aqueous solution was prepared by dissolving iron precursor (either Iron (III) chloride, Iron (III) sulfate, or Iron (III) nitrate) in distilled water. Polyester nonwoven fabric was dipped in the solution under vigorous stirring, and subsequently, $NaBH_4$ (0.04 M) was added, and the mixture was stirred vigorously for 30 min at 25 °C. Upon addition of $NaBH_4$, the color of the solution turned from yellow to black, indicating the reduction of the iron ions and *in-situ* formation of zero-valent particles (see Reaction 3.1). Afterward, the mixture was stirred for 4 h at 75 °C. Resulting Fe^0 immobilized PF was recovered from the solution followed by a mild wash with deionized water, dried overnight in a vacuum dryer, and preserved in an air-free desiccator.

$$2FeCl_3 + 6NaBH_4 + 18H_2O \rightarrow 2Fe^0 + 21H_2 + 6B\,(OH)_3 + 6NaCl \qquad (3.1)$$
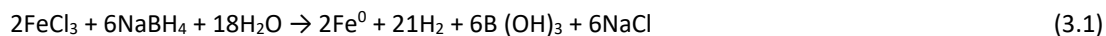
Ex-situ method: *The ex-situ* method consists of a two-step synthesis and immobilization method of zerovalent iron particles. Here, activated/modified polyester nonwoven fabric was dipped in aqueous iron precursor solution (either Iron (III) chloride, Iron (III) sulfate, or Iron (III) nitrate) and stirred vigorously for 4 h at 75 °C. After that, PF was recovered from iron solution followed by mild rinsing to remove unfixed iron ions. A separate solution of 0.04 M NaBH$_4$ has been prepared. NaBH$_4$ (0.04 M) solution was slowly dropped onto the as obtained PF, due to the reduction of iron ions into Fe^0, PF was immediately turned black (see Reaction 3.1). The drop of NaBH$_4$ solution continues until there was no hydrogen gas (as bubbles) indicating the complete reduction of iron ions into zero-valent iron. The resulting Fe^0 immobilized PF was recovered from the solution followed by a mild wash with deionized water, dried overnight in a vacuum dryer, and preserved in an air-free desiccator.

Immobilization of glucose oxidase enzyme on polyester nonwoven fabric

The physical adsorption method was used for immobilization of glucose oxidase enzyme on polyester nonwoven fabric (see Figure 3.11). Typically, Polyester nonwoven fabric was immersed into the enzyme solution with liquor ratio cm^2: ml = 1:3 to 1:5 at either *pH* 5.5 or 7.0 for 4 h at 4°C. The enzyme solution was prepared by dissolving glucose oxidase enzyme in 0.1 M potassium phosphate buffer solution (PBS). During the immobilization, the solution was shaken every 30 min. After the immobilization process, the enzyme immobilized polyester nonwoven fabric was carefully removed from the solution and successively rinsed to eliminate loosely attached enzymes. It is to be noted that, during each rinsing, a specific volume of buffer solution (0.01 M PBS) was used which was later studied to estimate the leaching of enzymes (after immobilization) during each rinsing cycle. Then, the resultant enzyme immobilized polyester nonwoven fabric were dried at 4 °C overnight and preserved in the fridge at ambient condition before studying the efficiency and robustness of immobilization.
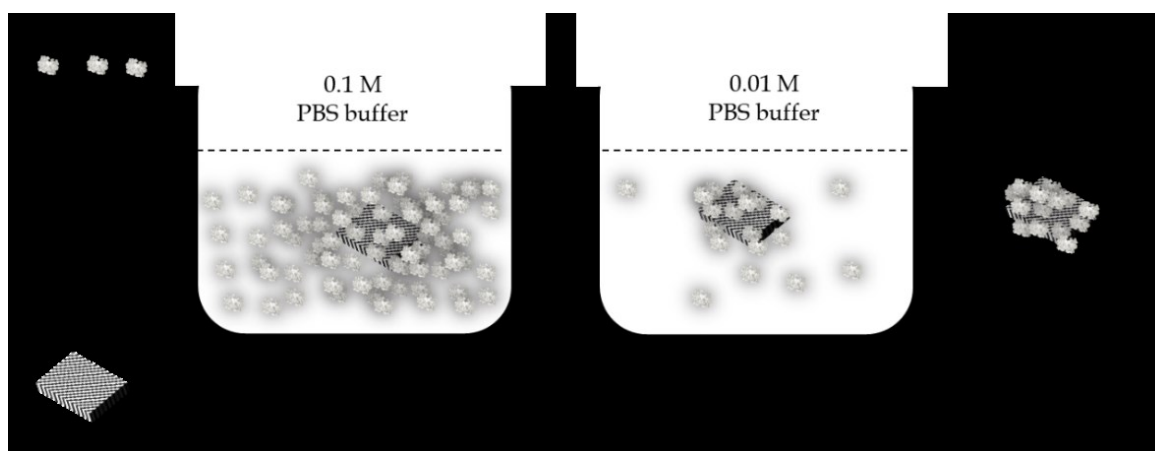
Figure 3. 11: Schematic illustration of physical adsorption Immobilization of glucose oxidase enzyme on PF.

3.3. Methods of material characterization

Various instruments for physical and chemical characterization techniques were used to study the materials before and after each modification stage. The overall characterization conducted in this thesis was divided into five key categories: methods of superficial analysis of materials (3.3.1.), methods of the enzyme activity assay (3.3.2.), methods of catalytic activity study (3.3.3.), methods of antibacterial activity study (3.3.4.), and methods of statistical analysis (3.3.5.).

3.3.1. Methods of superficial characterization

Surface analysis of the materials was done using several instruments and methods, such as capillary uptake measurement, sessile-drop goniometry, scanning electron microscopy (SEM), transmission electron microscopy (TEM), digital microscopy (DM), particle size measurement, electrokinetic measurements, x-ray photoelectron spectroscopy (XPS), x-ray diffraction (XRD), energy-dispersive x-ray spectroscopy (EDS), Fourier transform infrared (FTIR), chemical analysis, thermogravimetric analysis (TGA), and differential scanning calorimetry (DSC). It is to be noted that the necessity of the analysis was driven by the modifications of the PF and the materials involved in specific modifications.

Sessile-drop goniometry

To characterize the wettability of the polyester nonwoven fabric, sessile-drop goniometry was carried out using an optical tensiometer (Attension theta, Biolin scientific CO., Sweden, see Figure 3.12) to measure the contact angle. Automatic data collection panel of theta optical tensiometer records and allows the analysis of drop by using One Attension software as per the Young-Laplace equation [45]. Young`s contact angle of a liquid droplet on an ideal solid surface is defined by the mechanical equilibrium of the droplet under the action of three interfacial tensions (see Equation 3.1).

$$\gamma_{lv} cos\theta_Y = \gamma_{sv} - \gamma_{sl} \qquad\qquad (3.1)$$

Where θ_Y is the Young contact angle, γ_{lv}, γsv, and γsl represent the liquid-vapor, solid-vapor, and solid-liquid interfacial tensions, respectively. All the experiments were triplicated and the mean contact angle has been considered.
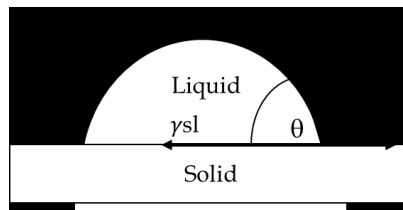
Figure 3. 12: Schematic illustration of Young`s equation describing the contact angle in terms of interfacial forces.

Capillary uptake measurement

To further understand the wettability of the samples, the analysis was carried out for rectangular-shaped nonwovens sample of size 3 cm x 5 cm mounted on the weighing position of the tensiometer. The sample nonwovens were progressively brought into contact with the surface of distilled water placed in a container on the movable stage and measured the weight of the water entrapped inside the fabric . After a progressive increase of weight of the sample with the time the final wetting force [$W_t (t_{end})$] of the samples were recorded, then the sample was resealed from the contact of water and measured the weight of the water entrapped inside the structure of the nonwoven by capillarity [$W_c(t_{end})$] read directly on the screen of the balance. After that, the meniscus weight (Wm) of the nonwovens was calculated using Equation 3.2. In all the experiments, t_{end} is 3 min.

$$W_m = W_t (t_{end}) - W_c (t_{end}) \qquad\qquad (3.2)$$

The water contact angle at the nonwoven sample surface could be determined from the calculated meniscus by using the following equation (Equation 3.3) where calculated meniscus weight (W_m) and its corresponding gravitational acceleration (g) is equal to the surface tension of the liquid (γ_L) and sample perimeter in contact with the liquid (ρ).

$$W_m \times g = \gamma_L \times Cos\,\theta \times \rho \qquad\qquad (3.3)$$

To confirm the hydrophilicity of the nonwoven material following plasma treatment, the use of the Balance 3S machine allows us to measure the weight of water absorbed by the nonwoven fabric as a function of time. The force exerted on the blade (F) is equal to the perimeter of the sample (ρ), the surface tension of water (γ), and the wetting angle (θ). If other parameters are known, the water contact angle can be obtained from Equation 3.4.

$$F = \rho * \gamma * \cos\theta \qquad\qquad (3.4)$$

Scanning electron microscope

ZEISS EVO15, MEB HR ZEISS Sigma 300 (Institut Universitaire de Technologie Chimie, Universite de Lille, France), The LEO Ultra 55, and JEOL JSM-7800F Prime microscope (Chalmers university of technology, Sweden) has been used to obtain the image and chemical information about the nano and microstructure of all types of materials used in this thesis. The LEO Ultra 55 is a dedicated high vacuum and high resolution scanning electron microscope (SEM) that allows for imaging with a resolution down to 1 nm. Before imaging in all the above devices, all samples were metalized by conductive materials.

Digital optical microscope

A Digital optical microscope (OM) from Dino-Lite has been used to gather the optical images of the sample. The instrument delivers 720p fluid live images at 20x~220x with adjustable polarization. The whole system comes with a stand that features precise fine-focus adjustment and quick release function.

X-ray photoelectron spectroscopy

X-ray photoelectron spectroscopy (XPS) study was carried out by a spectrophotometer (PHI 5500 ESCA, Physical Electronics INC., USA) equipped with monochromatic aluminum (Al) source (photon energy = 1486.6 eV). The binding energy (BE) positions were associated with reference to an adventitious carbon peak (C1s = 285.0 eV) before data analysis. Due to the insufficient conductivity, an electron neutralizer was used to compensate for the charge. Survey scan for the compositional evaluation (Energy range of 0 to 1100 eV; Step size of 0.4 eV/step), and the narrow scan for the chemical state analysis with selected range for individual elements and step size of 0.1 eV/step was performed.

Particle size measurement

The average size of the particles of any materials used in this thesis has been analyzed by image processing software ImageJ 1.40G by using images from SEM and TEM analysis. Here, a random quantity (100 -200) of sample (based on the materials) measurement use to be taken by referring to the scale on the images followed by the formulation of a size distribution histogram with standard deviation.

Electrokinetic measurement

Electrokinetic measurements were carried out to determine the ζ-potential of samples as a function of the *pH* values of the electrolyte solution (0.001 M KCl). The measurement was carried out using the streaming potential method, in which a liquid is forced to flow through two parallel plates contain samples and streaming potential is generated (Surpass, Anton Paar AB., Sweden). 0.01 M HCl and 0.01 M NaOH were used to adjust the *pH* values of electrolyte solution. The ζ-potential was calculated using the Helmholtz Smoluchowski Equation (see Equation 3.5).

$$\zeta = \frac{dl_{str}}{d_{\Delta p}} \times \frac{\eta}{\varepsilon \times \varepsilon_0} \times \frac{L}{A} \tag{3.5}$$

Where *dl/dp* is the slope of streaming current vs. differential pressure, η is electrolyte viscosity, ε represents the dielectric coefficient of electrolyte, ε_0 represents permittivity, *L* is the length of the streaming channel and *A* is the cross-section of the streaming channel.

X-ray diffraction

X-ray diffraction (XRD) analysis of the materials was carried out using Diffractometer Siemens D5000 at the Chalmers University of Technology, Sweden, equipped with Cu source (45*kV*, 40mA), Göbel mirror on a primary side and long Solar slits, and Sol'X energy-dispersive detector on the secondary side. The sample was rotating and a grazing-incidence geometry was used with an incident beam fixed at 10 degrees, step size of 0.05 degrees was used with 4s per step.

Fourier transform infrared spectroscopy

Fourier transform infrared (FTIR) chemical analysis of the polyester nonwoven fabrics were performed by using an FTIR spectrometer (Nicolet iS10, Thermo-Fisher Scientific CO., USA) to investigate the possible changes in surface functional properties of the materials. The spectra were taken between wavenumber 400 cm^{-1} to 4000 cm^{-1}. The samples were drilled before IR analysis, and background spectra were recorded on air.

Energy-dispersive X-ray spectroscopy

Energy-dispersive X-ray spectroscopy (EDX) analysis of the materials studied in this thesis was carried out using BRUCKNER axes EDX analyzer mounted with JEOL JSM IT100 SEM (described above) at Institut Universitaire de Technologie Chimie (Universite de Lille, France).

Thermogravimetric analysis

Thermogravimetric analysis (TGA) demonstrates the thermal degradation of the studied sample by measuring the change in the mass of the sample once it is heated giving a controlled temperature gradient. Thermogravimetric curves are plotted in integral (relative mass in % of initial mass; TG) and differential (a derivative of TG curve over time; DTG curves) forms. The peak at the DTG curve represents T_{max} of the composition and the temperature corresponding to 5 wt.% degradation in the TG curve is noted as T_{onset}. Approximately 10 mg of each sample was placed in a platinum crucible and TG and DTG curves were obtained (TGA Q500, TA Instruments Co., UK) under nitrogen flow (40 $cm^3.min^{-1}$) from 25 °C to 600 °C at a linear heating rate of 20 °C min^{-1}.

Differential scanning calorimetry

Differential scanning calorimetry (DSC) is a key technique to correlate temperatures with specific physical properties of the substances and direct determination of the enthalpy associated with the process of interest [288]. DSC measurement (DSC Q2000, TA Instruments Co., UK) was performed in a nitrogen atmosphere on approximately 5 mg of each sample. Samples were heated from 25 to 200 °C in Aluminum pans at a heating rate of 10 °C min^{-1}, held in isothermal condition for 2 min to destroy its anisotropy and cooled down at a cooling rate of 10 °C min^{-1} to 25 °C. Then it was heated up to 200°C with the same heating rate. All the thermal parameters were calculated on the second heating scan.

3.3.2. Methods of assessing enzyme immobilization

The enzyme assays can be split into two groups according to their sampling method: continuous assays, where the assay gives a continuous reading of activity, and discontinuous assays, where samples are taken, the reaction is stopped, and the concentration of substrates/products is then determined. In this thesis, continuous colorimetric enzymatic assays have been used to determine the concentration and kinetics of the immobilized enzymes with the help of a Lineweaver-Burk fitting plot. To contrast the loading, stability, and leaching of the immobilized enzymes, a robust quantitative analysis has been carried out on the prepared samples.

Colorimetric enzyme assay

The colorimetric enzyme assay was used to quantify the enzymes in a given substrate or solution. In colorimetric assays, the substrate is converted by the enzyme into a soluble, colored reaction product. This allows precise determination of the enzyme activity by optical density. The assay was carried out by using glucose oxidase assay kits provided by Megazyme ltd as per the instruction provided by the manufacturer. Typically, 0.5 ml D-glucose (0.5 M) was oxidized by glucose oxidase enzyme in presence of 2 ml POD (peroxidase enzyme, buffer, *pH* 7) solution with a chromogenic substrate which gives a color change at a fixed wavelength (λ_{510nm}). The difference in absorption (*ΔE*) at that point calculated real-time through a UV-vis spectrophotometer was used to quantify the active enzymes by referring to the absorption standard curve of free enzymes. In principle, Glucose oxidase activity was measured according to the enzyme's ability to catalyze the oxidation reaction of D-glucose. Hydrogen peroxide is released as a by-product of this reaction. The produced H_2O_2 enters in another reaction with p-hydroxybenzoic acid and 4-aminoantipyrine in presence of peroxidase enzyme (POD), which results in a pink-colored complex (quinoneimine dye complex) at 30° C and *pH* 7. The absorbance intensity of the colored complex was monitored at λ_{510nm} using a UV–vis spectrophotometer exactly after 20 min. From the absorbance difference (A_2-A_1) between the blank and GOx, $\Delta A_{510\,nm}$/20 min can be calculated. The activity values (U/L) are obtained by Equation 3.6.

U/L of sample solution = (mU/0.5 mL × 2000 × D)/1000 (3.6)

Here, 2000 is the conversion (0.5 mL as assayed to 1 L), 1/1000 is the conversion from mU to U and D is the dilution factor.

Quantitative study

Quantitative analysis of enzyme immobilized polyester nonwoven fabric was carried out from various approaches. The experimental data of enzyme activity for each calculation was availed by the enzymatic colorimetric assay as explained earlier. Initially, the total loaded enzyme, E_a (active) on each fabric was calculated by referring concentration of enzyme in-stock solution (mU/ml)-E_s to the concentration of enzyme on the remaining solution-E_r (active enzymes (mU/ml) in solution after used in immobilization) as explained in Equation 3.7.

$E_a = (E_s - E_r)$ (3.7)

The total active loaded enzyme in bio-functionalized Polyester nonwoven fabric was calculated (by using enzyme colorimetric assay) before rinsing and correlated with the leached enzyme during rinsing, E_r. While part of the enzyme deposited on the fabric, was strongly adsorbed, the unfixed enzymes were rinsed out. After each rinsing, the rinsed buffer solution (cm^2: ml = 1:5) was collected to quantify the leached enzyme on the solution until no leach was found afterward. The total amount of active enzymes leached (E_w) by rinsing was calculated by Equation 3.8.

$E_w = (E_{r1} + E_{r2} + E_{r3} + E_{r4 \ldots\ldots} + E_{rn})$ (3.8)

Here, $E_{r1}, E_{r2}, E_{r3}, E_{r4}$, and, E_{rn} represent the amount of enzyme washed-off during the 1st, 2nd, 3rd, 4th ..... n th wash, respectively.

Lineweaver-Burk fitting plot

This plot is a double reciprocal plot, which represents the graphics of the enzyme kinetics equation that was proposed by Hans Lineweaver and Dean Burk. It can be described as the graphical analysis method of the Michaelis-Menten equation (Equation 3.9).

$$\frac{1}{V} = \frac{Km}{Vmax} \frac{1}{[S]} + \frac{1}{Vmax}$$ (3.9)

From this equation, the enzyme kinetics like the apparent maximum velocity and apparent Michaelis-Menten constant can be determined. In this thesis, the response of our obtained samples that are bio-functionalized with GOx was evaluated in solutions, which contain different concentrations of substrate. Following these steps, the apparent Imax and Km were determined, which will help to understand the changes in the affinity of enzymes towards the substrate with different samples.

3.3.3. Methods of assessing catalytic pollutant removal

The activity of the prepared catalysts in pollutant removal was monitored (in terms of the removal of the pollutants and toxicity from treated water) with a UV-Vis spectrophotometer. The methods and instruments used to study catalytic pollutant removal performance of catalysts are described. In the end, the method used to assess the reusability of the catalysts is described in brief.

UV-visible (UV-Vis) spectroscopy

Pollutant removal was monitored by using a UV-Visible spectrophotometer. The instant-to-initial absorbance ratio of pollutants in the solution (A_t/A) was measured at different time intervals. Thus, changes in A_t/A allowed assessing the progress in removal. The removal or conversion percentage was calculated according to the concentration at predetermined time intervals by using Equation 3.10 [289].

$$\text{Conversion \%} = \frac{C - C_t}{C} \times 100 \tag{3.10}$$

Here, C is the initial concentration of pollutants; and C_t represents the concentration of pollutants at different time intervals during removal.

Theory of adsorption kinetics studies

The adsorption kinetics of pollutants at different times were analyzed by applying first-order and pseudo-first-order as well as second-order and pseudo-second-order kinetic models to recognize the solute absorption rate and transient behavior of the adsorption process.

First-order and pseudo-first-order kinetic model: The Lagergren pseudo-first-order model is based on the assumption that the rate of change of solute uptake with time is directly proportional to the difference in saturation concentration and the amount of solid uptake with time, which is generally applicable over the initial stage of an adsorption process. It is commonly observed that kinetics follows this Lagergren pseudo-first-order rate equation when adsorption occurs through diffusion through the interface . The Lagergren pseudo-first-order model can be described by Equation 3.11.

$$\frac{dq_t}{dt} = K_1 \left(q_e - q_t \right) \tag{3.11}$$

Where q_e and q_t (mg.g^{-1}) are the amounts of the amount adsorbed at equilibrium and at time *t*, respectively, K_1 is the equilibrium rate constant in the pseudo-first-order model (L.min^{-1}). After integration and applying the boundary conditions, Equation 3.12 obtained :

$$\log \left(q_e - q_t \right) = \log(q_e) - \frac{K_1}{2.303} t \tag{3.12}$$

The value of K_1 is found from the linear plots of $\log(q_e - q_t)$ versus t. If an adsorption process follows true first-order kinetics, then the intercept of $\log(q_e - q_t)$ versus t plots would be equal to log of experimentally determined q_e or adjusted to fit the experimental value. For slow adsorption process, true equilibrium can be difficultly reached, making it very difficult to measure q_e accurately .

Second-order and pseudo-second-order kinetic model: The pseudo-second-order kinetic model is based on the assumption that the rate-limiting step is chemical sorption or chemisorption and predicts the behavior over the whole range of adsorption. In this condition, the adsorption rate is dependent on adsorption capacity not on the concentration of adsorbate. One major advantage of this model over Laguerre first order is that the equilibrium adsorption capacity can be calculated from the model; therefore, there is theoretically no need to evaluate adsorption equilibrium capacity from the experiment. The differential equation for the pseudo-second-order kinetics has presented in Equation 3.13.

$$\frac{dq_t}{dt} = K_2 \ (q_e - q_t)^2 \tag{3.13}$$

After mathematical development, and taking into account the boundary conditions, the pseudo-second-order kinetic model is finally expressed as Equation 3.14.

$$\frac{t}{q_t} = \frac{1}{K_2 q_e{}^2} + \frac{t}{q_e} \tag{3.14}$$

With $\dfrac{1}{K_2 q_e{}^2} = \dfrac{1}{h}$

Where h is the initial sorption rate; q_e is the amount of the pollutant adsorbed at equilibrium (mg.g^{-1}), and K_2 is the equilibrium rate constant of the pseudo-second-order model (g. mg^{-1}. Min^{-1}). The plot of t/q_t as a function of t should give a linear relationship. From the slope $1/q_e$ and the intercept $1/h$), we can calculate the amount of adsorbate adsorbed at equilibrium and gives K_2, the second-order rate coefficient .

Theory of adsorption isotherm studies

The analysis of isotherms methods is an important way to represent the relationship between adsorbent and adsorbate in pollutant removal from water precisely. In this thesis, the models of Langmuir and Freundlich isotherms are applied to recognize the range and degree of favorability of adsorption.

Langmuir isotherms: Langmuir isotherms based on the Langmuir isotherm models assume a homogeneous surface with uniform adsorption energy and exclusive coverage of the adsorbent. Equation 3.15 presents the linearized form of the Langmuir isotherm model.

$$\frac{C_e}{q_e} = \frac{C_e}{q_m} + \frac{1}{q_m \ K_L} \tag{3.15}$$

Here, q_e (mg.g^{-1}) is the absorbed amount of the pollutants at equilibrium, C_e (mg.L^{-1}) is the equilibrium concentration of the pollutant solution, K_L is the Langmuir constant connected to the free energy of adsorption, and q_m (mg.g^{-1}) is the maximum adsorption capacity at a complete monolayer. The Langmuir isotherm parameters are determined from linear isotherm plots by placing C_e/ q_e over C_e.

Freundlich isotherm: The Freundlich model is applied to describe the adsorption of dye on a heterogeneous surface by multilayer adsorption. Equation 3.16 provides the linearized Freundlich isotherm adsorption model.

$$log q_e = \left(\frac{1}{n}\right) \log C_e + \log K_f \tag{3.16}$$

Here, q_e (mg.g^{-1}) is the absorbed amount of the pollutants per unit weight of the adsorbent, n is the Freundlich constant indicative of adsorption concentration of the adsorbents, and K_f is the Freundlich coefficient related to the adsorption capacity of the pollutant adsorbed onto the adsorbent per unit equilibrium concentration. Freundlich parameters can be calculated and the values of n and K_f are achieved from the linear isotherm plots of $log q_e$ versus $log C_e$ curves.

Toxicity removal study

Chemical oxygen demand (COD) analysis was carried out using COD vials provided by CHEMetrics, Inc. (USA) following the "ASTM D1252-06-chemical oxygen demand (dichromate oxygen demand) of water" test method B. Typically, COD measures the oxidizable organic matter content of polluted water. The samples reacted with an acidic solution of potassium dichromate in the presence of a catalyst and digested for 2 h at a temperature of 150 °C. Oxidizable organic compounds reduce the dichromate ion ($Cr_2O_7^{2-}$) to the chromic ion (Cr^{3+}). In the COD kits, the decrease in dichromate ion was measured calorimetrically at $\lambda_{620\,nm}$. The test results are expressed as the number of milligrams of oxygen consumed per litter of sample (mg/L COD) using Equation 3.17 [290].

COD (mg/L) = (23010 × A$_{620}$) − 3   (3.17)

Here, A$_{620}$ is the absorption of the COD solution at $\lambda_{620\,nm}$ after digested with the sample solution for 2 h at a temperature of 150 °C. Total dissolved solids (TDS) in the wastewater before and after treatment was measured by using Hanna Instruments *pH*, EC, TDS Combo Tester (HI98129 Hanna Instruments Ltd.). Principally, this device estimates the quantity of TDS by measuring the electrical conductivity of the water by passing a small current through it. The meter displays the TDS value in parts per million (ppm).

Reusability of catalysts immobilized polyester nonwoven fabrics

To study the recyclability and reusability of the catalysts immobilized PF, they were recycled from the reactor and washed with distilled water before reuse for another cycle under the same experimental conditions.

3.3.4. Methods of assessing antibacterial activity

The antibacterial properties of the catalyst-immobilized PF samples were evaluated through either disc diffusion and zone inhibitory analysis or optical density analysis of gram-positive and gram-negative bacteria strains. The antibacterial behavior was measured for each bacteria type, either individually or in combination.

Disc diffusion and zone inhibitory

Mueller Hinton agar plates were used for diffusion and zone inhibition analysis, the test is a semi-quantitative method where the antibacterial activity was assessed by examining the absence or presence of microbial growth in the contact zone between agar and specimen and on the eventual appearance of an inhibition zone according to ISO 20645. Typically, the samples (1 cm × 1 cm) were placed on the surface of the nutrient agar medium which was swabbed with the bacterial (10^6 CFU/cm^3) culture. The plates were incubated at 37 °C for 24 h to measure the zone of inhibition in millimeters formed around the catalyst. The results are expressed as inhibition zone (mm).

Optical density

Optical density analysis towards gram-positive and gram-negative bacteria strains were studied in this thesis to further understand the antibacterial behavior of the catalyst immobilized PF samples. The inhibition of bacteria was calculated by measuring the optical density at 630 nm using a UV-visible spectrophotometer at room temperature. In this method, the kinetics of antibacterial property of the catalysts towards the mixture of gram-positive and gram-negative bacteria strains has been studied as well.

3.3.5.   Method of statistical analysis

A full factorial experimental design was used to approximate the feasibility of the heterogeneous Fenton-like removal process, and, optionally, to make predictions from this approximation in a form of statistical modeling. In a full factorial experiment design, the experiment consists of two or more factors, where each factor is evaluated with discrete possible values or levels. The experimental units take on all possible combinations of these levels across all such factors. Findings from the experimental work are statistically verified using ANOVA analyses at a confidence interval of 95%.

Chapter 4

Immobilizing inorganic catalyst (zerovalent iron) on textile

Chapter outline

This chapter presents the results and analysis related to immobilizing the inorganic catalyst (zerovalent iron) on polyester nonwoven fabric (PF). The chapter comprises two studies, A and B, as illustrated in Figure 4.1. Study A investigated the effect of the reduction method (*in-situ* vs. *ex-situ*) on the loading, stability, and catalytic activity of Fe^0-immobilized PF. Study B explored the effects of the tailor-made PF surface on the loading, stability, and catalytic activity of the Fe^0-immobilized PF. In both studies, the Fe^0-immobilized PF catalysts were evaluated for their effectiveness in the removal of pollutants (organic and pathogenic) from water. The outcome of this chapter addressed two research questions (RQ 1 and RQ 2), paving the way to fabricating Fe^0-immobilized PF for wastewater treatment applications.
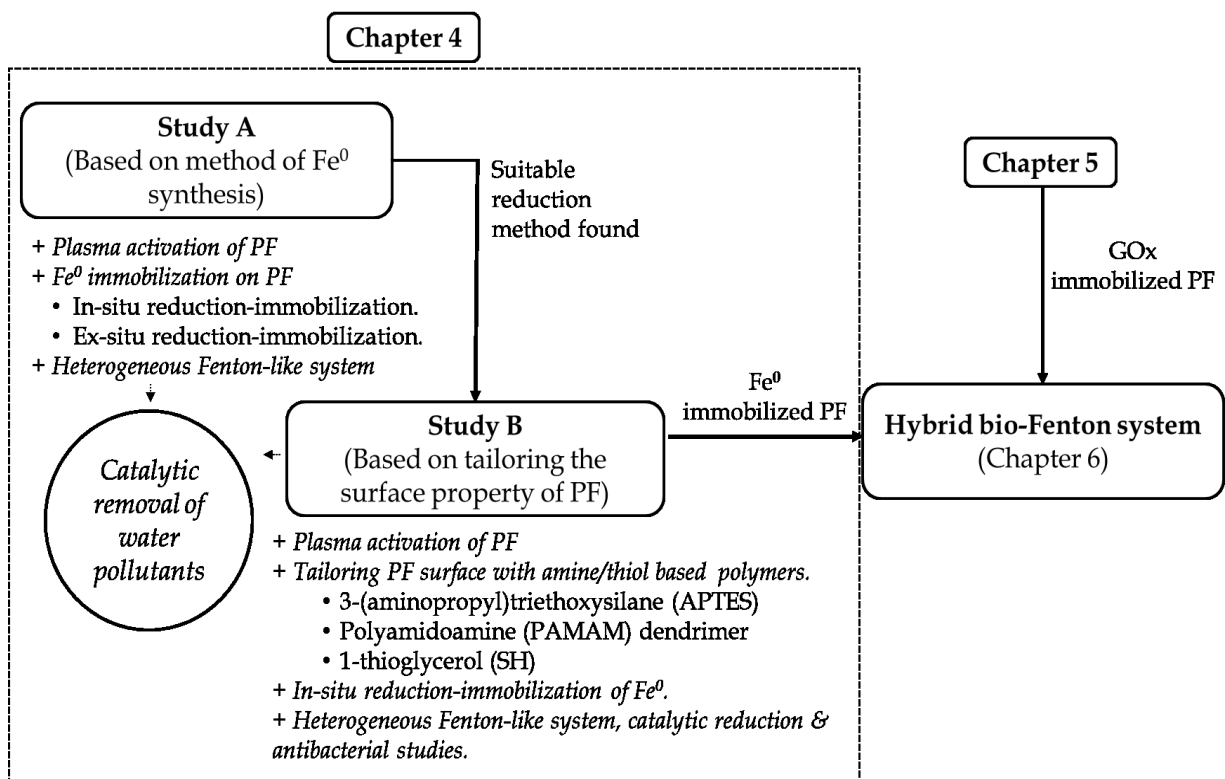
Figure 4. 1: Schematic presentation of the chapter outline and correlation to the thesis.

4.1. <u>Study A</u>: *In-situ* vs *ex-situ* reduction-immobilization of Fe^0 on polyester nonwoven fabric

4.1.1. Introduction

Inorganic catalysts from copper, zinc, magnesium, titanium, silver, iron, nickel, and their composites have been studied widely for various applications, ranging from chemical synthesis functional material to environmental remediation [291, 292]. Among them, Fe particles, especially zerovalent iron (Fe^0), are one of the most widely used inorganic catalysts for environmental remediation due to their high efficiency in pollutant removal and their low production cost [293]. Zerovalent iron has been recognized as a heterogeneous catalyst for both oxidative and reductive removal of pollutants from water. In an oxidative removal system (such as a Fenton/Fenton-like system), zerovalent iron particles generate hydroxyl radicals in the presence of water and hydrogen peroxide [294]. In a reductive system, Fe^0 produces hydroxyl radicals in the presence of a reducing agent (such as sodium borohydride) [184].

In a homogeneous system, it is highly resource-intensive to recover zerovalent iron particles from the system. Therefore, immobilization of zerovalent iron has been proposed as a suitable method of binding zerovalent iron particles to a support material, providing better reaction control and easier recovery. However, few studies have reported the use of textiles as the support material for the immobilization of Fe^0. Textiles are inexpensive and readily available in many forms, so the immobilization of iron particles on textiles can open new possibilities for robust fibrous catalytic systems for a wide range of applications. Xiao *et al.* (2009) [184] immobilized zerovalent iron nanoparticles in an electrospun polymer nanofiber textile for an environmental remediation application. Mia *et al.* (2019) [108] immobilized zerovalent iron on waste-silk fabric for Fenton-like removal of toxic water pollutants. Recently, Raji *et al.* (2021) [295] reported the immobilization of nano zerovalent iron on activated carbon cloth to fabricate Fenton-like catalysts.

In all of these studies, zerovalent iron was prepared by reducing Fe^{2+} or Fe^{3+} ions in an aqueous solution using sodium borohydride. This method was used because it is simple and can be safely performed in most chemistry labs. *In-situ* reduction and *ex-situ* reduction are the two most common methods of reduction synthesis of zerovalent iron particles when it comes to immobilization on textiles [184, 193]. *In-situ* reduction is a single-step process involving simultaneous dispersion, reduction, and immobilization of Fe^0 on textiles, whereas *ex-situ* reduction is a two-steps process, where iron ions are allowed to create a complex with the textile and then reduced in a separate bath after the textile is removed from the iron ion solution. Although both methods have been studied for the immobilization of zerovalent iron on textile support materials, there are no previous reports of zerovalent iron immobilized specifically on a polyester textile. There is also no comprehensive comparison of *in-situ* and *ex-situ* reduction methods for the immobilization of zerovalent iron particles on any form of textile.

Therefore, we began by comparing the two to identify the most suitable approach for the synthesis and immobilization of zerovalent iron particles on polyester textiles for wastewater treatment. As explained above, the hydrophobic surface of the PF had been activated by plasma eco-technology as an eco-friendly alternative to toxic chemical processes [66]. Hyperbranched dendrimers with hydroxyl terminal end functional groups were considered to integrate additional functional groups into the polyester fiber surface. The prepared PFs were compared in terms of loading, dispersion of different iron-size particles, and catalytic activity of the iron-immobilized PF in heterogeneous Fenton-like removal of water pollutants. All the catalysts were characterized with various experimental and instrumental tools to validate the observations. The results of Study A have been published in Publication II.

4.1.2.   Material preparation

Two methods, *in-situ* and *ex-situ*, were used for reduction-immobilization of Fe^0 on the polyester nonwoven fabric. Before the immobilization of Fe^0, the hydrophobic surface of PF has activated through plasma eco-technology treatment, followed by chemical grafting of hyperbranched dendrimers, following the method described in sections 3.2.1 and 3.2.2 of chapter 3 (illustrated in Figure 4.2).

During the atmospheric-pressure (air) plasma eco-technology treatment, PF samples were passed between the electrodes at a speed of 2 m per minute under standard atmospheric air conditions, with a glow discharge instigated by the potential difference (the dielectric barrier discharge or DBD) [97]. Before the plasma treatment, dirt and impurities were removed from the PF surface by Soxhlet extraction, as described in section 3.2.1 of chapter 3. Dendrimers (hyperbranched poly-(ethylene glycol)-pseudo-generation-5 dendrimer with hydroxyl end group functionality) were grafted on plasma-activated PF by chemical sorption, as described in section 3.2.2 of chapter 3. Both plasma-activated and dendrimer-grafted samples were investigated and compared in terms of *in-situ* and *ex-situ* reduction-immobilization of Fe^0, as described in section 3.2.3 of chapter 3.
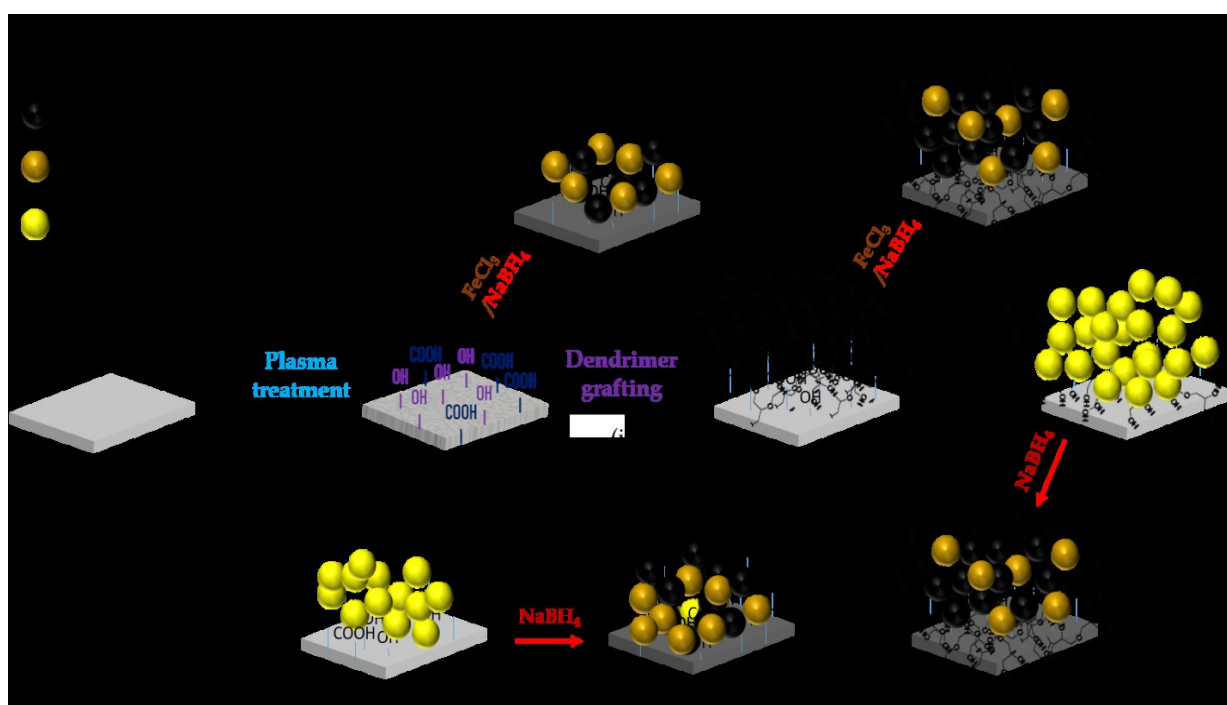
Figure 4. 2: Schematic illustration of material preparation steps for this study; (i) Plasma treatment; (ii) dendrimer grafting (iii and iv) in-situ and (v -vii or vi -viii) ex-situ reduction-immobilization of Fe^0 on PF.

4.1.3. Results: Study A

The result of study-A has been presented in three sections; the first two sections (sections ii and i) focused on the characterization of resultant material and the third section (section iii) discussed the catalytic application of resultant catalyst on a Fenton-like system for wastewater treatment. To mention resultant samples in data analysis and discussion, a short and common terminology of all samples were set based on their modifications as presented in Table 4.1.

Table 4. 1: Sample names and corresponding descriptions.

| Sample Name | Descriptions | | |
	Modification-1	Modification-2	Modification-3
Untreated PF	-	-	-
PF@AP	Plasma treatment	-	-
PF@Dr	Plasma treatment	PEG dendrimer grafting	-
In-PF-Fe^0	Plasma treatment	-	Fe^0 immobilization (*In-situ*)
Ex-PF-Fe^0	Plasma treatment	-	Fe^0 immobilization (*Ex-situ*)
In-PF@Dr-Fe^0	Plasma treatment	PEG dendrimer grafting	Fe^0 immobilization (*In-situ*)
Ex-PF@Dr-Fe^0	Plasma treatment	PEG dendrimer grafting	Fe^0 immobilization (*Ex-situ*)

4.1.3.1. Section (i): Characterization of surface activation of polyester nonwoven fabric and grafting of hyperbranched dendrimer

Characterization of surface activation of polyester nonwoven fabric and grafting of hyperbranched dendrimer was carried out through various instrumental and experimental tools and they include; sessile-drop goniometry, capillary uptake analysis, Fourier transform infrared spectroscopy, and energy-dispersive X-ray spectroscopy.

Wettability analysis

The wettability of PF before plasma treatment, after plasma treatment, and after dendrimer grating was comparatively studied through water contact angle (θ_{H_2O}) analysis using sessile-drop goniometry. The contact angle is a parameter of wettability, surface energy, and diffusion resistance. Figure 4.3 shows optical images of sessile water droplets deposited at the fabric surface (inset: picture of water contact angle). Results show that, θ_{H_2O} of untreated PF is as high as 141°, which is higher than that of polyester fiber surface (θ_{H_2O}= 80°). The high surface roughness due to irregularities of the nonwoven surface would account for such a high θ_{H_2O}.
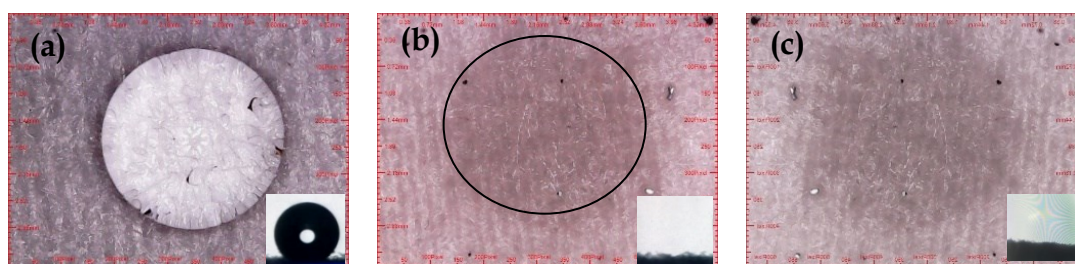
Figure 4. 3: Water contact angle measurement and optical images of sessile water droplet deposited at the surface of (a) Untreated PF, (b) PF@AP, and (c) PF@Dr; (inset: picture of water contact angle).

A decrease in water contact angle (θ_{H_2O}=0°) was recorded on plasma-treated PF. This can be due to the formation due to scissions of ester bonds (present at the polyester fiber) during plasma treatment, yielding hydrophilic terminal carboxyl and hydroxyl ends as confirmed in previous studies [296]. Similar to PF@AP, PF@Dr maintained the wettability of the fabric due to the presence of hydrophilic terminal groups (hydroxyl ends) of PEG dendrimers

while having θ_{H_2O}=0°. Since the droplet of water adsorbed immediately in both PF@AP and PF@Dr. Actual θ_{H_2O} of each samples cannot be measured in this process (due to high hydrophilicity). Therefore, samples were further studied with capillary uptake measurement.

Table 4. 2: Wettability analysis of PF samples.

Sample name	θ_{H_2O} [°] (sessile-drop goniometry)	Capillary uptake measurement	
		W_m (mg)	Calculated θ_{H_2O}[°]
Untreated PF	141	-	-
PF@AP	0	1453	1.46
PF@Dr	0	1650	0.68

Capillary uptake provides information about the transport mechanism of the water (and hence of reactional medium) into the pores of PF. Without a hydrophilic surface, there will be no capillary uptake due to the absence of polar functional groups. Results show, apart from the meniscus weight (234 mg), untreated PF did not show any capillary uptake, corresponding to its inherent hydrophobic surface. However, there is a consistency between the water contact angle measured by the sessile-drop goniometry analysis and capillary uptake; plasma treatment successfully activated the surface of PF showing a rise in capillary uptake (1453 mg). The low meniscus weight and water contact angle confirms the change in wettability at the outer surface and while higher capillary uptake shows activation of fiber surfaces in the inner core of the PF fabric. A further increase in capillary uptake (1650 mg) has been recorded when plasma-treated PF was functionalized with PEG dendrimer. This indicates that the abundance of terminal hydroxyl groups in the PEG dendrimer results in a slightly higher affinity towards water. The water contact angle of untreated PF and PF has been calculated using meniscus weight (W_m), the surface tension of water (γL), and sample perimeter in contact with water (ρ). Results showed that the calculated $\theta_{[H_2O]}$ of PF is 1.46, whereas the PF@Dr showed a calculated θ_{H_2O} of 0.68. Although there are negligible mathematical differences between the θ_{H_2O} of PF and PF@Dr, in this thesis, the θ_{H_2O} for both samples has been referred as θ_{H_2O}=0°.

Fourier transform infrared spectroscopy

Fourier transform infrared (FTIR) spectroscopy has been used to identify the integration of alleged polar functional groups on PF after plasma treatment and PEG dendrimer grafting. Resultant spectra have been presented in Figured 4.4. Results show, all samples demonstrated common bands in the region 1750-650 cm^{-1}, which were attributed to the stretching vibration of CH_2, C=O, aromatic C=C, and C-O of ester, indicating the structure of PET [297, 298]. The chain scission of the PET was reflected in the FTIR spectrum of PF@AP as the decrease in absorption intensity of IR bands corresponding to the carbonyl ester groups also band shifted a little to 1706 cm^{-1} from 1712 cm^{-1} [299]. New absorption was observed at 1530 cm^{-1} to 1660 cm^{-1} and at 1740-1800 cm^{-1}, which assigned to the asymmetrical stretching vibration of -COO, and coupling interaction between the two equivalent carbon bonds of carboxylate anion, as well as carboxylic acid. While a broad band near 3500 cm^{-1} was assigned to stretching vibration of OH [300]. The formation of such functional groups by air plasma treatment is well documented in the literature [301, 302]. Thus, FTIR results support that plasma treatment resulted in the incorporation of new polar functional groups like COO-, COOH, OH at the surface of polyester. The bands at 1471 cm^{-1} and 1117cm^{-1} present in PF@Dr arising from the vibration of the ethylene glycol can be due to the chemical grafting of hyperbranched PEG dendrimer [303]. Thus, these results reflect and validate the successful activation and grafting of dendrimer based on the changes in the conformational composition of polyester fabric.
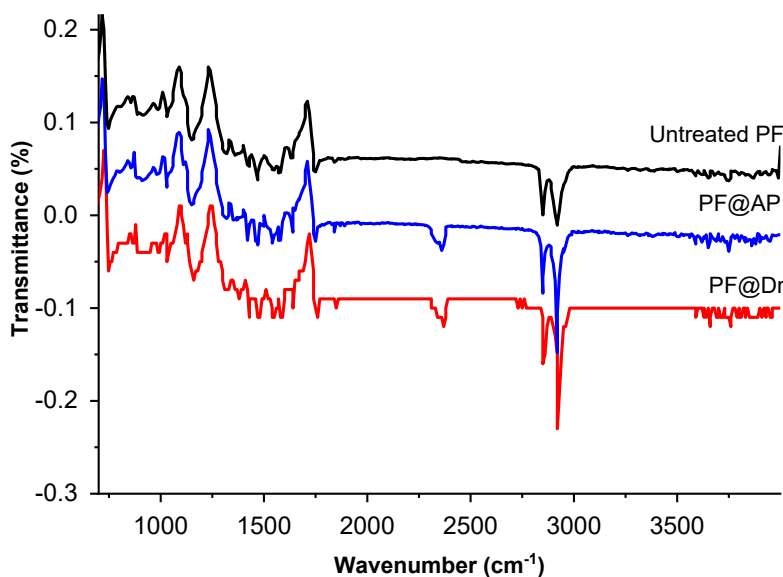
Figure 4. 4: Spectra from Fourier transform infrared spectroscopy of untreated PF, PF@AP, and PF@Dr.

Energy-dispersive X-ray spectroscopy

Energy dispersive X-ray (EDX) spectroscopy analysis based on atomic/elemental identification and the ratio has been obtained from atom percentage as summarized in Table 4.3 (obtained from EDX spectroscopy). The result shows the untreated PF contains an O/C atomic ratio of about 0.35 (65.33% C atom, 34.77% O atom). However, after plasma treatment of PF the O/C atomic ratio increases to 0.38 (62.13% C atom, 37.87% O atom). The increase in O atom indicates the chain scission of the PET and formation of oxygenated functional groups (COO-,COOH, OH) due to plasma treatment as assumed in FTIR analysis. Nevertheless, the O/C atomic ratio has further increased (0.43, 57.02% C atom, 42.98% O atom) after dendrimer grafting. An increase in oxygen atom can be explained by the presence of an abundant amount of hydroxyl functional group in the dendrimer, which contributed to the hydrophilicity of PF as explained in wettability analysis. This change in atomic ratio is directly linked to the respective chemical composition of PF surface, which stands clear validation of activation and successful grafting of the hyperbranched dendrimer. Sessile-drop goniometry, capillary uptake measurement, FTIR, and EDX analysis point to the same conclusion.

Table 4. 3: Atomic identification analysis of untreated PF, PF@AP, and PF@Dr.

Sample name	Atomic identification per scanned surface (EDX analysis)*		
	C atom %	O atom %	O/C
Untreated PF	65.33	34.77	0.35
PF@AP	62.13	37.87	0.38
PF@Dr	57.02	42.98	0.43

*Atoms peak regions: Carbon (C, 0.278 keV), Oxygen (O, 0.550 keV)

4.1.3.2. Section (ii): *In-situ/ex-situ* reduction-immobilization of Fe^0 on polyester nonwoven fabric

The effect of *in-situ* or *ex-situ* reduction method on the surface morphology, dispersion, particle size, and the thermal property of immobilized Fe^0 has been comparatively studied using several experimental and analytics tools, that includes, digital optical microscope, scanning electron microscope, high-resolution scanning electron microscope, energy-dispersive X-ray spectroscopy, X-ray diffraction, and thermogravimetric analysis. Results of this section validate the potential immobilization of Fe^0 particles on activated PF that in turn influences the catalytic performance of catalysts as discussed in the next and final section (section iii) of this study (study-A).

Morphological analysis

The initial confirmation of immobilization of Fe^0 on PF was carried out through visual characterization tools. Optical microscopic (OM) images presented in Figure 4.5 provide evidence of iron-like particles on the surface of the PF. A close observation of the images reveals distinct features (yellowish or blackish color) of each fibrous nonwoven textiles due to the immobilization of Fe^0. The changes in features can be due to either the differences in pre-treatment of PF or the method (*in-situ/ex-situ*) of reduction-immobilization of Fe^0 used.
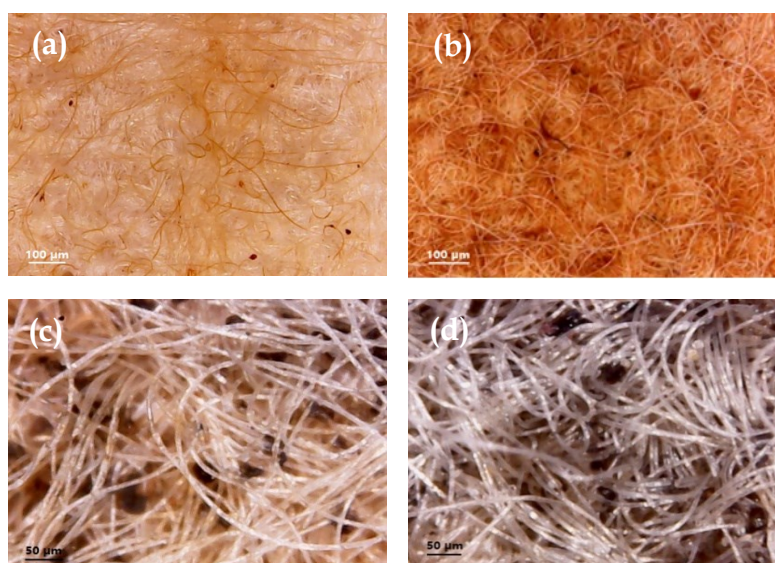
Figure 4. 5: Optical microscope images of (a) In-PF-Fe^0, (b) Ex-PF-Fe^0, (c) In-PF@Dr-Fe^0 and, (d) Ex-PF@Dr-Fe^0.

Further investigation on the samples reveals that all four samples contain immobilized iron particles (seen in atomic identification from EDX and XRD analysis), where In-PF-Fe^0 and Ex-PF-Fe^0 show yellowish micro/nano iron particles, and the dendrimer based fabrics, In-PF@Dr-Fe^0 and Ex-PF@Dr-Fe^0 show blackish iron particles trapped within the pores of the nonwoven. The differences in color of iron particles correspond to different stages of iron (either, zerovalent iron, iron oxide, or zerovalent iron with oxide shell) [304]. The blackish iron particles observed in In-PF@Dr-Fe^0 and Ex-PF@Dr-Fe^0 are more likely to be stable Fe^0 without an oxide shell whereas yellowish iron particles In-PF-Fe^0 and Ex-PF-Fe^0 is Fe^0 with oxide shell (an average shell thickness is in the range of 2.3-2.8 nm [248]) as illustrated in Figure 4.6. By contrasting iron the reduction methods, it can be seen that in both *in-situ* and *ex-situ* reduction-immobilization of Fe^0, this color-changing phenomena exists, however, a closer look reveals that, PF pre-treated with both plasma and dendrimer before Fe^0 immobilization shows blackish iron particles whereas

PF without a dendrimer coating showed yellow iron particles. These findings indicate that, with grafting of dendrimer on PF, better stability of immobilized Fe^0 particles can be achieved (yellowish iron particles indicate the formation of oxide layer on the Fe^0). To understand the immobilization, dispersion, and particle size distribution of immobilized Fe^0 particles on PF, further tests were carried using a scanning electron microscope (SEM) in variant scale (50 μm and 10 μm) and a high-resolution scanning electron microscope (HR-SEM) was used to better analyze the fibrous textile surfaces.

SEM and HR-SEM images in Figure 4.7 display the general distribution of spherical-shaped iron particles over the surface of PF. Samples show different distribution patterns of Fe^0 particles among themselves, which can be attributed to their preparation process. Clear differences between *in-situ* reduction vs *ex-situ* reduction as well as with dendrimer vs without dendrimer have been observed. By contrasting the samples prepared by the *in-situ* reduction method (In-PF-Fe^0 and In-PF@Dr-Fe^0) and *ex-situ* reduction method (Ex-PF-Fe^0 and Ex-PF@Dr-Fe^0), it can be seen that *in-situ* reduced samples showed a uniform distribution of iron particles without any formation of cluster or aggregates whereas *ex-situ* reduced samples showed a non-uniform distribution of iron in form of isolated particles and clusters. The Fe^0 particles in the *in-situ* reduced samples seem to be essentially localized on the surface of fibers, whereas the pores of nonwovens remain intact. On the other hand, the formation of iron particle clusters in the *ex-situ* reduced samples has been detected on the fiber surface as well as in the pores of nonwoven. From these observations, it can be concluded that there a clear influence of reduction-method on the distribution and integration of Fe^0 particles on PF.
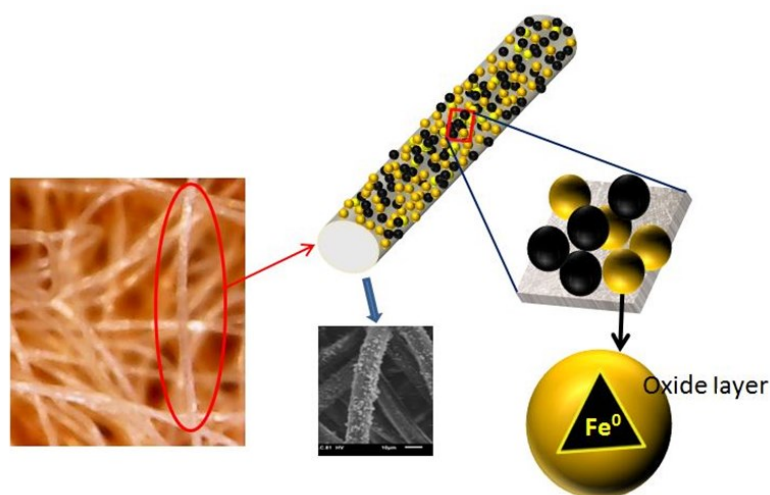
Figure 4. 6: Schematic illustration of zerovalent iron particles with oxide shell.

Nevertheless, when samples with or without dendrimer (In-PF-Fe^0 and In-PF@Dr-Fe^0) were compared, samples with dendrimer showed more densely integrated iron particles than those without dendrimer. This similar phenomenon can be observed for the *ex-situ* method for Ex-PF-Fe^0 and Ex-PF@Dr-Fe^0 when compared to the *in-situ* method. This is in line with the report by Mayers *et al.* (2011) [305] where they have mentioned that dendrimers can encapsulate more iron particles with the advantage of both templating and stabilizing the particles. Without a quantitative analysis, this observation cannot be considered a conclusive finding; therefore, a quantitative analysis of the loading was conducted through thermogravimetric analysis (discussed in the following section).

The morphology and dispersion of iron particles on PF are believed to be influenced by the size of the particles, hence a widespread investigation on particle size distribution was carried out from HR-SEM images. Results show iron particles formed in different samples have diameters as low as 50 nm. Nanoparticles of iron often aggregated and formed micro-particles with a diameter up to 25 μm as observed in Figure 4.5 and Figure 4.7. Among the four samples studied here, *in-situ* reduced samples showed comparatively finer particle sizes than that of *ex-situ* reduced samples. This result corresponds to the less aggregation of iron particles in the *in-situ* method as

compared to *ex-situ* as discussed earlier. The average particle sizes recorded for each sample are; In-PF-Fe^0 (170±55 nm) Ex-PF-Fe^0, (190±126 nm) In-PF@Dr-Fe^{0,} and (164±115 nm) Ex-PF@-Fe^0 (194±69 nm). Summarizing morphological analysis, it can be established that, as consistent with earlier discussion, the method of reduction of iron ions affects the overall morphology, distribution, and sizes of the iron particles which might have effects in further application of iron particles immobilized PF.
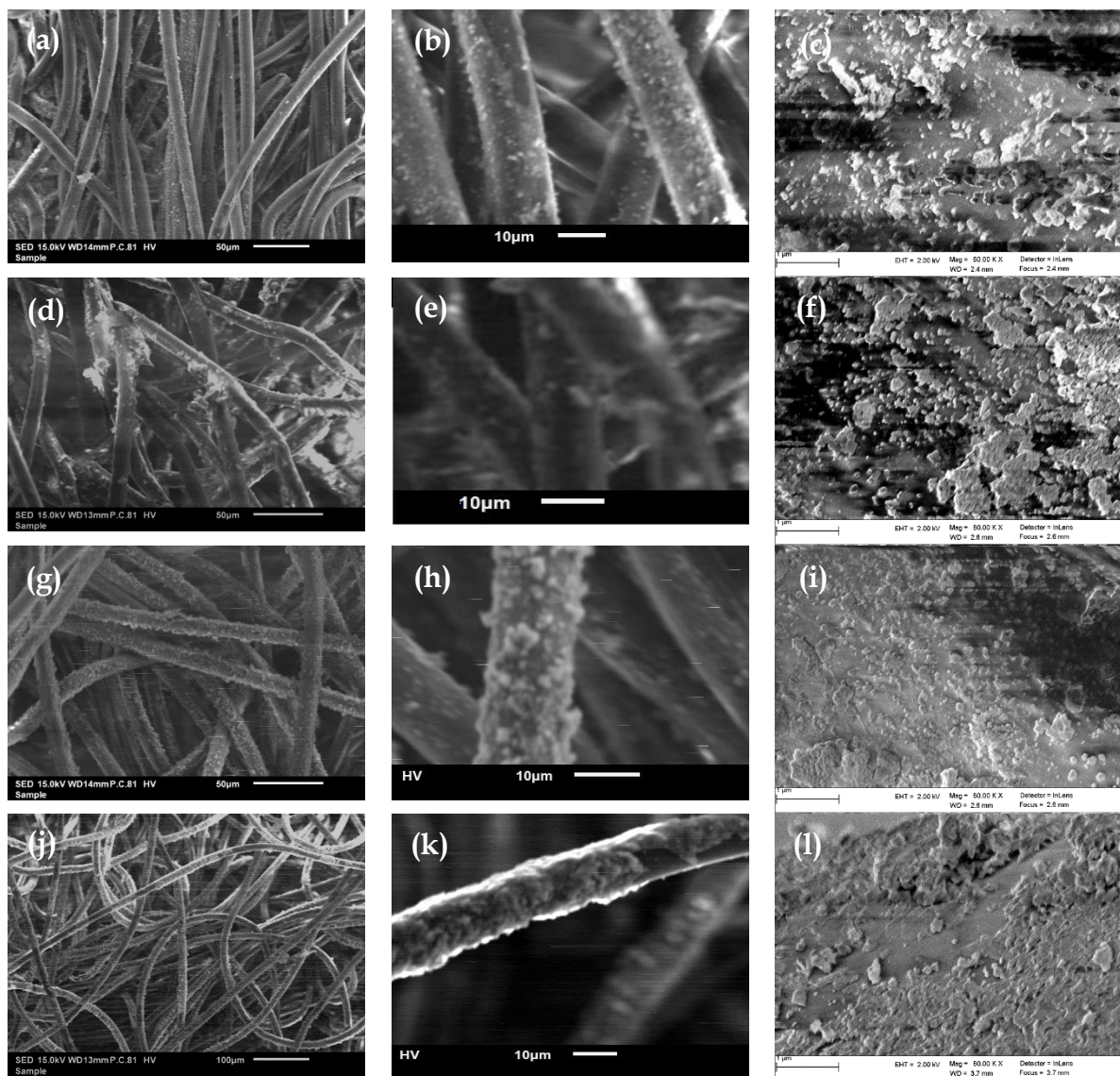
Figure 4. 7: SEM and HR-SEM images of (a-c) In-PF-Fe^0, (d-f) Ex-PF-Fe^0, (g-i) In-PF@Dr-Fe^0, and (j-l) Ex-PF@-Fe^0.

X-Ray analysis (EDX, XRD)

To validate the conclusion from the morphological analysis of Fe^0 immobilized PF samples, Energy-dispersive X-ray spectroscopy (EDX) has been carried out to identify the atoms present in the PF surface. This analysis aims to detect iron particles and corresponding atom% in a given area. Results gathered from the analysis have been summarized in Table 4.4. Examples of two spectra (PF before and after iron immobilization) have been provided in Figure 4.8. Spectral analysis showed that PF before iron immobilization showed characteristic peaks of O (0.278 *keV*) and C

(0.550 *keV*) of polyester. However, after Fe^0 immobilization, along with peaks of C and O, two new apparent peaks of iron (0.725 *keV* and 6.432 *keV*) were observed. This finding conclusively validates that, the particles immobilized in PF as visually observed in the morphological analysis are indeed iron particles. For a deeper understanding of Fe^0 immobilization on PF, atomic percentage and ratios from EDX analysis have been investigated to demonstrate the quantitative significance of iron particles in each sample. Atomic percentage analysis of the samples presented in Table 4.4 shows that the lowest iron content (18.81%) was found in In-PF-Fe^0 followed by In-PF@Dr-Fe^0 (21.06%) and Ex-PF-Fe^0 (22.30%). The highest atom% of iron has been found in Ex-PF@Dr-Fe^0 (26.98%). A closer look at the result reveals that, among *in-situ* and *ex-situ* reduced samples, *in-situ* reduced samples showed lower Fe atom% than that of *ex-situ* reduced samples indicating that, *ex-situ* reduction method integrates more iron particles than the *ex-situ* method. These results agree with the fact that the *ex-situ* reduction process entraps iron particles in both surface and pores of fabric as observed in morphological analysis (discussed earlier). In addition, when contrasting the samples based on the use of dendrimer, results show, the use of dendrimer increases the loading of iron particles by up to 0.90%, which validates the effects of dendrimer on loading as speculated during morphological analysis. Furthermore, atomic ratios (O/C, Fe/C, and Fe/O) analysis also provided the relative evidence that proves the effect of reduction-method and dendrimer on the loading, stability, and overall distribution of immobilized Fe^0 on PF.
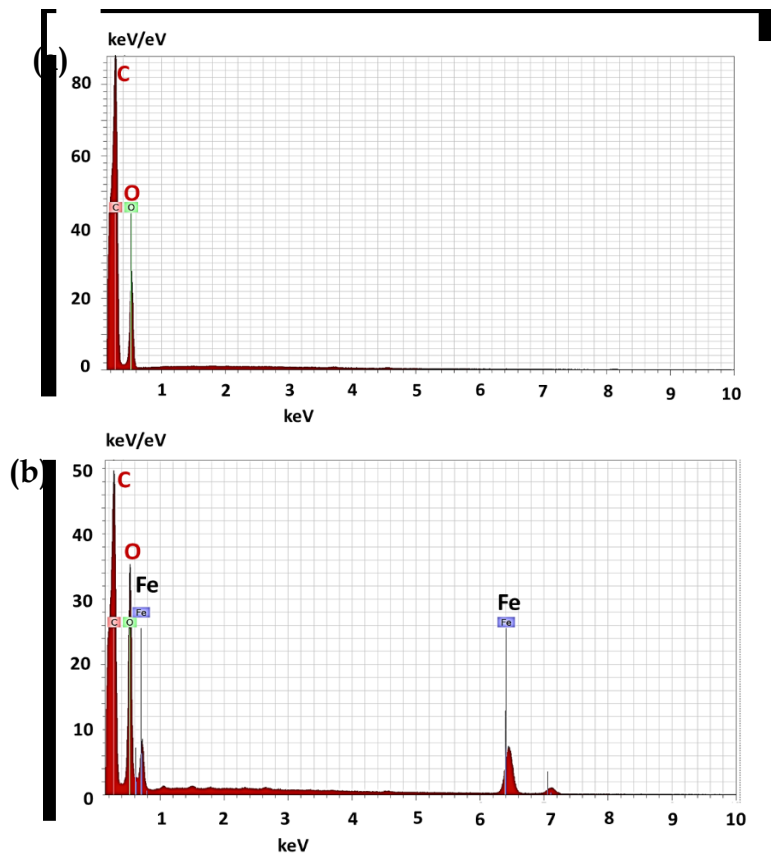
Figure 4. 8: Characteristics EDX spectra of PF; (a) before and (b) after Fe^0 immobilization. Carbon (C, 0.278 *keV*), Oxygen (O, 0.550 *keV*) and Iron (Fe, 0.725 *keV* and 6.432 *keV*).

Table 4. 4: Quantitative analysis of atomic identification per scanned surface of Fe^0 immobilized PF.

Sample name	Atomic identification per scanned surface (EDX analysis)*					
	C atom%	O atom%	Fe atom%	O/C	Fe/C	Fe/O
In-PF-Fe^0	57.23	23.96	18.81	0.41	0.33	0.79
Ex-PF-Fe^0	56.0	21.69	22.30	0.38	0.40	1.02
In-PF@Dr-Fe^0	57.20	21.72	21.06	0.38	0.37	0.97
Ex-PF@Dr-Fe^0	52.25	20.76	26.98	0.40	0.52	1.30

*Atoms peak regions: Carbon (C, 0.278 *keV*), Oxygen (O, 0.550 *keV*), and Iron (Fe, 0.725 *keV,* and 6.432 *keV*).

To determine the precise nature of iron particles immobilized on PF, all samples were characterized by X-ray diffraction (XRD) analysis. Results presented in Figure 4.9 showed that PF (without iron particles) showed no distinct peaks at any part of the spectra, whereas apparent peaks at the 2θ of 44.9° (110), 35.8° (311), and 31.6° (220) were found in samples with immobilized iron particles (In-PF-Fe^0, Ex-PF-Fe^0, In-PF@Dr-Fe^{0,} and Ex-PF@-Fe^0). The new peaks correspond to both zero-valent iron (α-Fe) and iron oxide (Fe$_2$O$_3$ and Fe$_3$O$_4$) crystalline phases [306, 307]. These results validate the successful synthesis and immobilization of zerovalent iron particles on the surface of PF. The presence of oxides peaks can be related to the formation of thin oxide layers on the surface of the zerovalent iron nanoparticles as illustrated in Figure 4.6. These results are in general consistent with reported work suggesting a core-shell structure for the zerovalent iron particles [248].
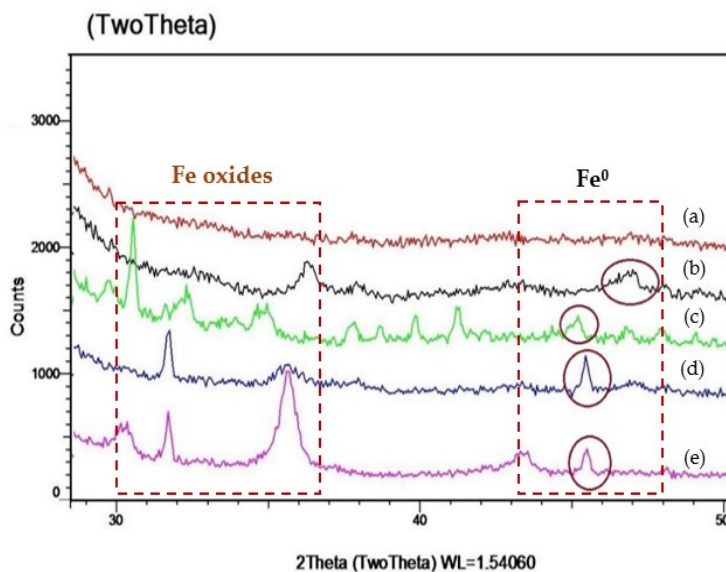
Figure 4. 9: X-ray diffraction analysis of (a) PF, (b) In-PF-Fe^0, (c) Ex-PF-Fe^0, (d) In-PF@Dr-Fe^0 and, (e) Ex-PF@-Fe^0.

Thermal property analysis

Thermogravimetric (TG) analysis of PF before and after dendrimer grafting and iron immobilization was carried out to investigate the changes in the thermal property of the fabric as well as perform a quantitative analysis of iron particles immobilized on PF. Results obtained from the TG analysis have been presented in Table 4.5 show that two common mass loss regions at around 350–450 °C and 500–800 °C are present in all samples. However, apart from common mass loss regions, dendrimer grafted samples (In-PF@Dr-Fe^0 and Ex-PF@Dr-Fe^0) showed an additional mass loss region from around 60°C to 150 °C, which is most probably due to evaporation of superficial water in the PF entrapped with the dendrimers. The mass loss region located around 360–450 °C is attributed to the thermal degradation of the PET polymer [308]. It can be seen that the modification of PF did not have a direct influence on the thermal property of the fabric. However, the observation regarding residual wt.% has been correlated to the number of iron particles immobilized on the polyester nonwoven fabric.

Therefore, after the thermal degradation of PET polymers in the PF, the remaining wt.% has been considered as the relative quantity of iron particles on the PF (provided that, no other additional materials were present on the fabric surface as concluded in EDX and XRD analysis). The summary of the results (w/w of immobilized Fe^0) on PF has been presented in Table 4.5 and comparatively studied based on their preparation methods (reduction method and use of dendrimer). Results show that the lowest iron content (13.26%) has been found in In-PF-Fe^0 followed by Ex-PF-Fe^0 (15.10%) and In-PF@Dr-Fe^0 (17.80%). The highest iron wt.% has been found in Ex-PF@Dr-Fe^0 (24.70%). These findings are also identical to the results found in EDX analysis.

Table 4. 5: Loading analysis of Fe^0 on PF, based on residual wt.% based on TG analysis.

Sample name	Weight loss regions			w/w % of immobilized Fe^0
	1st	*2nd*	*3rd*	on PF *(from TG analysis)*
In-PF-Fe^0	-	360–450 °C	500–800 °C	13. 26
Ex-PF-Fe^0	-	360–450 °C	500–800 °C	*15.10*
In-PF@Dr-Fe^0	60-150 °C	360–450 °C	500–800 °C	17.80
Ex-PF@Dr-Fe^0	60-150 °C	360–450 °C	500–800 °C	24.70

However, a comparative study of the result reveals that, among *in-situ* and *ex-situ* reduced samples, *in-situ* reduced samples showed lower Fe% than *ex-situ* reduced samples indicating that, *ex-situ* reduction method integrates more iron particles than *ex-situ* methods as consistent with the claim in EDX analysis. These results further validate that, higher amount of iron particles can be entrapped in PF through the *ex-situ* reduction method (in a common condition). In a separate comparison, results show that samples prepared with dendrimer showed comparatively higher iron particles than samples prepared without dendrimer. This means, TG analysis also provides evidence regarding the effectiveness of dendrimer in increasing the loading of iron particles, which has been claimed in earlier characterizations.

4.1.3.3. Section (iii): Application of Fe^0 immobilized PF on wastewater treatment

Resultant Fe^0 immobilized PF samples were used as catalysts in heterogeneous Fenton-like removal of pollutants from water in presence of hydrogen peroxide (H_2O_2). Malachite green (MG) dye was used as a model pollutant. The efficiency of Fe^0 immobilized PF in Fenton-like removal of MG dye was comparatively studied. Decoloration, removal kinetics, and mechanism of heterogeneous Fenton-like removal of MG dye have been measured or postulated based on the data availed from the UV-vis spectrophotometer. Toxicity reduction, as well as recyclability and reusability of Fe^0, immobilized PF was investigated as well. The results of this section will pave the way to the selection of an efficient reduction method (*in-situ /ex-situ*) for immobilization of Fe^0 on PF for environmental and green chemistry application.

UV-visible spectroscopy

To investigate the potential applications of Fe^0 immobilized PF, resultant samples (In-PF-Fe^0, Ex-PF- Fe^0, In-PF@Dr-$Fe^{0,}$ and Ex-PF@Dr-Fe^0) were used as a catalyst in heterogeneous Fenton-like removal of malachite green dye in water. The fenton-like reaction involves the combined use of ferrous ions and hydrogen peroxide (H_2O_2) to produce highly oxidation potential active oxygen species capable of degrading organic contaminants. Malachite green is a common basic organic dye-containing aromatic ring, which is resistant to traditional chemical and biological removal methods [309]. UV-visible spectroscopic analysis was used to study the decoloration of malachite green. Results obtained from UV-Visible spectroscopy are in Figure 4.10.
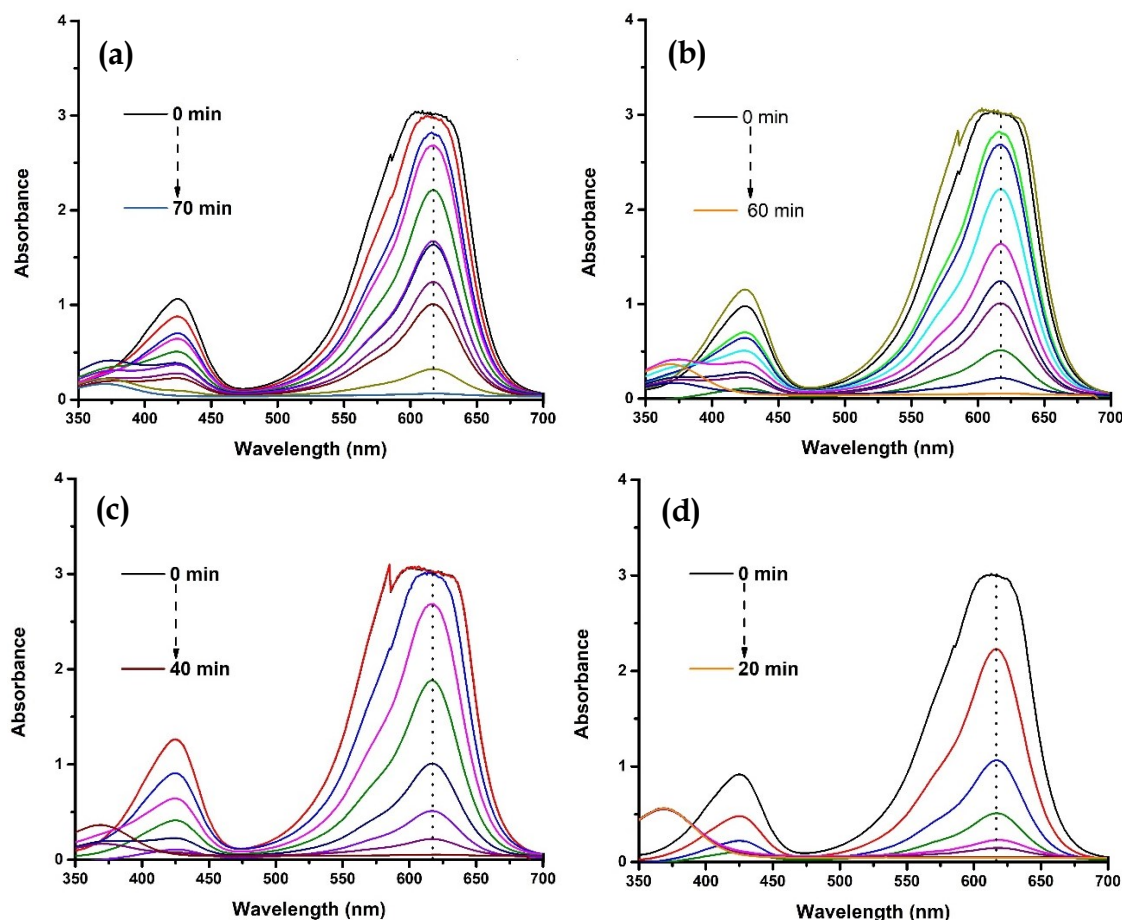
Figure 4. 10: UV-visible spectroscopy of Fenton-like removal of MG dye (λ_{620nm}) using (a) In-PF-Fe^0, (b) Ex-PF-Fe^0, (c) In-PF@Dr-Fe^0 and (d) Ex-PF@-Fe^0. Conditions: MG dye = 20 mg/L, Sample = 1 cm^2, H$_2$O$_2$ = (0.5 mL, 0.3 M).

Results show a characteristic absorption peak of malachite green at $\lambda_{620\,nm}$. It has been observed that the intensity of the peak flattens over 20 to 70 min when exposed to a heterogeneous Fenton-Like system. Four samples required four different treatment times to remove the same concentration of dye from water, which means that, the catalytic performances of the samples are not the same. The fastest removal of dye has been achieved by Ex-PF@Dr-Fe^0 (20 min) followed by In-PF@Dr-Fe^0 (40 min), Ex-PF-Fe^0 (60 min), and In-PF-Fe^0 (70 min). The removal of time corresponds to the number of factors such as speed of producing Fe^{2+}, speed of generation of hydroxyl radicals, and possible mass transfer limitations [176, 310-313]. As a control experiment, PF without iron particles was studied for removal of MG dye in a similar condition, which showed no removal of MG dye. This confirmed that immobilized iron directly participated in the removal of dyes from water. Indeed, the rate of color removal seems to be correlated to the amount of immobilized iron participating in the dye removal reaction.

The kinetics of the dye removal reaction was calculated using Origin 2018 software (version 9.5). The [instant /initial] absorbance ratio of the malachite green band at $\lambda_{620\,nm}$ (A$_t$/A), which accounts for the corresponding concentration ratio (C$_t$/C), allows plotting of Ln(C$_t$/C) as a function of time. Model validation of the pseudo-first-order kinetics for MG dye removal using Fe^0 immobilized PF has been obtained by the linear evolution in time of Ln(C$_t$/C), as supported by R^2 values over 0.98 (see Table 4.6). Plots also show that Fe^0 immobilized PF samples exhibited good linear relationships of Ln(C$_t$/C) versus reaction time following pseudo-first-order kinetics with respect to MG dye removal. These conclusions are consistent with the results found in the literature [82, 289, 314, 315]. As shown in Table 4.6, the Ex-PF@Dr-Fe^0 gives a considerably high catalytic efficiency by removing 98.24% MG dye at a rate constant of 0.1534 min^{-1}. Conversely, the MG dye removal using In-PF-Fe^0, Ex-PF- Fe^0, In-PF@Dr-Fe^0 showed considerable conversion (95.06% in at rate constant of 0.0569 min^{-1}, 96.86% at rate constant of 0.0645 min^{-1}, and 97.31% at rate constant of 0.0847 min^{-1}, respectively). Such a high conversion and rapid kinetics in

catalytic MG dye removal might be attributed to the good stability and immobilization of zero-valent iron particles ensuring the maximum coverage of active radicals for dye removal as supported by high "k" values.

Table 4. 6: Pseudo-first-order kinetics study for the Fenton-like removal of MG dye ($\lambda_{620\ nm}$).

Sample name	Removal Time (min)	MG Removal kinetics	
		*k(min^{-1})	**R^2
In-PF-Fe^0	70	0.0469	0.950
Ex-PF-Fe^0	60	0.0645	0.968
In-PF@Dr-Fe^0	40	0.0847	0.973
Ex-PF@Dr-Fe^0	20	0.1534	0.982

*k is the rate constant is expressed in min^{-1}.

**R^2 is the correlation coefficient of the linear regression.

Mechanism of Fenton-like removal of malachite green dye

Based on the results, a plausible mechanism for heterogeneous Fenton-like removal of MG dye using Fe^0 immobilized PF was postulated. The underlying mechanisms of removal of MG dye in the system of Fe^0 immobilized PF in presence of H_2O_2 were considered. The catalytic degradation of MG dye was attributed to the synergistic effect of the Fenton reaction that takes place in the presence of Fe^0 and H_2O_2 that produced highly reactive •OH radicals that can break the existing chromophore groups and triphenylmethane backbones in MG molecules, thus destroying the structure of MG dye. In the heterogeneous Fenton-like system, the generation cycle of hydroxyl radicals by heterogeneous Fenton-like mechanism and mineralization of MG dye was postulated and presented as Reaction 4.1–4.11. According to the reaction (4.1-4.4), Fe^0 initiated the reaction and lead to the generation of Fe^{2+} which is an integral element for Fenton reaction and •OH radicals formation [316] (see Reaction 4.5-4.9). In a second step, reactive species are formed which are responsible for MG dye degradation, with color removal and subsequent mineralization. For mineralization of the intermediates, a further step might take place where reaction intermediates underwent further oxidation and converted into nontoxic substances (see Reaction 4.10-4.11). The reaction mechanism is shown in the four key steps as follows:

(i)   The process of formation of iron (II) species

$Fe^0 + 2H^+$	$\rightarrow$	$Fe^{2+} + H_2$	(4.1)
$Fe^0 + H_2O_2 + 2H^+$	$\rightarrow$	$Fe^{2+} + 2H_2O$	(4.2)
$Fe^0 + O_2 + 2H^+$	$\rightarrow$	$Fe^{2+} + H_2O$	(4.3)
$Fe^0 + 2Fe^{3+}$	$\rightarrow$	$3Fe^{2+}$	(4.4)
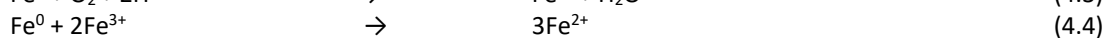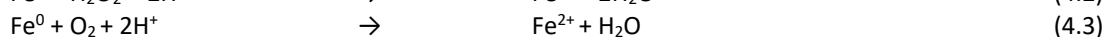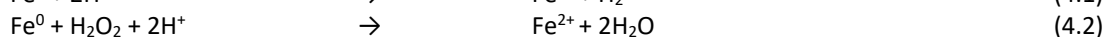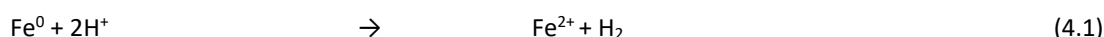
(ii)   The process of producing reactive species

$Fe^{2+} + H_2O_2$	$\rightarrow$	$Fe^{3+} + HO^- +$	•OH	(4.5)
$Fe^{3+} + H_2O_2$	$\rightarrow$	$Fe^{2+} + HO_2{}^\bullet +$	H^+	(4.6)
$Fe^{3+} + HO_2{}^\bullet$	$\rightarrow$	$Fe^{2+} + H^+ + O_2$		(4.7)
$Fe^{2+} + HO_2{}^\bullet$	$\rightarrow$	$Fe^{3+} + HO_2{}^-$		(4.8)
$H_2O_2 + 2H^+ + 2e^-$	$\rightarrow$	$2H_2O$		(4.9)
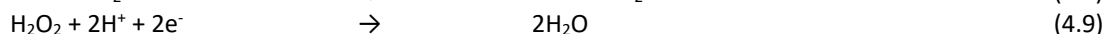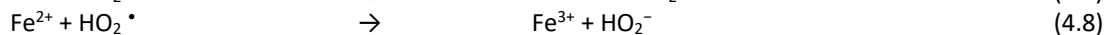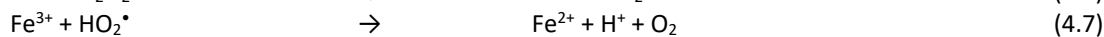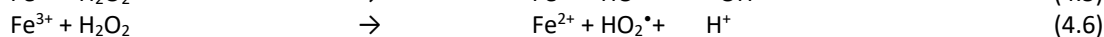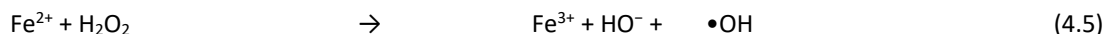
(iii)   The process of color removal of MG dye

MG molecules + •OH	$\rightarrow$	Oxidized MG	(4.10)

(iv)   The process of mineralization

Oxidized MG + •OH	$\rightarrow$	$CO_2 + H_2O$	(4.11)
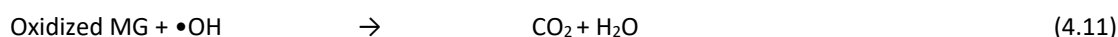
Toxicity reduction analysis

Decoloration implies the destruction of a color-bearing group of MG dye. Mostly the conversion of dye into a colorless organic entity is the result of decoloration of dyes; however, it does not reflect the complete mineralization of dye in nontoxic entities (CO_2 and H_2O). Therefore, it is important to study the toxicity reduction after decoloration of dye or colored pollutants from water. In this thesis, chemical oxygen demand (COD) of the treated and untreated (dye-containing water) water was comparatively studied. Pollutants do not only cause the COD of the treated water, but it can also be due to the leaching of catalyst in the water during treatment. To estimate the leach of iron in water during Fenton-Like removal of MG dye, total dissolved (TDS) analysis was carried out as well. Results from COD and TDS analysis along with color and *pH* of water have been presented in Table 4.7.

Results showed that the heterogeneous catalysts (prepared in this thesis) provided a clear treated water after Fenton-like removal of MG dye whereas the homogeneous Fenton system left yellowish water containing dissolved solids (should be dissolved iron oxides [176] produced during radical generation). These dissolved solid has to be separated from the treated water with additional processes before releasing them for further use. Separated solids known as iron sludge is secondary pollutants from this system, whereas, in the heterogeneous system (using catalyst from this thesis), there was no formation of iron sludge which indeed a significant achievement.

Table 4. 7: Toxicity reduction analysis of water after Fenton-like removal of MG dye.

Sample name	Color	*pH*	TDS (ppm)	Relative COD reduction (%)
Homogeneous Fenton	Yellowish	3	730	-
In-PF-Fe^0	Clear	5	52	29.0
Ex-PF-Fe^0	Clear	5	229	59.6
In-PF@Dr-Fe^0	Clear	5	128	66.2
Ex-PF@Dr-Fe^0	Clear	5	189	54.2

Nevertheless, it requires acidic pH (pH=3) to catalyze a homogeneous Fenton reaction, whereas the resultant heterogeneous catalyst was studied in pH=5. Therefore, during MG dye removal, the pH of the homogeneous Fenton reaction was 3, and the pH of the homogeneous Fenton reaction was 5. The pH of the MG dye removal reaction has reflected on the pH of treated water. The result shows that, treated water with homogeneous Fenton reaction left with high acidic pH, which requires strong neutralization, whereas in heterogeneous Fenton reaction using Fe^0 immobilized textile, the pH of treated water was around 5 which can be released after dilution (discharge standard of pH is pH 6-9) or light neutralization. Needless to say, the *pH* closer to 7 of treated water is more favorable to achieve discharge standard of *pH* [82, 311] which will eventually reduce the cost and increase the potential of large-scale application.

Total dissolved solids (TDS) analysis of treated water reveals that high TDS (730 ppm) has been found in water treated with homogeneous Fenton system, whereas a comparatively lower TDS has been recorded in heterogeneous Fenton treated water. While comparing the four heterogeneous catalysts, it can be seen that, among all, the lowest TDS has been found in In-PF-Fe^0 (52 ppm) followed by In-PF@Dr-Fe^0 (129 ppm) and Ex-PF@Dr-Fe^0 (189 ppm). A 440% increase in TDS has been noticed in Ex-PF- Fe^0 (229 ppm) as compared to In-PF-Fe^0. The increase in TDS can be explained by the leaching of immobilized iron particles from PF during removal reaction and later conversion into oxides. A clear pattern in TDS analysis shows that, as compared to *ex-situ* reduced samples, *in-situ* reduced samples showed lower TDS which indicates high leaching stability of iron particles in PF. In addition, when two *ex-situ* reduced samples were compared, dendrimer grafted samples showed lower TDS but an opposite phenomenon was observed in the case of *in-situ* reduced samples. These findings conclude that there is no significant effect of dendrimer grafting in the TDS parameter (corresponds to leaching of iron particles). However, COD reduction has been negative in the homogeneous catalysis, which means the total amount of COD has increased in the homogeneous Fenton-system (compared to untreated water). This is most probably due to the interference of iron oxides during the COD test. The relative reduction in COD for water by each PF sample was calculated by referring to the COD of untreated water as 100%. Results shown in Table 4.7 reveal that, where there

is no COD reduction in the homogeneous Fenton system, heterogeneous catalysts (In-PF-Fe^0, Ex-PF-Fe^0, In-PF@Dr-Fe^0, and Ex-PF@Dr-Fe^0) showed a considerable COD reduction (up to 66.23%). The highest COD reduction was achieved by In-PF@Dr-Fe^0 (66.23%) and the lowest was by In-PF- Fe^0 (29%).

Recyclability and reusability of Fe^0 immobilized polyester nonwoven fabrics

One of the important advantages of immobilization of catalysts is the possibility to be recovered and reused. Here, the reusability of Fe^0 immobilized PF samples (In-PF-Fe^0, Ex-PF- Fe^0, In-PF@Dr-Fe^0, and Ex-PF@Dr-Fe^0) were studied in heterogeneous Fenton-like removal of MG dye. The result shows the potential reusability of Fe^0 immobilized PF samples for seven cycles without significantly losing the performance of MG dye removal. The best reusability was provided by In-PF@Dr-Fe^0 and Ex-PF@Dr-Fe^0 samples. A confirmation in this regard was obtained from the morphological analysis where the presence of a considerable amount of iron particles was found on the fiber surface of all samples, which endorses their potential reusability. Further details about the reusability of the catalysts are available in Publication II.

4.1.4. Discussion: Study A

The purpose of this study was to find a suitable reduction method for the stabilization and immobilization of zerovalent iron particles on polyester nonwoven fabric. Based on the available literature on the reduction synthesis of zerovalent iron particles, sodium borohydride (NaBH$_4$) was used as the reducing agent [293, 317]. The hydrophobic surface of the polyester nonwoven fabric was activated through resource-efficient plasma eco-technology instead of the harsh chemical alkaline hydrolysis activation process. Plasma activation of polyester fabric is a well-established and well-documented technology. Our results show that the plasma treatment created polar groups (-COO, -COOH, -OH) on the surface of the PET fibers, as concluded through multiple analysis methods (sessile droplet goniometry, capillary uptake, FTIR, and EDX). Radicals were created on the surface of the polyester fibers, which triggered the rupture of the ester bond in the polyester, as described by Leroux *et al.* (2009) [88]. These radicals were converted into polar groups through the interaction with O$_2$ from the air that had been used as gas discharge. These polar groups allow the polyester fabric to undergo dipolar interactions, van der Waals forces, or hydrogen bonding with water and other materials, thereby activating the surface.

As indicated in Riccardi *et al.* (2003) [318], Sanchis *et al.* (2006) [319], Leroux *et al.* (2009) [88], and many other reports [66, 320], the functional groups created are prone to suffer an aging process due to the reorganization of the surface polar groups that tend to bury themselves below the surface. This is why hyperbranched dendrimer grafting was subsequently carried out, ensuring the durability of the activated state of the polyester, as we provided additional hydrophilic surface functional groups from the characteristic chemical structure of the dendrimer used in this study. XPS analysis reveals the further increase in atom% of O dendrimers were grafted, which confirms the integration of additional hydrophilic surface functional groups. This is further supported by the higher wettability (low water contact angle, high capillary uptake) of the dendrimer-grafted polyester fabric compared with the plasma-activated polyester fabric.

Analysis of the reduction-immobilization of zerovalent iron particles on activated polyester nonwoven fabric (activated by either plasma alone or plasma with dendrimers) showed that the use of reduction methods (both *in-situ* and *ex-situ*) to produce zerovalent iron particles has synergistic effects on the performance of the immobilization on the PF. Characterization of the samples by various tools confirms that the method of reduction of iron ions affects the overall morphology, distribution, and sizes of the iron particles. We found that *in-situ* reduction-immobilization results in uniform distribution of iron particles without any cluster or aggregates, whereas the opposite was observed in *ex-situ* reduced-immobilized iron particles. Furthermore, *in-situ*-reduced iron particles were observed to be essentially localized only on the surface of polyester nonwoven (the pores of the nonwoven remained intact in most cases). However, *ex-situ*-reduced iron particles were detected both on the

fiber surface and in the pores of nonwoven. These changes in particle size and the cluster formation were related to the molar concentration of $NaBH_4$. A higher concentration of $NaBH_4$ in *in-situ* reduction (higher than the stoichiometric requirement) reacted with water molecules, resulting in the formation of hydrogen gas. This increased the collusion of particles, leading to aggregation, as explained by Turabik *et al.* (2017) [317].

Dendrimer grafting on PF was found to positively influence the stability, loading, and dispersion of iron particles, but did not affect the size of the iron particles during the reduction-immobilization. Another conclusion related to the effect of surface chemical properties of PF in overall performance in applications of zerovalent iron immobilized textile in pollutant removal as they (zerovalent iron immobilized textile) integrated more iron particles in the textile surface.

As reported in numerous other studies [321], nanoscale iron particles are replacing micro iron particles and have proven to be a fairly effective reductant and catalyst for a wide variety of common environmental contaminants, including chlorinated organic compounds and metal ions [322]. In this study, samples with immobilized zerovalent iron particles on polyester nonwoven fabric acted as catalysts in the removal of pollutants from water. The highest catalytic efficiency of Ex-PF@Dr-Fe^0 during the removal of MG was also found to be correlated to the efficiency of iron immobilization (stability, size, and loading percentage). Furthermore, both the reduction method and the surface modification with dendrimers affected the catalytic efficiency of iron particles immobilized on PF in the removal of MG dye in a heterogeneous Fenton-like system (as observed in the results). However, the toxicity reduction analysis (based on TDS and COD analysis) was inconclusive. Although a clear pattern was observed in the decolorization of the dye, the toxicity reduction and leaching analyses yielded no clear results. Therefore, in our next study, we focused on tailoring the surface of the PF using polymers with specific terminal end functional groups for the robust immobilization of zerovalent iron particles on polyester nonwoven fabric.

4.2. <u>Study B</u>: Tailoring the surface of polyester nonwoven fabric with amine/thiol groups for the immobilization of Fe^0

4.2.1. Introduction

A tailor-made surface with favorable surface functional groups may contribute to the robust immobilization of zerovalent iron on polyester nonwoven fabric, leading to higher loading, better dispersion, and greater stability of the immobilized Fe^0 particles.

For that, the integrated surface functional groups must remain stable for a relatively long time, and the interactions between zerovalent iron nanoparticles and the functional groups on the surface must be strong enough to keep the iron particles anchored to the surface during catalytic application [323]. (3-aminopropyl)triethoxysilane (APTES) is one of the most popular linkage reagents for metal particle immobilization. It provides amine groups for immobilizing the metal particles, while the three hydrolyzable ethoxy groups ensure robust anchoring of the silane to the surface of the support matrix [193]. Another interesting functionality comes from thiol groups, which can also bind metal particles to the surface through strong covalent bonding [324, 325]. Polyamidoamine (PAMAM) dendrimers constitute one family of dendrimers that have been used to stabilize small metal clusters of a defined size. Consisting of an ethylenediamine (EDA) core with repeating amidoamine branches, PAMAM dendrimers have been shown to act as hosts to many metal ions, including Cu^{2+}, Pt^{2+}, Pd^{2+}, Ni^{2+}, Fe^{2+}, Au^{3+}, and Ru^{3+} [326]. Upon chemical reduction of the metal ion/dendrimer complexes, the PAMAM polymer matrix encapsulates and subsequently stabilizes the metal clusters, preventing agglomeration [327].

Although these polymers have proven useful in many instances, their application in immobilizing inorganic catalysts on textile supports, particularly zerovalent iron particles, has not been studied before now. Therefore, we tailored the surface of the polyester nonwoven fabric with polyamidoamine dendrimers, 3-(aminopropyl)triethoxysilane, and 1-thioglycerol, to help immobilize Fe^0 particles and explore their catalytic activity in both oxidative and reductive pollutant removal systems. Statistical modeling of the oxidative system (to identify the influence of key factors in the pollutant removal) has been carried out through a full factorial experiment design. The success of tailoring the surface of the polyester nonwoven fabric was evaluated through various characterization methods, including sessile droplet goniometry, optical microscopy (OM), scanning electron microscopy (SEM), Fourier transforms infrared (FTIR) spectroscopy, ζ potential, wettability analysis, thermogravimetric analysis (TGA), and differential scanning calorimetry (DSC). The results of study B have been published in Publications III, IV, and V.

4.2.2. Material preparation

Polyamidoamine dendrimer, 3-(aminopropyl)triethoxysilane and 1-thioglycerol were dispersed on plasma-activated PF surface to endure a tailor-made surface with specific functionality. A schematic illustration describing preparations of tailor-made PF surface for immobilization of Fe^0 particles is demonstrated in Figure 4.11. Typically, activation of PF surface was carried out through atmospheric pressure (air) plasma treatment using Coating Star atmospheric pressure plasma treatment machine manufactured by Ahlbrandt System (Germany) according to the treatment parameter provided in *section 3.2.1 of* chapter 3. Before activation, PF was cleaned through Soxhlet extraction by the virtue of solvent (petroleum ether) vaporization and condensation process as per the method described in *section 3.2.1* of chapter 3. Chemical grafting of both amine (PAMAM and APTES) and thiol (SH) group-rich polymers has been carried out according to the methods described in *section 3.2.2* of chapter 3. After

successful dispersion of either PAMAM, APTES, or SH on PF, resultant PF was used for immobilization of Fe^0 particles through the *in-situ* reduction-immobilization method as described in section 3.2.1 of chapter 3.
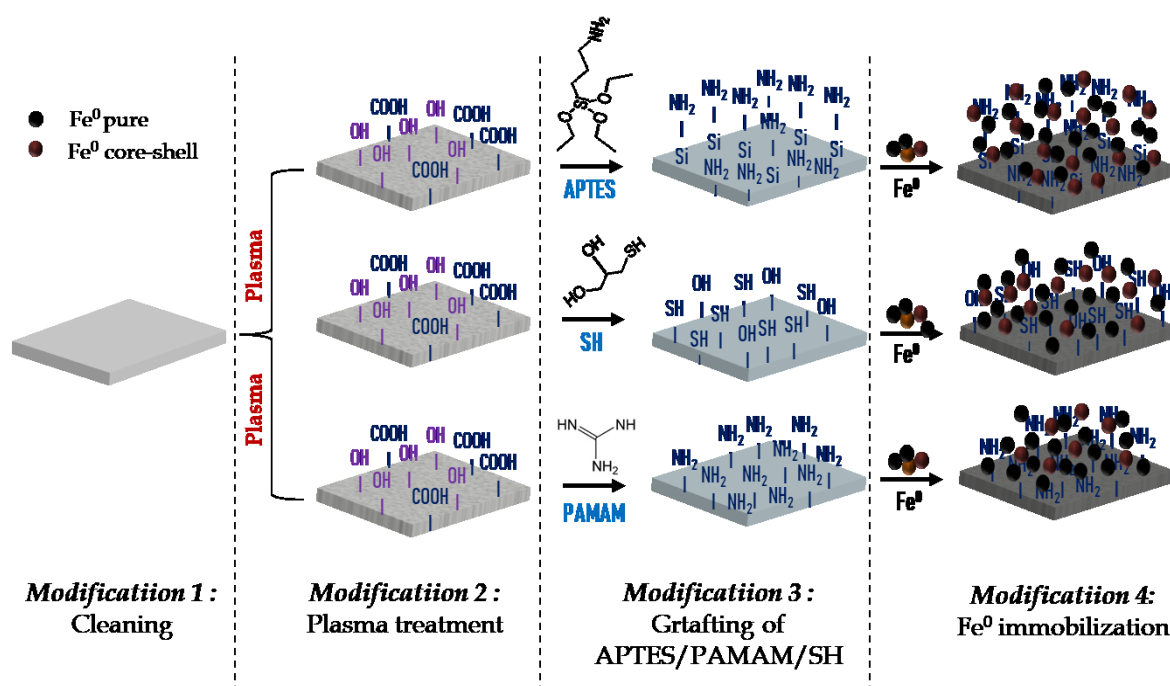
Figure 4. 11: Schematic illustration of surface activation, modification, and immobilization of Fe^0 particles on PF.

4.2.3. Results: Study B

Following the same model of Study-A, the results of study-B have also been provided in three different sections. Section (i) and section (ii) presents the results related to the characterization of as obtained catalysts, whereas section (iii) provides results related to the application of Fe^0 immobilized PF as catalysts in both oxidative (Fenton-like) and reductive (catalytic reduction) removal of pollutants from water. Common terminology of samples was set (see Table 4.8) based on their underwent modifications.

Table 4. 8: Sample names and corresponding descriptions.

Sample Name	Descriptions		
	Modification-1	Modification-2	Modification-3
Untreated PF	Pristine	-	-
PF@AP	Plasma treatment		-
PF-NH$_2$	Plasma treatment	PAMAM grafting	-
PF-Si-NH$_2$	Plasma treatment	APTES grafting	
PF-SH	Plasma treatment	Thioglycerol grafting	-
PF-Fe^0	Plasma treatment	-	Fe^0 immobilization
PF-NH$_2$-Fe^0	Plasma treatment	PAMAM grafting	Fe^0 immobilization
PF-Si-NH$_2$-Fe^0	Plasma treatment	APTES grafting	Fe^0 immobilization
PF-SH-Fe^0	Plasma treatment	Thioglycerol grafting	Fe^0 immobilization

4.2.3.1. Section (i): Characterization of tailor-made polyester nonwoven fabric

Characterization of PF before and after PAMAM, APTES, or SH grafting was carried out through series of tools and techniques that includes; sessile droplet goniometry, optical microscope (OM) and scanning electron microscope (SEM), Fourier transform infrared (FTIR) spectroscopy, thermogravimetric analysis (TGA) and differential scanning calorimetry (DSC).

The wettability of PF before and after PAMAM (-NH$_2$), APTES (Si-NH$_2$), or SH grafting based on the contact angle of deposed water drop into the surface was investigated based on sessile droplet goniometry. Results presented in Figure 4.12 show that plasma-activated PF is hydrophilic in nature showing characteristics of water contact angle ($\theta_{H_2O}= 0°$). Study-A already discussed the results related to activation of PF by plasma treatment. The hydrophilic surface of PF turned into hydrophobic after tailoring the surface with chemical grafting of PAMAM, APTES, or SH. This change in surface features corresponds to the successful grafting of all three polymers as supported by previous studies [193, 328, 329]. The θ_{H_2O} recorded for PF-NH$_2$, PF-Si-NH$_2$ and PF-SH are 98.0°, 110.5° and 101.7°, respectively.

(a) **(b)** **(c)** **(d)**
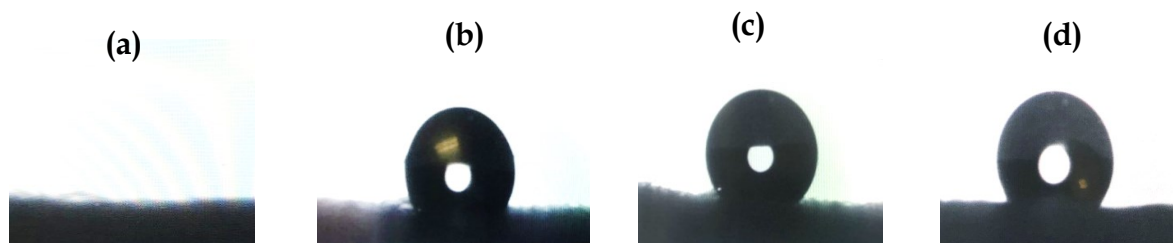
Figure 4. 12: Water contact angle analysis of PF based on sessile droplet goniometry; (a) PF@AP, (b) PF-NH$_2$, (c) PF-Si-NH$_2$, and (d) PF-SH.

Conclusive investigation of grafting on either PAMAM, APTES, or SH on PF surface was carried out through Fourier transform infrared (FTIR) spectroscopy analysis. Resultant spectra assembled in Figure 4.13 for better comparison show the presence of strong peaks at 712–1242 cm^{-1}, 1650–1713 cm^{-1} in all samples corresponding to ether, carboxyl, and carbonyl groups in ester [330]. Detailed analysis of the peaks reveals that bands at 1410 cm^{-1} and 1577 cm^{-1} represent the C–C and C–H bond stretching vibration of the phenyl ring. On the other hand, the band at 1239 cm^{-1} and 1095 cm^{-1} is due to C–O stretching [331]. Furthermore, presumably asymmetrical and symmetrical stretching of CH$_2$ and CH$_3$ appeared at 2951 cm^{-1} and 2848 cm^{-1} respectively. The above analysis provides evidence of the characteristics of polyester fabric. Moreover, characteristic stretching of O–H groups near 3428 cm^{-1} has also been observed in all samples. The presence of O–H groups confirms the presence of hydrophilic groups (either –COOH or –OH) due to plasma activation. Analyzing spectra of PF-NH$_2$ and PF-Si-NH$_2$ reveals that, along with other peaks of PF, new peaks are appearing around 3100 cm^{-1} to 3700 cm^{-1} regions. The high intensity and clear peaks around corresponds to the primary amino groups (-NH$_2$) [332] which can be either from PAMAM or APTES on respective samples. However, the spectra of APTES-grafted PF showed a change on the peaks at 957 cm^{-1}, suggesting the presence of Si-OH stretching vibration, whereas the peaks at 3396 cm^{-1} and 1633 cm^{-1} are attributed to the O-H vibration. The peaks obtained at 1070 cm^{-1} and 800 cm^{-1} are attributed to the stretching vibrations of Si-O-Si most probably corresponding to the silica network created around the polyester fibers during the chemical modification process [193]. On the other hand, the prominent broad band around 3600–3000 cm^{-1} and a minuscule vibration band at 2535 cm^{-1} has been observed in PF-SH samples, the new peaks correspond to O–H and S–H [333] which might be attributed to 1-thioglycerol. The above discussion gives sufficient evidence to conclude the successful grafting of PAMAM, APTES, or SH on PF surface. These grafted polymers provide a tailor-made surface of PF with either amine or thiol functional groups. The effect of tailor-made surfaces on the physical behavior of PF (such as wettability and thermal property) has also been studied through thermogravimetric analysis and sessile droplet goniometry (discussed in the later part).
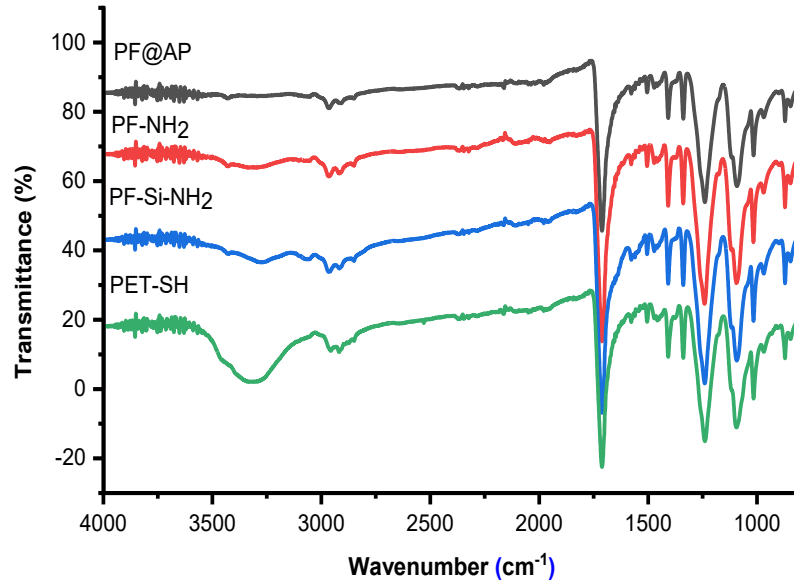
Figure 4. 13: FTIR spectra of polyester nonwoven fabric before and after chemical grafting of either PAMAM, APTES, or SH; Here (a) PF@AP, b) PF-NH$_2$, (c) PF-Si-NH$_2$, and (d) PF-SH.
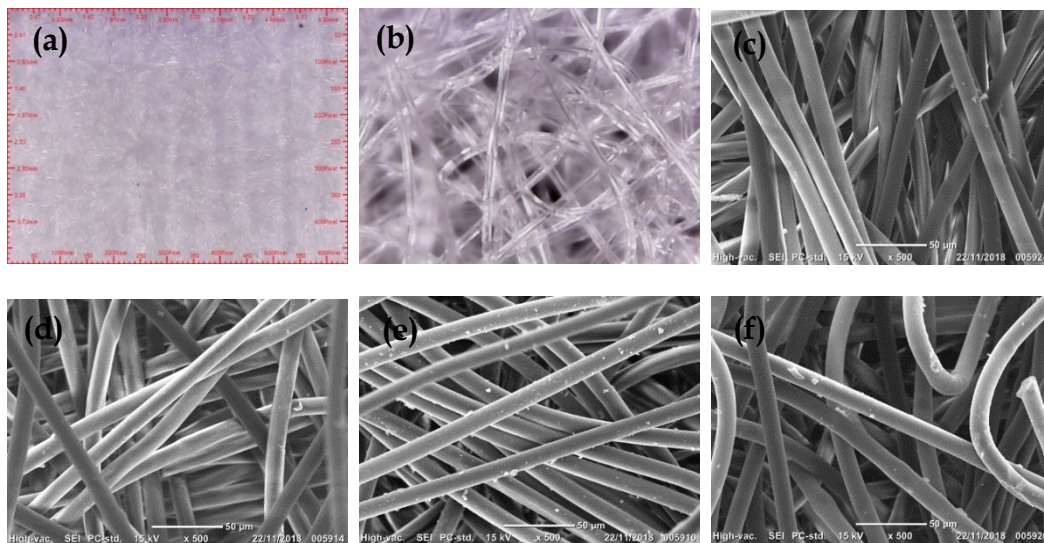
Figure 4. 14: OM and SEM images of polyester nonwoven fabric before and after chemical grafting of APTES, PAMAM or SH; (a-c) PF@AP, (d) PF-NH$_2$, (e) PF-Si-NH$_2$ and, (f) PF-SH.

The morphological analysis of polyester nonwoven fabric before and after chemical grafting of either APTES, PAMAM, or SH was carried out through a digital optical microscope (OM) and scanning electron microscope (SEM). The instrument and protocol used to gather OM and SEM images have been described in section 3.3.1 of chapter 3. Images presented in Figure 4.14 shows that untreated PF has a randomly oriented network of fibers with a smooth surface. However, after grafting of PAMAM, APTES, or SH on PF, a distribution of white-like grains on the fiber surface has been detected. Since those grains appeared on the PF surface after chemical grafting of respective polymers, one can assume that the white-like grains on the PF surface could be PAMAM, APTES, SH on PF-NH$_2$, PF-Si-NH$_2$, and PF-SH, respectively.
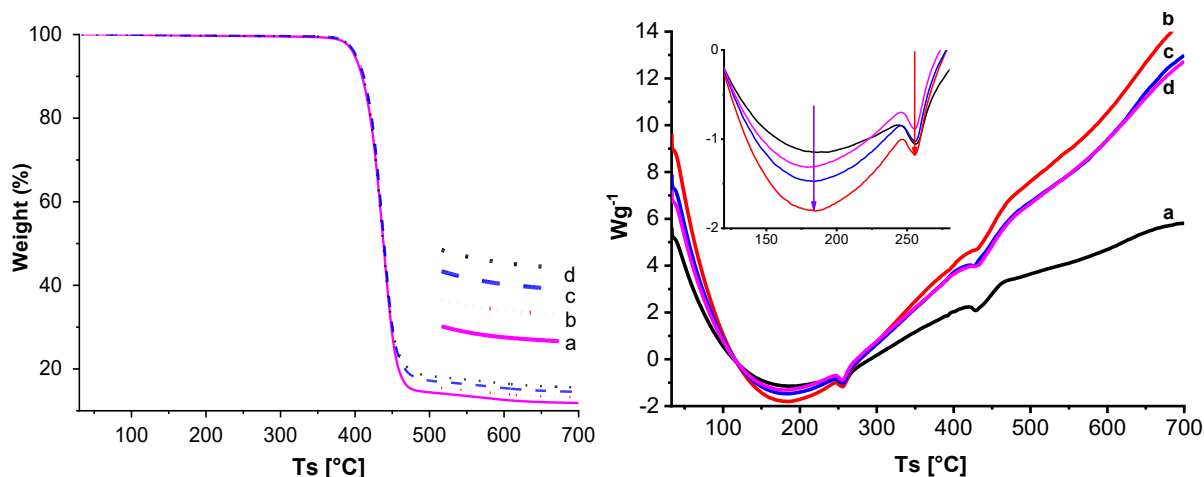
Figure 4. 15: (Left) TGA and (Right) DSC analysis of PF samples (a) PF, (b) PF-NH$_2$, (c) PF-Si-NH$_2$, and (d) PF-SH.

Thermal behavior of the PF after tailoring the surface with PAMAM, APTES, or SH was investigated through thermogravimetric analysis (TGA) and differential scanning calorimetry (DSC). Results from TGA and DSC analysis presented in Figure 4.15 show three mass loss regions located around 60–150°C, 350–450°C, and 500–700°C for all samples. The first weight loss region below 100°C can be explained by the evaporation of superficial water present in the sample while the other regions might be associated with the decomposition of the fiber constituents [334]. A closer look at the wt.% indicates that the lower total weight losses in PF-NH$_2$, PF-Si-NH$_2$, and PF-SH than that of PF indicating the thermal stability improvement. When compared among the PAMAM, APTES or PF-SH grafted samples, SH showed the highest thermal stability improvement followed by PF-Si-NH$_2$ and PF-NH$_2$. Additionally, DSC measurements showed that the maximum heat flow was higher for all the modified materials than the untreated PF. Therefore, increased thermal stability was confirmed after grafting of PAMAM, APTES, or SH. Summary from wettability, IR analysis, the morphological and thermal analysis provides substantial evidence of successful tailoring of PF surface using Polyamidoamine dendrimer, 3-(aminopropyl)triethoxysilane, and 1-thioglycerol which will be used for immobilization of Fe^0 (as discussed in the following section).

4.2.3.2. Section (ii): Results and analysis related to immobilizing Fe^0 on tailor-made polyester nonwoven fabric

To apprehend the changes in the surface of PF samples due to the immobilization of Fe^0, morphological analysis of the resultant samples was conducted through various tools. Figure 4.16 presents the images from the digital optical microscope (OM), scanning electron microscope (SEM) and particle size distribution histogram of Fe^0 immobilized PF based on high-resolution scanning electron microscope through ImageJ-image processing software. Visual analysis of OM images displays that, Fe^0 immobilized PF showed brownish-colored irregularly shaped layered clusters in the surface of PF. These clusters are probably Fe^0 particles that are immobilized on PF.

SEM images reveal that integration of Fe^0 particles on PF surface induced a thorough change in surface morphology, resulting in the formation of bulkier clusters of much smaller size particles. This trend can be explained in terms of the appearance of strong interaction between iron particles and functional groups in the surface (Fe: NH$_2$|SH) due to PAMAM, APTES, or SH grafting, that promotes not only the structural morphology of iron particles but also particle binding and interaction. This suggests a predominantly physical and non-stoichiometric condensation of Fe^0 particles through interaction with the organic entanglement. Modification of PF and crosslinkers used showed slight differences in the dispersion of the Fe^0 particles. While comparing the surface morphology among PF-Fe^0, PF-Si-NH$_2$-Fe^0, PF-NH$_2$-Fe^{0,} and PF-SH-Fe^0, it can be seen that all the samples

have an uneven distribution of particles, both on the surface of the fibers as well as within the inter-fiber pores. Immobilization and entrapment of iron particles certainly increase the loading efficiency, which in turn will translate into the catalytic property. Along with the dispersion, a distinct variation in shapes and aggregates has also been noticed. The shape of the iron particles in PF-NH$_2$-Fe^0 and PF-SH-Fe^0 was found to have more stable spherical shapes with fewer aggregates than that of PF-Si-NH$_2$-Fe^0 and PF-Fe^0, which can lead to higher stability of iron particles when immobilized on PAMAM and 1-thioglycerol grafted surface.
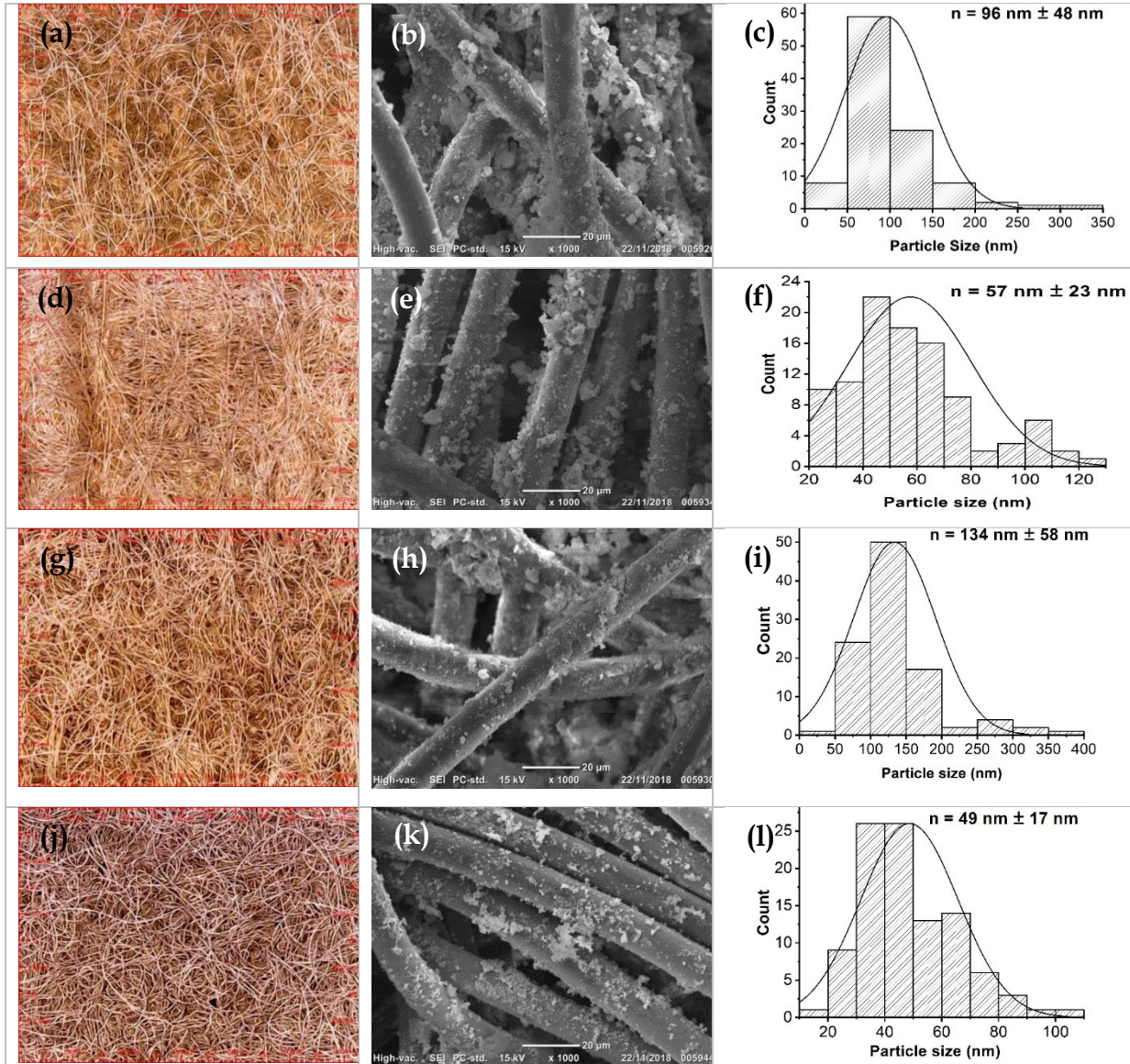
Figure 4. 16: OM, SEM images and particle size distribution histogram of Fe^0 immobilized PF; (a-c) PF-Fe^0, (d-f) PF-Si-NH$_2$-Fe^0, (g-i) PF-NH$_2$-Fe^0 and (j-l) PF-SH-Fe^0; (n represents size of the particles).

The size distribution histograms of the iron particles show an irregular distribution of iron particles with an average size ranges from 10-150 nm. Given the inverse relationship between size and the dispersion of the particles, aggregation of several small particles into one big particle can be the cause for bigger particle size in samples. Analysis of individual samples reveals that the finest iron particles (49±17 nm) size of iron particles were deposited on PF-SH-Fe^0 followed by PF-Fe^0 (96±23 nm), PF-Si-NH$_2$-Fe^0 (57±23 nm), and PF-NH$_2$-Fe^0 (134±58 nm) which indicates less agglomeration of nanoparticles and better stability. On the other hand, studies to investigate the

changes in fiber diameter due to the immobilization of the iron particles reveals that there was a noticeable increase (about 9.6%) in fiber diameter due to the deposition of the iron.

The element composition and the nature of the chemical bonding of Fe^0 immobilized PFs were evaluated by X-ray photoelectron spectroscopy (XPS). The main photo-peaks are presented in relative atomic content (a.t%) and summarized in Table 4.9. Results show predominant C1s, O1s, and Fe2p spectra in all samples, which indicates successful immobilization of Fe^0 in all samples. However, a variation in the content that has been observed could be related to the grafting and loading efficiency of Fe^0 particles on the PF surface. A close look at the results shows that, highest 9.3 a.t% of Fe2p was recorded for PF-Si-NH$_2$-Fe^0 followed by PF-SH-Fe^0 (9.0 a.t%), PF-NH$_2$-Fe^0 (5.6 a.t%)and PF-Fe^0 (4.8 a.t%). It is worth mentioning that, in both PF-NH$_2$-Fe^0 and PF-Si-NH$_2$-Fe^0 there has been a detection of N1s of 1.6 a.t% and 0.6 a.t%, which could be due to the presence of amine from PAMAM and APTES. On the other hand, PF-SH-Fe^0 showed a small amount of S2p, which may be due to the presence of SH in thioglycerol. These results conclusively support the claim of successful grafting of PAMAM, APTES, or SH on plasma-activated polyester nonwoven fabric, as well as immobilization of Fe^0.

Table 4. 9: Relative atomic content (a.t%) of the surface chemical composition of the samples (from XPS analysis).

Sample Name	C (a.t %)	O (a.t %)	Fe (a.t %)	N (a.t %)	Si (a.t %)	S (a.t %)
PF-Fe^0	22.8	53.8	4.8	-	-	-
PF-NH$_2$-Fe^0	57.2	34.3	5.6	1.6	-	-
PF-Si-NH$_2$-Fe^0	38.2	42.7	9.3	0.6	2.1	-
PF-SH-Fe^0	51.2	36.0	9.0	-	-	0.9
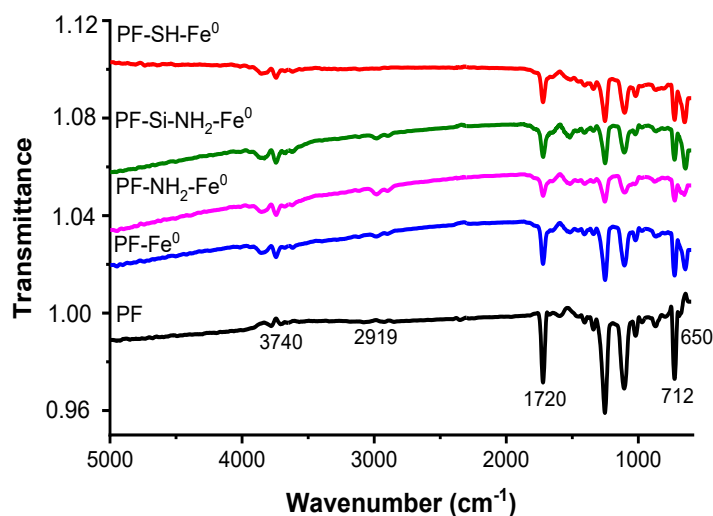
Figure 4. 17: FTIR spectra of PF, PF-Fe^0, PF-NH$_2$-Fe^0, PF-Si-NH$_2$-Fe^0, and PF-SH-Fe^0.

Infrared studies of Fe^0 immobilized PF samples were carried out to identify the concentration and nature of the functional groups. The FTIR analysis of PF-Fe^0, PF-NH$_2$-Fe^0, PF-Si-NH$_2$-Fe^0, and PF-SH-Fe^0 with having PF as a reference has been displayed in Figure 4.17. The PF demonstrated some bands in the 1720-650 cm^{-1} region which were attributed to the stretching vibration of CH$_2$, C=O, and aromatic C=C, indicating the structure of polyester fibers [335, 336]. On the other hand, marked changes are registered after the incorporation of iron nanoparticles, with a slight decay in band intensity noticed for the 3740 cm^{-1} and 2919 cm^{-1} peak associated with the asymmetric stretching vibration of NH$_2$ and C-H aliphatic groups [337]. This was a significant signal that suggests compaction of the organic entanglement, most likely due to the appearance of strong interactions between iron nanoparticles and hydroxyl groups Fe: OH, and metal with amine Fe: NH$_2$ [308, 336, 338, 339]. Thus, agglomeration of nanoparticles can easily produce, as supported by OM and SEM microscopy. Hence, shifts of the OH stretching band from 3734 cm^{-1} for PF-SH-Fe^0 to 3745 cm^{-1} towards higher wavenumbers provided evidence in this regard.

Moreover, the intensity of C-H, C=O, and C-O bands was decreased after Fe loading, suggesting the interaction of Fe with N-H, C-N, and O-H groups of the C-H chain. The same trend was already reported in the literature for metallic nanoparticles, which interact with NH_2, CH, and OH groups [308, 334, 338-340]. Afterward, these results demonstrate that both amine (-NH_2) or thiol (-SH) grafting and Fe^0 particles insertion contribute to the stabilization, due to the strong Fe: SH|NH_2 interaction and structure compaction around Fe^0, and possible synergy between the N, S and O atoms in Fe^0 stabilization remains to be elucidated. Particularly, this effect was more pronounced for thioglycerol grafting.
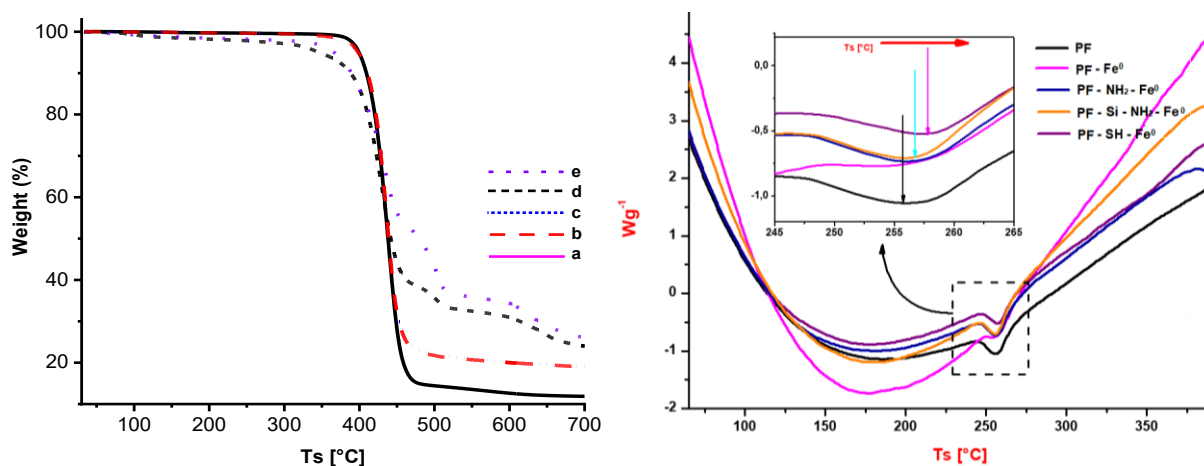
Figure 4. 18: (Left) Thermogravimetric analysis of PF samples; (a) PF, (b) PF-Fe^0, (c) PF-NH_2-Fe^0, (d) PF-Si-NH_2-Fe^0 and (e) PF-SH-Fe^0 and (Right) DSC analysis of PF, PF-Fe^0, PF-NH_2-Fe^0, PF-Si-NH_2-Fe^0 and PF-SH-Fe^0.

Table 4. 10: Summary of particle size and w/w (%) of Fe^0 immobilized on PF.

Sample name	Weight loss regions (TG analysis)			w/w % of immobilized Fe^0 on PF *(from TG analysis)*
	1st	*2nd*	*3rd*	
PF-Fe^0	50-150 °C	350–500 °C	500–800 °C	18.94
PF-NH_2-Fe^0	50-150 °C	350–500 °C	500–800 °C	19.02
PF-Si-NH_2-Fe^0	50-150 °C	350–500 °C	500–800 °C	24.12
PF-SH-Fe^0	50-150 °C	350–500 °C	500–800 °C	26.10

Thermal behaviors of Fe^0 immobilized PF samples were studied through thermogravimetric analysis (TGA) and differential scanning calorimetry (DSC) (see Figure 4.18). Along with the thermal behaviors, the loading of Fe^0 in terms of the amount of Fe^0 deposited on PF-Fe^0, PF-Si-NH_2-Fe^0, PF-NH_2-Fe^0, and PF-SH-Fe^0 were studied through thermogravimetric analysis (TGA). Analysis of PF has been conducted as well as a reference sample. TGA graph shows that grafting of amine/thiol and immobilization of Fe^0 particles played an important role to improve the thermal stability of PF. Three mass loss regions were observed for all the samples, which are located around 60–150°C, 350–500°C and 500–700°C. The first weight loss region below 100°C can be explained by the evaporation of superficial water present in the sample while the other regions might be associated with the decomposition of the fiber constituents [334].

As summarized in Table 4.10, the total weight loss of the samples is not the same, as a concept, the highest weight loss corresponds to the lowest loading of the additional materials, for this case iron particles. Regarding the PF sample, PF-Fe^0 had the highest weight loss (with residual content of 18.94%) as compared to its counterparts. The lowest weight loss was recorded for PF-SH-Fe^0, which translates to the high residual content (26.10%) of Fe^0. The reason for the high loading of enzyme on PF-SH-Fe^0 can be related to the possible synergy between the S and O atoms present in the tailor-made PF surface. Additionally, DSC measurements showed that the maximum heat flow was higher for all Fe^0 immobilized PF samples than the reference PF, which attributes to the increased thermal stability. These results show that the chemical grafting of APTES, PAMAM, or SH and immobilization of iron particles have a synergetic effect which leads to thermal stability improvement of polyester nonwoven fabrics.
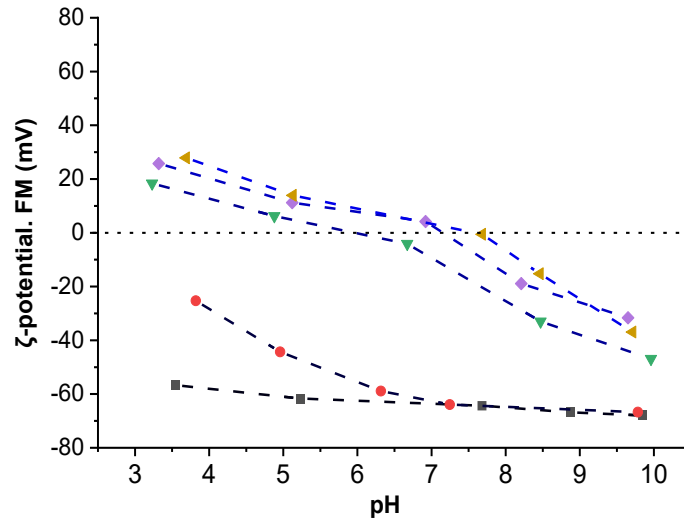
Figure 4. 19: The ζ-potential value of samples as a function of the pH of the electrolyte solution; (■) Untreated PF, (●) PF@AP, (▼) PF-NH$_2$-Fe^0 (◆) PF-Si-NH$_2$-Fe^0 and, (◄) PF-SH-Fe^0.

The isoelectric point (iep = $pH|\zeta = 0$) can be determined through the streaming-potential values of untreated PF, PF, PF-Fe^0, PF-NH$_2$-Fe^0, PF-Si-NH$_2$-Fe^{0,} and PF-SH-Fe^0 has been observed by electrokinetics and measured as ζ-potential. The summary of the ζ-potential analysis of the samples is presented in Figure 4.19. It can be seen that the isoelectric point of untreated PF is pH = 3.9 which means that a negative surface charge will be observed for the polyester fibers for pH higher than 3.9. Due to the further addition of –OH and –COOH groups during plasma treatment of the PF (PET), the surface charge and isoelectric point were further negative starting from -6.89 mV at pH=3.45 to -49.23 mV at pH=9.91. A negatively charged surface containing –OH and –COOH groups may pose an ideal environment for robust electrostatic incorporation of cationic iron ions (Fe^{3+}) followed by reduction and immobilization into polyester fabrics. Upon immobilization of Fe^0, the isoelectric point of PF-NH$_2$-Fe^0, PF-Si-NH$_2$-Fe^{0,} and PET-SH-Fe shifted to pH around 7 signifying an increase in ζ-potential due to the loading of iron particles.
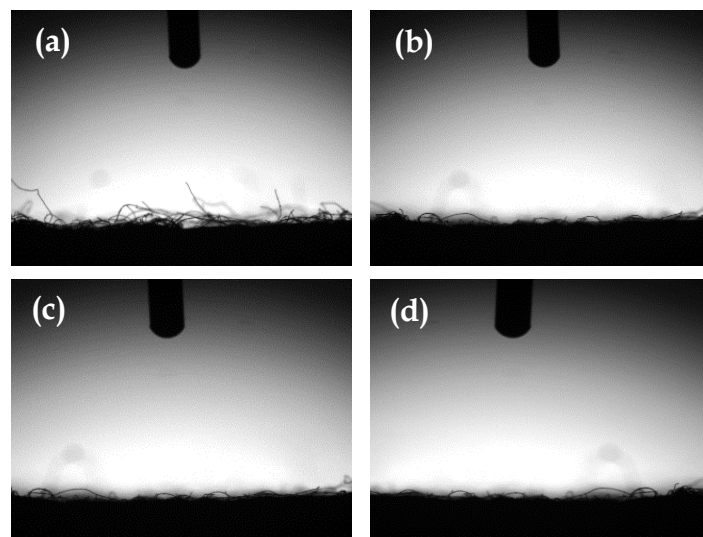
Figure 4. 20: Water contact angle of deposed drop into Fe^0 immobilized PF; (a) PF-Fe^0, (b) PF-NH$_2$-Fe^0, (c) PF-Si-NH$_2$-Fe^0 and (d) PF-SH-Fe^0.

The water contact angle of deposed drop into Fe^0 immobilized PF surfaces were investigated through sessile droplet goniometry. Results showed that, although all samples (PF-NH$_2$, PF-Si-NH$_2$, and PF-SH) showed a characteristic hydrophobic surface before iron immobilization (discussed earlier), there has been a shift in the wettability of the samples after immobilization of Fe^0 particles. The water contact angle measured for PF-Fe^0, PF-NH$_2$-Fe^0, PF-Si-NH$_2$-Fe^0, and PF-SH-Fe^0 is nearly 0°, which means that all samples are hydrophilic in nature (see Figure 4.20). This phenomenon would be beneficial to facilitate the diffusion or transfer rate of organic molecules from aqueous solution to the surface of adsorbents during the catalytic reaction (for example dye removal) [193, 341] (as discussed in the following sections).

4.2.3.3. Section (iii): Application of Fe^0 immobilized polyester nonwoven fabrics in wastewater treatment

Application of resultant Fe^0 immobilized PF samples in pollutants removal from water has been studied in Heterogeneous Oxidative (Fenton-like) or reductive (catalytic reduction) removal of colorants and phenolic contaminants and inhibit microbial pathogens from wastewater. Detailed results from all applications have been presented and analyzed in the following sections.

4.2.3.3.1. Heterogeneous Fenton-like removal of crystal violet dye from water

Resultant Fe^0 immobilized PF (PF-Fe^0, PF-NH$_2$-Fe^0, PF-Si-NH$_2$-Fe^0, and PF-SH-Fe^0) catalysts were studied in heterogeneous Fenton-like removal of crystal violet (CV) dye (50 mg.L^{-1}) in presence of hydrogen peroxide (H$_2$O$_2$). The degradation reactions were studied in a quartz cuvette placed in the UV-Vis spectrophotometer, the absorbance was registered immediately at room temperature where absorbance was recorded at predetermined time intervals to monitor the progress of the removal reaction. Based on that removal kinetics by fitting on pseudo-first-order kinetics model was calculated and mechanism of heterogeneous Fenton-like removal of CV dye has postulated (provided in the following discussion). Fenton-like removal of CV dye as a function of time was studied by UV-vis spectrophotometer and plotted as shown in Figure 4.21.

The removal reactions of CV dye using different Fe^0 immobilized PF samples (PF-Fe^0, PF-NH$_2$-Fe^0, PF-Si-NH$_2$-Fe^0, and PF-SH-Fe^0) were carried out under the same experimental conditions. The Fenton-like reaction uses ferrous ions (Fe^{2+}) and hydrogen peroxide (H$_2$O$_2$) to generate highly oxidation potential active oxygen species (such as hydroxyl free radicals) capable of degrading CV dye. The characteristic absorption peak observed at $\lambda_{590\ nm}$ was attributed to the intensity of CV dye [342]. As shown in Figure 4.21a-d, the intensity of the absorbance at $\lambda_{590\ nm}$ rapidly decreased, while exposed to a Fe^0 immobilized PF sample (that ultimately provides Fe^{2+}) and hydrogen peroxide, suggesting rapid generation of hydroxyl radicals that oxidized CV dye into colorless degraded intermediates. All samples were found to be effective towards the removal of CV dye in a heterogeneous Fenton-like environment providing complete degradation by 22-68 min. A close look at the color removal performance of the individual sample shows that significantly fast removal (98.87% in 22 min) performance was achieved by PF-SH-Fe^0 compared to other samples (98.56 % in 35 min, 98.35 % in 52 min, 94.77 % in 68 min for PF-Si-NH$_2$-Fe^0, PF-NH$_2$-Fe^0 and PF-Fe^0, respectively) . Fast removal might be attributed to the stability, disparity, and quantity of iron particles that were strongly immobilized on the PF surface, ensuring the maximum exposure of reagent to the presence of ferrous ions (Fe^{2+}) thus leading to efficient production of striking hydroxyl free radicals for oxidation of dye.
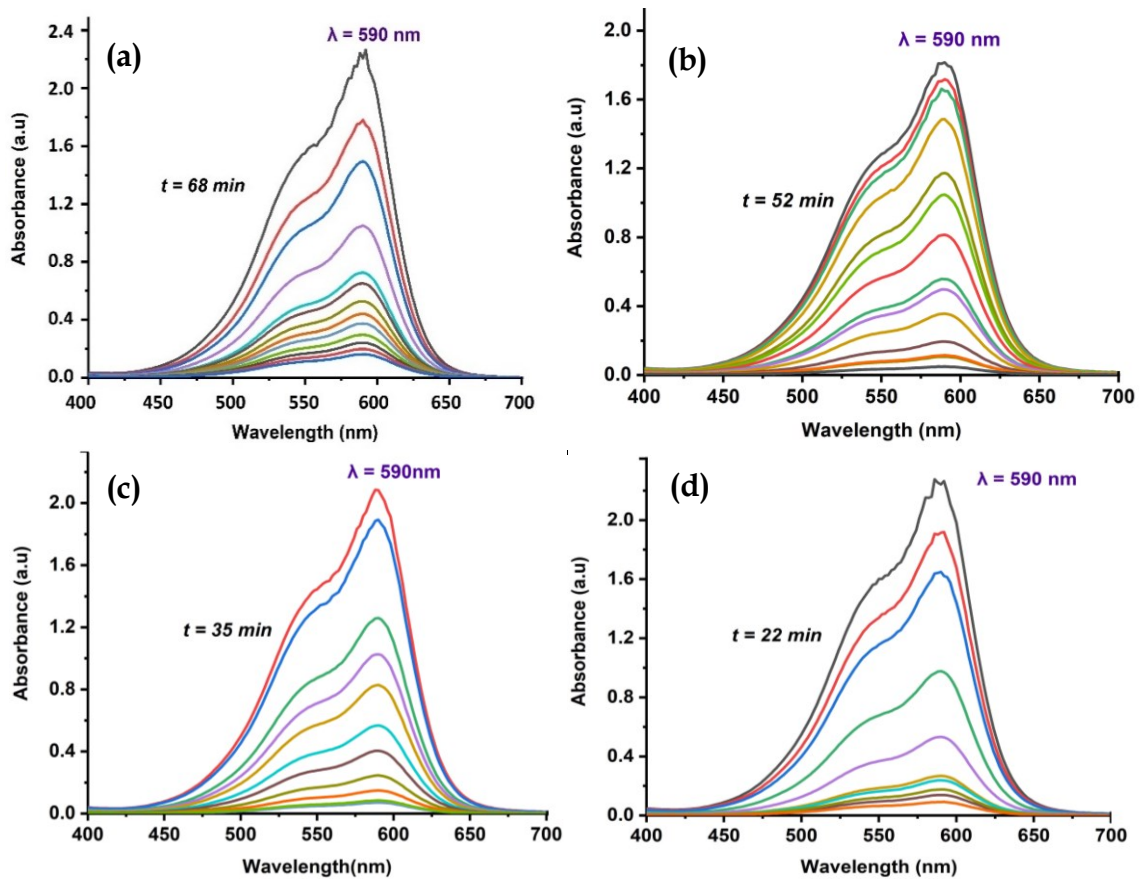
Figure 4. 21**:** UV-visible spectroscopy of heterogeneous Fenton-like removal of CV dye using Fe^0 immobilized PF samples; (a) PF-Fe^0/H_2O_2, (b) PF-NH_2-Fe^0/H_2O_2, (c) PF-Si-NH_2-Fe^0/H_2O_2, and (d) PF-SH-Fe^0/H_2O_2. [Conditions: CV dye = 50 mg.L^{-1}), H_2O_2 = 500 µL (0.3 M), pH=5, T= 25°C].

Removal reaction kinetics is one of the most important characteristics that represent the catalytic efficiency of the Fe^0 immobilized PF samples and, therefore, largely illustrate the potential applications [343]. Herein, the kinetic experiments of heterogeneous Fenton-like removal of CV dye with the use of Fe^0 immobilized PF samples in presence of hydrogen peroxide were conducted by investigating the degradation rate versus the degradation time, and the results are shown in Table 4.11. The [instant /initial] absorbance ratio of the CV dye band at $\lambda_{590\,nm}$ (A_t/A), which accounts for the corresponding concentration ratio (C_t/C), allows plotting of Ln (C_t/C) as a function of time as shown in Figure 4.22a-b. The removal performance of the membranes is presented in Figure 4.22c. Model validation of reaction kinetics for CV dye removal using Fe^0 immobilized PF samples are obtained by linear evolution in time of Ln(C_t/C), as supported by R^2 values 0.958, 0.897, 0.953, 0.953 for PF-Fe^0/H_2O_2, PF-NH_2-Fe^0 /H_2O_2, PF-Si-NH_2-Fe^0/H_2O_2, and PF-SH-Fe^0 /H_2O_2, respectively. Plots summarized in Table 4.11 shows that all samples exhibited good linear relationships of Ln (C_t/C) versus reaction time following pseudo-first-order reaction kinetics with respect to complete removal of CV dye. It is evident that among all samples the rate constant and removal performance of PF-SH-Fe^0/H_2O_2 is the highest (0.1922 min^{-1}, 98.87%).
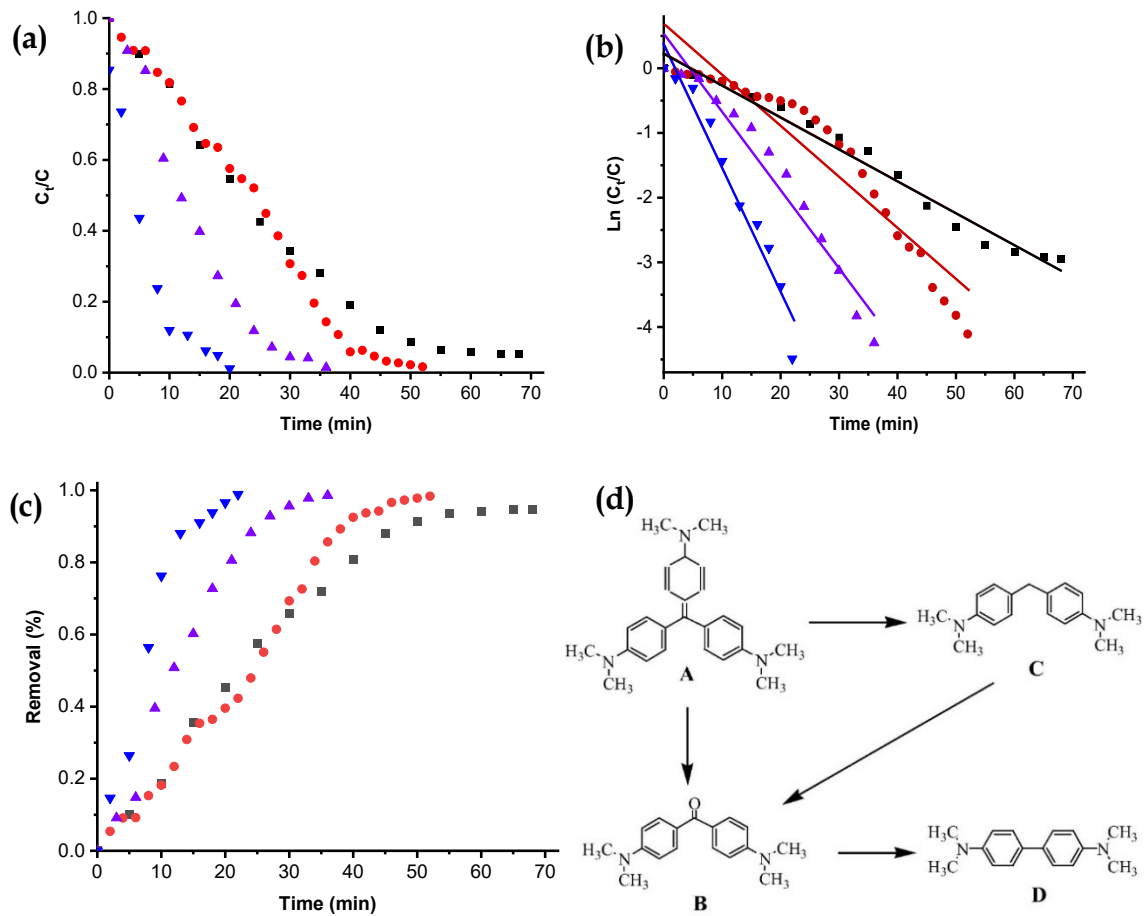
Figure 4. 22: Evolution of (a) C_t/C, (b) $Ln(C_t/C)$, (c) the removal yield in respect to time and (d) initial mineralization pathway of CV dye. (■) PF-Fe^0/H$_2$O$_2$, (●) PF-NH$_2$-Fe^0/H$_2$O$_2$, (▲) PF-Si-NH$_2$-Fe^0/H$_2$O$_2$, and (▼) PF-SH-Fe^0/H$_2$O$_2$ [Conditions: CV = 50 mg.L^{-1}, H$_2$O$_2$ = 500 μL (0.3 M), pH=5, T= 25°C].

Table 4. 11: Kinetics studies for heterogeneous Fenton-like removal of CV dye.

Sample Name	CV Conc. (mg.L^{-1})	[a]Time (min)	[b]k (min^{-1})	[c] (R^2)	Removal %
PF-Fe^0/H$_2$O$_2$	50	68	0.0494	0.958	94.77
PF-NH$_2$-Fe^0/H$_2$O$_2$	50	52	0.0789	0.897	98.35
PF-Si-NH$_2$-Fe^0/H$_2$O$_2$	50	35	0.1208	0.953	98.56
PF-SH-Fe^0/H$_2$O$_2$	50	22	0.1922	0.953	98.87

[a] Reaction time required for complete CV dye removal.

[b] k: rate constant for the 1st order kinetics, and is expressed in min^{-1}.

[c] R^2: correlation coefficient of the linear regression.

Postulated mechanism of crystal violet dye removal

The ability of zerovalent iron (immobilized on PF) to create iron ions, followed by involvement in a Fenton-like reaction in the presence of hydrogen peroxide, produces a high oxidation potential of hydroxyl free radical (•OH), which has a standard oxidation-reduction potential of 2.8 *V* (Reaction 4.12-4.16). Based on the mechanism of

Fenton-like reaction and previous reports [332, 344, 345] an initial mineralization mechanism for CV dye has also been suggested (see Figure 4.22d). It can be seen that there are many pathways for mineralization of CV dye as a function of interaction $^\bullet$OH, that are generated through Fenton reaction. Based on the theories of the Fenton/Fenton-like system, the removal of CV dye was attributed to the synergistic effect caused by radicals and other reactive species on the central carbon portion of the CV dye structure (Figure 4.22d-A) [39]. As found in the results discussed earlier, upon oxidation, the dye becomes colorless, indicating the removal of the color-bearing group and possible conversion into degraded intermediates. In the initial assumption, Palma-Goyes et $al.$ (2010) [345] and Guzman-Duque et $al.$ (2011) [346] suggested that due to oxidation CV may degrade into 4-(N, N-dimethylamino)-4'-(N', N'-dimethylamino) benzophenone (Figure 4.22d-B) or 4-(N, N-dimethylamino)-4'-(N', N'-dimethylamino) diphenylmethane (Figure 4.22d-C). However, a secondary degradation of these degraded intermediates occurs due to constant interaction with hydroxyl free radicals in the reaction bath and further degradation into 4-(N, N-dimethylamino)-4'-(N', N'-dimethylamino) dimethylaniline (Figure 4.22d-D) [344]. Finally, the gradual cleavage of the aromatic degraded intermediates would lead to carboxylic acids before dissociation into H_2O and CO_2 (mineralization) as illustrated in Reaction 4.16-4.17.

The postulates reaction steps for mineralization of CV dye are as follows;

(i)   The process of producing iron ions and reactive species

$$Fe^0 + 2H^+ \rightarrow Fe^{2+} + H_2 \tag{4.12}$$
$$Fe^0 + 2Fe^{3+} \rightarrow 3Fe^{2+} \tag{4.13}$$
$$Fe^0 + H_2O_2 + 2H^+ \rightarrow Fe^{2+} + 2H_2O \tag{4.14}$$
$$Fe^{2+} + H_2O_2 \rightarrow Fe^{3+} + HO^- + {}^\bullet OH \tag{4.15}$$
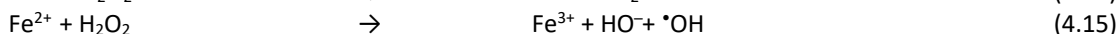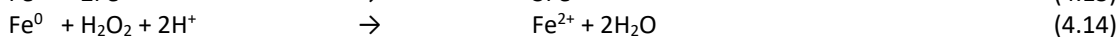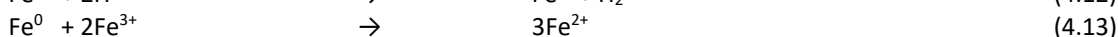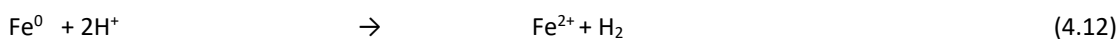
(ii)   The process of crystal violet dye removal

$$CV\ molecules + {}^\bullet OH \rightarrow Degraded\ intermediates\ of\ CV \tag{4.16}$$

(iii)   The process of mineralization

$$Degraded\ intermediates\ of\ CV + {}^\bullet OH \rightarrow CO_2 + H_2O \tag{4.17}$$
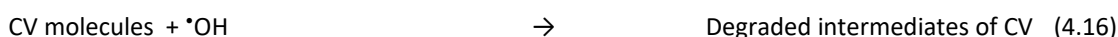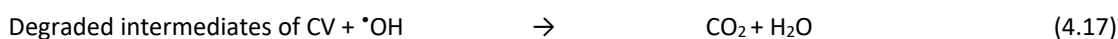
Toxicity reduction analysis

An important parameter for any pollutant removal procedure is the elimination of toxicity. The heterogeneous Fenton-like process for the elimination of crystal violet (CV) dye from the water was extensively studied based on chemical oxygen demand (COD). The samples were analyzed for COD reduction immediately after complete decolorization. The reduction of COD was calculated as a percentage of the initial COD of the CV dye in water before any treatment (assumed to be 100%). We found that, based on their COD results, all Fe^0-immobilized PF samples were capable of reducing the toxicity of the water. The highest relative COD reduction (78%) was observed after Fenton-like removal of CV dye using PF-SH-Fe^0/H_2O_2. The lowest COD reduction among the Fe^0-immobilized PF samples was observed for PF-Fe^0/H_2O_2 (32%). This can be attributed to either poor efficiency in the mineralization of the CV dye or leaching of Fe^0 particles from the PF into the solution (due to poor binding) during the CV dye removal reaction. The incomplete reduction of COD for all samples after complete color removal can be due to the remaining degraded intermediates (discussed earlier). Based on the results, it was concluded that PF-SH-Fe^0/H_2O_2 had superior catalytic properties with maximum mineralization of the degraded intermediates of CV dye into nontoxic elements. This can be due to the stabilization, uniform dispersion, and strong binding of Fe^0 particles. This conclusion is supported by SEM, XPS, TGA, and DSC analysis. Nevertheless, for all samples, a longer reaction between the degraded intermediates and radicals may improve the COD reduction performance, as suggested by Liu et $al.$ (2019) [347]. A longer treatment after CV dye removal should be considered; however, this suggestion requires further testing.

Recyclability and reusability of Fe^0 immobilized polyester nonwoven fabric

Reusability analysis of all samples has been carried out in subsequent removal of CV in the same experimental condition. Reusability analysis of the sample also provides evidence of the robustness of Fe^0 particles immobilization, which corresponds to the stability of Fe^0 particles. Results show that satisfying the basic motivation for immobilization of Fe^0 particles on PF, all samples showed the potential of reusability for a minimum four-cycle application to a maximum seven seven-cycle application without a significant decrease in removal performance. The least four-cycle reusability was found in PF-Fe^0 where as both PF-NH_2-Fe^0 and PF-Si-NH_2-Fe^0 showed the potential of six cycles of reusability. The highest reusability among four samples was found in PF-SH-Fe^0, which can be used for up to seven cycles. A close look at the reusability study of PF-Fe^0 shows a substantial decline in removal performance after three/four repeated use, which can be explained by loosely attached iron nanoparticles on the fabric, which may be leached to the solution during subsequent CV dye removal. Fe^0 particles immobilized on PAMAM, APTES and SH grafted samples on the other hand have a more robust and stability of iron nanoparticles providing at least above 90% removal even after seven reuses. This can be explained by the key role of amine/thiol functional groups that bind and shielded the Fe^0 particles and prevented leaching, which results in high durability".

Statistical modeling and optimization

In general, the Fenton process is influenced by many factors (such as pH of the reaction medium, the temperature, the hydrogen peroxide concentration, and the amount of catalyst) and is needed to optimize this process for assessing their measurable performances [169]. The conventional optimization process was determined through the interaction of the individual factors at-a-time while keeping all other conditions constant, this approach does not take into account cross-effects from the factors considered and leads to a poor optimization result [348]. Therefore, to better investigate the key factor in this newly developed system and optimize the removal of CV dye from water using Fe^0-immobilized PF, the individual effects of the factors were studied through a full factorial design using the methods and tools explained in section 3.3.5 of chapter 3. For all three samples (PF-NH_2-Fe^0, PF-Si-NH_2-Fe^0, and PF-SH-Fe^0), a full factorial design was set up by combining two factors and three levels. Table 4.12 presents the factors, their levels, and the response. According to the number of control parameters and their levels, a distinct full factorial design has been selected (L^{27}) to determine the optimal number of experiments in triplicates (see also Table 4.13). In the end, a passive response in terms of the relative concentration of dye at equilibrium was recorded for each trial run. The results from each trial run were evaluated in Minitab® 17 graphical and statistical analysis tool based on the main effects, interactions, ANOVA, and a response table.

Table 4. 12: Matrix of experiment's factors, their levels, and response.

Sample name	Factors	Level			Response
		A	B	C	
PF-NH_2-Fe^0	pH (X1)	5	7	9	Dye Conc., Q_e (%)
	$[H_2O_2]_{\mu l}$ (X2)	100	300	500	Dye Conc., Q_e (%)
PF-Si-NH_2-Fe^0	pH(X1)	5	7	9	Dye Conc., Q_e (%)
	$[H_2O_2]_{\mu l}$ (X2)	100	300	500	Dye Conc., Q_e (%)
PF-SH-Fe^0	pH(X1)	5	7	9	Dye Conc., Q_e (%)
	$[H_2O_2]_{\mu l}$ (X2)	100	300	500	Dye Conc., Q_e (%)

Note: Q^e is the concentration of a pollutant at equilibrium.

Table 4. 13: L^{27} full factorial design of experiment based on factors, levels, and response data [Relative dye concentration at equilibrium (%)].

RunOrder	PtType	Blocks	Factors		Relative Dye Concentration, Q_e (%)		
			pH (X1)	[H₂O₂] (X2)	PF-NH₂-Fe⁰	PF-Si-NH₂-Fe⁰	PF-SH-Fe⁰
1	1	1	5	100	0.8070	0.7501	0.7022
2	1	1	5	300	0.4354	0.5101	0.4469
3	1	1	5	500	0.0109	0.0243	0.0228
4	1	1	7	100	0.9625	0.9512	0.9654
5	1	1	7	300	0.8418	0.8626	0.7384
6	1	1	7	500	0.4209	0.4543	0.4481
7	1	1	9	100	0.9412	0.9837	0.9801
8	1	1	9	300	0.9501	0.9402	0.9619
9	1	1	9	500	0.9459	0.9932	0.9454
10	1	1	5	100	0.8319	0.7978	0.6421
11	1	1	5	300	0.4158	0.5498	0.4106
12	1	1	5	500	0.0108	0.0183	0.0208
13	1	1	7	100	0.9572	0.9403	0.9132
14	1	1	7	300	0.8198	0.7806	0.7002
15	1	1	7	500	0.4351	0.4199	0.4278
16	1	1	9	100	0.9803	0.9967	0.9903
17	1	1	9	300	0.9308	0.976	0.9625
18	1	1	9	500	0.9512	0.952	0.9398
19	1	1	5	100	0.8197	0.8212	0.7233
20	1	1	5	300	0.4637	0.4889	0.3606
21	1	1	5	500	0.0103	0.0199	0.0199
22	1	1	7	100	0.9498	0.9731	0.9573
23	1	1	7	300	0.8219	0.8195	0.7498
24	1	1	7	500	0.4664	0.4821	0.4302
25	1	1	9	100	0.9309	0.971	0.9863
26	1	1	9	300	0.9578	0.9804	0.9512
27	1	1	9	500	0.9141	0.9436	0.9607

By analyzing the main effects of the parameters, the general trends of each factor's influence on the process have been identified. Results show that, regardless of the type of sample (PF-NH₂-Fe⁰, PF-Si-NH₂-Fe⁰, and PF-SH-Fe⁰), changes in level in both X1 and X2 significantly altered the response in a linear model, which validates the statistically significant effect of pH and [H₂O₂]$_{\mu l}$ on the response. This is consistent with various reports [109, 349-351]. The interaction effects of the factors at both a low and a high level of another factor have been studied. The interaction plots for PF-NH₂-Fe⁰ for the factors pH and [H₂O₂]$_{\mu l}$ show that the interactions between X1$_{A \times B}$ and X2$_{B \times C}$ are significant. The remaining interactions, X1$_C$ and X2$_A$, show a nearly straight effect, forming a parallel-like line, meaning these two conditions are not related. On the other hand, the interaction between X1$_A$ and X2$_C$ has the most significant relationship (see Figure 4.23). The interaction plots of the other samples (PF-Si-NH₂-Fe⁰ and PF-SH-Fe⁰) show trends to those of PF-NH₂-Fe⁰. The overall scenario concludes that CV dye removal efficiency increases with increasing concentration of hydrogen peroxide and with decreasing pH, consistently with the main effects. This also indicates that the interaction plots are suitable for exploring the process parameters.

The main effects and interaction plots suggest the optimal levels for each factor, but do not indicate which factor has the most significant impact on the output, and do not assess the contribution of each factor. Instead, this was determined by the ANOVA, which is a robust method for evaluating the contribution of each factor and the significance of the optimization model [352]. This was accomplished by determining the Fischer's test value (F-value) and the sum of squares, which were used to evaluate the significance of the parameters; p values below 0.05 or 5% were considered statistically significant [353]. ANOVA results for PF-NH₂-Fe⁰, PF-Si-NH₂-Fe⁰, and PF-SH-Fe⁰ indicate that among the significant parameters, the pH has a large influence on the removal efficiency, with an

F-value of 2045.59, 866.65, and 1314.62 PF-NH$_2$-Fe^0, PF-Si-NH$_2$-Fe^0, and PF-SH-Fe^0, respectively. The p value was 0.000 for all samples. The concentration of hydrogen peroxide was also significant (p = 0.000), but had a lower influence than the pH, with F-values of 1496.75, 594.62, and 615.72 for the PF-NH$_2$-Fe^0, PF-Si-NH$_2$-Fe^{0,} and PF-SH-Fe^0, respectively.
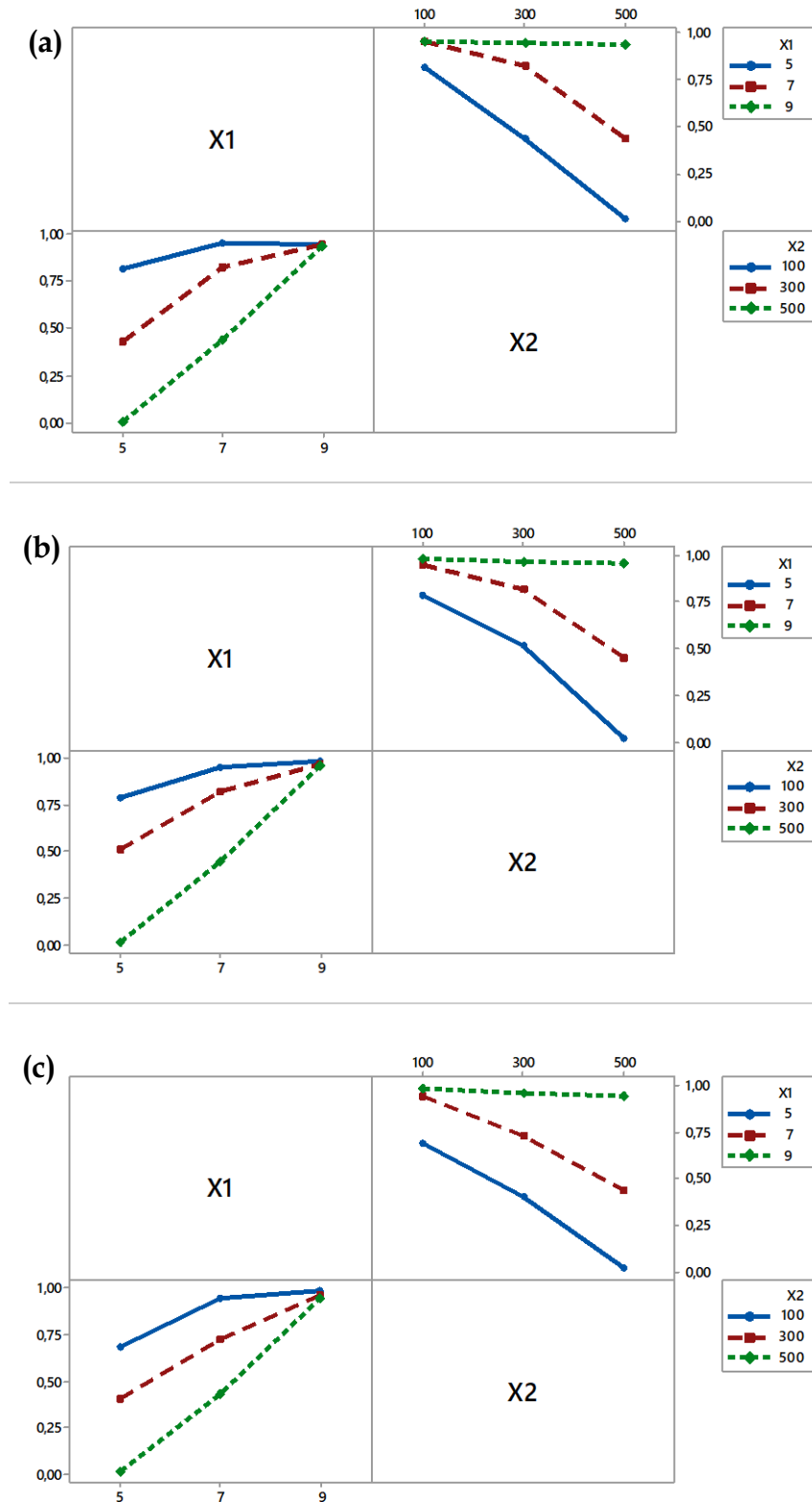
Figure 4. 23: Interaction plots for CV dye conc. (%) of (a) PF-NH$_2$-Fe^0, (b) PF-Si-NH$_2$-Fe^0 and (c) PF-SH-Fe^0 [Response : Dye concentration (%)].

The model summary shows string correlation, expressed by R^2 value over 98 for all three samples. On the other hand, by comparing the F-values among the three samples while considering all factors and levels, we found that the type of catalyst does not have any significant impact on the CV dye removal. The two-way interaction between the factors also has an overall significant impact on CV dye removal. However, extensive analysis with the coefficient of each interaction identifies that the interaction between $X1_B$ and $X2_A$ is not significant in PF-Si-NH$_2$-F^{0}e, $X1_A$, and $X2_B$, or $X1_B$ and $X2_B$ in PF-SH-Fe. The influence of each factor is also expressed as the percent contribution (p %). From the results, it can be seen that the pH has the percent contribution of 46.72% in PF-NH$_2$-Fe^0, 48.70% in PF-Si-NH$_2$-Fe^0, and 51.46% in PF-SH-Fe^0, while the $[H_2O_2]_{\mu l}$ has 34.19% in PF-NH$_2$-Fe^0, 33.42% in PF-Si-NH$_2$-Fe^0, and 27.456% in PF-SH-Fe^0. These findings indicate that, although both factors have significant influence over the CV dye removal efficiency, pH has a higher influence than $[H_2O_2]_{\mu l}$.
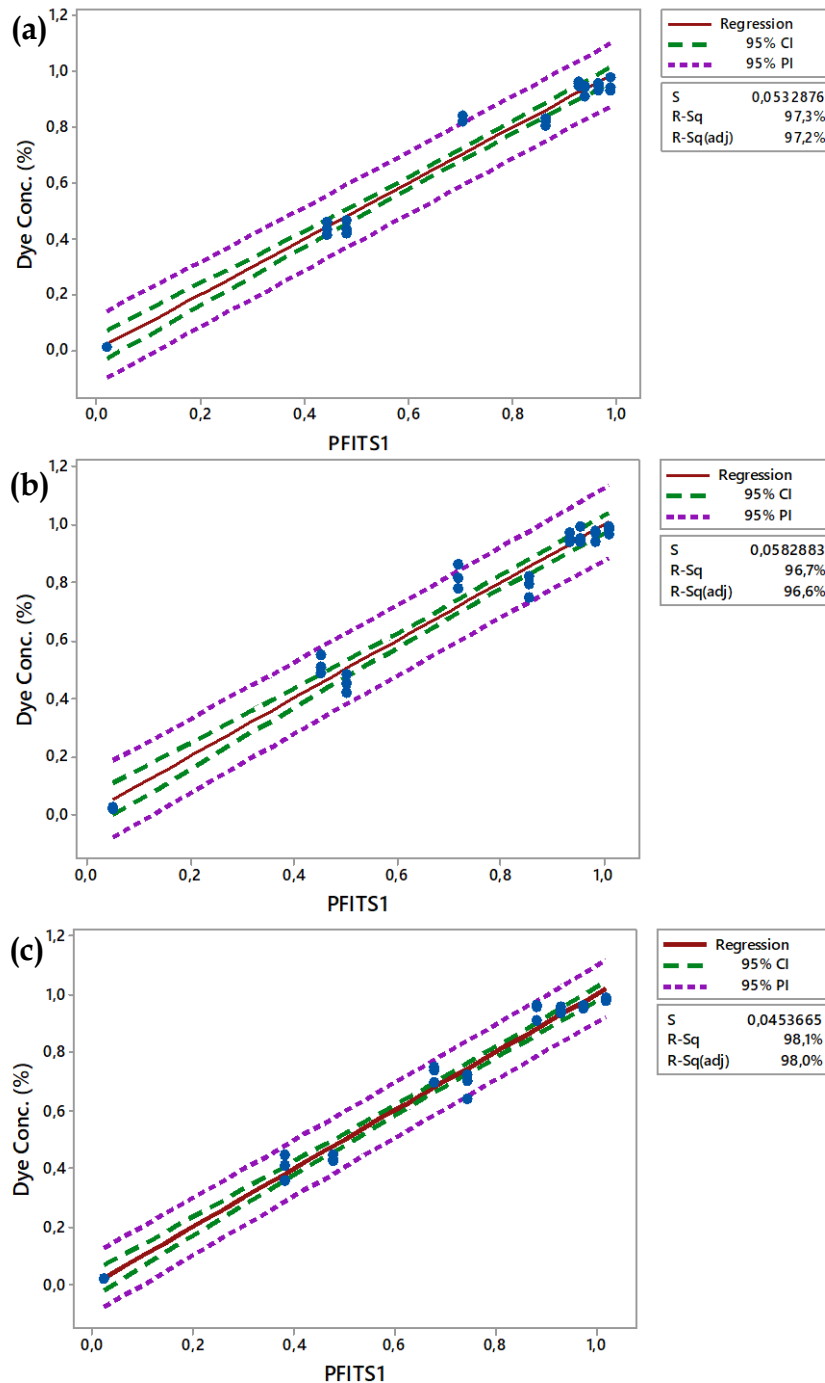
Figure 4. 24: Fitted plots for CV dye concentration (%); [CV conc. (%) = -0.00000 + 1.000 PFITS1]; (a) PF-NH$_2$-Fe^0, (b) PF-Si-NH$_2$-Fe^0 and (c) PF-SH-Fe^0; [CI = confidence interval, PI=prediction interval].

A detailed study among the three samples indicates that the influences of the pH had the most significant effect on PF-SH-Fe^0, followed by PF-Si-NH$_2$-Fe^0 and PF-NH$_2$-Fe^0, whereas [H$_2$O$_2$]$_{\mu l}$ had the greatest effect on PF-NH$_2$-Fe^0, followed by PF-Si-NH$_2$-Fe^0 and PF-SH-Fe^0. The greater influence of pH over [H$_2$O$_2$]$_{\mu l}$ can be explained by the synergic effect of pH on the stabilization of hydrogen peroxide and the formation of reactive species, which ultimately performs the removal of CV dye. Under unlikely pH conditions (such as pH<7), there could be no removal of CV dye, whereas, under favorable pH conditions, removal would occur regardless of [H$_2$O$_2$]$_{\mu l}$, though efficiency may be affected by [H$_2$O$_2$]$_{\mu l}$ [349, 354].

Fitted plots were made of the predicted versus actual values for the responses for PF-NH$_2$-Fe^0, PF-Si-NH$_2$-Fe^0, and PF-SH-Fe^0. Results from all samples show that the points reflect the deviation of the actual values from the predicted or fitted values. The graph (see Figure 4.24) indicates that the model is significant because the residuals are close to the diagonal line. In addition, the Pearson correlation coefficient between the predicted and actual values for the responses was 1.000, with a p-value of 0.000, which indicates a strong relationship between the predicted and actual values for all three samples [355, 356]. In addition to providing valuable insight into the roles of the factors, the model provides a rationale for creating a kinetic model that would deepen the understanding of the mechanisms and kinetics of the heterogeneous Fenton-like removal of complex pollutants in wastewater using the Fe^0-immobilized PF samples fabricated during Study B of this chapter.

4.2.3.3.2. Heterogeneous catalytic reduction of phenolic compound and colorants from wastewater

Catalytic reduction of various pollutants (phenolic compound and colorants) from water has been studied by using Fe^0 immobilized PF in presence of NaBH$_4$. The monitoring of the reduction of pollutants was conducted through UV-vis spectroscopy. The data presentation involves studies related to catalytic reduction of 4-nitrophenol (4-NP) and methylene blue (MB) dye, kinetics studies of the reduction reaction. Based on the results a general mechanism for catalytic reduction of pollutants has been postulated. The outcome of this section will validate and strengthen the potentiality of newly developed Fe^0 immobilized PF samples that are not only effective in the oxidative system but also in the reductive system.

Catalytic reduction of 4-nitrophenol

Reduction removal of 4-NP has been carried out by using Fe^0 immobilized PF (PF-Fe^0, PF-NH$_2$-Fe^0, PF-Si-NH$_2$-Fe^0, and PF-SH-Fe^0) as catalysts and NaBH$_4$ as reducing agent. Briefly, 2 mL of water was taken and to it, 1mg of 4-Nitrophenol (0.1 mM) and 100 mg of NaBH$_4$ (0.1 M) solution were added. To the above solution, 500 mg/L of catalysts and their intermediates were added to initiate the reactions. The degradation reactions were carried in a quartz cuvette placed in the UV-Vis spectrophotometer, the absorbance was registered immediately at room temperature to investigate the reduction and degradation kinetics. The absorbance was recorded at predetermined time intervals to monitor the progress of the reduction reaction.

UV-vis spectroscopy results presented in Figure 4.25 show a strong absorption peak at 400 nm corresponding to the 4-nitrophenol [83]. It is to be noted that, the initial UV band at 298 nm under neutral or acidic condition has been observed, which upon addition of NaBH$_4$ solution, made the band shift from 298nm to 400nm immediately, this corresponded to a color change from light yellow to yellow-green due to the formation of 4-nitrophenolate ion. As seen in Figure 4.25a-d, upon addition of catalyst, the intensity of the peak at 400nm slowly reduces until it flattens (means complete reduction). The result shows that, while the characteristic absorption peak of 4-NP at 400 nm is gradually decreasing, a new peak at ~300 nm develops which is ascribed to 4-aminophenol (4-AP). This change was due to the formation of 4-nitrophenolate ions under alkaline conditions [357, 358]. The formation of 4-AP confirms the reduction of 4-NP [359]. A comparative study among the four samples shows that the complete

reduction of 4-NP takes place within 12-30 min where the fast reduction was observed within PF-SH-Fe^0/NaBH$_4$ (12 min) followed by PF-NH$_2$-Fe^0/NaBH$_4$ (15 min), PF-Si-NH$_2$-Fe^0/NaBH$_4$ (30 min) and PF- Fe^0/NaBH$_4$ (30 min). The particularly high catalytic activity of PF-SH-Fe^0 could be explained by the presence of high loading and stability of Fe^0 particle on thiol grafted PF, this results in enhancement of faster electrons transfer from BH$_4^-$ ions to the nitro group of 4-NP, reducing it to 4-AP [357]. Overall, all tailor-made catalysts showed substantially high catalytic activity which signifies the key role of thiol and amines groups in iron loading and stabilization as consistent to the SEM, TGA, EDX and XPS analysis (in section 4.2.3.2).
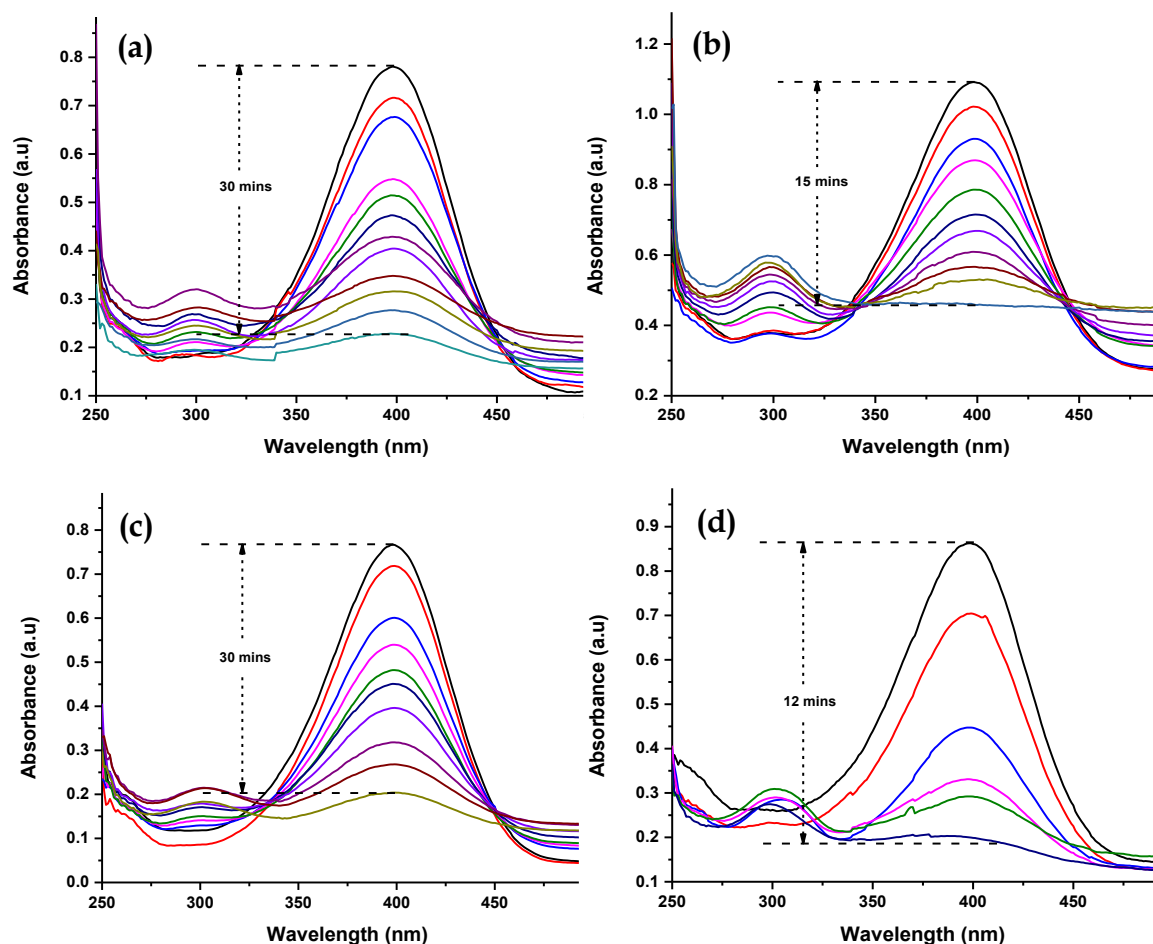
Figure 4. 25: UV-vis spectra for the catalytic reduction of 4-NP using Fe^0 immobilized PF sample; (a) PF-Fe^0/NaBH$_4$ (b) PF-NH$_2$-Fe^0/NaBH$_4$, (c) PF-Si-NH$_2$-Fe^0 /NaBH$_4$ and (d) PF-SH-Fe^0/NaBH$_4$. [Conditions: 4-NP = 0.1 mM, [NaBH$_4$]=0.1 M; Catalyst = 500 mg/L, pH=5, T= 25°C].

Kinetics of reduction is one of the most significant features of catalytic performance and thus shows mainly the potential applicability of the catalyst [343]. The kinetics of the reduction reaction was carried out by considering the concentration of NaBH$_4$ as constant during the catalytic reduction process. Hence, the rate constant of the reaction can be obtained by considering pseudo-first-order kinetics [314]. The [instant /initial] absorbance ratio of the 4-NP band at 400 nm (A$_t$/A), which accounts for the corresponding concentration ratio (C$_t$/C), allows plotting Ln(C$_t$/C) as a function of time (Figure 4.26). For the first-order kinetics model, the 4-NP reduction is confirmed and obtained by the linear evolution in time of Ln(C$_t$/C), more particularly for PF-SH-Fe^0/NaBH$_4$, as supported by R^2 values which are above 0.99. Table 4.14 summarizes the catalytic kinetic plots of the samples. All the plots show good linear relationships of Ln(C$_t$/C) versus reaction time and follow pseudo-first-order kinetics with respect to 4-NP reduction. The rate constant was found to be 3.426× 10^{-1} min^{-1} in PF-SH-Fe^0/NaBH$_4$, which was higher than those registered for the others samples; PF-NH$_2$-Fe^0 /NaBH$_4$ (6.158× 10^{-2} min^{-1}), PF-Si-NH$_2$-Fe^0 /NaBH$_4$ (9.380× 10^{-2} min^{-1}). By contrasting the kinetics of reactions among the samples, it can be concluded that the best catalytic

activity is registered for PF-SH-Fe^0/NaBH$_4$, which can be attributed to the presence of a strong synergistic interaction between SH and Fe^0 particles to produce a new activated site in the PF samples, as supported by the higher k.
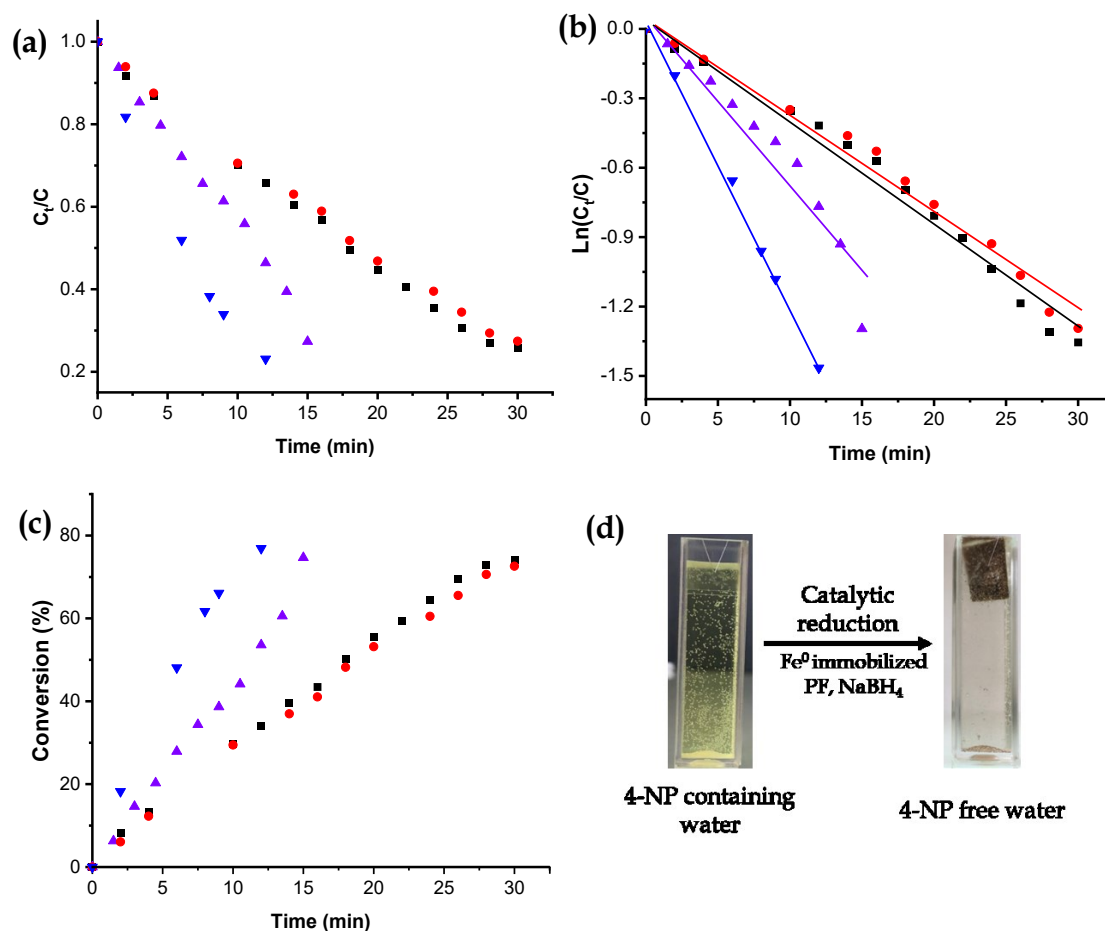
Figure 4. 26: Evolution of (a) C$_t$/C, (b) Ln(C$_t$/C), (c) the conversion yield in time at room temperature for 4-NP and (d) digital image of reduction of 4-NP using Fe^0 immobilized PF sample; (■) PF-Fe^0/ NaBH$_4$, (●) PF-NH$_2$-Fe^0/ NaBH$_4$, (▲) PF-Si-NH$_2$-Fe^0/ NaBH$_4$, and (▼) PF-SH-Fe^0/ NaBH$_4$. Conditions: 4-NP = 0.1 mM, [NaBH$_4$]=0.1 M; Catalyst = 500 mg/L, pH=5, T= 25°C].

Table 4. 14: Pseudo-first-order kinetics study for the catalytic reduction of 4-NP using Fe^0 immobilized PF.

Sample name	*Time (min)	**K (min^{-1})	***R^2
Untreated PF	>30	--	--
PF-Fe^0/ NaBH$_4$	30	4.685×10^{-2}	0.979
PF-Si-NH$_2$-Fe^0/ NaBH$_4$	15	9.380×10^{-2}	0.924
PF-NH$_2$-Fe^0/ NaBH$_4$	30	6.158×10^{-2}	0.980
PF-SH-Fe^0/ NaBH$_4$,	12	3.426×10^{-1}	0.996

* Reaction time for maximum conversion yields.

** k is the rate constant for the 1st order kinetics and is expressed in min^{-1}.

*** R^2 is the correlation coefficient of the linear regression.

Langmuir and Freundlich isotherms models for the adsorption of 4-NP using Fe^0 immobilized PF samples have also been studied (see Figure 4.27). The results summarized in Table 4.15 indicate that the PF-SH-Fe^0 adsorbent has high adsorption affinity towards 4-nitrophenol than the untreated PF. This could be due to the higher percentage

of Fe^0 particles immobilized into PF, which is more effective in the adsorption process. This confirms that the adsorption of 4-nitrophenol on all samples (PF-NH$_2$-Fe^0, PF-Si-NH$_2$-Fe^0, and PF-SH-Fe^0) is favorable. It was found that the Langmuir isotherm model fits well with the equilibrium data. The Freundlich model also reveals a good correlation.
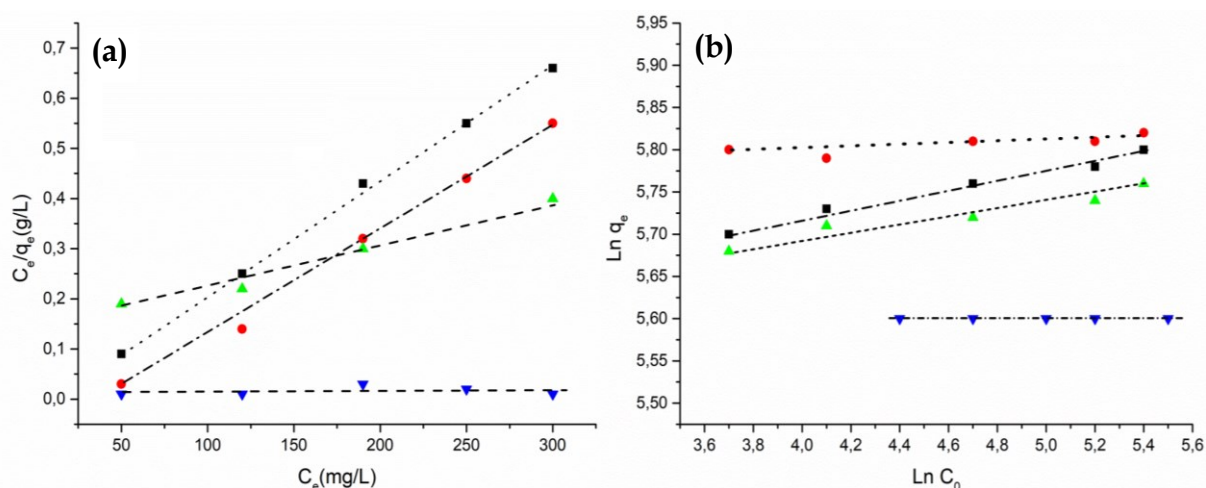
Figure 4. 27: Langmuir (a) and Freundlich (b) isotherms models for the adsorption of 4-NP using Fe^0 immobilized PF samples; (▼) Untreated PF, (●) PF-NH$_2$-Fe^0, (▲) PF-Si-NH$_2$-Fe^0 and (■) PF-SH-Fe^0 [Note: q_e (mg.g^{-1}) is the absorbed amount of the 4-NP at equilibrium, C_e (mg.L^{-1}) is the equilibrium concentration of the 4-NP solution].

Table 4. 15: Langmuir and Freundlich parameters for adsorption of 4-NP using Fe^0 immobilized PF.

Sample name	Freundlich isotherm			Langmuir isotherm		
	K_F (mg/g) (L/mg)1/n	1/n	R^2	q_m (mg/g)	K_L (L/mg)	R^2
Untreated PF	270.30	0.812	--	191.56	0.123	--
PF-Si-NH$_2$-Fe^0/ NaBH$_4$	186.08	0.541	0.920	293.30	0.061	0.989
PF-NH$_2$-Fe^0/ NaBH$_4$	191.82	0.640	0.909	269.91	0.081	0.993
PF-SH-Fe^0/ NaBH$_4$	173.77	0.144	0.995	350.60	0.051	0.995

K_f is the Freundlich coefficient, and n is the Freundlich constant.
K_L is the Langmuir constant, and q_m (mg.g^{-1}) is the maximum adsorption capacity at a complete monolayer.

Catalytic reduction of methylene blue dye

The catalytic activity of Fe^0 immobilized PF (PF-Fe^0, PF-NH$_2$-Fe^0, PF-Si-NH$_2$-Fe^0, and PF-SH-Fe^0) samples were also evaluated on the catalytic reduction of MB dye in the presence of NaBH$_4$. Figure 4.28 shows the results of UV-vis spectra during the reduction of MB. Results show a strong double peak at 665 nm in all samples, which is attributed to MB dye. Upon addition of catalysts and reducing agents, a decrease in the intensity of the peaks for all samples was observed. The decrease in intensity of the peaks corresponds to the decoloration of MB dyes causes by reduction. The complete reduction of MB was achieved between 18-45 min. Each sample required a different time to reduce the same concentration of MB solution, which further indicates the effectiveness of each catalyst. By comparing the samples among themselves, it can be seen that the fastest reduction of MB reaches 97.9 % in 16 min using PF-SH-Fe^0/ NaBH$_4$, which is consistent with the results obtained in 4-NP reduction, suggesting again that SH played a key role in the immobilization of Fe^0 particles and then the catalytic reduction of MB.
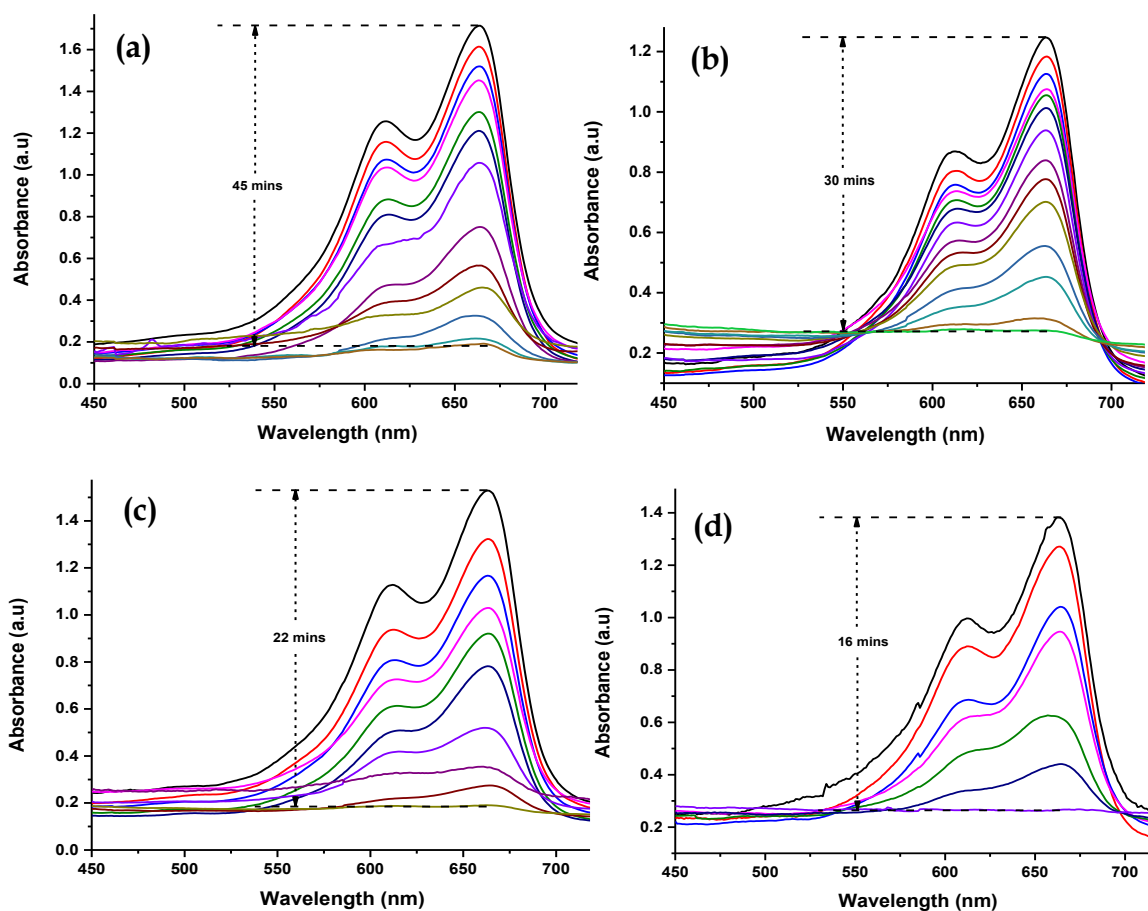
Figure 4. 28: UV-vis spectra for the catalytic reduction of MB using Fe^0 immobilized PF sample; (a) PF-Fe^0/NaBH$_4$ (b) PF-NH$_2$-Fe^0/NaBH$_4$, (c) PF-Si-NH$_2$-Fe^0 /NaBH$_4$ and (d) PF-SH-Fe^0/NaBH$_4$. [Conditions: MB dye = 0.5 mM, [NaBH$_4$]=0.1 M; Catalyst = 500 mg/L, pH=5, T= 25°C].

Such rapid kinetics in catalytic degradation of MB is attributed to the good stability, dispersion, and strong crosslink between -SH groups and Fe^0 particles on the PF surface, ensuring the maximum exposure of active sites during pollutant removal.   The complete reduction of MB by other samples was 45 min, 30 min, and 22 min for PF-Fe^0/NaBH$_4$, PF-NH$_2$-Fe^0/NaBH$_4$, PF-Si-NH$_2$-Fe^0/NaBH$_4'$ respectively. Here the longest treatment time required was with PF-Fe^0/NaBH$_4$ alike 4-NP degradation study (studied earlier). Control experiments carried out using PF-NH$_2$-Fe^0, PF-Si-NH$_2$-$Fe^{0,}$ or PF-SH-Fe^0 without using NaBH$_4$ showed no removal of MB dye. The characteristic absorption property of heterogeneous catalysts (alone) noticed during the control experiment was insignificant to be reported.

The [instant /initial] absorbance ratio of the MB band at 665 nm (A$_t$/A), which accounts for the corresponding concentration ratio (C$_t$/C), allows plotting Ln(C$_t$/C) as a function of time that helps to understand the kinetics of reduction reaction of MB dyes (see Figure 4.29). For the pseudo-first-order kinetics model, MB reduction is confirmed and obtained by the linear evolution in time of Ln(C$_t$/C), more particularly for PF-Si-NH$_2$-Fe^0/ NaBH$_4$, as supported by R^2 values over 0.97. Table 4.16 summarizes the catalytic kinetic plots of the samples. All the plots show good linear relationships of Ln(C$_t$/C) versus reaction time and follow pseudo-first-order kinetics with respect to MB reduction. The rate constant was found to be 12.32× 10^{-1}min^{-1} in PF-SH-Fe^0/NaBH$_4$, which was higher than those registered for the others samples; PF-NH$_2$-Fe^0 /NaBH$_4$ (4.292× 10^{-2} min^{-1}), PF-Si-NH$_2$-Fe^0/NaBH$_4$ (7.664× 10^{-2} min^{-1}). The lowest rate constant has been observed in PF-Fe^0/ NaBH$_4$ (4.609× 10^{-2} min^{-1}). By contrasting the kinetics of reactions among the samples, it can be concluded that the best catalytic activity is registered for PF-SH-Fe^0/NaBH$_4$ as it like 4-NP reduction. However, based on the concentration of pollutants reduced and time required, it is evident that the reduction performance of Fe^0 immobilized PF in the removal of MB dye is higher compared to those of 4-NP.
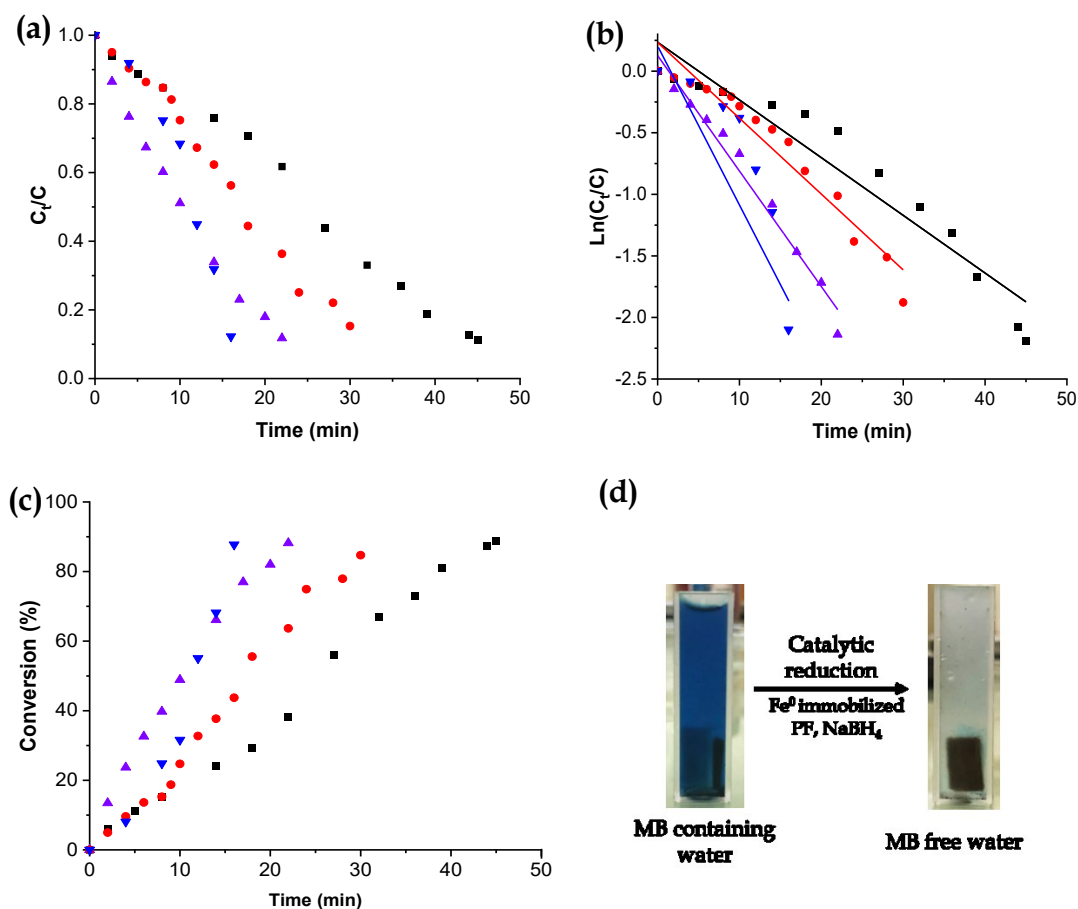
Figure 4. 29: Evolution of (a) C_t/C, (b) $Ln(C_t/C)$, (c) the conversion yield in time at room temperature for 4-NP and (d) digital image of reduction of MB using Fe^0 immobilized PF sample; (■) PF-Fe^0/ $NaBH_4$, (●) PF-NH_2-Fe^0 / $NaBH_4$, (▲) PF-Si-NH_2-Fe^0/ $NaBH_4$, and (▼) PF-SH-Fe^0 / $NaBH_4$. Conditions: MB = 0.5 mM, [$NaBH_4$]=0.1 M; Catalyst = 500 mg/L, *pH*=5, T= 25°C].

Table 4. 16: Pseudo-first-order kinetics study for the catalytic reduction of MB dye using Fe^0 immobilized PF.

Sample name	*Time (min)	**k (min^{-1})	***R^2
Untreated PF	>30	--	--
PF-Fe^0/ $NaBH_4$	45	4.609× 10^{-2}	0.9174
PF-Si-NH_2-Fe^0/ $NaBH_4$	22	7.664× 10^{-2}	0.9737
PF-NH_2-Fe^0/ $NaBH_4$	30	4.292× 10^{-2}	0.9358
PF-SH-Fe^0/ $NaBH_4$	16	12.32× 10^{-1}	0.9041

* Reaction time for maximum conversion yields.

** k is the rate constant for the 1st order kinetics and is expressed in min^{-1}.

*** R^2 is the correlation coefficient of the linear regression.

Catalytic reduction of mixture of 4-NP and MB dye

The catalytic performance of all samples (PF-Fe^0, PF-NH_2-Fe^0, PF-Si-NH_2-$Fe^{0,}$ or PF-SH-Fe^0) were also evaluated against water having the mixture of both 4-NP and MB. Aqueous 4-NP and MB solutions give a strong absorption

peak at 420 nm and 665 nm as shown in Figure 4.30. It was discussed already that 4-NP gives an absorption peak at 400 nm and MB gives an absorption peak at 650 nm. Thus, the peak appearance at 420 nm and 665 nm were due to the chemical interaction of two organics molecules in water. Peak position intensity at 665 nm decreases with the addition of catalyst. However, the band registered at 420 nm slightly decreases. Afterward, the peak UV–visible spectra were recorded continuously, and with time the peak intensity at 665 nm (MB) disappeared. This result is of great importance, which demonstrates the hard conversion of NO_2 from 4-NP in NH_2 from 4-AP. This can be accentuated by the unavoidable protonation of 4-NP groups, thereby favoring the reduction of MB. Such interactions explain the slight shifts observed for the main UV-vis bands of these molecules. Later, a new peak appeared at 250 nm with increasing intensity, indicating a worthy conversion process (*i.e* 4-NP to 4-AP). Therefore, it can be stated that the samples exhibited excellent activity and the reduction of the mixture takes between 18-32 min. Aligning with the individual reduction of pollutants, PF-SH-Fe^0/ NaBH$_4$ showed the fastest (18 min) reduction of MB followed by PF-Si-NH$_2$-Fe^0/ NaBH$_4$ (20 min), PF-NH$_2$-Fe^0/ NaBH$_4$ (30 min), and PF-Fe^0/ NaBH$_4$ (32 min). Current results are consistent with the effectiveness of reduction of 4-NP, MB when studied separately (discussed earlier).
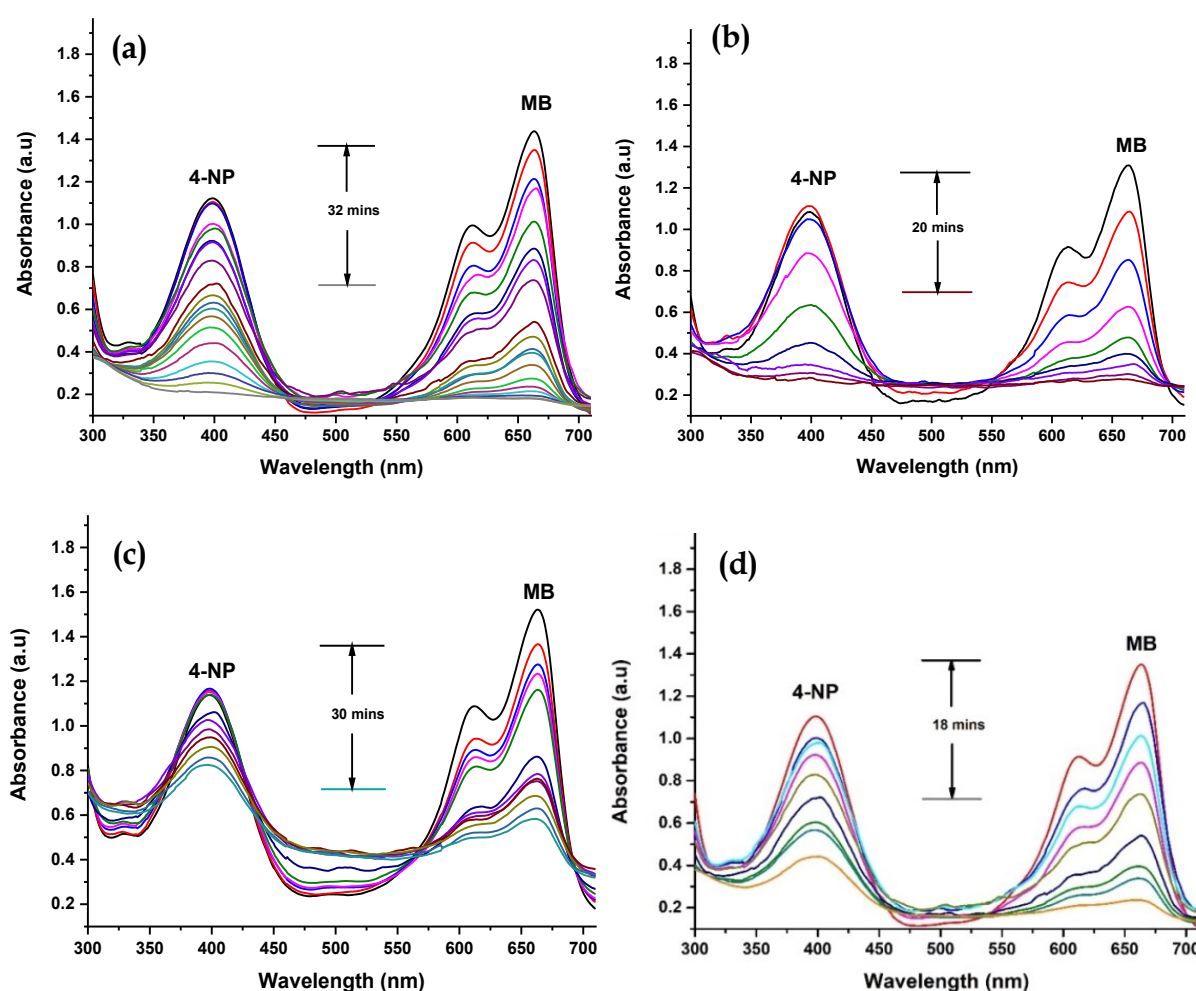
Figure 4. 30: UV-vis spectra for the catalytic reduction of mixture of 4-NP and MB using Fe^0 immobilized PF sample; (a) PF-Fe^0/NaBH$_4$ (b) PF-NH$_2$-Fe^0/NaBH$_4$, (c) PF-Si-NH$_2$-Fe^0 /NaBH$_4$ and (d) PF-SH-Fe^0/NaBH$_4$. [Conditions: 4-NP = 0.1 mM, MB = 0.5 mM, [NaBH$_4$]=0.1 M; Catalyst = 500 mg/L, pH=5, T= 25°C].

Postulated mechanism of heterogeneous catalytic reduction of 4-NP and MB

As mentioned above, the changes in catalytic activity were attributed to the synergistic effect of Fe particles and NaBH$_4$. The postulated mechanism for the catalytic reduction and degradation of 4-NP and MB dye is represented in Figure 4.31. As known, the insertion of Fe^0 particles on the surface of PF leads to the introduction of catalytic property. Here, when the Fe^0 immobilized PF is used as a catalyst for reduction of 4-NP and MB dye, BH$_4^-$ ions produced by dissociation of NaBH$_4$ absorbed onto the Fe^0 particles and then discharge H$^-$ on the surface [360]. Afterward, electrons are accumulated on the surface of Fe^0 immobilized PF. Herein, this behavior can be explained by electron transfer, where a vacant region in the Fe^0 particles is produced, which terminates to an electron-enriched area. These abundant electrons can accelerate the uptake of electrons by 4–NP or MB dye and result in the reduction.
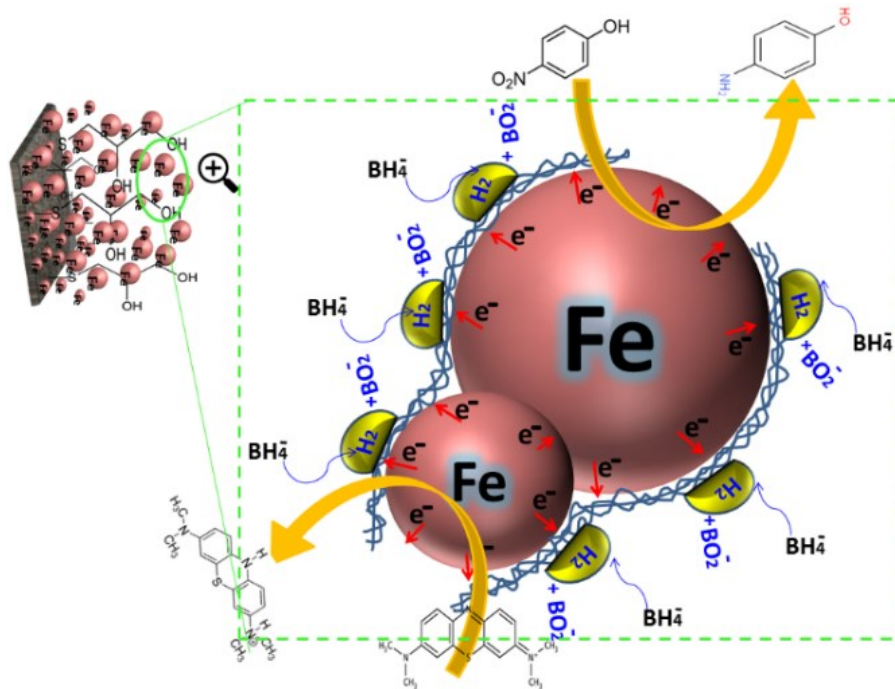
Figure 4. 31: A postulated mechanism for the catalytic reduction and degradation of 4-NP and MB dye.

Leaching of catalyst and total dissolved solids analysis of treated water

The leaching and total dissolved solids (TDS) analysis of treated water was calculated from the data collected during the reduction of 4-NP (which will correspond to MD reduction as well). Results summarized in Table 4.17 showed a high concentration of TDS in PF-Fe^0/ NaBH$_4$ treated reduced 4-NP water compared to the other sample. The higher TDS values are attributed to the odd release of iron particles from the PF surface during the catalytic reduction process. Such a drawback was already reported by several works previously published. However, Fe^0 particle immobilized on APTES, PAMAM or SH grafted PF samples were found to markedly reduce the leaching of catalysts (as well as wastewater toxicity), where TDS concentration decreased from 484 ppm to 113 ppm. Maximum 77% relative reduction of TDS has been observed for PF-SH-Fe^0/ NaBH$_4$ followed by 68%, 48% reduction on PF-Si-NH$_2$-Fe^0/ NaBH$_4$, PF-NH$_2$-Fe^0/ NaBH$_4$, respectively. The highest TDS reduction in the thiol-grafted sample is due to the robust incorporation of Fe nanoparticles in the PF (*explained in previous discussions*) that limits the leaching.

Table 4. 17: Leaching of catalyst and total dissolved solids analysis of treated water.

Sample Name	Treated water color	TDS (ppm)
PF-Fe^0/ NaBH$_4$	Clear (brownish tone)	484.0
PF-Si-NH$_2$-Fe^0/ NaBH$_4$	Clear (brownish tone)	153.0
PF-NH$_2$-Fe^0/ NaBH$_4$	Clear (brownish tone)	251.0
PF-SH-Fe^0/ NaBH$_4$	Clear (brownish tone)	113.0

Reusability of Fe^0 immobilized polyester nonwoven fabrics

The reusability study of Fe^0 particle immobilized PF on both catalytic reductions of 4-NP and MB was carried out. The result indicates that all Fe^0 particle immobilized PF samples can be recycled and reused more than seven seven-cycles without obvious decline conversion processes. All an increase in the required time to complete the reduction of pollutants is necessary after each cycle application. Overall reusability performance of all APTES, PAMAM, and SH samples is very promising in every aspect of a heterogeneous system. This can be explained by the efficient effect of APTES, PAMAM, and SH, which could serve as an effective shield to prevent leaching, which results in decent durability.

4.2.3.3.3. Antibacterial study of Fe^0 immobilized polyester nonwoven fabric

The evidence of the antibacterial property of Fe^0 particle immobilized PF samples were gathered to introduce the multifunctional property of the resultant materials. Two different methods based on qualitative and quantitative analysis have been used to study the antibacterial property are (a) disc diffusivity and zone inhibitory analysis and (b) optical density analysis.
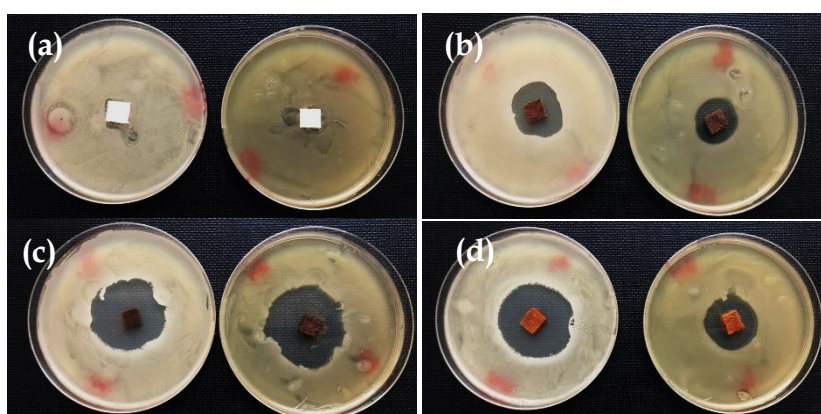
Figure 4. 32: Diffusivity and zone inhibitory test of differently iron-immobilized fibrous membranes; (left) Staphylococcus epidermidis; (right) Escherichia coli ; (a) PF, (b) PF-Si-NH$_2$-Fe^0 (c) PF-NH$_2$-Fe^0 and (d) PF-SH-Fe^0.

At first, the antibacterial activities of the samples (PF-Si-NH$_2$-Fe^0, PF-SH-Fe^0, and PF-NH$_2$-Fe^0) were studied under natural conditions through diffusivity and zone inhibitory analysis against both gram-positive and gram-negative bacteria (*S. epidermidis* and *E. coli*) strains. Before placing samples on Petri-dishes containing inoculated bacteria,

the sample was wetted with a drop of distilled water to maximize the effect of immobilized Fe^0 particles. A blank experiment conducted using an untreated PF showed no inhibition zone, which means the PF does not possess antibacterial behavior if it does not contain zero-valent iron. However, upon immobilization of Fe^0 particles, PF samples effectively inhibited the bacterial growth showing inhibition zones with diameter varying from 21 mm to 38 mm (see Figure 4.32) (According to ISO 20645 standard, the outspreading up to 1 mm inhibition zone and no growth under specimen or no inhibition zone is accepted as effective) [361, 362].

Table 4. 18: The zone of inhibition[a] (mm) analysis of samples according to test method ISO 20645.

Sample Name	*Staphylococcus epidermidis*	*Escherichia coli*
PF	-	-
PF-Si-NH$_2$-Fe^0	26 mm	21 mm
PF-NH$_2$-Fe^0	35 mm	26 mm
PF-SH-Fe^0	35 mm	38 mm

[a]Mean values were given in the table after performing three tests of each analysis.

These results are of great importance and can be explained by the strong capacity of the iron nanoparticle immobilized on polyester nonwoven fabric to alter the membrane of *E. coli* and S*. epidermidis*, inducing cell wall rupture. This iron nanoparticle's synergistic antibacterial activity is consistent with the process previously described [290, 363, 364]. The inhibition zone diameter (see Table 4.18) reveals that the PF-SH-Fe^0 and PF-NH$_2$-Fe^0 catalysts were more robust compared to PF-Si-NH$_2$-Fe^0. This may be attributed to the existence of a significant amount of stabile iron particles, their mass, particle size, and large surface area [365] as well as the antibacterial property of polyamidoamine dendrimer [290].

As a comprehensive investigation of the antibacterial effect of the resulting catalysts (PF-Si-NH$_2$-Fe^0, PF-SH-Fe^0, and PF-NH$_2$-Fe^0), optical density analysis was also performed. Result presented in Figure 4.33 showed that the samples of amine and thiol-based linkers are effective in inhibiting the growth of bacteria strains in water. The removal efficiency was investigated by computing the kinetics derived from UV-vis spectroscopic results. It was found that the thiol (SH) based PF-SH-Fe^0 catalyst removed the maximum (average 86%) bacteria at $2.398×10^{-2}$/min which can reach up to 99.97% depending on the time and amount of catalyst used. According to the discussion about the elimination of organic compounds (dyes, phenols) from water, the explanation for the higher effectiveness of the PF-SH-Fe^0 membrane against catalytic action against bacteria strains (antibacterial effect) is also due to the higher stability of immobilized zerovalent iron nanoparticles of textile surface.
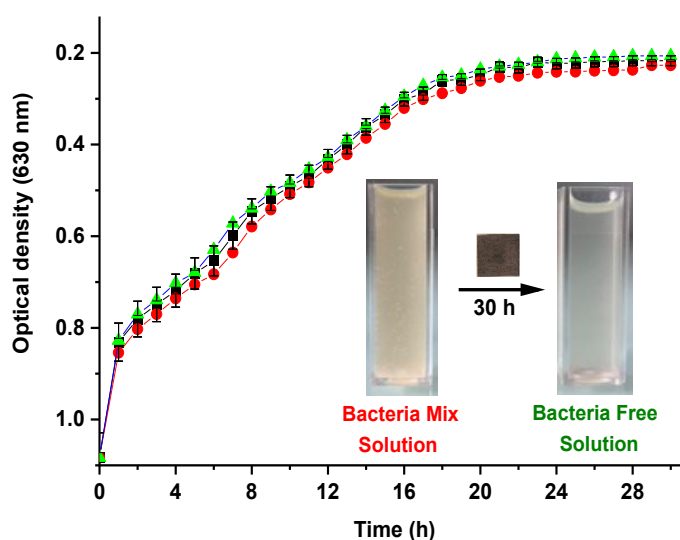
Figure 4. 33: Optical density analysis of antibacterial property of the PF samples the mixture of gram-positive and gram-negative bacteria strains; (●) PF-Si-NH$_2$-Fe^0 (■) PF-NH$_2$-Fe^0 and (▲) PF-SH-Fe^0.

4.2.4. Discussion: Study B

This study investigated the effects of tailor-made polyester nonwoven fabric (PF) on the immobilization of zerovalent iron. A tailor-made PF surface with amine/thiol functional groups was fabricated by chemical grafting of either 3-(aminopropyl)triethoxysilane (APTES), polyamidoamine dendrimer (PAMAM), or 1-thioglycerol (SH). Before that, the hydrophobic surface of the PF had been activated by plasma eco-technology, as described in Study A. The results and mechanisms related to plasma activation of the polyester nonwoven fabric have already been discussed in section 4.1.4 of chapter 4.

Chemical grafting of APTES, PAMAM, and SH on plasma-activated PF was validated through various tools and techniques, including sessile droplet goniometry, OM, SEM, FTIR, TGA, and DSC. As explained in the introduction of this thesis, a number of studies recommend using APTES, PAMAM, and SH as the binder for various functional materials. The active functional groups of the selected polymers created ionic interaction while the polymers spread over the surface of the PF as a coating. This was observed in SEM analysis of the prepared samples. The overall coating significantly influenced the chemical properties of the polyester nonwoven fabric. Wettability analysis through sessile droplet goniometry revealed an interacting phenomenon, where it was found that the PF with grafted PAMAM, APTES, and SH was completely hydrophobic in nature, while the PF samples before the grafting had been highly hydrophilic due to the activation through the plasma eco-technology treatment. This overall alteration of the surface chemical properties of the host material due to the grafting of PAMAM, APTES and SH has been reported in their other applications as well [193, 366-369].

Iron particles were immobilized on the prepared tailor-made polyester nonwoven fabric with amine/thiol group functionality. Results from multiple analyses suggested strong interactions between the iron particles and the functional groups on the surface (Fe: NH_2|SH) due to the grafting of PAMAM, APTES, and SH. This had been anticipated based on extensive characterization of the samples. The structure of both APTES and PAMAN includes amine (-NH_2) terminal groups. These groups served to immobilize and interact with iron nanoparticles through electrostatic interaction. However, in the case of thioglycerol, the terminal groups were hydroxyl (-OH), which were exposed for attachment to the iron nanoparticle surface (see Figure 4.34).
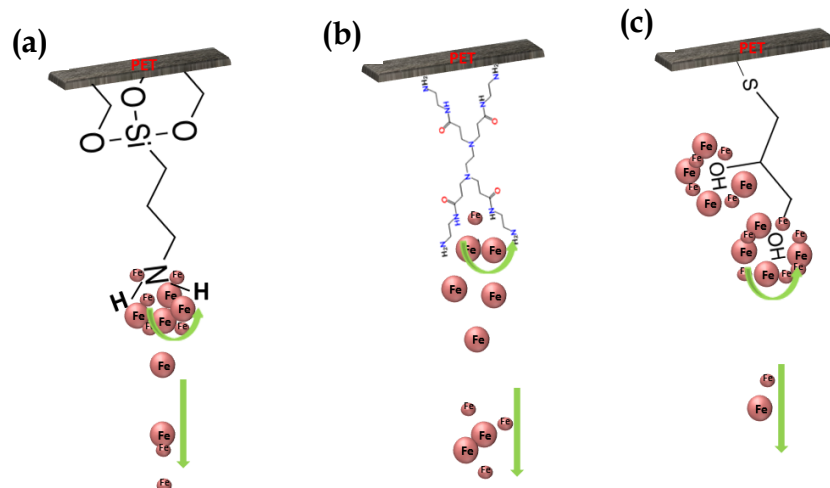
Figure 4. 34: Illustration of the abstraction of iron nanoparticles from the (a) APTES-grafted PF, (b) PAMAN-grafted PF and, (c) SH-grafted PF surfaces.

In this case, when thiol or amine came into contact with the iron particles, the weakest portion of the bridge structure broke, resulting in a rupture. The difference between thiol and amine may explain the resulting rupture force. Thiol grafting led to strong dispersion of the iron particles, observed through SEM, optical

microcopy, and catalytic activities. The interaction force of thiol is greater than that of amines and is the most likely source of the breakup with iron nanoparticles.

Size distribution analysis of zerovalent iron particles shows that the type of functional groups on the surface of the PF also influenced the structural morphology of the *in-situ*-synthesized iron particles. The dispersion and size of the particles are related to the aggregates formed from iron particles due to strong magnetic attraction among them [370]. Higher aggregation leads to larger (and irregular) particles. Strong interaction between thiol groups and iron explains the lower particle size on PF-SH-Fe^0. Furthermore, the density of the immobilized iron particles was higher for SH-grafted PF than APTES- or PAMAM-grafted PF. This is due to the high affinity of sulfur atoms for iron nanoparticles [371].

The prepared PF samples with immobilized zerovalent iron were used as catalysts either in a heterogeneous Fenton-like system (in the presence of H_2O_2), in a catalytic reductive system (using $NaBH_4$ as a reducing agent), or in a pathogen inhibition system for the removal of organic and pathogenic contaminants from water. During the application in the heterogeneous Fenton-like system (in the presence of H_2O_2), the zerovalent-iron-immobilized PF catalysts were effective in removing a high concentration of crystal violet dye from water in as little as 22 min. Nevertheless, it is well known that H_2O_2 molecules can be decomposed effectively to hydroxyl radicals ($^•OH$) by zerovalent iron particles [372]. The $^•OH$ produced can effectively mineralize many pollutants (including colorants, phenolic compounds, and various POPs), as reported in numerous studies [373, 374]. The influence of various factors in removal performance was investigated experimentally and explained through statistical modeling, revealing that the pH and the concentration of H_2O_2 affected the efficiency of the pollutant removal. (Although this is similar to the conventional process with a solution of zerovalent iron, there are other advantages to immobilization.) In the catalytic reductive system (using $NaBH_4$ as the reducing agent), the performance of the zerovalent-iron-immobilized PF catalysts was extensively assessed for both colorants and phenolic compounds (individually and in a mixture). The results showed that the samples had high catalytic activity in pollutant removal. The removal performance was closely related to the interaction between zerovalent iron particles and the reducing agent, whose mechanism has already been established elsewhere [375]. The results of pathogen inhibition and the removal of pathogenic contaminants from water using the prepared fabric samples effectively validated the catalytic activity of the immobilized zerovalent iron. This finding is consistent with the study done by Lee *et al.* (2008) [365]

In summary, it can be stated that, following zerovalent iron immobilization of PF, the main findings of Study –A and Study-B (of Chapter 5) also indicates that, immobilized glucose oxidase enzyme on tailor-made PF surface retained catalytic activity (as validated through various analysis) without compromising the inherent catalytic performance of GOx. The conclusion also delivers the answers to RQ 1 (Research question 1) and RQ 3 (Research question 3) of this thesis. The following chapter (Chapter 6) will seek the answer to the final research question of this thesis.

"

Research Question 1 (RQ 1): How feasible is textile as a support material for catalyst immobilization?
Research Question 2 (RQ 2): Can we immobilize inorganic catalysts (Fe^0) on textiles without compromising their inherent catalytic performance?

"

Chapter 5

Immobilizing biocatalyst (glucose oxidase enzyme) on textile

Chapter outline

This chapter presents the results of immobilizing the biocatalyst (glucose oxidase, GOx) on polyester nonwoven fabric (PF). Enzyme immobilization is a widespread empiric technology that yields stable, active, and reusable enzymes. The performance of the immobilized enzymes depends on several factors, but the binding interaction between the support matrix and the enzyme is crucial. This chapter explores different ways of tailoring the surface of the PF to achieve stable and robust immobilization of GOx. The studies have been divided into two categories and termed Study-A and Study-B, and presented in Figure 5.1.
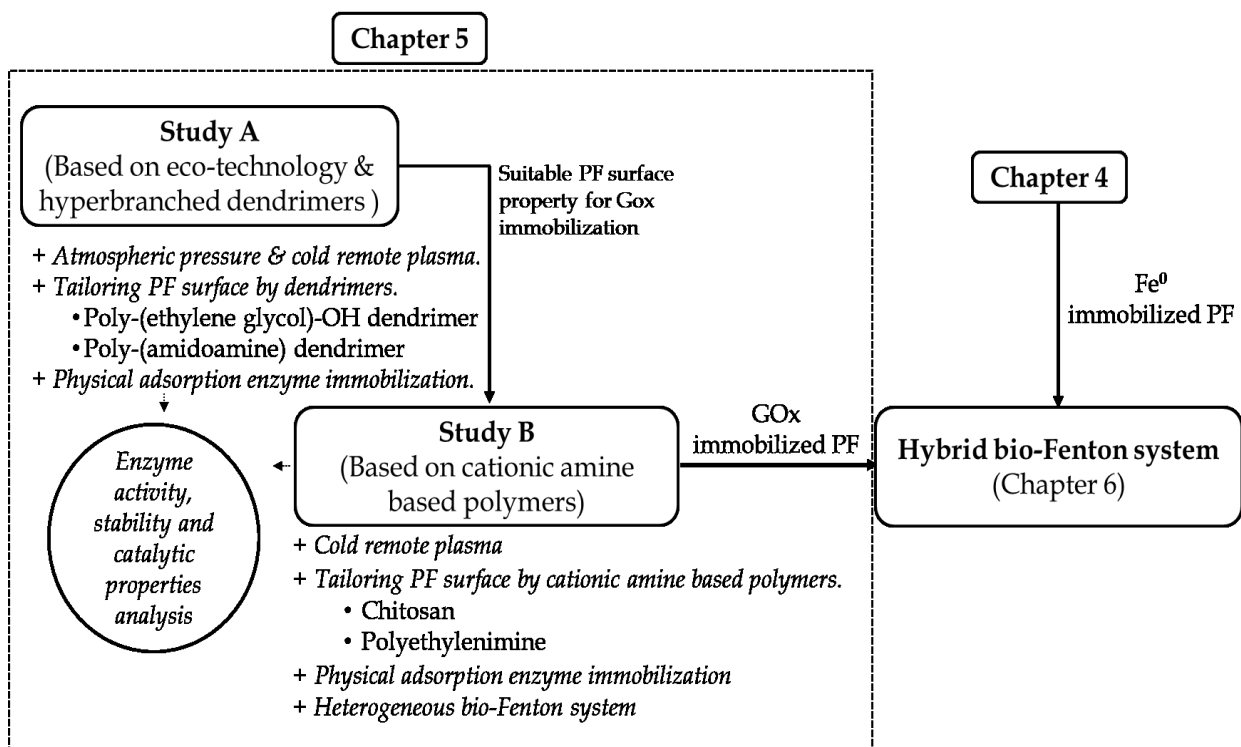
Figure 5. 1: Schematic presentation of the chapter outline and correlation to the thesis.

Study A focuses on the competitive advantages of using plasma eco-technology (either atmospheric-pressure or cold remote plasma) and hyperbranched dendrimers (with either -OH or -NH$_2$ end terminal groups based) for

robust immobilization of GOx on the PF surface. Based on the results of Study A, Study B deals with tailoring the surface of the PF with cationic amine-based polymers (either chitosan or polyethylenimine). Catalytic loading, activity, and stability (leaching, washing, and temperature) of the immobilized GOx were compared to determine the optimal conditions for the robust immobilization of GOx on PF. The catalytic behaviors of the prepared GOx-immobilized PF were analyzed in terms of their antibacterial properties (Study A) and as a catalyst in a heterogeneous bio-Fenton system for the removal of water pollutants (Study B). The outcome of this chapter addresses research questions 1 and 3.

5.1. <u>Study A</u>: Eco-technology and hyperbranched dendrimers for immobilizing glucose oxidase enzymes on polyester nonwoven fabric

5.1.1. Introduction

Glucose-1-oxidase (GOx) (D-glucose: oxygen-1-oxidoreductase) is a naturally produced redox enzyme that catalyzes the oxidation of D-glucose into D-glucono-1,5-lactone or D-glucono-δ-lactone and hydrogen peroxide using molecular O_2 as an electron acceptor [129, 257, 376]. The immobilization of GOx would allow faster regeneration and better regulation of the reactor configuration and reaction output [377-380]. Several materials have been proposed as supports for GOx immobilization, such as carbon felt [129], gold nanostars [4], cellulose nanocrystals [381], carbon nanotubes [382, 383], nanofibers [384], metal nanoparticles [6, 7], and textiles (such as PF [124]). GOx immobilization on PF is complicated, as PF is highly inert, with low surface energy. Consequently, the PF fiber surface must be activated before it interacts with the surrounding environment. Several PF activation processes are available including alkaline hydrolysis [385], photo-induced irradiation [386], electron beam irradiation [387], enzymatic hydrolysis [84], and plasma eco-technologies [296].

Plasma eco-technology is a cost-effective, resource-efficient, and eco-friendly process (no harmful solvents, no chemical waste, and less degradation of the specimen) for the surface activation of PF. Several studies have reported the effectiveness of plasma treatment activation through the integration of the desired functional groups, such as hydroxyl, carboxyl, amine, amide, etc., by selecting the appropriate plasma-discharge parameters (i.e., the type of gas, treatment time, input power, etc.) [388, 389]. Vesel *et al.* (2008) reported that a change in nano-roughness (~10 nm) of the PF by the plasma containing oxygen [66] and nitrogen [390] may have a significant effect on protein immobilization [388].

Dendrimers are highly branched (hyperbranched) fractal-like macromolecules with well-defined monodisperse architecture, three-dimensional structures, shape, and topology. They are polymers with a regular structure and a high density of end groups [391]. Hyperbranched dendrimers are eco-friendly and can form complexes with other molecules via molecular encapsulation and both covalent and non-covalent interactions [276]. Several studies reported strong interactions between the GOx enzyme and dendrimers due to the presence of multiple functional groups in the dendrimers. This polyvalence property of dendrimers enables self-assembly into aggregates through a combination of interactions [277-282]. The end uses of dendrimers have been extensively described in biotechnology and biomedical applications, but information about the use of dendrimers for GOx immobilization on surface-activated is rather limited. Therefore, we investigated the influence of both plasma eco-technology and hyperbranched dendrimers in the robust immobilization of GOx on PF. Air atmospheric plasma and cold remote plasma with a mixture of nitrogen and oxygen gases (N_2+O_2) have been used to activate the hydrophobic PF surface, followed by chemical grafting of either poly-(ethylene glycol)-OH dendrimers or PAMAM dendrimers. GOx immobilization was then done through a physical adsorption method. The surface activation of the PF by plasma

eco-technology was validated based on results from wettability (sessile droplet goniometry and capillary uptake) and x-ray photoelectron spectroscopy (XPS) analysis (already described in chapter 4). The effectiveness of plasma eco-technology and hyperbranched dendrimers in the immobilization of GOx on PF was compared in terms of GOx loading, activity, stability (wash and thermal), and catalytic inhibition of pathogenic bacteria strains. The results of this study have been published as Publication VI.

5.1.2.   Material preparation

The first step of material preparation involved activation of the PF through plasma eco-technology, using either air atmospheric plasma or cold remote plasma with N_2+O_2. After that, either poly-(ethylene glycol)-OH or poly-(amidoamine) hyperbranched dendrimers were chemically grafted on the plasma-activated PF. In the third and final stage, physical adsorption immobilization of GOx was carried out on both plasma-activated and dendrimer-grafted PF samples. The effects of each treatment on loading, stability, and catalytic activity of the immobilized GOx were comparatively studied through various mathematical and instrumental tools. The schematic illustration in Figure 5.2 presents the steps of material preparation for this study (Study A).
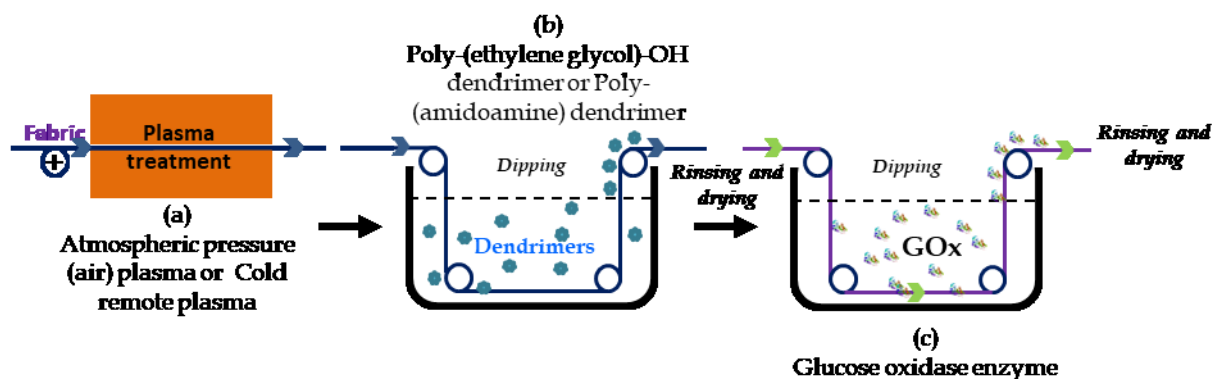
Figure 5. 2: Schematic illustration of path of material preparation for this study; (a) activation of PF through plasma eco-technology, (b) hyperbranched dendrimers grafting on plasma-activated polyester nonwoven fabrics, (c) physical adsorption immobilization of GOx enzyme on polyester nonwoven fabrics.

Two different types of plasma treatment were used for the activation of polyester nonwoven fabric, as described in section 3.2.1 in chapter 3. Air atmospheric plasma treatment was chosen due to its effectiveness in activating polyester nonwoven fabric by integrating polar functional groups, yielding a carboxyl- and carbonyl-rich surface, as explained in earlier studies [296]. On the other hand, cold remote plasma with N_2+O_2 was used to activate the surface of the polyester nonwoven fabric by integrating amine, amide, and carboxyl functional groups [66, 129]. Typically, in atmospheric-pressure (air) plasma eco-technology treatment, the fabric was passed at a speed of 2 m per minute between two electrodes (with an inter-electrode distance of 1.5 mm) under standard atmospheric air conditions, with a glow discharge (dielectric barrier discharge or DBD) instigated by the potential difference [97]. The plasma treatment was carried out at a power of 60 kJm^{-2} with a frequency of 26 kHz and was applied to both sides of the fabric. For the cold remote plasma eco-technology treatment, the PF was positioned in the sample slot of the cold remote plasma eco-technology treatment device. Mixtures of N_2 and O_2 gases were excited by means of a microwave (800 W, at 2.45 GHz) to create a plasma discharge. Nitrogen gas flow was 1,230 sccm, and oxygen flow was 89 sccm at 3.8 mbar. After the plasma treatments, the polyester fabric samples were stored in aluminum foil to avoid deterioration before use.

After plasma activation, the PF samples were further activated through chemical grafting of hyperbranched poly-(ethylene glycol)- pseudo-generation-5 dendrimers with hydroxyl (-OH) end groups, as well as poly-(amidoamine) (PAMAM) dendrimers consisting of an alkyl-diamine core and tertiary amine branches. The method is described in

section 3.2.2 in chapter 3. The resulting dendrimer-grafted polyester nonwoven fabric samples were filtered, washed, and dried overnight (at ambient temperature) before characterization and use.

Finally, the glucose oxidase enzyme was immobilized on the plasma-treated and dendrimer-grafted PF, as described in section 3.2.3 of chapter 3. Typically, the PF samples were immersed in the enzyme solution (prepared by dissolving glucose oxidase in a 0.1 M potassium phosphate buffer solution) with a liquor ratio (cm^2: ml) of 1:3 for 4 hours at 4 °C and a pH of 5.5. The resulting GOx-immobilized PF samples were gently filter-dried before characterization and use.

5.1.3. Results: Study A

The results of Study A have been divided into three different sections. Section (i) presents the results of the surface activation through plasma eco-technology and validates the hyperbranched dendrimer grafting on the plasma-activated PF. Section (ii) provides a comparative analysis of the efficiency of each enzyme-immobilized textile in terms of the loading of GOx, activity, and the stability (leaching, washing, and temperature) of the immobilized GOx. This section contains key results related to the extent of the enzyme loading and enzyme stability under various conditions, which is critical for the robust catalytic application. Finally, section (iii) provides evidence of catalytic activity in the GOx-immobilized PF samples. After appropriate characterization of the materials through various quantitative and qualitative analyses, this section discusses the application of GOx-immobilized PF samples in catalytic inhibition of the growth of bacterial strains. This is the first study to confirm the antibacterial activity of immobilized GOx on a fibrous textile support material. Although the validation of atmospheric-pressure (air) plasma activation of PF has already been discussed in chapter 4, the results are discussed again here for comparison with cold-plasma-activated PF. A common terminology was established for all samples, based on their modification, as presented in Table 5.1.

Table 5. 1: Sample names and corresponding descriptions.

Sample Name	Descriptions		
	Modification-1	*Modification-2*	*Modification-3*
Untreated PF	-	-	-
PF@AP	Atmospheric pressure plasma	-	-
PF@CRP	Cold remote plasma	-	-
PF@AP-PEG	Atmospheric pressure plasma	PEG-OH dendrimer grafting	-
PF@CRP-PEG	Cold remote plasma	PEG-OH dendrimer grafting	-
PF@AP-PAM	Atmospheric pressure plasma	PAMAM dendrimer grafting	-
PF@CRP-PAM	Cold remote plasma	PAMAM dendrimer grafting	-
PN@AP/GOx	Atmospheric pressure plasma	-	GOx immobilization
PN@CRP/GOx	Cold remote plasma	-	GOx immobilization
PN@AP-PEG/GOx	Atmospheric pressure plasma	PEG-OH dendrimer grafting	GOx immobilization
PN@AP-PAM/GOx	Atmospheric pressure plasma	PAMAM dendrimer grafting	GOx immobilization
PN@CRP-PEG/GOx	Cold remote plasma	PEG-OH dendrimer grafting	GOx immobilization
PN@CRP-PAM/GOx	Cold remote plasma	PAMAM dendrimer grafting	GOx immobilization

5.1.3.1. Section (i): Characterizations of plasma activation and dendrimer grafting on polyester nonwoven fabric

Various instrumental and analytic tools such as sessile droplet goniometry, capillary uptake, X-ray Photoelectron Spectroscopy, and Fourier transform infrared spectroscopy analysis were used to investigate and validate the physical and chemical changes in the surface of PF due to the plasma activation as well as grafting of hyperbranched dendrimers. The results of this section are greatly important, as they will provide evidence related to the surface chemical property of PF surface before GOx immobilization.

X-ray Photoelectron Spectroscopy (XPS) analysis indicated the changes in the surface chemical property of PF after plasma treatments and dendrimer grafting. The elemental composition of the samples summarized in Table 5.2 shows that untreated PF samples have a nominal O/C atomic-ratio around 0.3, which has been increased to 0.5 after atmospheric pressure (air) plasma treatment. This occurrence of an increase in O/C atomic-ratio was due to the chain scissions of ester bonds and the formation of carboxyl and hydroxyl terminal groups as consistent with earlier reports [66, 290]. On the other hand, on samples treated by cold remote plasma with N_2+O_2, detection of N (0.6%), can be due to the presence of amino groups on PF surface as consistent with the literature [129]. After dendrimer grafting, further changes in samples surface chemical property have been observed indicating a successful grafting of dendrimers on PF fibers. Deeper information obtained from elemental composition analysis revealed that even after dendrimer grafting-all samples showed the presence of some sort of oxygenated groups. However, samples treated through either cold remote plasma with N_2+O_2 and/or grafting of PAMAM dendrimer showed the presence of characteristics amino-functional groups. It has been observed that the final treatment of the samples has a prominent influence on the surface property of PF. These results validate the claim of surface activation of PF surface through plasma treatments.

Table 5. 2: Physico-chemical properties of polyester nonwoven fabrics before and after plasma treatment (based on XPS analysis)

Sample name	Elemental composition (ratio)	Remarks
Untreate PF	O/C = 0.30, N : 0%	-COOR groups
PF@AP	O/C = 0.50, N : 0%	-OH, -COOH groups
PF@CRP	O/C = 0.38, N : 0.6%	OH, -COOH, -NH$_2$ groups
PF@AP-PEG	O/C = 0.53, N : 0%	-OH, -COOH groups
PF@CRP-PEG	O/C = 0.43, N : 0.2%	OH, -COOH, -NH$_2$ groups
PF@AP-PAM	O/C = 0.40, N : 0.5%	OH, -COOH, -NH$_2$ groups
PF@CRP-PAM	O/C = 0.36, N: 0.62%	OH, -COOH, -NH$_2$ groups

Fourier transform infrared (FTIR) spectroscopy analysis was carried out to scrutinize the outcomes of XPS analysis. Briefly, spectra showed that untreated PF demonstrated some bands in the region 1720-650 cm^{-1}, and a double peak at 2830 cm^{-1} and 2960 cm^{-1} region which were attributed to the stretching vibration of CH$_2$, C=O, aromatic C=C, and stretching vibration of =C–H of aldehyde doublet, present on the surface of polyester fibers [335, 336]. Along with these vibrations and stretching, strong peaks of ether (950–1200 cm^{-1}), carboxyl and carbonyl groups (1650–1710 cm^{-1}) are also visible in all samples indicating that the core structure of polyester has not been altered due to the plasma treatments. On PF@AP, several weak peaks appearing in the region at 3700–3684 cm^{-1} were attributed to O–H stretching possibly due to the integration of new polar hydroxyl and carboxyl groups. Along with similar stretching, weak stretching at region 3346 cm^{-1} observed in PF@CRP was assigned to the stretching vibration of both carboxyl and secondary amine groups [129]. Both XPS and FTIR analyses point out the successful activation of PF (through plasma treatment) and grafting of hyperbranched dendrimers.

To understand the wettability of resultant plasma-activated and dendrimer grafted PF samples, water contact angle (θ_{H_2O}) using sessile-drop goniometry has been measured and validated by capillary uptake measurements as per the method described in section 3.2.1 and section 3.2.2 of chapter 3. Table 5.3 summarizes the findings of wettability analysis (Figure 5.3 shows the capillary uptake curve of PF samples). Results show that the sessile water droplet in untreated PF remain on the surface while recording θ_{H_2O} as high as 141° (showing no meniscus weight,

W_m), which is considerably higher than that of regular PET fibers. The high θ_{H_2O} of PF can be due to the exceptional surface roughness of the nonwoven fabric caused by irregular orientation of fibers. The θ_{H_2O} has been significantly reduced after plasma treatment of PF through both atmospheric pressure (air) plasma treatment and cold remote plasma with N_2+O_2. Since the droplet disappeared very rapidly, the water contact angle of the resultant plasma-treated samples was considered to be 0°. The reduction in water contact angle indicates the wettability of the PF samples might be due to the integration of polar functional groups [296]. The polar surface characteristics of plasma-treated PF samples were further validated by the significant rise in meniscus weight (PF@AP = 1460 mg, PF@CRP= 919 mg) as obtained through capillary uptake measurement.
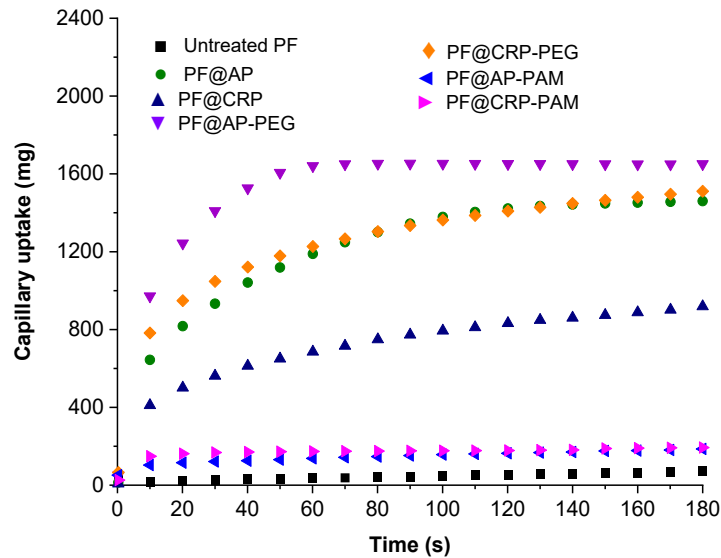
Figure 5. 3: Capillary uptake measurement of untreated PF (■), PF@AP (●), PF@CRP (▲), PF@AP-PEG (▼), PF@CRP-PEG (♦), PF@AP-PAM (◄), and PF@CRP-PAM (►).

Table 5. 3: Wettability analysis of polyester nonwoven fabrics samples.

Sample name	θ_{H_2O} [°] (sessile-drop goniometry)	Capillary uptake measurement	
		W_m (mg)	Calculated θ_{H_2O} [°]
Untreated PF	141	-	-
PF@AP	0	1460	1.46
PF@CRP	0	919	2.30
PF@AP-PEG	0	1650	0.83
PF@CRP-PEG	0	1476	1.44
PF@AP-PAM	102	-	-
PF@CRP-PAM	109	-	-

As confirmed by XPS and FTIR analyses, dendrimer grafting causes alterations in the surface property of plasma-treated PF samples. While the wettability of PF sample was increased by 1.13% (PF@AP vs PF@AP-PEG), and 1.60% (PF@CRP vs PF@CRP-PEG) when hyperbranched poly-(ethylene glycol)-OH dendrimer was grafted as analyzed through capillary uptake measurement, PAMAM dendrimer grafted plasma-treated PF samples showed total hydrophobicity as confirmed in both sessile-drop goniometry and capillary uptake analysis. The increase in wettability after hyperbranched poly-(ethylene glycol)-OH dendrimer grafting can be explained by the integration of highly concentrated hydroxyl groups present in the dendrimer [296]. The decrease in wettability after PAMAM dendrimer grafting may be due to the high integration of N as amino groups. Similar phenomena have been reported by Mutel *et al.* (1993) [392] and Arfaoui *et al.* (2016) [66]. These clear changes in the surface property of PF validate the successful grafting of both dendrimers. Detail discussion of this study is available on Publication VI.

5.1.3.2. Section (ii): Results related to immobilization of GOx on plasma/dendrimer grafted polyester nonwoven fabric

The yield of loading, activity, and stability of immobilized GOx on plasma and dendrimer grafted PF has been studied according to the methods described in section 3.3.2 of Chapter 3. All the data presented in this section was collected through a colorimetric assay of the GOx enzyme.

Table 5.4 shows the summary of quantitative analysis of GOx immobilized PF samples in terms of yield of loading and yield of active immobilized GOx. Results showed that treatments and modification of PF surface provided a visible influence on the activity of GOX. The highest yield of loading of GOx was recorded as 31% (PF@CRP-PAM/GOx), whereas the lowest was 20% (PF@AP-PEG/GOx). The changes in loading performance correspond to the affinity of GOx to the surface of PF. A close look at the data reveals interesting facts where a sample with the abundance of amino groups showed a higher yield of GOx loading than that with no amino groups. Some samples modified with both amino and oxygenated functional groups were moderate in loading efficiency such as; PF@CRP-PEG/GOx secured the loading of 22% GOx and loading yield of PF@AP-PAM/GOx was 26%. For the case of samples modified with both amino and oxygenated functional groups, the outer functional groups were found to be critically important as the orientation of functional groups plays a significant role if prepared through the methods presented in this thesis. The presence of amino-functional groups of PF surface was more successful than that of oxygenated functional groups, which is in agreement with the existing literature [66]. This can be explained by the attraction between two amino acids to form a peptide link as explained by David *et al.* (1987) [393].

Table 5. 4: Yield of loading and active immobilized GOx on polyester nonwoven fabric samples.

Sample name	The yield of loading (%)	The yield of active immobilized GOx (%)	Leached active immobilized GOx (%)
PF@AP/GOx	21	62	48
PF@CRP/GOx	27	74	37
PF@AP-PEG/GOx	20	68	42
PF@AP-PAM/GOx	26	78	39
PF@CRP-PEG/GOx	22	70	41
PF@CRP-PAM/GOx	31	81	38

Loading of GOx on PF samples does not provide the actual information about the status of the enzyme (denatured/active) as this was measured through an indirect method. Therefore, the yield of active immobilized enzymes was calculated through a direct approach. Results summarized in Table 5.4 showed that the amount of active immobilized GOx on PF varies significantly from sample to sample. The yield of active immobilized GOx can be as high as 81% whereas the lowest yield of active immobilized enzyme was 62%. A whopping 19% difference between the PF@CRP-PAM/GOx and PF@AP-PEG/GOx points out a critical factor responsible for such results. The yield of active immobilized enzymes is usually related to several factors which include, the orientation of GOx, the interaction between GOx: PF, blocking of active sites, and presence of inhibitor during immobilization. The highest active immobilized enzyme on PF@CRP-PAM/GOx corresponds to a favorable surface of PF which ensured proper orientation of GOx during immobilization, which did not react with sensitive functional groups of GOx and ought to bring a better GOx: PF interaction. Critical observation of the results reveals a pattern, where samples modified with both oxygenated and amino-functional groups showed better yield in active immobilized enzyme than that with only oxygenated functional groups. This argument is in line with the analysis on the yield of loading and might be driven by the same principle.

The stability of immobilized GOx on PF and the influence of integrated functional groups on PF: GOx complex has been studied as a function of successive rinses, reusability, and temperature. Rinsing of the GOx immobilized PF samples are particularly indispensable, as this process will remove loosely attached enzyme on PF surface, which may otherwise leach during catalytic application. All samples were subjected to a successive cycle of rinsing using the same amount of PBS buffer solution. Based on the preliminary studies, six rinsing cycles were considered for any loss of active immobilized GOx. Results presented in Table 5.4 show high leaching of immobilized GOx after a

total of six rinses with the highest 48% and lowest 37% leaching of GOx. All samples were seen to be stable after six rinsing cycles, although for the first cycles over 50% of total GOx were leached. Leaching came to a stop after four cycles for PF@CRP/GOx and PF@CRP-PAM/GOx and six cycles for all other samples (see Figure 5.4). This phenomenon is particularly important as it indicates that six cycles would be sufficient to remove all unfixed GOx from PF.
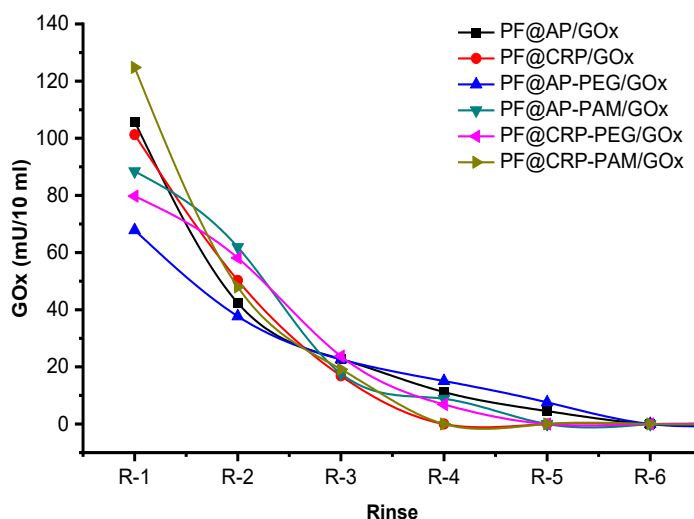
Figure 5. 4: Leaching study based on the stability of immobilized GOx as a function of successive rinses; PF@AP/GOX (■), PF@CRP/GOx (●), PF@AP-PEG/GOx (▲), PF@CRP-PEG/GOx (◄), PF@AP-PAM/GOx (▼) and PF@CRP-PAM/GOx (►).

Detailed analysis of the samples reveals distorted data set (proximity of the results between samples) where a clear conclusion could not be reached. Nonetheless, within the boundary of the data, amino-groups integrated PF samples showed better immobilization of GOx providing high stability of immobilized GOx in terms of leaching during rising cycles. An observation further reveals that, while PF@CRP/GOx shows the lowest leaching of GOx, and this was among the highest in the case of PF@CRP-PEG/GOx and PF@CRP-PAM/GOx. This phenomenon can be correlated to GOx loading on PF, as the surface with amino-functional groups predominantly provides a high affinity to the GOx. Such great affinity attracts a large quantity of GOx on the surface: most of them are loosely adsorbed on the fiber surface, and contribute to the high leaching. It is to be noted that, even with such high leaching, the total remaining active immobilized GOx on amino-functional groups integrated PF surface is higher than that of oxygenated groups integrated PF sample. Conversely, the low affinity of hydroxyl groups results in a fewer amount of loosely attached enzymes on their surface. However, an exception on characteristics has been observed in the PF@AP-GOx sample, where the highest amount of enzymes (among all samples) was found to be leached off during rinsing. This can be attributed to the presence of carboxyl groups along with hydroxyl groups integrated through plasma treatment [66]. Leaching of enzyme carried out on buffer solution has been further supported with the results related to reusability of the GOx immobilized PF. Here the activity of GOx immobilized PF was calculated after successive reuse cycles. A decrease in the quantity of active immobilized GOx was considered as a lost enzyme during reuse.

Figure 5.5 shows the results related to the stability of immobilized glucose oxidase enzyme on polyester nonwoven fabric as a function of reusability cycles. Results showed a sharp decrease in enzymatic activity of all GOx immobilized PF samples in the first three cycles. After the third cycle, a moderate to least decrease in activity was observed until the fifth cycle. All samples showed a stable activity after fifth cycle use showing no/insignificant decrease in enzyme activity. The decrease in enzyme activity after each reuse cycle corresponds to either the leaching of active enzyme or denaturation of enzyme on the process. The loss of enzyme during reusability can occur either in the bath of application or during the recycling process. Since the assay analysis provides the best possible condition for the enzyme to perform, in those conditions, denaturation of the enzyme is most unlikely. Therefore, the leaching of the enzyme during each cycle has been considered as the main cause of reduction in enzyme activity.
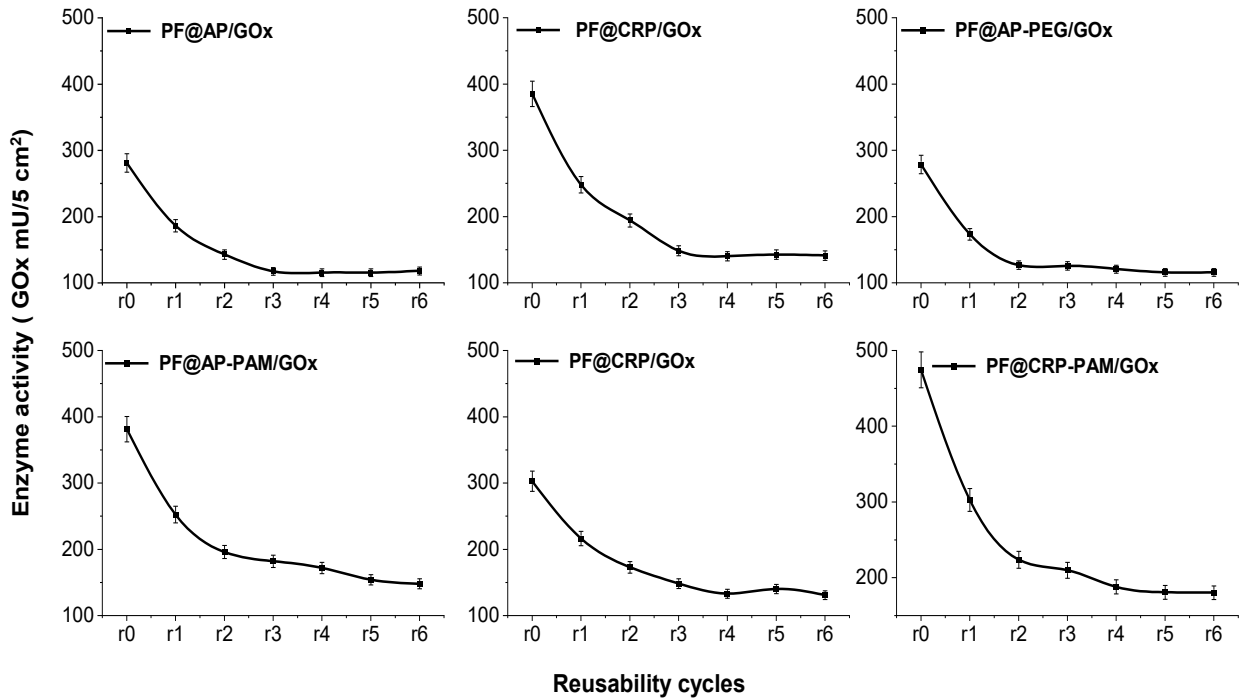
Figure 5. 5: Stability of immobilized glucose oxidase enzyme on polyester nonwoven fabric as a function of reusability cycles.
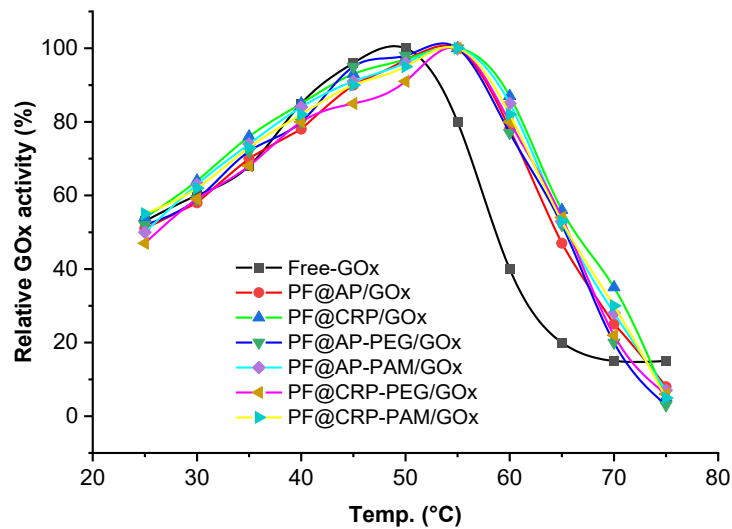
Figure 5. 6: Stability of immobilized GOx as a function of temperature; Free GOx (■), PF@AP/GOX (●), PF@CRP/GOx (▲), PF@AP-PEG/GOx (▼), PF@CRP-PEG/GOx (◄), PF@AP-PAM/GOx (♦) and PF@CRP-PAM/GOx (►).

The performance of the enzyme is sensitive to its surrounding stimuli. Here, the influence of temperature on the stability of immobilized GOx was comparatively studied at different temperatures from 25°C to 75°C. All GOx immobilized polyester nonwoven fabrics were comparatively studied by referring to the stability of free-GOx at the same temperatures. Data were normalized with the maximum value of operation seen both in free and immobilized GOx to help compare the behaviors of free and immobilized GOx. The relative activity (maximum active immobilized enzymes found on primary samples corresponding to 100% of relative activity) obtained for each temperature used with free and immobilized GOx is plotted in Figure 5.6. Results show a slight shifting of the enzyme activity optimal temperature between the free and immobilized GOx. Free GOx displayed a maximum

activity at 50 °C which decreased by 50% at ~60 °C and continued to decline until the activity was absent at 75°C indicating enzyme denaturing due to temperature-related destruction of the enzyme structure as consistent to the literature [394, 395]. In contrast, all immobilized GOx reached the highest activity at 55 °C which decreased by 50% at ~65 °C indicating an increase in improvement of thermal stability of the immobilized enzyme. The sharp decrease in the activity of immobilized GOx can be correlated to the glass transition temperature (Tg) of PF which is around 65-70°C. Mobility of polymer chains in the amorphous region of PET fiber, at a temperature above Tg causes melting of PET and deactivation and/or losing GOx [66]. However, a progressive increase in activity of the immobilized GOx (at neutral pH) provides evidence for the lasting potential of the enzymatic reaction, which will further ensure better reaction control over free-GOx for industrial practices.

Lineweaver-Burk fitting of the activity of GOx

The initial reaction rate of experiments conducted at different glucose concentrations (2 mM to 50 mM) was evaluated using the Michaelis-Menten model of enzyme kinetics [396] and the Lineweaver-Burk method was used to estimate the apparent Michaelis constant (K_m) and maximum velocity of the reaction (V_{max}) as summarized in Table 5.5. K_m and V_{max} were determined by incubating the GOx (free and immobilized) with varying concentrations of the substrate; the results can be plotted as a graph of rate of reaction against concentration of substrate, and will normally yield a hyperbolic curve. As indicated in the table, the immobilized GOx showed a decrease in V_{max}, and an increase in the value of K_m as compared to the free GOx (V_{max} =2.86 mM min^{-1}, K_m=5.80 mM). The increase in the value of K_m could be attributed to the lower accessibility of the active sites of immobilized GOx to the glucose molecules. The decrease in V_{max} value as a result of immobilization is considered to be associated with the lower affinity of the substrate to the enzyme active site. However, when comparing the results among immobilized GOx samples, it can be seen that minimum reduction in V_{max} as well as the minimum increase in K_m, were observed in PF@CRP-PAM/GOx, which again confirm the highest enzymatic catalytic activity of enzyme immobilized on PF with amine surface functional groups.

Table 5. 5: Kinetics parameters of free and immobilized GOx

Sample name	V_{max} (mM min^{-1})	K_m (mM)
Free GOx	2.86	5.80
PF@AP/GOx	1.52	7.11
PF@CRP/GOx	2.10	6.38
PF@AP-PEG/GOx	1.38	8.11
PF@AP-PAM/GOx	1.98	6.75
PF@CRP-PEG/GOx	1.68	6.47
PF@CRP-PAM/GOx	2.21	6.16
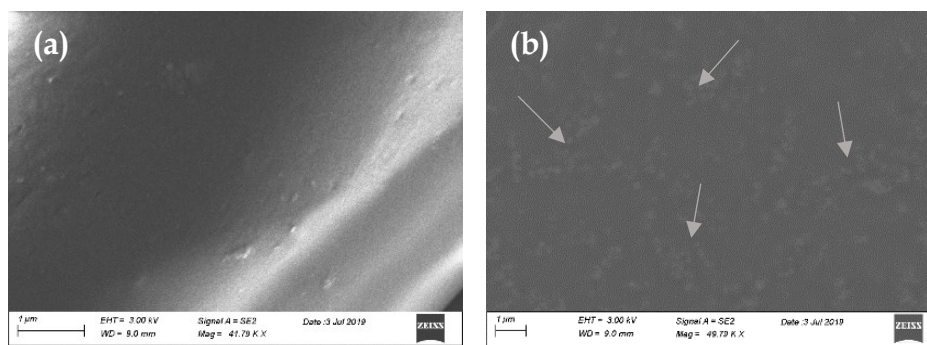
Figure 5. 7: SEM images of the surface of (a) untreated PF and (b) GOx immobilized PF (PF@CRP-PAM/GOx).

A qualitative analytic test by scanning the electron microscope exposes uniformly or exclusively scattered bright points of immobilized fiber enzymes (see Figure 5.7b), but untreated polyester displays a reasonably smooth surface (see Figure 5.7a) as consistent with the report by Kahoush *et al.* (2019) [129].

5.1.3.3. Section (iii): Results related to the antibacterial activity of GOx immobilize PF

To study the catalytic application of resultant GOx immobilized PF, the antibacterial activity of all GOx immobilized samples were investigated under natural conditions through diffusivity and zone inhibitory analysis against both gram-positive and gram-negative bacteria (*S. epidermidis* and *E. coli*) strains. Before place the sample on Petridis, the sample was wetted quickly in a glucose solution that will oxidize into hydrogen peroxide. Produced hydrogen peroxide is responsible for rapturing the bacterial cell wall, which later shows an apparent antibacterial property. A blank experiment was conducted using an untreated PF. The results of antibacterial activity analysis of untreated PF and GOx immobilized PF has been presented in Table 5.6 based on the diameter/outspreading of the inhibition zone (area of inhibition of bacterial growth). According to ISO 20645 standard, the outspreading up to 1 mm inhibition zone and no growth under specimen or no inhibition zone is accepted as effective [361, 362]. Results from Table 5.6 shows that untreated PF has no inhibition zone, which means the PF does not possess antibacterial behavior in pristine form. However, all GOx immobilized PF samples showed effective inhibition of bacterial growth showing inhibition zone varied from 19 mm to 41 mm. As obtained high inhibition zone conclusively validates the immobilization of GOx on PF and their superior antibacterial property in presence of D-glucose.

Table 5. 6: The zone of inhibition (mm) analysis according to test method ISO 20645.

Sample name	*Staphylococcus epidermidis*	*Escherichia coli*
Untreated PF	-	-
PF@AP/GOx	19 mm	23 mm
PF@CRP/GOx	21 mm	29 mm
PF@AP-PEG/GOx	31 mm	33 mm
PF@AP-PAM/GOx	38 mm	38 mm
PF@CRP-PEG/GOx	39 mm	38 mm
PF@CRP-PAM/GOx	41 mm	35 mm

5.1.4. Discussion: Study A

This study shows that the hydrophobic surface of non-woven polyester fabric was activated by both atmospheric-pressure (air) plasma and cold remote plasma. The surface of the activated polyester nonwoven fabric was further modified by chemical grafting of amine- and hydroxyl-end hyperbranched dendrimers, which later were used for immobilization of glucose oxidase enzyme, yielding a polyester fabric with bio-catalytic activity. However, there was substantial variation in the efficiency of enzyme immobilizing between the two plasma treatments and two different dendrimers. Wettability analysis demonstrated the effects of the different treatments on the surface roughness and capillary uptake of the PF. Following surface activation, there was a significant decrease in water contact angle, corresponding to an increase in hydrophilicity of the fabric. Primarily, the radicals formed during the plasma treatment due to the scission of ester bonds created a polar surface with end functional groups such as C–O, C=O, C=N, N–H, and N–C–O, confirmed by FTIR analysis. The addition of O_2 in the cold remote plasma treatment produced polar terminal groups, giving PF@CRP a hydrophilic surface, whereas the presence of N_2 explains the formation of amino/imide/amide groups on the polyester surface. These polar groups integrated into plasma-treated polyester allow the formation of van der Waals forces or hydrogen bonds between the PF and

dendrimers. Upon grafting of the dendrimers, the PF could be divided into two groups, one with hydroxyl functional end groups and the other with amine functional end groups. Both functional groups provided favorable conditions for enzyme immobilization [397, 398].

The loading of the GOx enzymes on the polyester surface was influenced by the functional groups integrated by the plasma treatment and dendrimer grafting. Amino acids are organic compounds containing amine ($-NH_2$) and carboxyl ($-COOH$) functional groups and are the sole element (from protein) of all known enzymes [399-401]. Therefore, this is apparent that amine groups would provide the most favorable conditions for robust enzyme immobilization. Since the polyester fabric was functionalized by plasma and dendrimers, yielding amine and hydroxyl groups, the enzymes covalently bonded with the polyester fabric by reacting with the corresponding functional groups. The results showed that amine groups provide better enzyme immobilization efficiency than hydroxyl groups. The active sites of amine functional groups brought a large number of enzymes to the fiber surface. On samples where the estimated number of amine functional groups is higher, higher enzyme affinity was observed. In addition to hydrogen bonding with carbonyl groups, covalent bonding with the amino acids of the enzymes [402, 403] can lead to reduced leaching of the enzyme into the reaction medium. Lower leaching of enzymes consequently extends the reusability. Additionally, the PF is inherently a 3D porous material composed of cylindrical fibers with high porosity. While high porosity can allow easy inflow and outflow of reaction mixtures (substrates or products), the total surface area of the fibers per unit area of the nonwoven material is high enough to allow for the fixation of a sufficient amount of enzymes. Hydrophilization of the PF surface via plasma treatment and/or dendrimer grafting would not only improve this flow of liquid but would also create specific functional groups, allowing enzymes to be immobilized with the appropriate access to the active sites, hence improving bioactivity.

In summary, the glucose oxidase enzyme was securely immobilized on the polyester surface modified with plasma and hyperbranched dendrimers. The plasma treatment activated the hydrophobic polyester surface by introducing hydrophilic groups, such as terminal hydroxyl and amine groups, that facilitated the grafting of the dendrimers. The synergistic effect of the hydroxyl, carboxyl, amine, and amide groups enabled enzymes to be immobilized on the textile surface and remained active, maintaining stability and reusability properties. This study also validates the first attempt to confirm the antibacterial activity of the glucose oxidase enzyme immobilized on a fibrous textile, showing high antibacterial activity (zone inhibition of up to 41 mm). This means that enzyme-immobilized textiles are robust catalysts capable of bio-catalysis in a heterogeneous catalytic system. These findings lead us to our next study, where we investigated the effect of cationic amine-rich polymers grafted on the textile surface for improved immobilization of GOx for use in a heterogeneous bio-Fenton system to remove toxic pollutants from water.

5.2. <u>Study B:</u> Tailoring surface of the polyester nonwoven fabric by cationic amino-based polymers for immobilizing glucose oxidase enzyme

5.2.1. Introduction

The higher density of oxygenated and amine functional groups at the surface of the support matrix allows higher enzyme loading (more binding sites to immobilize additional enzymes on the surface) and robust immobilization (a single enzyme may interact with multiple points on the support material). Kuo *et al.* (2012) [404] reported that a coating of chitosan (an amine-rich natural polymer) on Fe_3O_4 nanoparticles led to robust loading of lipase, which retained 83% of its activity even after twenty repeated use cycles. Chitosan is a natural polymer with unique physicochemical properties [405]. Verma *et al.* (2020) [405] and Kamaci *et al.* (2020) [406] reported that the polycationic structure of chitosan (with both oxygenated and amine functional groups) can interact with the anionic or negatively charged part of enzymes and bind them securely to the support material, ensuring stability.

Other studies, by Rios *et al.* (2019) [407] and Virgen-Ortíz *et al.* (2017) [408], reported the effectiveness of polyethylenimine (PEI), an amine-rich polymer, for the robust immobilization of enzymes on various support materials. PEI is a cationic polymer, which contains primary, secondary, and/or tertiary functional amine groups [409]. It exhibits low toxicity and ease of separation and is used in many applications. Changni *et al.* (2020) reported that PEI can form ionic bonds with around 70–80% of all proteins contained in crude extracts [410].

However, neither of the two amine-rich polymers has been studied for its effectiveness in modifying the textile surface for immobilization of proteins/enzymes. Therefore, this study has been devoted to modifying and preparing polyester textiles to function as a favorable host/support material for the robust immobilization of GOx. This was done by grafting amine-rich functional groups on the PF surface using simple and eco-friendly processes and less toxic or non-toxic polymers will be a solicitous approach for such purpose.

Therefore, in this study, we have investigated the potential of amine-rich polymers such as polyethylenimine and chitosan for the immobilization of GOx, as well as their bio-catalytic activities. The structural features of the treated PF samples at each stage of modifications were studied using analytic and instrumental techniques such as sessile-drop goniometry, electrokinetic measurement (streaming-potential analysis), x-ray photoelectron spectroscopy (XPS), Fourier transforms infrared (FTIR) spectroscopy, and so on. The loading, stability, and activity of the immobilized GOx on different samples were compared. Finally, the enzyme-immobilized polyester textiles were studied for their bio-catalytic activities in a heterogeneous bio-Fenton system for the removal of toxic pollutants from water.

5.2.2. Material preparation

The material preparation in this study involved the activation of polyester nonwoven fabric (PF) through plasma eco-technology; surface modification of PF through chemical grafting of either chitosan (CS) or polyethylenimine (PEI) on the plasma-activated PF; and immobilization of the GOx enzyme on both activated and functionalized PF, as described in sections 3.2.1 and 3.2.2 of chapter 3 (see Figure 5.8).

The plasma treatment of the PF was carried out at a plasma power of 1500 W in the presence of He, O_2, and N_2 gases (in a 1:0.2:1 ratio). The fabric was slid between two electrodes (d = 2.5 mm) at 2.0 m per minute under atmospheric pressure conditions (22 ±2 °C). The treatment was applied to both sides. The treated fabric was

referred to as PF@AP. To avoid aging, the activated PF samples were stored in an airtight dark chamber before use. The freshly surface-activated PF samples were further modified by chemical grafting of one of the two preselected amine-rich polymers (CS and PEI). For that, the PF@AP was soaked separately in either a CS solution (4.0 g·L^{-1}, 1 M acetic acid, pH of 4) or a PEI solution (4.0 g·L^{-1}, pH of 5) for 1 h at 60 °C with gentle magnetic stirring. Both CS and PEI solutions had been prepared earlier, stirred for 24 h, and balanced for 2 h before chemical grafting on PF. The treated PF samples were referred to as PF@AP-PEI and PF@AP-CS. The samples were rinsed with warm ultrapure water, dried at 60 °C, and stored in a desiccator before further use.
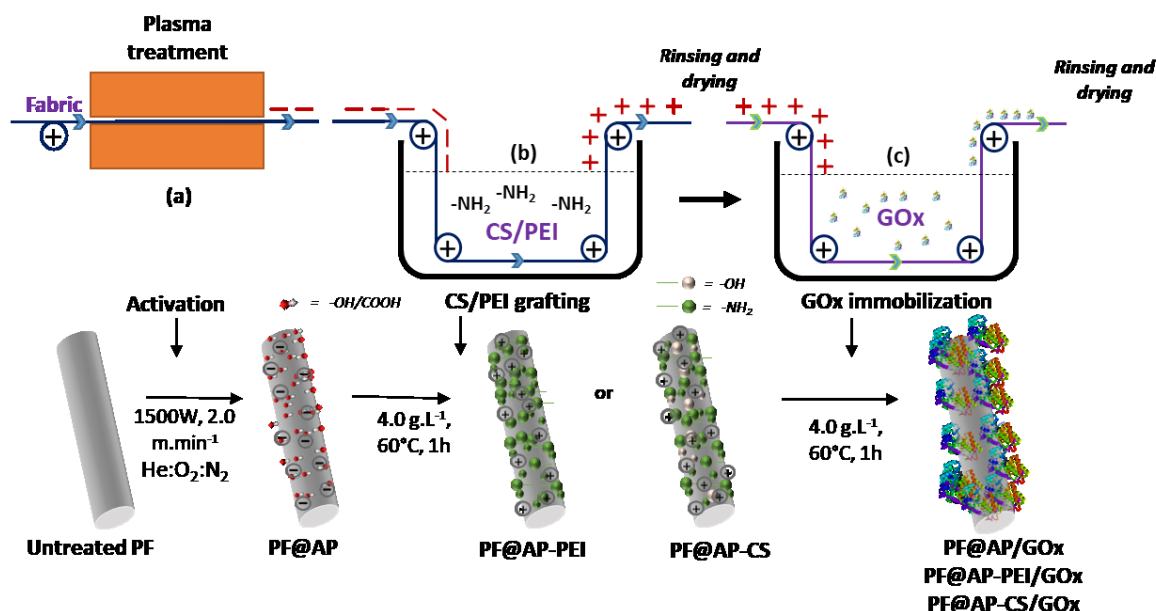
Figure 5. 8: Schematic illustration of (a) activation of PF through plasma eco-technology, (b) surface functionalization through chemical grafting of either CS or PEI on plasma-activated PF, and (c) immobilization of GOx on both activated and functionalized PF.

Finally, the prepared PF samples were immersed in the GOx enzyme solution (cm^2: ml = 1:3) at two different pH levels (5.5 and 7.0) for 4 h at 4 °C. The GOx solution had been prepared by dissolving GOx (0.190 U·ml^{-1}) in a 0.1 M phosphate buffer solution (PBS). During the immobilization, the solution was shaken every 20 min. The enzyme-immobilized PF samples (referred to as PF@AP/GOx, PF@AP-PEI/GOx, and PF@AP-CS/GOx) were carefully removed from the solution, dried at 4 °C overnight, and preserved under ambient conditions before characterization and use.

5.2.3. Results: Study B

Similar to Study A, the results of Study B have are also presented in three sections. Section (i) presents the evidence related to the surface activation of PF through plasma eco-technology and the validation of the chemical grafting of amine-rich polymers (chitosan and polyethylenimine) on plasma-activated PF. Once the validation of plasma activation and grafting of amine-rich polymers was achieved, resultant samples were used to immobilize the glucose oxidase enzyme. Section (ii) provides a comparative analysis of the efficiency of each sample at GOx immobilization, based on the loading of GOx, activity, and the stability (leaching, washing, and temperature) of the immobilized GOx. The final section (section iii) presents the application of the prepared materials (GOx-immobilized PF) in a heterogeneous bio-Fenton system for the removal of toxic pollutants from water. This is the first attempt to use GOx-immobilized textiles for this application. Although the validation of the plasma activation of PF has already been discussed in Chapter 4, it is discussed again here for comparison with the surface

functionalization with CS and PEI. For ease of reference, samples were assigned abbreviated names based on their modifications, as presented in Table 5.7.

Table 5. 7: Sample names and corresponding descriptions.

Sample Name	Descriptions		
	Modification-1	*Modification-2*	*Modification-3*
Untreated PF	-	-	-
PF@AP	Atmospheric pressure plasma	-	-
PF@AP-CS	Atmospheric pressure plasma	Chitosan grafting	-
PF@AP-PEI	Atmospheric pressure plasma	Polyethylenimine grafting	-
PF/GOx	-	-	GOx immobilization
PF@AP/GOx	Atmospheric pressure plasma	-	GOx immobilization
PF@AP-CS/GOx	Atmospheric pressure plasma	Chitosan grafting	GOx immobilization
PF@AP-PEI/GOx	Atmospheric pressure plasma	Polyethylenimine grafting	GOx immobilization

5.2.3.1. Section (i): Results related to activation of PF and grafting of cationic amino-based polymers

The wettability of the polyester fabric before and after surface activation was studied using sessile-drop goniometry. Deionized water droplet was placed on the front side of fabrics and a camera with a display performance of 60 frames per second (fps) was used to determine the initial water contact angle (θ_{H_2O}). Sessile-drop goniometry measures the static contact angle. However, for a rough surface such as textile, the liquid moves around before it settles and the wetting phenomenon is more than a static state. In a typical manner, the angle of contact defines the roughness and presence of hydrophilic/hydrophobic groups of the material's surface. Higher the roughness and hydrophilic groups will provide lower water contact angle ($\theta_{H_2O} = 138°$) and vice-versa. The report of θ_{H_2O} analysis of untreated PF, PF@AP, PF@AP-PEI, and PF@AP-CS have been displayed in Figure 5.9. Results of untreated and activated PF showed a sharp decline in θ_{H_2O} from 138° to 0°. This result is consistent with the result and explanation of our previous study that has been discussed earlier in *chapter 5*. The decline of water contact angle indicates the integration of hydrophilic surface groups (–COOH, –OH, –NH₂) on the surface of PF as consistent with other literature [388, 411, 412].

(a)   **(b)**   **(c)**   **(d)**
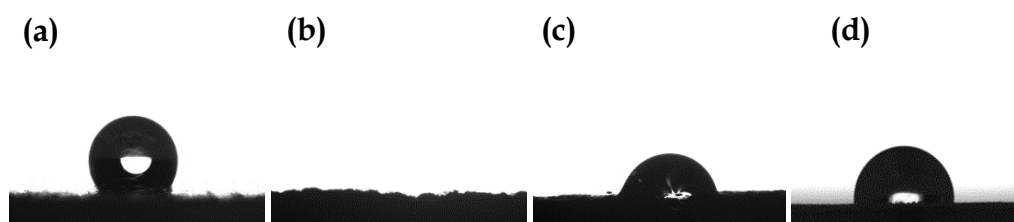
Figure 5. 9: Contact angle analysis of (a) untreated PF, (b) PF@AP, (c) PF@AP-PEI, and (d) PF@AP-CS.

Upon grafting of CS and PEI on plasma-treated polyester fabric (PET-CS, PET-PEI) the contact angle of modified nonwoven fabrics has risen to 98° and 75° respectively (see Figure 5.9c-d). Grafting of CS onto the polyester could introduce surface groups such as hydroxyl, amide, and carboxyl, which contributed to H-bond formation with water, hence the water contact angle, is lower than that of untreated PF. Between PF@AP-PEI and PF@AP-CS, the water contact angle of PF@AP-PEI was smaller than that of PF@AP-CS resulting from the introduction of the higher

number of amino groups to the fabric surface by PEI. Therefore, the wettability of PF@AP-PEI was better than that of PF@AP-CS. However, both of them contain favorable surface functional groups to bind with amino acids of the enzyme.
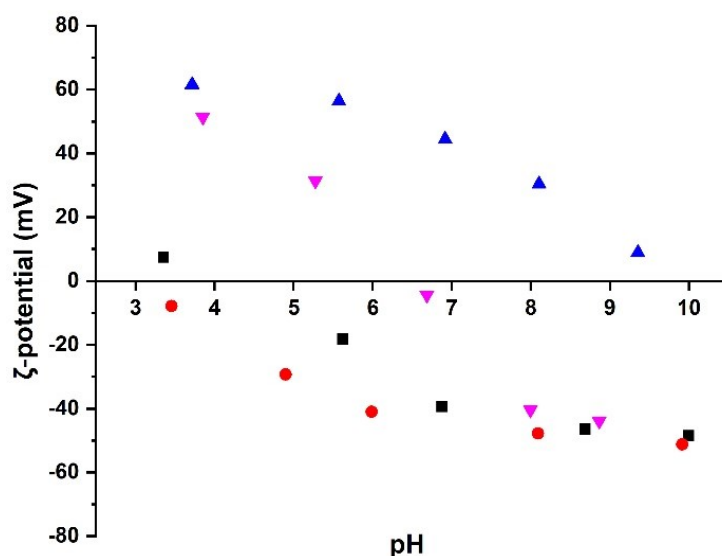
Figure 5. 10: ζ-potential values determined for untreated PF (■), PF@AP (●), PF@AP-PEI (▲), and PF@AP-CS (▼) in dependence on pH of an aqueous 10^{-3} M/L KCL solution.

The isoelectric point (iep = $pH|\zeta = 0$) observed by electrokinetics was measured as the streaming potential to determine the ζ-potential values. The ζ-potential values of untreated and functionalized PF samples are shown in Figure 5.10. Untreated PF has an isoelectric point of $pH = 4.0$ which indicates that the surface charge of polyester is negative for pH higher than 4.0. The negative surface charge of polyester is due to the dissociation of end-terminal functional groups (–OH and –COOH) of the polymer. After plasma activation, PF seems to be carrying a negatively charged surface in all pH ranges, which indicates the formation of additional hydrophilic functional groups on the surface due to the plasma treatment. This is in correlation with the water contact angle analysis of PF@AP-PEI (see the previous section). However, after functionalization of fabrics by amine-rich cationic polymers, the degree of carboxylic groups decreases, and positively charged functional groups are present on the surface of the textile. This results in increasing the value of isoelectric points. PF@AP-PEI carries a positive surface charge for any range of pH. PF@AP-CS has an isoelectric point of 6.7.

FTIR chemical analysis was performed on untreated and functionalized PF to identify their chemical composition and possible functional groups. Spectra of all samples were normalized by equalizing the height of absorption peak at 1712 cm^{-1}, which represents C=O stretch (ester) (see Figure 5.11). An overview of the spectra reveals that there are several common peaks present in all samples. For example, the peak at 1015 cm^{-1} indicates plane vibration of the benzene ring, the peaks at 1091and 1238 cm^{-1} represent C-O stretch (ester), and absorption at 2965 cm^{-1} is due to the asymmetric C-H stretching. All these common peaks are identical to polyester PET [330]. However, after the fabric was plasma-treated, a new but weak stretching at region 2965 cm^{-1} was observed in PF@AP which is assigned to the stretching vibration of OH that overlaps C-H [129]. Identified OH vibration can be due to the integration of polar functional groups (possibly both –OH and –COOH) on the surface of PF due to plasma treatment. Analysis of FTIR of CS and PEI functionalized PF reveals new peaks between 1550 and 1700 cm^{-1}, which correspond to NH bonds. However, it has been assumed that peaks at 1560 and 1650 cm^{-1} might be covered by strong C=O peak of CS. Along with that, PF@AP-PEI has additional peaks at 1576 cm-^{1} and in 3427 cm^{-1}, these peaks also represent N-H bonds.
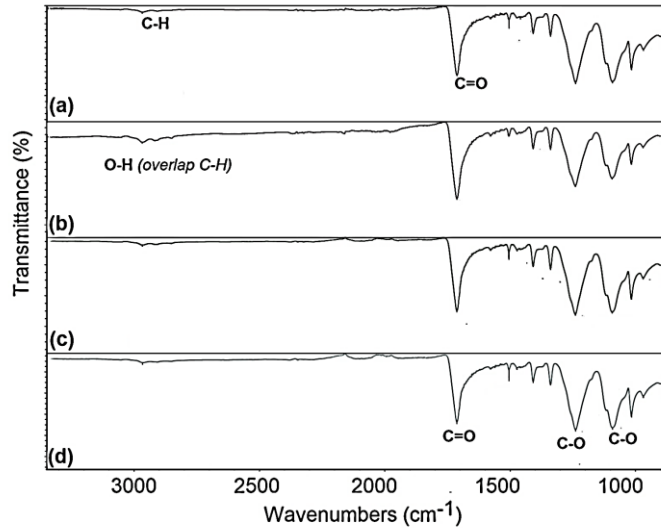
Figure 5. 11: Fourier transform infrared (FTIR) chemical analysis of PF samples; (a) untreated PF, (b) PF@AP, (c) PF@AP-CS, and (d) PF@AP-PEI.

Relating to the above characterization of the materials, a randomly selected group of samples (untreated PF, PF@AP, and PF@AP-PEI) were evaluated by X-ray photoelectron spectroscopy to identify the changes in element composition and the nature of the chemical bonding due to the subsequent surface treatments of PF. Wide scan XPS spectra of samples are presented in Figure 5.12. Results summarized in Table 5.8 show that a control sample contains 76.4 a.t% carbon and 21.1 a.t% oxygen, which after plasma activation changed into 75.4 a.t% carbon and 24.6 a.t% oxygen indicating an increase in oxygen due to the formation of –COOH and –OH groups on the PF surface (see Figure 5.12a-b). A detailed study on PF@AP illustrates that; the sample consists mainly of C and O in a ratio around 3:1. The majority of the carbon (i.e. 60 % of the area) refers to the C≡C and C=C bonding type in the hydrocarbon chain, whereas 40% of the area corresponds to C=O, C-O, and COO⁻. O1s, on the other hand, shows 90% of the signal area is for C=O, C-O, and -OH. All features in the O1s and part of C1s correspond to polyester, i.e. the characteristics functional group along with hydrophilic groups. After chemical grafting of polyethylenimine (PEI), nitrogen was detected in the surface composition along with characteristic oxygen and carbon, which is mainly imine (398.0 eV), pyrrolic/secondary amine (400.0 eV, C_4H_9N/R_2NH), and tertiary amine/graphitic-N/protonated imine (401.5 eV, $R_3N/R_2R=N^+$). The C to O ratio is 4:1. In C1s, 50 % of the area refers to a hydrocarbon chain that consists of C-C and C≡C and around 50 % refers to the carboxylic (COO-) of polyester, the overall changes indicate the successful grafting of PEI.
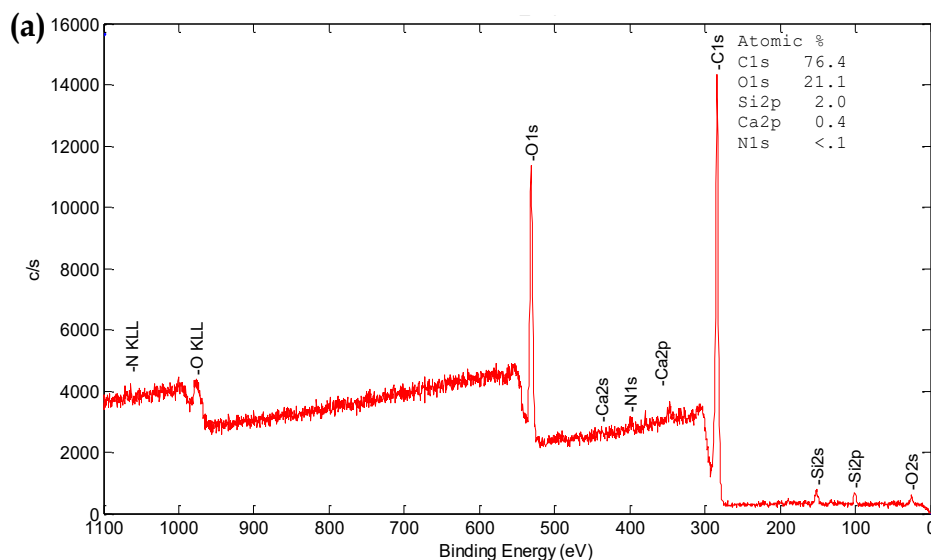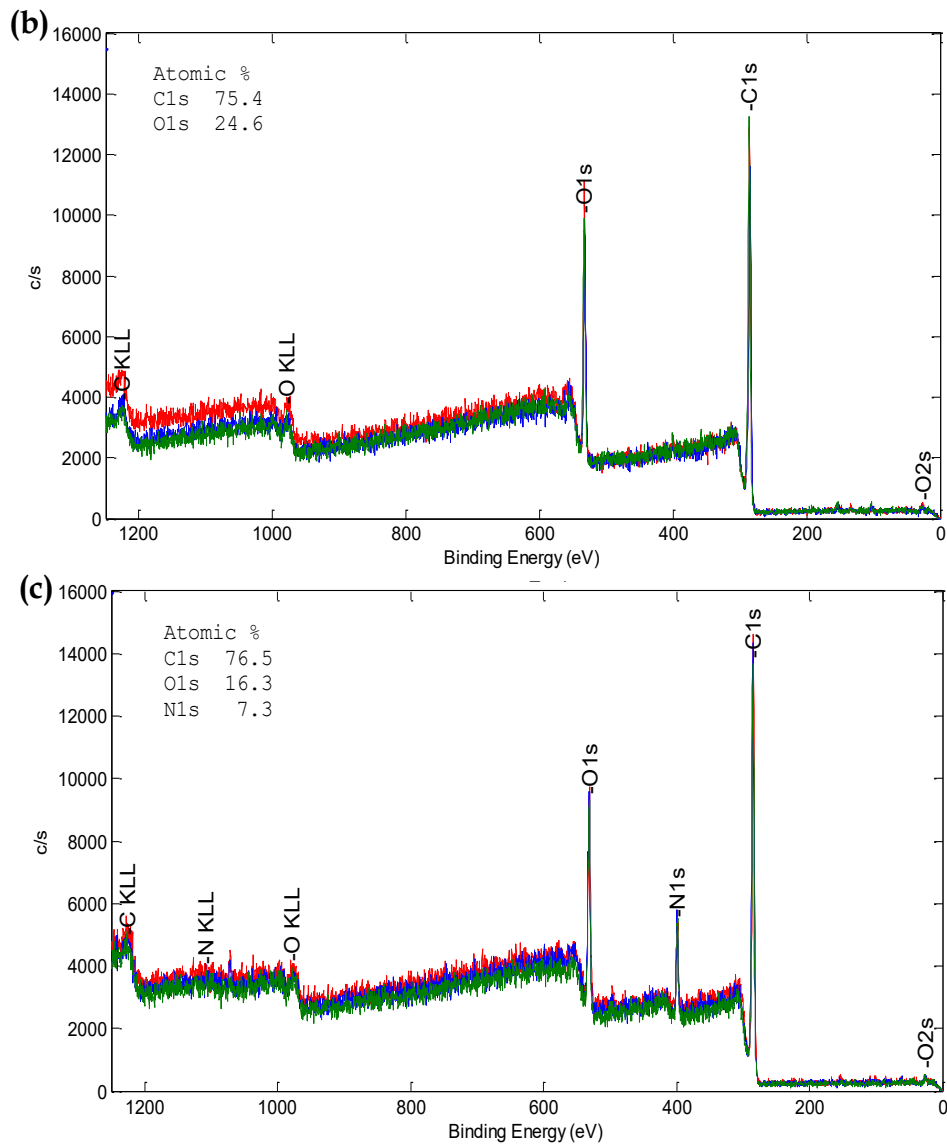
Figure 5. 12: Wide scan XPS spectra of (a) untreated PF, (b) PF@AP and (c) PF@AP-PEI.

Table 5. 8: Atomic proportion (a.t %) of the surface chemical composition of the samples (XPS analysis).

Sample name	C (a.t %)	O (a.t %)	N (a.t %)
Untreated PF	76.4	21.1	<0.1
PF@AP	75.4	24.6	0
PF@AP-PEI	74.6	18.0	7.4

5.2.3.2. Section (ii): Results related to immobilization of GOx on tailor-made PF

The total yield of immobilized GOx was measured for PF/GOx, PF@AP/GOx, PF@AP-PEI/GOx, and PF@AP-CS/GOx using the glucose oxidase assay kit following the protocol described in section 3.2.3 of Chapter 3. The loading of the enzyme was calculated on a passive approach, where the quantity of remaining active enzyme on the solution after immobilization was measured. Immobilization of GOx enzyme on PF was carried out at two different *pH*

conditions (*pH* 5.5 and *pH* 7.0) and compared systematically. As shown in Figure 5.13, all samples were able to load GOx on the surface under given immobilization conditions. The result indicates that PEI grafted polyester fabrics were the most effective towards immobilization of GOx having more than 55% loading efficiency whereas chitosan (CS) grafted PF had 42% loading efficiency. High loading efficiency on PEI and CS grafted PF corresponds to the effectiveness of amine and amide functional groups that electrostatically attracts enzyme to the surface of the fabric. Among modified polyester fabrics, plasma-treated PF had the lowest loading efficiency (28%) which can be due to the low affinity of enzymes towards hydroxyl functional groups present in the fabrics (due to plasma treatment) as confirmed in our previous reports [66]. When enzymatic activities are compared for enzymes adsorbed at *pH* 7.0 and *pH* 5.5, it has been confirmed that *pH* 5.5 was more effective on immobilization process compared to *pH* 7.0 in all samples, which is in agreement with Kahoush *et al.* (2019) [129].
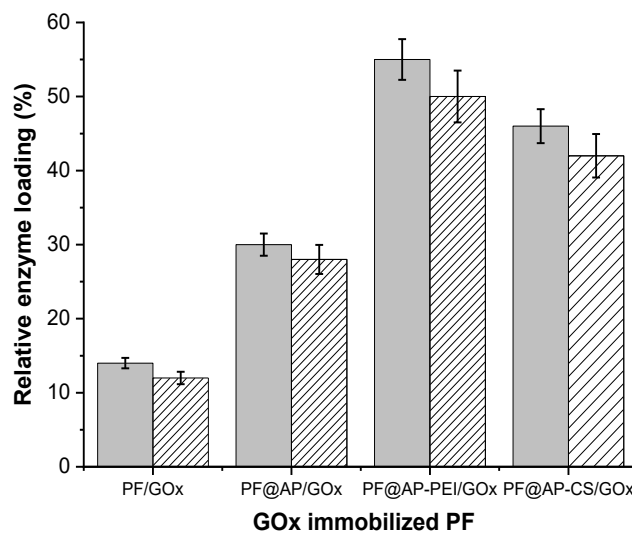
Figure 5. 13: Relative loading efficiency of GOx (%) on polyester nonwoven fabric; PF/GOx, PF@AP/GOx, PF@AP-PEI/GOx and PF@AP-CS/GOx. [pH-5.5 (left column ▬) and pH-7.0 (right column ▨)].

Loading of enzymes on the support matrix does not guarantee the activity and stability of the immobilized enzyme. Therefore, we have calculated actual stable and active immobilized GOx for all samples. Results presented in Figure 5.14 displayed that, following an efficient loading; PF@AP-PEI/GOx (*pH*-5.5) delivered a robust immobilization of GOx while having 78% of active immobilized enzyme of the surface. The remaining 29% enzyme might have denatured during immobilization or blocked their active sites. Immobilized in the same pH, PF@AP-CS/GOx provided 71% of active immobilized GOx followed by 54% for PF@AP/GOx and 28% for PF/GOx. The lowest active immobilized GOx was found in PF/GOx sample. Comparing the results between pH 5 and pH 7, it can be seen that, slightly acidic medium in GOx immobilization provides better efficiency in loading and stability of the immobilized enzyme. Nonetheless, the sample prepared on *pH* 7.0 also provided as high as 73% of the active immobilized enzyme (found in PF@AP-PEI/GOx) followed by PF@AP-CS/GOx (68%), PF@AP/GOx (51%), and PF/GOx (21%).

The influence of integrated functional groups on the stability of immobilized GOx has been studied as a function of rinse frequency. Consecutive rinsing of GOx immobilized PF removes loosely attached enzyme from the surface. Results in Figure 5.15 (and summarized in Table 5.9) demonstrate that after ten rinses, almost all the loaded enzymes on the untreated polyester fabrics have been washed away. However, enzymes immobilized on PF@AP/GOx, PF@AP-PEI/GOx, and PF@AP-CS/GOx (at *pH* 5.5) were found to be securely bound and stable even though, a certain % (46%, 22%, and 29%) of the active loaded enzyme were leached from PF@AP/GOx, PF@AP-PEI/GOx, and PF@AP-CS/GOx, respectively. The lowest leaching of the enzyme during rinse was found in PF@AP-PEI/GOx, which can be due to the presence of the higher amount of amide/amine functional groups on the fabric surface that might strongly bind with the amine/carboxyl groups in GOx. On the other hand, enzymes immobilized on PF at *pH*-7.0 were found to be less stable to rinsing than those immobilized at *pH* 5.5, yet the difference is not factually significant.
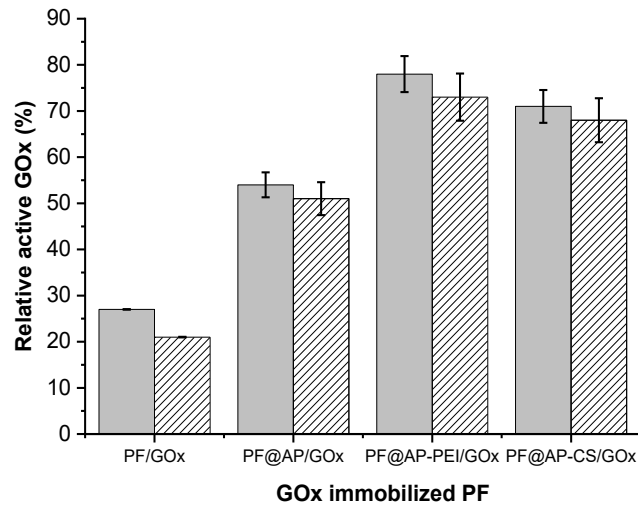
Figure 5. 14: Relative yields of the active immobilized GOx (%) on polyester nonwoven fabric; PF/GOx, PF@AP/GOx, PF@AP-PEI/GOx, and PF@AP-CS/GOx. [pH-5.5 (left column⬛️) & pH-7.0 (right column▨)].
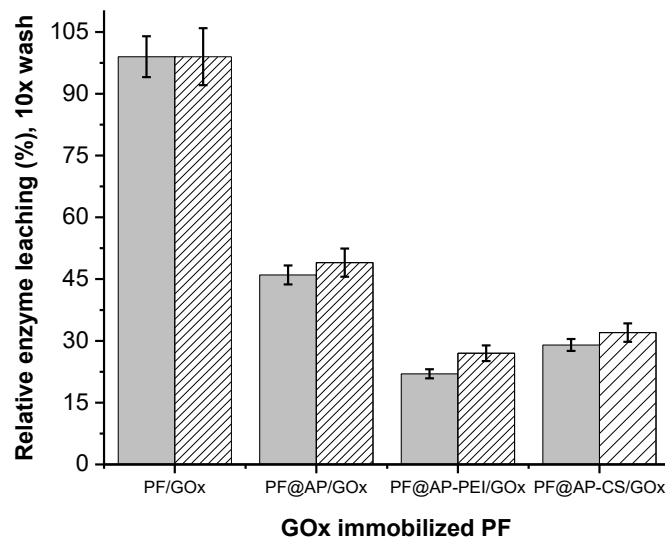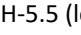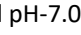
Figure 5. 15: Relative leaching of the enzyme (%) during 10 mild wash of GOx immobilized polyester nonwoven fabric; PF/GOx, PF@AP/GOx, PF@AP-PEI/GOx, and PF@AP-CS/GOx. [pH-5.5 (left column ⬛️) and pH-7.0 (right column ▨)].

Table 5. 9: Summary of loading, leaching, and yield of the active GOx on PF.

Sample name	Loading, %		Leaching, % (10x wash)		Active immobilized GOX, %	
	pH 5.5	*pH 7.0*	*pH 5.5*	*pH 7.0*	*pH 5.5*	*pH 7.0*
PF/GOx	14	12	99	99	0	0
PF@AP/GOx	30	28	46	49	54	51
PF@AP-PEI/GOx	55	50	22	27	78	73
PF@AP-CS/GOx	46	42	29	32	71	68

The stability of immobilized enzymes and the usability of resultant GOx immobilized PF samples were studied through the activity of enzymes after each reusability cycle. The enzyme reusability study as shown in Figure 5.16 was carried out, where all the parameter remains constant for each cycle analysis. It can be seen from the results that, the enzymatic activity of all samples showed a sharp decrease in activity during the first few reusability cycles, which later exhibited a moderate decrease up to five cycle applications followed by no/insignificant decrease in enzyme activity until 15-cycle applications. The decrease in enzyme activity initial reusability cycles can correspond to either denaturation of GOx or leaching of GOx during recycling processes. The stability of enzyme activity after five-cycle use corresponds to the robustness of immobilized GOx. It is safe to say that, in ideal conditions, as obtained GOx immobilized PF can be reused for manifolds (more than 15 cycles).

A comparative study between PF/GOx, PF@AP/GOx, PF@AP-PEI/GOx, and PF@AP-CS/GOx reveal that, after achieving stability, PF@AP-PEI/GOx showed the highest relative enzyme activity, which may be explained by the high loading and active immobilized GOx enzymes. Following that, PF@AP-CS/GOx showed the second-best catalytic performance, where the lowermost performance was recorded in PF/GOx. The catalytic performance of GOx immobilized on amine-rich cationic polymer grafted PF can be explained by the better binding ability of CS/PEI through possible covalent interaction between amine groups of the PF and carboxylic groups of a primary amine in enzyme molecules.
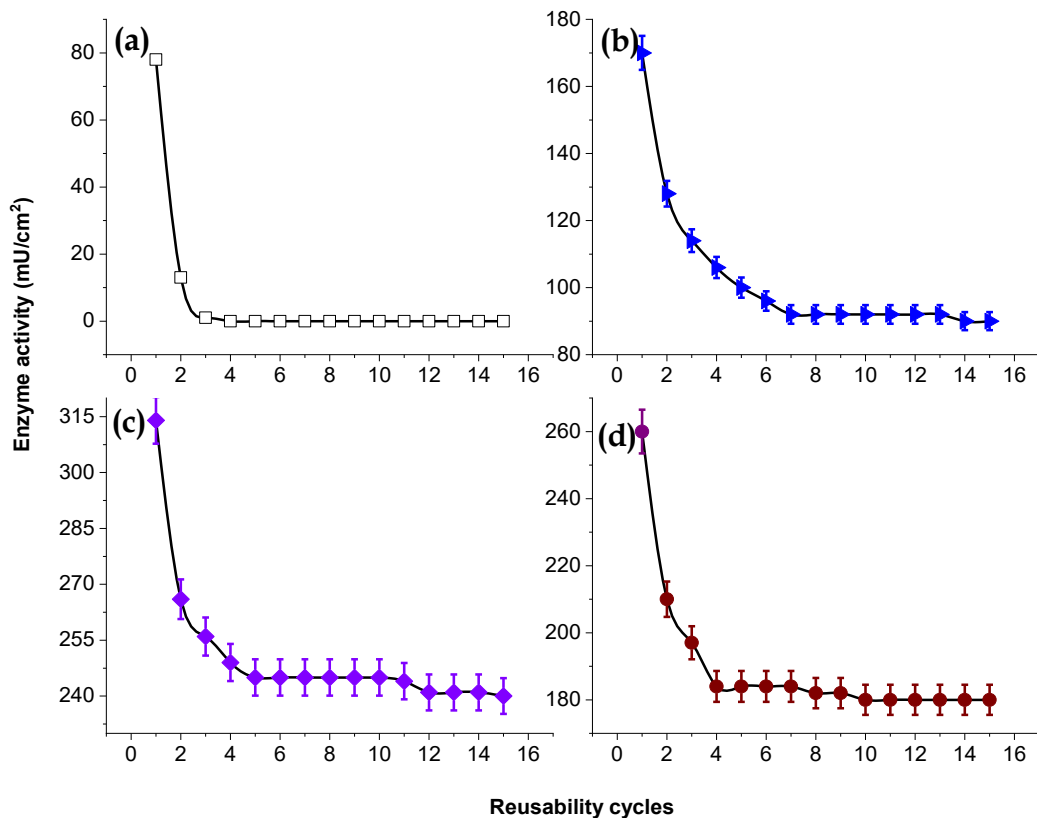
Figure 5. 16: Relative enzyme activity (%) vs number of reusability cycles of (a) PET-GOx [□]; (b) PET-AP-GOx [►]; (c) PET-PEI-GOx [♦]; and (d) PET-CS-GOx [●] *(pH-5.5).*

As discussed in the previous study (study-A), the thermal stability of immobilized GOx sample was comparatively studied by referring to the thermal stability of free-GOx. The activity of free GOx and immobilized GOx - PF@AP-PEI/GOx (as the most effective sample based on previous analysis) were measured at different temperatures from 25 °C to 75 °C. To better compare the behavior of free and immobilized GOx. Data were normalized to the highest value of activity displayed by both free and immobilized GOx. The findings of this study are presented in Figure 5.17. Results show characteristics maximum activity of free-GOx at 50 °C which decreased by 50% at ~60 °C and

125

denatured at 75 °C, which is consistent with study-A and other literature [394, 395]. In contrast, PF@AP-PEI/GOx showed maximum relative activity at 55 °C, showing an increase in thermal stability of the immobilized enzyme by ~5 °C. Above 65 °C, a sharp reduction in relative enzyme activity in both free-GOx and PF@AP-PEI/GOx has been noticed, which can be due to the destruction of GOx structure at high temperature as explained elsewhere [66].
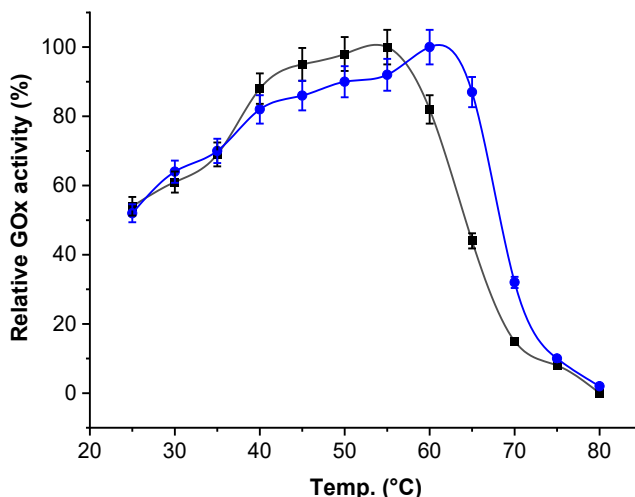
Figure 5. 17: Stability of GOx as a function of temperature. Free GOx (■), PF@AP-PEI/GOx (●).

At different glucose concentrations (2 mM to 50 mM) the initial rate of reaction was evaluated using the Michaelis-Menten model of enzyme kinetics [396] and the Lineweaver-Burk method was used to estimate the apparent Michaelis constant (K_m) and maximum velocity of the reaction (V_{max}) as summarized in Table 5.9. As shown in the results, GOx showed a decrease in V_{max}, and an increase in the value of K_m for all immobilized GOx as compared to the free GOx (V_{max}=2.94 mM min^{-1}, K_m=5.74 mM). The increase in the value of K_m could be attributed to the lower accessibility of the active sites of immobilized GOx to the glucose molecules. The decrease in V_{max} value as a result of immobilization is considered to be associated with the lower affinity of the substrate to the enzyme active site. In general, minimum reduction in V_{max} as well as the minimum increase in K_m were observed for PF@AP-PEI/GOx (Table 5.10), which also confirm the highest enzyme activity in line with the arguments discussed earlier.

Table 5. 10: Kinetics parameters of free and immobilized GOx.

Sample name	V_{max} (mM min^{-1})	K_m (mM)
Free GOx	2.94	5.74
PF@AP/GOx	1.48	7.32
PF@AP-PEI/GOx	2.32	6.08
PF@AP-CS/GOx	2.10	6.38

Overall results indicate that, tailoring the surface of polyester nonwoven fabric with amino rich polymers indeed an operative approach for high GOx loading and improve the stability of immobilized GOx. Such high loading and stability of GOx on PF surface provide sufficient notional strength to be used as heterogeneous biocatalysts to catalyze a bio-Fenton system bioremediation application, which has been investigated in upcoming sections of this thesis.

5.2.3.3. Section (iii): Results related to the catalytic performance of resultant catalysts in heterogeneous bio-Fenton system

The application of resultant GOx immobilized PF samples were investigated in the removal of crystal violet dyes in a heterogeneous bio-Fenton system. The catalytic activity of GOx immobilized PF was evaluated in a bio-Fenton system where removal of crystal violet dyes as a model pollutant was carried out. Bio-Fenton reaction involves the combined use of biomolecules (such as enzymes), β-D-glucose, and ferrous sulfate to produce highly oxidation potential active oxygen species (OH•) capable of degrading organic contaminants such as crystal violet. Crystal violet is a triphenylmethane dye regarded as a biohazard substance as it is poisonous and carcinogenic [413, 414]. Crystal violet dye is being extensively used in textiles, medicine as well as in paints and printing ink, which is resistant to traditional chemical and biological removal methods, and therefore needs immediate attention [415-417]. Removal of CV in the heterogeneous bio-Fenton system was monitored in real-time through UV-vis spectroscopy and presented in Figure 5.18.
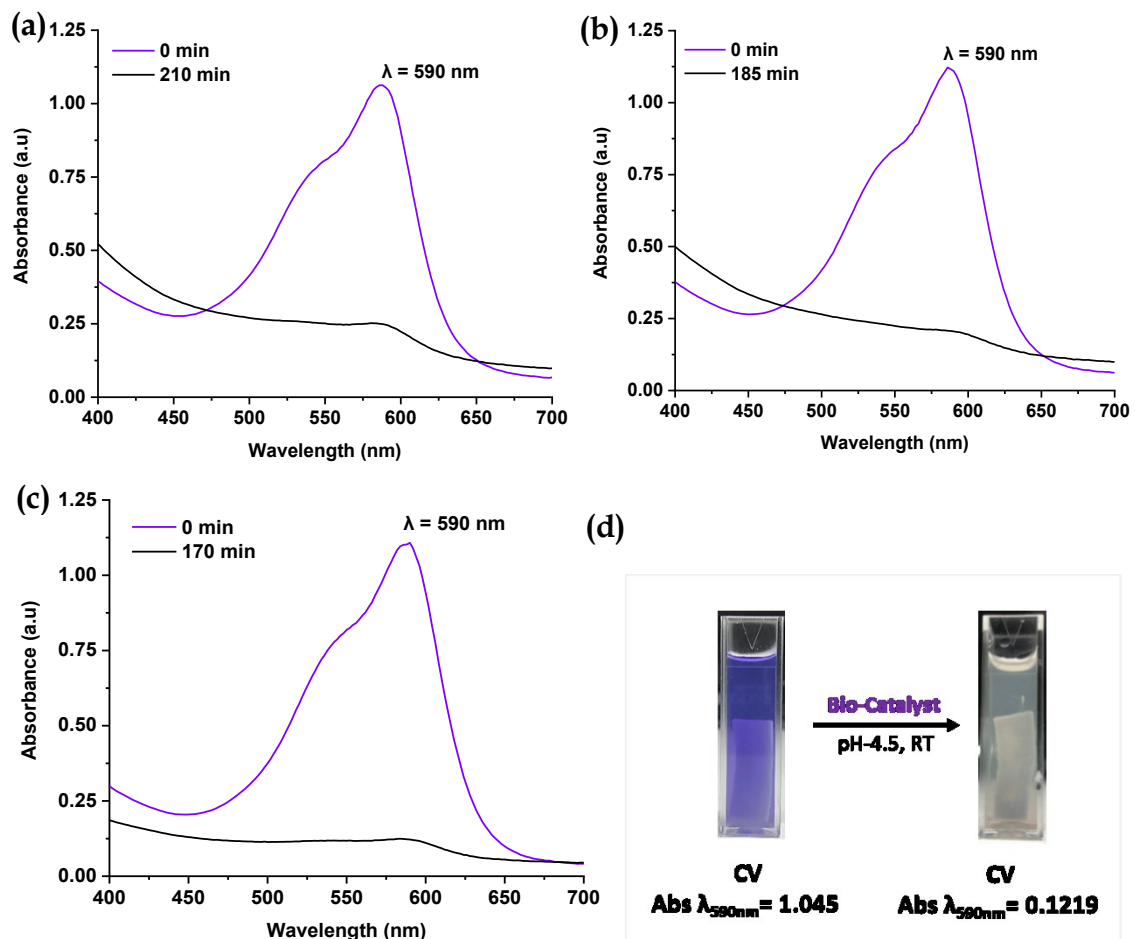
Figure 5. 18: UV-visible spectroscopy of removal of CV dye (λ_{590nm}) through the bio-Fenton system using GOx immobilized PF; (a) PF@AP/GOx, (b) PF@AP-CS/GOx and (c) PF@AP-PEI/GOx and (d) Digital images illustrating the color removal of CV dye.

Results show the characteristic absorption peak observed at $\lambda_{590\,nm}$ attributed to the intensity of crystal violet dyes [342]. It can be seen that the peak of CV dye at $\lambda_{590\,nm}$ significantly decreased within 170 min to 215 min depending on the type of sample (PF@AP/GOx, PF@AP-PEI/GOx, or PF@AP-CS/GOx) used. The gradual decrease in the

intensity of the peak at $\lambda_{590\ nm}$ indicates the decoloration of CV dye as confirmed by conversion over time (see Figure 5.19c). In Parallel to the designed removal reaction, a control removal reaction was carried out without using enzymes where no decrease in color intensity was recorded. Among three (03) samples studied in this report, PF@AP-PEI/GOx showed the fastest degradation of CV dye where 88.69% color removal was achieved within 170 min, at a constant rate of 0.01188 min^{-1}, with a correlation coefficient of the linear regression of about 94.378. Comparatively, the slower rate constant observed with the other samples, could be due to the participation of a lower amount of GOx in H_2O_2 production, which could then generate OH• radicals that are responsible for color removal. The color removal using PF@AP/GOx, PF@AP-CS/GOx reaches 81.94% in 210 min and 82.39 % in 185 min respectively. Such a high conversion in all fibrous samples might be attributed to the good stability and immobilization of glucose oxidase enzyme ensuring the maximum production of hydrogen peroxides (and active radicals) for dye degradation. Indeed, the rate of color removal seems to be correlated to the number of enzyme units immobilized on each nonwoven as discussed in previous sections.

The [instant /initial] absorbance ratio of the crystal violet dyes band at $\lambda_{590\ nm}$ (A/A$_0$), which accounts for the corresponding concentration ratio (C$_t$/C), allows plotting of Ln (C$_t$/C) as a function of time as shown in Figure 5.19a-b. Model validation of the Pseudo-first-order kinetics for CV color removal with the bio-functionalized fibrous catalyst is obtained by the linear evolution in time of Ln(C$_t$/C), as supported by R^2 values beyond 0.97. Plots summarized in Table 5.11 shows that all samples (PF@AP/GOx, PF@AP-PEI/GOx, or PF@AP-CS/GOx) exhibited good linear relationships of Ln(C$_t$/C) versus reaction time following pseudo-first-order kinetics with respect to CV dye removal. These results are consistent with those found in previous reports [345, 417-419].
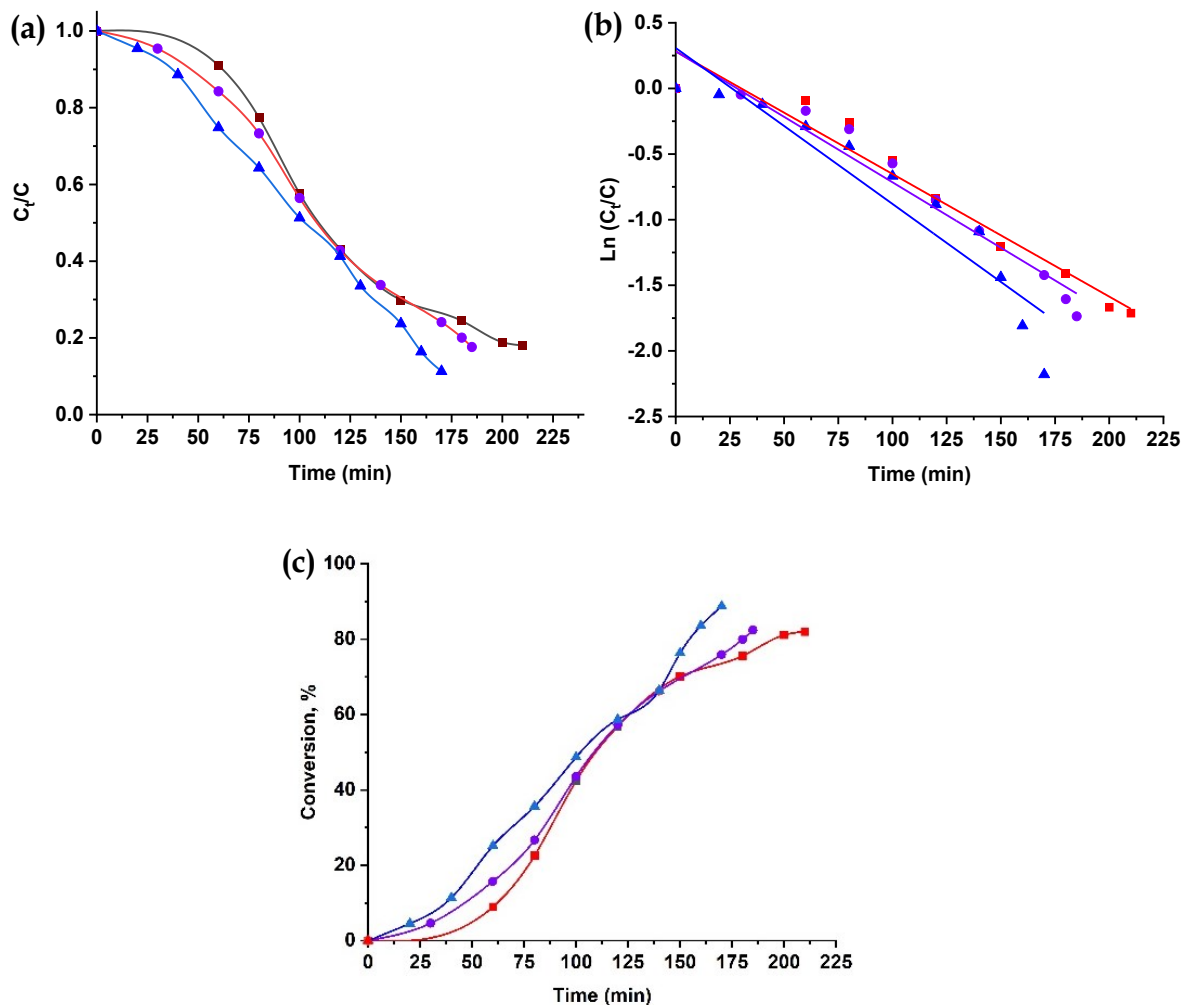
Figure 5. 19: Evolution of the (a) (C$_t$/C), (b) Ln (C$_t$/C), and (c) conversion, % as a function of time for (■) PF@AP/GOx, (●) PF@AP-CS/GOx and (►) PF@AP-PEI/GOx.

Results are of great interest due to the effective and complete removal of CV through a heterogeneous bio-Fenton system. The removal of crystal violet dyes in the system attributed to the synergistic effect involves multi-step reaction which allows generation of highly reactive •OH radicals followed by oxidation of CV into non-toxic substances [39]. Based on that, the plausible underlying mechanism of removal of crystal violet dye in a bio-Fenton system using enzyme immobilized fibrous samples has been postulated.

Table 5. 11: Kinetics study for removal of CV ($\lambda_{590\ nm}$).

Sample name	Pollutants Conc. (mg.L^{-1})	[a]Time (min)	[b]k (min^{-1})	[c](R^2)	Conversion, %
PF@AP/GOx	10	210	0.00934	0.974	81.94
PF@AP-CS/GOx	10	185	0.00997	0.972	82.39
PF@AP-PEI/GOx	10	170	0.01188	0.943	88.69

[a]Reaction time required for complete color removal.
[b]k is the rate constant expressed in min^{-1}
[c]R^2 is the correlation coefficient of the linear regression.

It has been estimated that, before the dye removal reaction, an initial CV solution containing CV dyes, β-D-glucose, and Fe_2SO_4 was prepared where dissociation of Fe_2SO_4 into Fe^{2+} and SO_4^- took place (see Reaction-5.1). After the addition of fibrous catalyst (containing GOx), a simple enzymatic glucose oxidation reaction takes place in the solution and there is the *in-situ* generation of hydrogen peroxide (H_2O_2) as explained in Reaction-5.2. Herein the presence of Fe^{2+} and H_2O_2 in the solution initiates Fenton reaction (due to the use of bio-molecules/enzymes for in-situ generation of reagents, so-called bio-Fenton) and produces highly oxygen potential hydroxyl radicals (•OH) (see Reaction 5.3). •OH has a standard oxidation-reduction potential of 2.8V and is capable to degrade complex organic compounds.

$$Fe_2SO_4.7H_2O \quad + \quad H_2O \quad \xrightarrow{\hspace{2cm}} \quad Fe^{2+} \quad + \quad SO_4^- \quad\quad (5.1)$$

$$C_6H_{12}O_6 \quad + \quad H_2O \quad + \quad O_2 \quad \xrightarrow{(GOx)} \quad C_6H_{12}O_7 \quad + \quad H_2O_2 \quad\quad (5.2)$$

$$Fe^{2+} \quad + \quad H_2O_2 \quad \xrightarrow{\hspace{2cm}} \quad Fe^{3+} \quad + \quad {}^\bullet OH \quad + \quad OH^- \quad (5.3)$$
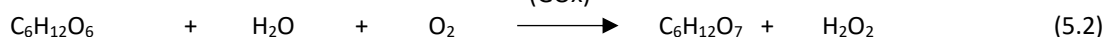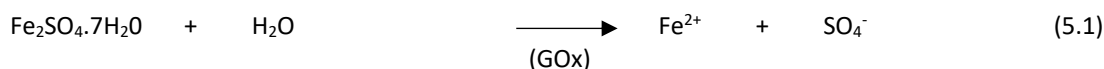
It can be seen that there are a number of pathways for mineralization of crystal violet dye as a function of interaction with oxidizing species such as hydroxyl free radicals, generated through bio-Fenton reaction. As found in the UV-Visible spectroscopy, the intensity of crystal violet dyes reduces over time, indicating the removal of the color-bearing group and possible conversion into degraded intermediates followed by secondary degradation into nontoxic substances as illustrated in Reaction 5.4-5.5.

$${}^\bullet OH \quad + \quad \text{Crystal violet} \quad \xrightarrow{\hspace{2cm}} \quad \text{Degraded intermediates} \quad\quad (5.4)$$

$$\text{Degraded intermediates} \quad + \quad {}^\bullet OH \quad \xrightarrow{\hspace{1.5cm}} \quad H_2O \quad + \quad CO_2 \quad\quad (5.5)$$
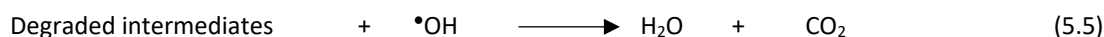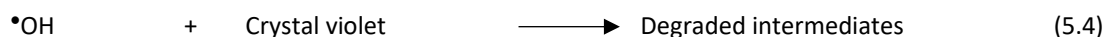
An assumption by *Palma-Goyes et al.* (2010) [345] and *Guzman-Duque et al.* (2011) [346] suggested that hydroxyl free radicals and other reactive species react with the central carbon portion of crystal violet dye structure and degrade them into reaction intermediates such as 4-(N, N-dimethylamino)-4'-(N', N'-dimethylamino) benzophenone or 4-(N, N-dimethylamino)-4'-(N', N'-dimethylamino) diphenylmethane. After that, these degraded intermediates follow secondary degradation due to constant interaction with hydroxyl free radicals in further intermediates before finally being mineralized into carboxylic acids before dissociation into H_2O and CO_2 [344].

5.2.4. Discussions: Study B

The polyester nonwoven fabric used in this study is inherently a 3D material composed of cylindrical fibers and with high porosity. While high porosity can allow easy inflow and outflow of the reaction mixtures (substrates or products), the total fiber surface per unit area of the nonwoven material is high enough to allow a sufficient amount of enzymes to be fixed. The addition of favorable surface functional groups on the PF surface via plasma treatment and grafting of PEI and CS should not only improve this flow of liquid but also create a specific environment allowing enzymes to be immobilized with maximum accessibility to their active sites. This would lead to improved bioactivity. The possible sequences of chemical modifications of the polyester fabric by plasma treatment, CS/PEI grafting, and enzyme immobilization is shown in Figure 5.20.
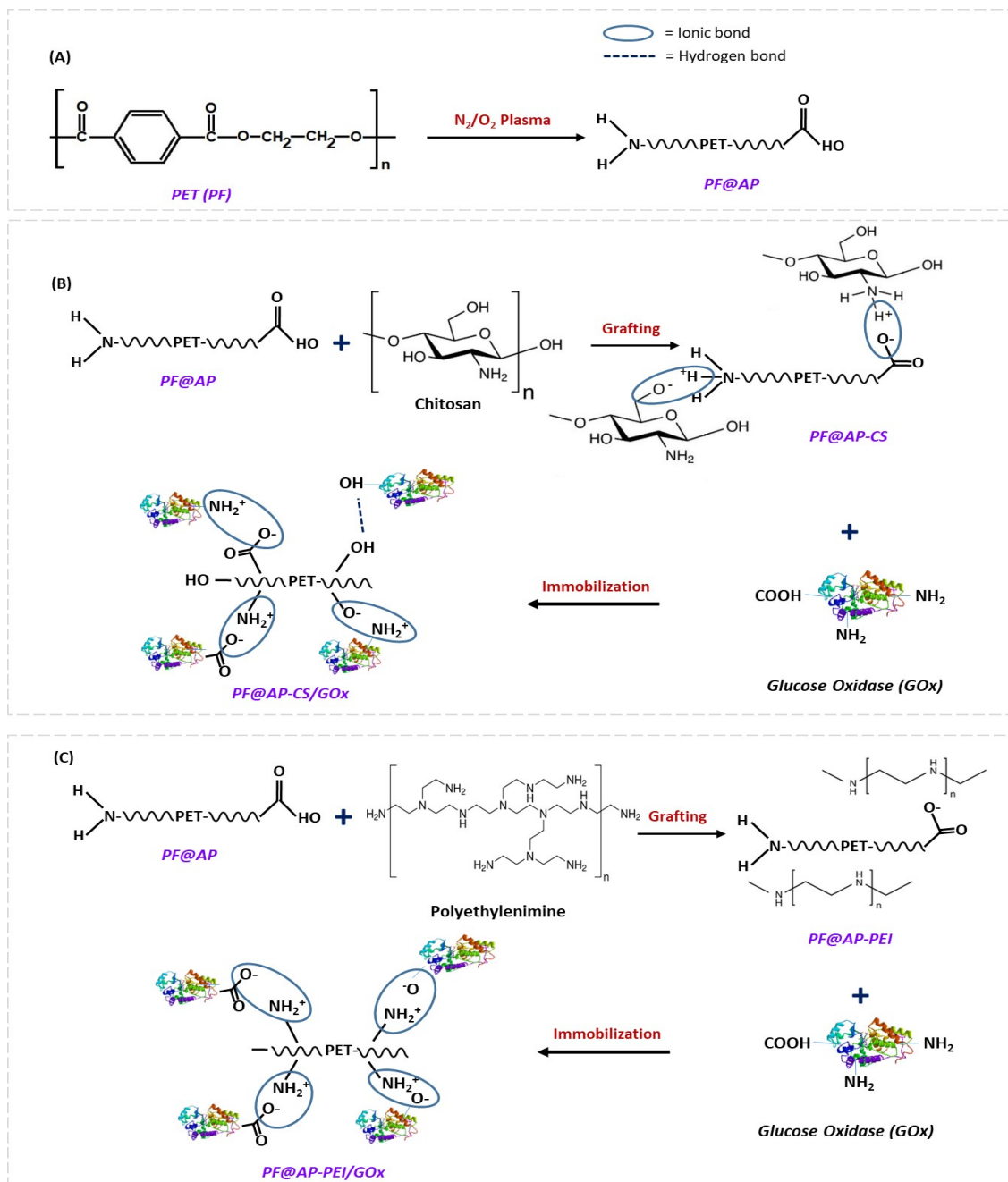
Figure 5. 20: Pathway of possible chemical modifications of PF due to (A) plasma treatment, (B) chitosan grafting followed by GOx immobilization, and (c) polyethylenimine grafting followed by GOx immobilization.

This study confirms that both the plasma treatment and the subsequent functionalization of polyester nonwoven fabric with cationic amine-rich polymers (PEI and CS) effectively activated the surface of the polyester. The functionalized polyester fabrics were broadly favorable for the immobilization of the glucose oxidase enzyme while maintaining robust bio-catalytic activity. The surface chemical properties of the polyester fabrics following plasma activation and grafting of crosslinkers performed very differently (depending on their defining functional groups) during enzyme immobilization. Wettability analysis revealed the effects of the different treatments on the water contact angle of the polyester nonwoven fabrics. Following surface activation through plasma treatment, there was a significant decrease in water contact angle (from 138° to 0°), corresponding to an increase in the hydrophilicity of the fabrics. This is primarily due to the radicals formed on the PET fiber surface during the plasma treatment from the scission of ester bonds. The radicals create a polar surface with end functional groups such as C–O, C=O, C=N, N–H, and N–C–O. These groups were confirmed by FTIR and XPS analysis. The addition of O_2 during plasma treatment produces polar terminal groups that create a hydrophilic surface, while higher nitrogen content can be explained by the formation of amine, imide, and amide groups on the polyester surface.

During PEI/CS grafting, further $-NH_2$ groups were integrated, and at the same time, the hydrophilicity of the plasma-treated polyester fabric decreased (observed through an increase in contact angle). However, while the treated surface became less hydrophilic, the grafted $-NH_2$ surface terminal groups were found to provide favorable conditions for robust enzyme immobilization, as explained in the analysis above. This is consistent with many previous reports [397, 398]. This observation is further supported by the fact that amino acids are organic compounds containing amine ($-NH_2$) and carboxyl ($-COOH$) functional groups, which are also the main components of the protein structure of enzymes [399-401]. In polyester fabrics activated by $O_2 + N_2$ plasma, followed by grafting of $-NH_2$-rich crosslinkers, the relevant functional groups in the enzymes may have covalently or ionically bonded with the polyester fabric [402, 403], leading to more robust immobilization, as illustrated in Figure 5.20B-C. Clearly, amine groups have provided the most favorable conditions for robust enzyme immobilization.

The extent of immobilization was found to directly influence the biocatalytic activity of the prepared GOx-immobilized PF, as observed during the removal of CV dye in a heterogeneous bio-Fenton system. Increasing the enzyme concentration sped up the removal reaction because there was more D-glucose available to bind and produce hydrogen peroxide [253]. The fastest pollutant removal was achieved by PF@AP-PEI/GOx, which was also the GOx-immobilized PF sample with the best loading yield, activity, and stability (as explained in the Results section).

In summary, the main findings of Studies A and B of Chapter 5 are that the glucose oxidase enzyme immobilized on a tailor-made PF surface retained catalytic activity (as validated through various analyses) without compromising the inherent catalytic performance of the GOx. This conclusion addresses research questions 1 and 3. The next chapter (chapter 6) seeks to answer the final research question of this thesis.

"

Research Question 1 (RQ 1): How feasible is textile as a support material for catalyst immobilization?
Research Question 3 (RQ 3): Can we immobilize biocatalysts (GOx) on textiles without compromising their inherent catalytic performance?

"

Chapter 6

Heterogeneous bio-Fenton system using immobilized catalyst: Proof of concept

Chapter outline

This chapter is dedicated to the proof of concept of a heterogeneous bio-Fenton system for removing pollutants from water using both immobilized inorganic catalysts and biocatalysts. Here, both zerovalent iron and glucose oxidase was immobilized on the same type of textile support matrix to achieve total heterogeneity of the system. This has never been done before. The outcome of this chapter presents the direct answer to research question 4 and provides supporting evidence for research questions 1, 2, and 3.

6.1. Introduction

The bio-Fenton reaction is the latest addition to the class of Fenton-like reactions. It was first proposed by Chun-Hua *et al.* (2010) [185] and later used by Afzal *et al.* (2012) [17] in a catalytic application. Although this technology is a decade old, it has received very little attention so far. The primary advantage of a bio-Fenton system is the *in-situ* sustainable production of hydrogen peroxide (mainly through oxidizing D-glucose using a biocatalyst or enzyme), which reduces the chance of accidents and improves safety in the work environment. Furthermore, this method has low power consumption, making it very cost-effective. The bio-Fenton system is considered a green and sustainable alternative to the conventional Fenton reaction and other advanced oxidation processes in general.

The most commonly used enzyme in the bio-Fenton system is glucose oxidase, although alcohol oxidase has also been reported. Glucose oxidase is well known to catalyze the oxidation reaction of D-glucose, producing D-glucono-1,5-lactone as the main product and hydrogen peroxide as a by-product (see reaction 5.1). The resultant hydrogen peroxide is released into the system and further reacts with iron species (provided beforehand) to generate reactive species capable of oxidizing pollutants in water. A handful of studies have reported using this system to remove pollutants from water. Karimi *et al.* (2012) [17] reported the decolorization of malachite green in a bio-Fenton system (using free GOx and FeSO$_4$). Eskandarian *et al.* (2014) [16] reported decolorizing Acid Blue 113 textile azo dye (AB 113) in a bio-Fenton system (using free GOx and FeSO$_4$). Advancing the technology further, Elhami *et al.* (2015) [18] designed a heterogeneous bio-Fenton catalyst for the removal of colorants from water using immobilized glucose oxidase on a Kissiris/Fe$_3$O$_4$/TiO$_2$ composite. Kahoush (2019) [34] also reported the removal of toxic reactive dyes from water through a heterogeneous bio-Fenton system using GOx immobilized on carbon felt. Recently, Ravi *et al.* (2020) [13] described the removal of trichloroethylene in a bio-Fenton oxidation system (free GOx and FeSO$_4$). A close look at the literature shows that most of these studies were performed with enzymes in their free state, which leads to some additional steps after the treatment to denature the enzyme in the solution. Moreover, the loss of enzymes increases operational costs. An enzyme immobilization process would improve the system, ensuring the reusability of the biocatalysts and facilitating the extraction of the proteins from the reaction medium when needed, without any further steps. Only two of the studies deal with the immobilization of enzymes; one used a rare volcanic material and the other has used carbon felt (which is sturdy but expensive).

These expensive and unusual support materials require additional preparation steps, which is not ideal from a sustainability point of view. Therefore, a cheaper flexible support material for immobilizing enzymes is greatly needed. In addition, most studies on removing pollutants in a bio-Fenton system discuss only the decolorization of the pollutant, without doing toxicity reduction measurements. Furthermore, there has been no research on using the immobilization of iron species in a bio-Fenton system. This leads to the formulation of the hypothesis of this study. The hypothesis is based on using the glucose oxidase enzyme to generate hydrogen peroxidegeneration, and using zerovalent iron particles to generate Fe^{2+}. Details of the hypothesis, its theoretical background, and the prediction of the experimental analysis are explained below. The validation of the hypothesis has been conducted through the removal of crystal violet colorant in a heterogeneous bio-Fenton system using immobilized enzyme and immobilized iron on polyester nonwoven fabric.

Hypothesis

The concept of this study is based on the use of immobilized glucose oxidase and immobilized zerovalent iron on polyester nonwoven fabric as heterogeneous catalysts in a bio-Fenton reaction. This hypothesis was tested in this thesis. The null hypothesis is that immobilized glucose oxidase and immobilized zerovalent iron will be ineffective in catalyzing a heterogeneous bio-Fenton reaction and will not be able to remove toxic pollutants from water. The alternative hypothesis is that immobilized glucose oxidase and immobilized zerovalent iron will be effective in catalyzing a heterogeneous bio-Fenton reaction and will be able to remove toxic pollutants from water.

A heterogeneous bio-Fenton system can be influenced by many factors, such as the concentration of catalysts (GOx and Fe^0), the concentration of substrate (D-glucose), the concentration of pollutants, pH, temperature, and the reaction medium. In this study, these factors were considered the dependent variables, therefore they will be and subjected to testing, while the catalyst used in this study (see from chapters 4 and 5) were considered an independent variable. Given the aim of this study, the proof of concept was limited to a single type of pollutant.

Theoretical correlation

The bio-Fenton reaction involves the generation of reactive species such as hydroxyl radicals ($^{\bullet}OH$) with the help of biological entities. The typical example of a bio-Fenton reaction is catalyzed by the *in-situ* generation of H_2O_2 from glucose oxidase (see Reaction 6.1) and by the subsequent formation of $^{\bullet}OH$ in the presence of Fe^{2+} (see Reactions 6.2–6.3).
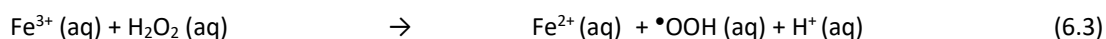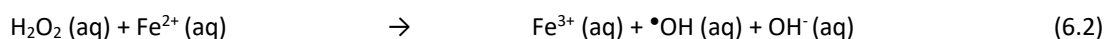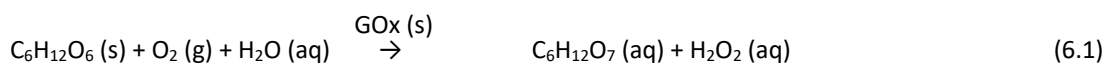
$$C_6H_{12}O_6 \text{ (s)} + O_2 \text{ (g)} + H_2O \text{ (aq)} \xrightarrow{\text{GOx (s)}} C_6H_{12}O_7 \text{ (aq)} + H_2O_2 \text{ (aq)} \tag{6.1}$$

$$H_2O_2 \text{ (aq)} + Fe^{2+} \text{ (aq)} \rightarrow Fe^{3+} \text{ (aq)} + {}^{\bullet}OH \text{ (aq)} + OH^- \text{ (aq)} \tag{6.2}$$

$$Fe^{3+} \text{ (aq)} + H_2O_2 \text{ (aq)} \rightarrow Fe^{2+} \text{ (aq)} + {}^{\bullet}OOH \text{ (aq)} + H^+ \text{ (aq)} \tag{6.3}$$

Glucose oxidase specifically oxidizes β-D-glucose at its first hydroxyl group, utilizing molecular oxygen as the electron acceptor to produce D-gluconolactone and hydrogen peroxide, as shown in Reaction 6.1 [253]. Under standard conditions, one unit of GOx can oxidize 1.0 µmole of β-D-glucose to D-gluconolactone and H_2O_2 per min at a pH of 5.1 and 35 °C. The optimal pH for glucose oxidase is 5.1, although it has a broad activity pH range of 3.6-7. Based on the above principle, a homogeneous bio-Fenton reaction is presented as Reaction 6.4, where $C_6H_{12}O_6$ and Fe^{2+} are among the reactants, producing mostly $C_6H_{12}O_7$, Fe^{3+}, $^{\bullet}OH$, and OH^- through a chain of reactions. In this process, H_2O_2 is both produced and consumed in the system.

GOx (s)

$$C_6H_{12}O_6 \text{ (s)} + Fe^{2+} \text{ (s)} + O_2 \text{ (g)} + H_2O \text{ (aq)} \rightarrow C_6H_{12}O_7 \text{ (aq)} + Fe^{3+} \text{ (aq)} + {}^{\bullet}OH \text{ (aq)} + OH^- \text{ (aq)} \quad (6.4)$$
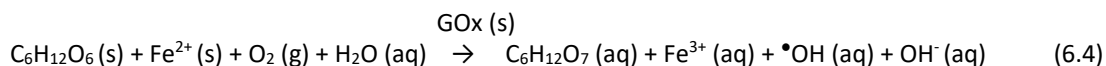
According to the theory of zerovalent iron, Fe^0 has a standard reduction potential (E^0) of −0.440 V for the half-reaction between the Fe^{2+}/Fe^0 couple (see Reaction 6.5), which confirms that Fe^0 is an effective electron donor regardless of its particle size. The interaction of Fe^0 with water (H_2O, an electron receptor) and in some cases with dissolved oxygen (O_2) in the reaction environment produces Fe^{2+} (see Reaction 6.6-6.7), which is a key reagent in the Fenton reaction.

$$Fe^{2+} \text{ (s)} + 2e^- \rightarrow Fe^0 \text{ (s)} \quad (6.5)$$

$$Fe^0 \text{ (s)} + H_2O \text{ (aq)} \rightarrow Fe^{2+} \text{ (aq)} + H_2 \text{ (g)} + 2OH^- \text{ (aq)} \quad (6.6)$$

$$Fe^0 \text{ (s)} + O_2 \text{ (aq)} + H^+ \rightarrow Fe^{2+} \text{ (aq)} + H_2O \text{ (aq)} \quad (6.7)$$
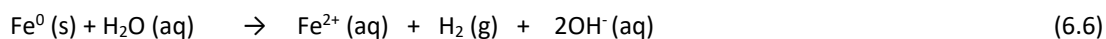
Theoretically, GOx and Fe^0 should not undergo any significant chemical changes during immobilization, which has been confirmed in separate studies for both catalysts [420]. In the past, Fe^0 has also shown its effectiveness in catalyzing a Fenton reaction in the presence of H_2O_2 [109, 176, 411, 421-423]. This was also confined in our study (see chapter 4). As reported by Arjunan *et al.* (2013) [424], Fe^0 immobilized on polyvinyl alcohol (PVA) showed similar catalytic behavior as free Fe^0 during the removal of pollutants from water (see Reaction 6.8). Detailed discussions related to immobilized Fe^0 can be found in Litter *et al.* (2017) [178], Phenrat *et al.* (2019) [425], and Pasinszki *et al.* (2020) [426].

$$Fe^0/PVA \text{ (s)} + H_2O \text{ (aq)} \rightarrow Fe^0/PVA \text{ (s)} + Fe^{2+} \text{ (aq)} + H_2 \text{ (g)} + 2OH^- \text{ (aq)} \quad (6.8)$$
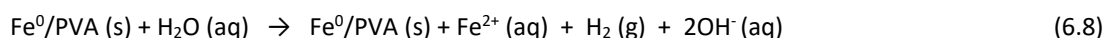
Immobilized GOx has already been tested as a catalyst in the bio-Fenton reaction. Elhami *et al.* (2015) [18] reported the immobilization of glucose oxidase on a Kissiris/Fe_3O_4/TiO_2 composite as a heterogeneous bio-Fenton catalyst for the removal of colorants from water. In a similar study, Kahoush (2019) [34] also showed that immobilized GOx on carbon felt can catalyze a bio-Fenton reaction to remove colorants from water (see Reactions 6.9–6.10). Although in both cases, immobilized GOx was used, the precursor for Fe^{2+} had not been immobilized, which poses a serious problem later by creating secondary pollutants (iron sludge). Our work is the first to address this problem, since the hypothesis includes the immobilization of both the GOx and the Fe^{2+} precursor (Fe^0), as well as proposing the use of polyester textiles as the support material for their immobilization. A polyester support material can be an inexpensive, strong, and flexible alternative to complex or noxious material used earlier, such as Kissiris/Fe_3O_4/TiO_2, carbon felt, or silica.

CF/GOx (s)

$$C_6H_{12}O_6 \text{(s)} + O_2 \text{ (g)} + Fe^{2+}\text{(s)} + H_2O \text{ (aq)} \rightarrow C_6H_{12}O_7 \text{ (aq)} + Fe^{3+} \text{ (aq)} + {}^{\bullet}OH \text{ (aq)} + OH^- \text{ (aq)} \quad (6.9)$$

$$\text{Remazol blue RR} + {}^{\bullet}OH \text{ (aq)} \rightarrow \text{Degraded Remazol blue RR (aq)} + CO_2 \text{ (g)} + H_2O \text{ (aq)} \quad (6.10)$$
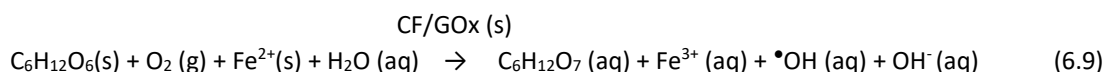
The above discussion on theoretical background provides a substantial correlation with the alternative hypothesis, which emphasizes the need for proper testing as provided in this study.

Predictions

Based on the theoretical background analysis and recently published literature, a heterogeneous bio-Fenton system should be able to catalyze a bio-Fenton reaction. The bio-Fenton reaction should produce reactive species that would contribute to the dye degradation by oxidizing the dye (studied in this thesis). However, pollutant removal using such a system may prove inefficient due to the involvement of multi-step reaction design. This study aims to test the hypothesis experimentally to yield information that would help design an efficient system for removing pollutants from water.

6.2. Material preparation

The material preparation included the design of the reactor (a heterogeneous bio-Fenton system), preparation of the Fe^0-immobilized polyester nonwoven fabric, and preparation of the GOx-immobilized polyester nonwoven fabric. A detailed description of the materials, method, and preparation parameters used at each step can be found below.

Design of a heterogeneous bio-Fenton system

A bio-Fenton system requires no specific configuration. Most of the published studies were carried out in an Erlenmeyer flask, which contained the reaction mixture (heterogeneous bio-Fenton catalyst, a certain concentration of pollutants, and glucose), kept at constant temperature, and stirred. The configuration of the reactor in this study is shown in Figure 6.1.
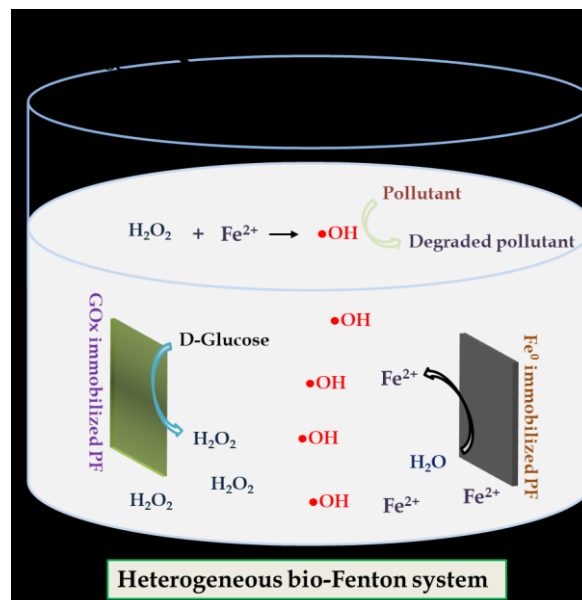
Figure 6. 1: Schematic illustration of the configuration of the reactor designed for this study.

The Fe^0-immobilized polyester nonwoven fabric (PF@SH-Fe^0) was reused from the study in chapter 4. The preparation method of the selected Fe^0-immobilized polyester nonwoven fabric is discussed in detail in section 4.2.2 of chapter 4. Similarly, the GOx-immobilized polyester nonwoven fabric was reused from the study in chapter 5. PF@AP-CS/GOx was selected for the bio-Fenton system. The preparation method of PF@AP-CS/GOx has been described in detail in section 5.2.2 of chapter 5.

Heterogeneous bio-Fenton system for removal of crystal violet dyes

The trial of a heterogeneous bio-Fenton system for removal of crystal violet (CV) dyes was performed in a 25 mL beaker containing 10 mL of reaction mixtures at constant shaking. The reaction mixtures were prepared using predefined amounts of crystal violet dye and D-glucose. Immobilized GOx and Fe^0 were added just before initiating the removal reaction. The effect of catalysts concentration (1 cm^2/5ml, 2 cm^2/5ml and 3 cm^2/5ml), D-glucose concentration (0.5, 1.0 and 1.5 g/L), CV dye concentration (10 mg/L), pH (3, 5, 7, 9), temperature (15, 25, 35, 45 and 55°C) was studied. The removal of crystal violet dye was monitored using a UV-Vis spectrophotometer. The instant-to-initial absorbance ratio of the crystal violet solution (A/A$_0$) was measured before and after the removal process. Thus, changes in A/A$_0$ could be used to assess the progress of color removal. The color removal or conversion percentage corresponds to the removal of the crystal violet dye, which was calculated using the concentration of CV dye in the system at predetermined time intervals [289]. The absorbance spectra of crystal violet dye, D-glucose, and dissolved iron (see Figure 6.2) are all distinct and can be measured accurately.
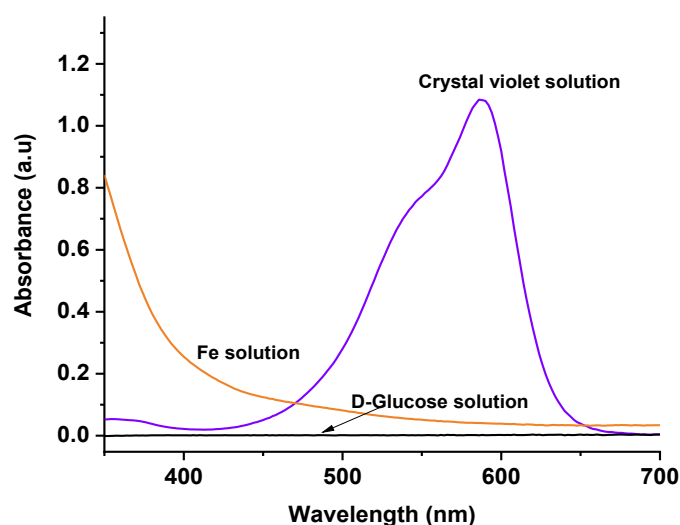
Figure 6. 2: Absorbance spectra of crystal violet dye, D-glucose, and Fe solution.

6.3. Results

The results of this study consist of the data related to the removal of crystal violet dye in the heterogeneous bio-Fenton system using immobilized organic and inorganic catalysts. Color removal, removal kinetics, influencing factors, and toxicity reduction were evaluated. Based on the results, a mechanism has also been proposed for the removal of crystal violet dye in the experimental system. For the characterization and analysis of the catalysts themselves, see chapters 4 and 5.

UV-Vis spectroscopy

A general removal reaction of crystal violet dyes using catalyst-immobilized textiles was carried out under the following conditions: catalyst concentration of 2 cm^2/5 mL; D-glucose concentration of 1.0 $g \cdot L^{-1}$; CV dye concentration of 10 $mg \cdot L^{-1}$; pH of 3; and temperature of 35 °C. UV-visible spectroscopic measurements were done to find the concentration of CV dye before and after the removal process (see Figure 6.3). The results show a characteristic absorption peak at $\lambda_{590\,nm}$, which can be attributed to crystal violet dye [342]. The intensity of the peak begins decreasing over time once all the reactants and catalysts are in the reaction system. A reference removal reaction was also carried out, where D-glucose was not added to the solution. The results showed no removal of CV dye (see Figure 6.3a), except for slight absorption due to the characteristic absorption properties of heterogeneous catalysts. On the other hand, in the actual experiment (where all necessary reagents were provided), the intensity of the peak at $\lambda_{590\,nm}$ decreased, which indicates the decolorization of crystal violet dye (see Figure 6.3b). A 93% decolorization of crystal violet dye in water was achieved for the first trial (270 min), as measured through UV-Vis spectra. This removal efficiency is attributed to the good stability and robust immobilization of the catalysts in the PF, ensuring maximum catalytic activity for the bio-Fenton reaction.
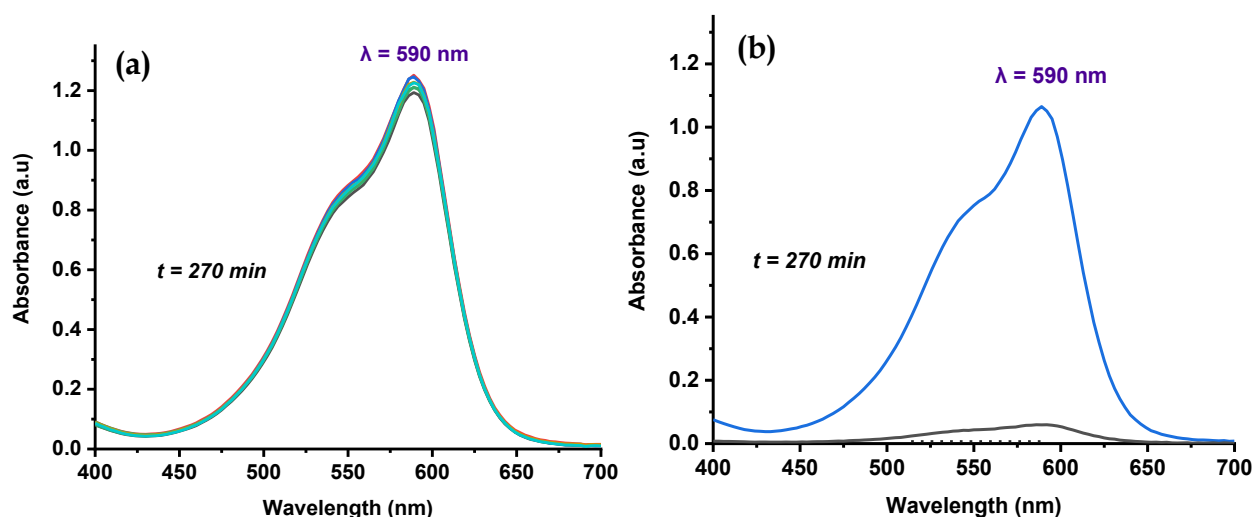
Figure 6. 3: UV-Vis spectroscopy of removal of CV (λ_{590nm}) (a) through heterogeneous bio-Fenton system (a) reference experiment, (b) actual experiment; [Conditions: Catalysts (cm^2): CV dye (mL) = 2:5; D-glucose =1.0 g/L and pH=3.0, Temp. =35°C].

The kinetics of removal of the CV dye were also evaluated based on the instant /initial absorbance ratio of the crystal violet dye band at $\lambda_{590\,nm}$ (A_t/A), which corresponds to the concentration ratio (C_t/C), allowing Ln (C_t/C) to be plotted as a function of time. The pseudo-first-order kinetics for crystal violet dye removal was used to validate the model through the linear evolution over time of Ln (C_t/C), supported by R^2 values beyond 0.94. The plot shows good linear relationships between Ln (C_t/C) and reaction time following pseudo-first-order kinetics for crystal violet dye removal. These results are consistent with those found in previous reports [345, 417-419]. In summary, these results provide the initial and most important validation of the alternative hypothesis. However, decolorization does not indicate that the water has been detoxified, especially for complex pollutants like crystal violet dye. They can maintain their toxicity even after losing their chromophore group. The following section presents the evidence for toxicity reduction of the water following the decolorization of the crystal violet dye.

Toxicity reduction analysis of treated water

Most studies on bio-Fenton systems did not evaluate the toxicity reduction by their system, which is readily unanticipated for pollutant removal from water [34]. We evaluated the toxicity of the water before and after the removal of crystal violet dye in the heterogeneous bio-Fenton system based on the chemical oxygen demand (COD) analysis following the method described in section 3.3.3 of chapter 3. Relative COD analysis was carried out based on the COD of the untreated water solution (containing crystal violet dye). The results presented in Figure 6.4 show that the COD of the treated (decolorized) water was reduced by 12% compared to untreated water
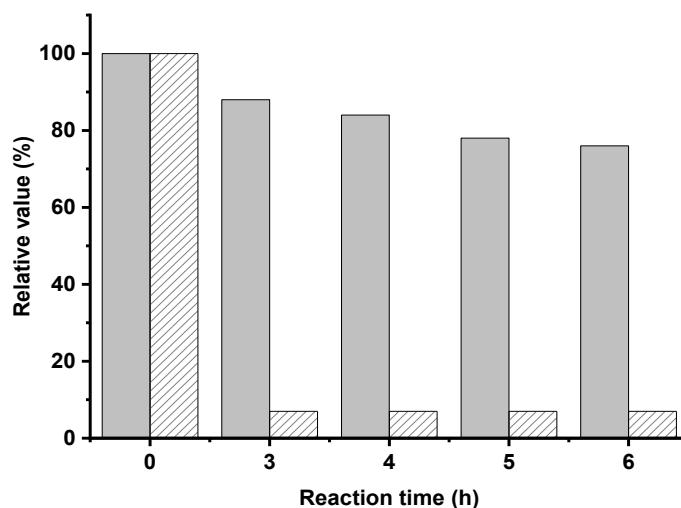
Figure 6. 4: Toxicity reduction study of treated water based on chemical oxygen demand analysis; relative COD concentration (▬), relative CV dye concentration (▨). [Conditions: Catalysts (cm^2): CV (mL) = 2:5; D-glucose =1.0 g/L and pH=3.0, Temp. =35°C].

Nevertheless, the COD of the treated water was measured immediately after the decoloration reaction, which showed poor performance in toxicity reduction. It could be explained by the incomplete mineralization of the crystal violet dye and/or by high D-glucose concentration in the treated water. According to the theory of the incubation of catalysts (especially for GOx), the longer the incubation time of the GOx with its substrate, the more product would be formed. However, the rate of product formation is not a simple linear function of incubation time [427]. Selecting the appropriate incubation time depends on a compromise between various factors (pH, temperature, the concentration of reagents, and so on). As a general rule, incubation should be long enough to allow a moderate amount of product to form, and also long enough to make errors in timing insignificant, but not so long that there is detectable leveling off of the curve [428, 429].

Hence, both implicit reasons for poor COD removal were tested by providing additional incubation time (3 h) for the catalysts after decolorization reached equilibrium. This would allow intermediate products of CV to undergo further breakdown, leading to the mineralization of both the pollutants and the remaining D-glucose, which can be oxidized. The additional removal time had a positive effect. After one additional hour, the COD reduction reached up to 16%, which further increased to 22% after two hours and 24% after 3 hours. Based on the parameters used, the equilibrium of COD reduction had been achieved at that point. Presumably, a more complete toxicity reduction could be achieved by optimizing the reaction.

Effects of pH and temperature

In a Fenton reaction, the pH is a significant parameter. The lifetime of hydrogen peroxide and Fe^{2+} is very sensitive to the solution pH. As reported in many studies, an acidic pH provides the most favorable conditions for the Fenton reaction and the subsequent oxidation of pollutants in water [34, 169, 430]. We evaluated the effect of pH on the removal of crystal violet dye in our system. Consistent with the literature, acidic pH led to more efficient removal of CV than neutral or basic pH. The decrease in the reaction rate at pH values over 5.5 is due to the formation of oxides and the disintegration of hydrogen peroxide into water and oxygen [431]. It is clear that a pH of 3 is highly favorable, and a pH of 6 and above is exceedingly unfavorable for the proposed system.

Increasing the temperature intensifies the conventional Fenton reaction by improving both the oxidation rate and the degree of mineralization of the pollutants [432]. Therefore, the effect of temperature on the removal of CV in the proposed system was investigated at temperatures of 15, 25, 35, 45, and 55 °C. The experiments were conducted at an initial CV dye concentration of 10 mg·L^{-1}, catalyst concentration 2 cm^2/5 mL, D-glucose concentration 1.0 g·L^{-1}, and pH 3.0. The results showed that faster removal could be achieved by increasing the temperature up to a certain level, consistently with earlier reports [433-435]. Significantly, while a gradual increase in temperature may positively affect the Fenton reagents, temperatures over 55 °C are not recommended. Above this temperature, GOx starts to undergo heat-related destructions (see the discussions in chapter 5).
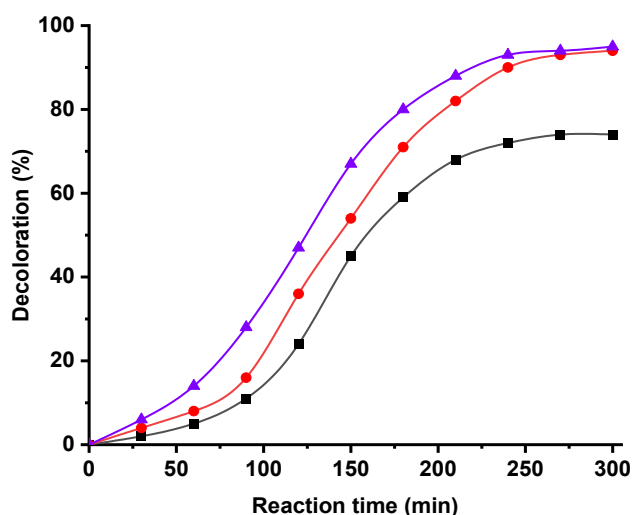
Figure 6. 5: Decoloration of crystal violet dyes at various D-glucose concentrations; D-glucose 0.5 g/L (■), 1.0 g/L (●) and 1.5 g/L (▲); [Conditions: Catalysts (cm^2): CV dye (mL) = 2:5, pH=3.0, and Temp. = 35°C].

Effect of D-glucose and catalysts concentration

The control trial experiment in the decolorization study reveals the importance of D-glucose in the heterogeneous bio-Fenton system. Without D-glucose, there is no hydrogen peroxide in the system, and it cannot function. The production of hydrogen peroxide depends on the concentration of D-glucose in the solution. We evaluated the effect of D-glucose concentration (0.5, 1.0, and 1.5 g·L^{-1}) on the decolorization rate. The concentration of CV dye, concentration of catalysts, pH, and temperature were kept constant at the levels described in UV-Vis spectroscopy analysis. As shown in Figure 6.5, increasing in D-glucose concentration has caused an increase in the decolorization rate. However, at a certain point, the curve reached a plateau. Once all the GOx is bound to a substrate, the presence of additional substrate has no positive effect on the reaction, as the available enzymes are saturated and

already working at their maximum rate. However, sometimes the excess amount of D-glucose may cause mass transfer and diffusion limitations, which may slow down the reaction [250, 254, 436].

A similar phenomenon was observed with the concentration of catalysts (GOx and Fe^0). The results related to the effect of the concentration of catalysts on the removal of crystal violet dye in the heterogeneous bio-Fenton system were inconclusive and will not be discussed in detail. Nonetheless, the pollutant removal efficiency may decrease in presence of higher amounts of the catalyst, as excessive exposure to catalysts may cause undesirable reactions. Although Fe^0 functions independently when it comes to the substrate, the actual removal reaction depends on the rate of hydrogen peroxide production by GOx. Therefore, the two catalysts are interrelated. This interrelation is best defined by the standard concentration study, rather than by an experimental design and statistical modeling. This study is a proof of concept; therefore, we did not do a detailed parameter study with statistical modeling.

Recyclability and reusability of immobilized catalysts

The main reason for using immobilized catalysts was to ensure easy recovery of the catalyst and eliminate secondary pollutants. Therefore, the recyclability and reusability of the immobilized catalysts (both Fe^0 and GOx) were investigated through repeated cycle application in the removal of crystal violet dye under the same experimental conditions. The results show that both catalysts were successfully recycled after the first application and were used for the second. The efficiency of CV removal during the second application cycle was reduced from the first one; this can be attributed to either leaching of the catalysts during recycling or loss of catalytic activity due to interactions among constituents in the reaction bath during the removal reaction. This matches previous studies (in chapters 4 and 5) on the reusability of the two catalysts.

The mechanism of removal of crystal violet dye

The results are of great interest due to the effective and complete removal of the crystal violet dye in the heterogeneous bio-Fenton system. The removal of the dye can be plausibly attributed to the synergistic effect involving a multi-step reaction, which led to the generation of highly reactive $^\bullet OH$ radicals, followed by oxidation of crystal violet dye into non-toxic substances [39]. Based on that, the plausible underlying mechanism of removal of crystal violet dye in a bio-Fenton system using catalysts immobilized textile is postulated. It is estimated that before the removal reaction, an initial CV dye solution containing crystal violet dyes, D-glucose was prepared. The addition of a Fe^0-immobilized PF sample released Fe^{2+} into the system and prepared the environment. After the addition of GOx-immobilized PF, a simple enzymatic glucose oxidation reaction takes place in the solution and generates hydrogen peroxide (H_2O_2) in situ. The presence of Fe^{2+} and H_2O_2 in the solution initiates the bio-Fenton reaction and produces highly reactive hydroxyl radicals ($^\bullet OH$). $^\bullet OH$ has a standard oxidation-reduction potential of 2.8 V and can degrade complex organic compounds. There are a number of conduits for the mineralization of CV dye as a function of the interaction with this oxidizing species. As observed with UV-Vis spectroscopy, the intensity of crystal violet dye decreases over time, indicating the removal of the color-bearing group and possible conversion of the dye into degraded intermediates, followed by secondary degradation into nontoxic substances. Palma-Goyes et al. (2010) [345] and Guzman-Duque et al. (2011) [346] suggested that hydroxyl free radicals and other reactive species react with the central carbon portion of CV dye structure and degrade the dye into reaction intermediates such as 4-(N, N-dimethylamino)-4'-(N', N'-dimethylamino) benzophenone or 4-(N, N-dimethylamino)-4'-(N', N'-dimethylamino) diphenylmethane. After that, these degraded intermediates undergo secondary degradation into further intermediates due to continued interaction with hydroxyl free radicals, before finally mineralizing into carboxylic acids and dissociating into H_2O and CO_2 [344].

6.4. Discussion

The objective of this study was to provide a proof of concept of the heterogeneous bio-Fenton system using catalysts immobilized on a textile. This study is categorically different from the other related reports because of its innovative idea to immobilize both catalysts, GOx and Fe^0, on a solid support material. This study also made its mark by using polyester nonwoven fabric as an inexpensive, porous, strong, and flexible support material for immobilizing both GOx biocatalysts and Fe^0 inorganic catalysts. Both innovative approaches were tested and critical experimental evidence was gathered. The results support the alternative hypothesis (that immobilized glucose oxidase and immobilized zerovalent iron would be effective in catalyzing a heterogeneous bio-Fenton reaction and would be able to remove toxic pollutants from water).

The removal of CV dye from water in the proposed system involved several distinct reaction stages. Since this study is the first of its kind, we took the liberty of naming the stages the initial, action, and saturation stages (see Figure 6.6). The CV dye removal curve shows that the initial stage was slowest in terms of removal of CV dye, followed by the saturation stage. The fastest reaction rate occurred at the action stage. These observations are key to understanding the proposed system. The slow reaction rate at the initial stage can be explained by the absence of hydrogen peroxide at the beginning of the reaction. When hydrogen peroxide is enzymatically produced, more is needed to initiate the removal of CV dye in the bio-Fenton reaction than when the hydrogen peroxide is added to the system. A certain time interval is necessary to produce a sufficient amount of hydrogen peroxide; initially, the only Fenton reactant in the solution is Fe^{2+}. This imbalance between Fenton reactants can explain the phenomenon observed at the initial stage. After that, when the reaction solution was supplied with a sufficient amount of hydrogen peroxide, the action stage started. This was when the maximum removal of CV dye took place. The final stage of CV dye removal in the heterogeneous bio-Fenton system is the saturation stage, where the CV dye removal proceeds at a constant rate until it reaches a plateau. This can be explained by the mechanism of catalytic reactions: "a catalytic reaction is limited to a maximum speed to a certain stage; after that, increases in catalysts or substrate concentration will not have any impact on their catalytic behavior. This assumption merits more extensive study.
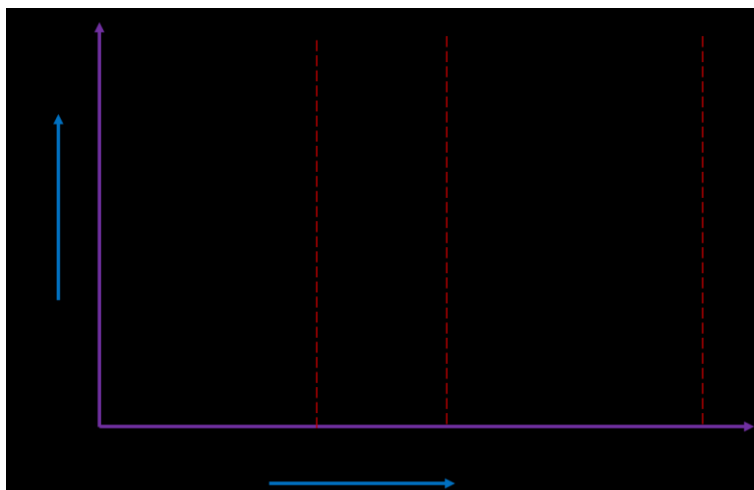
Figure 6. 6: Postulated reaction stages involved in the heterogeneous bio-Fenton system using immobilized catalysts.

After considerable time, 93% removal of the crystal violet dye was achieved in this system. The proof of concept is successful, with sufficient progress in color removal; however, the performance of the system in terms of toxicity reduction was substandard and requires further scrutiny. Chemical oxygen demand (COD) reduction of the treated water reached a maximum of 24% after 7.5 h of incubation time, although color removal was achieved in a much

shorter time. These observations are critical for understanding the mechanism of the system. The feasibility of this lab-scale process for industrial applications will depend on the specific technology cycle adopted the available setup and further optimization.

The effects of several influencing factors on the performance of the system were evaluated. As with the conventional Fenton reaction, the removal of CV dye was more efficient at an acidic pH than at a neutral or basic pH, which was not surprising. A pH of 6 and above seems exceedingly unfavorable for the proposed system [431]. Increasing the temperature improved the proposed system by increasing both the oxidation rate and the degree of mineralization of the pollutants [432]. It was found that, with increasing D-glucose concentration, the decolorization rate of the proposed system has also increased. However, this increase in removal rate due to the increase in D-glucose concentration takes place only until the curve reaches a plateau. A similar phenomenon was also observed when the effects of the concentration of catalysts (GOx and Fe^0) were evaluated.

This study is the first experimental proof of concept of the innovative heterogeneous bio-Fenton system that uses catalysts immobilized on textiles. Although this work significantly enriches the knowledge of bio-Fenton systems through various experimental data, it has several limitations. This study lacks detailed investigations of the mechanism of the pollutant removal, the interaction between the catalysts, the effect of the concentration of reactive species generated per unit time, and the identification of key decision factors. The proposed system itself also has some critical limitations, which concern both the output and the prospect of further development. They are (a) the need for a long incubation time to remove the pollutants; (b) poor COD reduction due to leaching of the catalysts (particularly Fe^0) and the use of COD-inflammatory chemicals (such as D-glucose); (c) specific reaction condition requirements (pH, temperature); (d) difficulties with the storage of the catalyst-immobilized textile before, during, and after the application. Other challenges involve the textile structure, modification of the textile surface, integration of favorable surface functional groups, and so on. Further studies should assess the effectiveness of the immobilized GOx after contact with iron ions. It may also be worthwhile to test two connected reactors with one immobilized catalyst per reactor (one reactor for producing H_2O_2 and the second, for mixing H_2O_2 with iron ions and pollutants). In this case, the iron ions would not affect the GOx, and neither would the glucose affect the COD measurements in the pollutant-degrading reactor.

The entire concept of bio-Fenton reactions and the heterogeneous bio-Fenton system is fairly new, and there are endless opportunities for improvement. Much of the research on catalyst immobilization for other applications can be applied to the proposed system, including the use of resource-efficient processes and the global campaign for rejecting complex processes and harsh conditions for the immobilization of catalysts on textiles. These possibilities can significantly improve the performance of the heterogeneous bio-Fenton system while opening doors to the implementation of large-scale eco-friendly wastewater treatment.

Chapter 7

General conclusions and future directions

Chapter outline

$\mathbf{T}$he final chapter of the thesis presents the overall summary of the thesis, concluding remarks, and scientific contributions and highlights of the various studies conducted under the framework of this thesis. The chapter also further addresses the challenges of the work and suggests future directions of the domain.

7.1. Summary

Driven by the identified researched gaps in the domain, this multidisciplinary thesis has achieved several goals related to immobilizing inorganic catalysts and biocatalysts on a porous textile support material for use in heterogeneous wastewater treatment systems. The general framework and structure of the thesis have been carefully designed to present the results systematically to ensure that the concept and findings are clear.

Chapter 1 provides a clear introductory background of catalyst immobilization on textiles and the research gaps that motivated the work, leading up to the specific research questions. Chapter 2 presents a comprehensive overview of the literature related to catalysts, catalytic systems, immobilization of catalysts, surface functionalization of textiles, catalytic pollutant removal from water, and so on. The literature review provides the rationales behind the choice of materials used in various sections of the thesis. Details of the materials and methods used to achieve the research objectives are presented in chapter 3, along with information about the instruments and parameters used in all the studies. After that, the thesis discusses the results obtained from the immobilization on textiles of zerovalent iron particles (chapter 4) and glucose oxidase (chapter 5).

We investigated several approaches to immobilizing the catalysts. All were based on the literature review and grounded in theory. The success of immobilization of Fe^0 particles on PF depends on two main factors: (a) the method of synthesis and immobilization of the Fe^0 particles, and (b) the surface-chemical properties of the PF. This thesis has explored both factors in separate experiments. The methods of synthesis and immobilization of Fe^0 particles were studied by investigating the effect of the methods of reducing iron ions to Fe^0 (*in-situ* vs. *ex-situ*) on loading, stability, and catalytic activity of the immobilized Fe^0 particles. After identifying the best method of reducing Fe ions into Fe^0 particles, another study explored ways of tailoring the surface of PF for robust Fe^0 binding. In both studies, the Fe^0-immobilized PF catalysts were effective in the removal of organic and pathogenic pollutants from water in either a heterogeneous Fenton-like system or a catalytic reduction system.

Enzyme immobilization is a widespread empiric technology used to obtain more stable, active, and reusable enzymes. The performance of immobilized enzymes depends on several factors, the most important of which is the binding interaction between the support matrix and the enzyme. We have explored different ways of tailoring the surface of the PF to achieve stable and robust immobilization of GOx. The first of two studies carried out in this domain focused on the competitive advantages of plasma eco-technology (either atmospheric-pressure or cold

remote plasma) and hyperbranched dendrimers (with either -OH or -NH$_2$ end terminal groups) for the robust immobilization of GOx on PF. Based on the results of the first study, the second study focused on tailoring the surface of the PF with cationic amine-based polymers (either chitosan or polyethylenimine). Catalytic loading, activity, and stability (leaching, washing, and temperature) of the immobilized GOx were compared to determine the best method for robust immobilization of GOx on PF. The catalytic behaviors of the prepared GOx-immobilized PF were evaluated in terms of their antibacterial properties and catalytic performance in the heterogeneous bio-Fenton system for the removal of water pollutants.

Chapter 6 of the thesis is related to all the research questions and provides the results related to the heterogeneous bio-Fenton system using both inorganic catalysts and biocatalysts immobilized on textiles. Both zerovalent iron and glucose oxidase was immobilized separately on the same type of textile support matrix to achieve total heterogeneity of the system. This thesis is the first published report of such a system and the first experimental proof of concept of this innovative idea.

7.2. General conclusions

The research for this thesis was done in three phases, where the first phase dealt with immobilizing inorganic catalysts on textiles; the second phase dealt with immobilizing biocatalysts on textiles; and the third and final phase, with the proof of concept of the heterogeneous bio-Fenton system using both inorganic catalysts and biocatalysts immobilized on textiles. The followings are the conclusions from all three phases.

Conclusions related to immobilizing inorganic catalysts on textiles

Two interconnected studies were involved in the investigation of immobilizing inorganic catalysts on textiles. The first, Study A, yielded the following conclusions.

(a) The main finding of this study is the experimental evidence for a simple approach to stabilizing and immobilizing iron particles on PF. It has been conclusively shown that the method of reducing iron (either *in-situ* or ex-situ) to produce zerovalent particles, as well as the surface chemistry of the functionalized polyester textile, has synergistic effects on the success of the immobilization of Fe^0 on PF.

(b) Characterization of the samples using various tools suggests that the method of reducing iron ions affects the overall morphology, distribution, and size of the iron particles. This variable during the preparation of samples also affected the further application of the iron particles immobilized on PF in the removal of malachite green dye in a heterogeneous Fenton-like system.

(c) Dendrimer grafting on the PF was also found to influence the stability, loading, and dispersion of iron particles.

(d) Another conclusion concerns the role of the surface chemical properties of the PF in overall performance. In many instances, further integration of hydroxyl groups facilitated the achievement of the goal. This suggests that the PF surface can be tailored to maximize the potential of the system. These findings offer a new direction for designing a robust Fenton-like system using Fe^0-immobilized PF for wastewater treatment.

Based on the findings of Study A, the subsequent Study B focused on tailoring the PF surface using polymers with specific terminal end functional groups for robust immobilization of zerovalent iron particles. An extensive study was conducted, and the results were presented in three separate sections as follows:

(a) Section (i): The first section of the study was related to activation and grafting of polyamidoamine dendrimer, 3-(aminopropyl) triethoxysilane, and 1-thioglycerol on plasma-activated polyester nonwoven fabric. Analysis based on sessile droplet goniometry, microscopic analysis (digital optical microscopy and scanning electron

microscopy), Fourier transform infrared (FTIR) spectroscopy and thermal property analysis confirmed successful activation and grafting of the selected polymers on PF surface. Results further suggest integration of specific surface functional groups on the PF surface to facilitate the immobilization of zerovalent iron particles.

(b) Section (ii): The second section confirmed the successful immobilization of zerovalent iron particles on surface-activated and modified polyester nonwoven fabrics. Results from the size distribution histogram of the iron particles showed an irregular distribution of iron particles with an average size of 10–150 nm. Out of the three polymers, 1-thioglycerol provided the most favorable PF surface for iron immobilization, leading to better dispersion, higher loading, and superior stability. This performance of 1-thioglycerol can be explained by synergy among Fe, S, and O atoms on the tailor-made PF surface.

(c) Section (iii): This section concluded that, as the prepared Fe^0-immobilized PF samples were effective in catalyzing a Fenton-like reaction (in the presence of hydrogen peroxide), they were effective in removing crystal violet dye from water. The highest dye removal yield was 98.87% in 22 min with a rate constant of 0.1919 min^{-1} (R^2 = 95.36) for zerovalent iron immobilized on 1-thioglycerol grafted polyester nonwoven textile. This sample also achieved a 78% toxicity reduction as assessed by COD analysis. These catalysts immobilized textiles could be reused for up to seven repeated cycles. Kinetics and a reaction mechanism of color removal were proposed based on the above results. In addition, the samples showed substantial antibacterial activity against pathogenic bacterial strains (*Staphylococcus epidermidis, Escherichia coli*) evaluated by disc diffusion-zone inhibitory and optical density analysis. These findings are important because they confirm the possibility of using textile-based flexible catalysts in heterogeneous Fenton-like systems for environmental and green chemistry applications.

Statistical optimization assessing the individual effect of two main factors, pH (X1) and concentration of hydrogen peroxide ($[H_2O_2]_{\mu l}$, X2) and their interaction effects on the removal process was determined at a 95% confidence level using an L^{27} design. The results show that increasing the pH to over 5 reduces dye removal efficiency, whereas increasing $[H_2O_2]_{\mu l}$ up to the equilibrium point increases dye removal. The type of catalyst-immobilized textiles (PF-NH$_2$-Fe^0, PF-Si-NH$_2$-Fe^0, and PF-SH-Fe^0) did not have a statistically significant effect. The factorial experiments suggest a significant synergistic interaction effect between the pH and $[H_2O_2]_{\mu l}$, as expressed by the values of the coefficient of interactions and analysis of variance.

The prepared catalysts showed similar efficiency in catalytic reduction (using NaBH$_4$ as reducing agent) of a persistent organic pollutant (4-nitrophenol, 4-NP) and a toxic colorant (methylene blue, MB). The highest conversion rate was 99.6% in 12 min for PF-SH-Fe^0, providing chemical stability and reusability over seven consecutive cycles without leaching of immobilized iron particles. Leaching and detoxification assessment by TDS analysis showed a 77% reduction in toxicity of the pollutants after treatment.

Both studies create new directions for designing robust Fenton-like systems using multifunctional Fe^0-immobilized polyester nonwoven fabrics for wastewater treatment.

Conclusions related to immobilizing biocatalysts on textiles

This part of the thesis is also based on the two studies on tailoring the surface of the PF for stable and robust immobilization of GOx. The first study (Study A) investigated the use of eco-technology and hyperbranched dendrimers for immobilizing redox enzymes on textiles and concluded the following.

(a) Robust grafting of glucose oxidase enzyme on the polyester surface can be achieved by modifying the PF surface with plasma treatment and hyperbranched dendrimers.

(b) The surface-modified polyester showed a sufficient quantity of surface-active groups after plasma treatment and dendrimer grafting, confirmed by wettability, SEM, and XPS analysis.

(c)   Enzyme activity analysis reveals that modified polyester with amino-terminal functional groups provides the most favorable conditions for enzyme immobilization, providing up to 31% enzyme loading while maintaining 81% of the immobilized enzymes' activity.

(d)   The study also confirmed the antibacterial activity of glucose oxidase enzyme immobilized on a fibrous textile (zone inhibition up to 41 mm). This area of research is still at an early stage.

Based on the conclusion of Study A regarding the effectiveness of amino-terminal groups for the robust immobilization of glucose oxidase enzyme on PF, Study B investigated the effectiveness of the tailor-made PF surface (modified through chemical grafting of either polyethylenimine or chitosan) for the immobilization of glucose oxidase (GOx) enzyme. This study concluded the following:

(a)   Grafting of polymers rich in amino groups on PF creates very favorable conditions for enzyme immobilization, as reflected in high loading (55.46%), good operational stability (78.37%), and thermal stability (~60 °C) with excellent recyclability (60% activity/15 cycles) and low leaching (22%) of the immobilized GOx.

(b)   The kinetic parameters of the enzymatic reaction revealed relative mass transfer and diffusion limitation of the immobilized GOx, observed in the apparent Michaelis constant (K_m) and maximum reaction velocity (V_{max}).

(c)   This study also found that the GOx-immobilized PF was effective in the removal of pollutants (10 mg·L^{-1} crystal violet) from water in a heterogeneous bio-Fenton system (using D-glucose and dissolved FeSO$_4$). The highest pollutant removal achieved was 88.69% at 1.19×10^{-2} min^{-1}.

Both studies on immobilizing biocatalysts on textiles yielded important results for the proof of concept of immobilizing biocatalysts on fibrous textiles and their application in the heterogeneous bio-Fenton system.

Conclusions related to the heterogeneous bio-Fenton system using immobilized inorganic catalysts and biocatalysts

This part of the thesis is a proof of concept of a heterogeneous bio-Fenton system for water pollutant removal using immobilized catalysts (both zerovalent iron and glucose oxidase immobilized on the textile support material), without the addition of hydrogen peroxide. Up to 93% removal of crystal violet dyes was achieved in this system. Toxicity reduction was difficult to access using COD analysis because of the presence of organic glucose and its organic oxidation product in the reactor. Further studies should focus on other methods of toxicity characterization and other reaction system designs, where iron ions are kept separate from immobilized enzymes. Overall, the proof of concept was successful and a more detailed study of this system should be done in the future.

7.3. Contributions and highlights

In this thesis, various novel approaches have been investigated, which not only contribute to the literature in the related domains of this thesis, but also significantly advances the areas of surface activation of textiles, modification by chemical grafting of specific polymers, and immobilization of various functional catalyst materials. Some of the main contributions and highlights are the following.

(a)   This thesis took a new approach by immobilizing inorganic catalysts and biocatalysts in polyester nonwoven fabric, and used the fabric for wastewater treatment, testing a new support material for catalyst immobilization, and pioneering eco-friendly and resource-efficient alternatives for a wastewater treatment system.

(b) Combining a textile with a catalytic system, this thesis has contributed to the domains of both technical/multifunctional textiles and heterogeneous catalysts. This is the first attempt to immobilize two different catalyst types (inorganic catalyst and biocatalyst) on the same type of textile. This is also the first trial of a Fe^0-immobilized textile catalyst used to catalyze a heterogeneous Fenton-like reaction to remove toxic pollutants from water.

(c) The detailed statistical modeling of a heterogeneous Fenton-like system is particularly important, as it will help other researchers navigate the complicated mechanism of heterogeneous Fenton-like systems. To the best of our knowledge, the statistical modeling presented here is the first for the use of a Fe^0-immobilized textile as a catalyst. The model is particularly useful because the Fe^0-immobilized textile proved to be very effective in both oxidative and reductive wastewater treatment systems.

(d) This work took a sustainable approach to the preparation of support materials from catalyst immobilization, using resource-efficient eco-technologies (plasma eco-technology, dendrimers, biopolymers).

(e) In general, this detailed study of catalytic wastewater treatment (including the kinetics and mechanism) using immobilized catalysts for both oxidative and reductive treatments contributes to the general knowledge of catalytic systems, to the knowledge of Fenton and bio-Fenton processes, but also the advancement and scaling up of an efficient and sustainable wastewater treatment system.

7.4. Challenges and future directions

Although this study has extensively investigated the concept of immobilizing catalysts on textiles, it failed to address several points, which can be studied further in the future. The challenges and future directions based on the findings of this thesis are presented below.

Immobilizing inorganic catalysts on textiles

Through microscopic analysis, we observed agglomeration of zerovalent iron particles on the textile surface. Agglomeration reduces the specific surface area and consequently limits the reactivity of the immobilized zerovalent iron. Therefore, it is important to increase the stability and minimize the agglomeration of the particles. Various additives should be tested for this purpose, such as surfactants, polymers, water-soluble starch, carboxymethyl cellulose, cellulose acetate, and polyacrylic acid, which may act as stabilization agents for immobilized zerovalent iron on textiles. The reaction mechanism of pollutant removal with Fe^0-immobilized PF is rather complex and little understood. More studies should be performed on this avenue. The current trends of Fe^0 synthesis and immobilization on textiles have led to the surface passivation of dry Fe^0 particles with a thin oxide layer, which reduces their reactivity. This, too, needs to be addressed in the future.

This thesis focused only on polyester nonwoven textiles as the support matrix for immobilization of Fe^0 particles. However, other forms and types of textiles (from both natural and synthetic sources) with optimized surface chemistry/structure can also be investigated. Furthermore, immobilization methods have a significant influence on the success of immobilizing inorganic catalysts. Rather than immobilization by physical adsorption, other methods can be tested, such as layer-by-layer immobilization and coating by resource-efficient printing technology. Other inorganic catalysts can also be tested for immobilization on textiles, such as silver (Ag), copper (Cu), aluminum (Al), titanium (Ti), zinc (Zn), and nickel (Ni).

Immobilizing biocatalysts on textiles

Biocatalysts are often highly desirable for catalyzing various complex reactions under mild conditions. In this era of sustainability and green technology, their importance in different fields is growing exponentially. However, despite all the advantages of immobilizing enzymes, significant challenges remain to overcome before the process

can be used on a large scale. Various phenomena may lead to a total or partial loss of catalytic activity of the immobilized biocatalysts. Here are a few examples: (i) waste of enzymes during immobilization; (ii) enzyme leaching into the medium; (iii) blocking of the active sites of enzymes; and (iv) interaction of the textile surface with the immobilized enzymes. There are endless possibilities for further research in the field of biocatalyst immobilization on textiles. Advances in textile processing promise other efficient substrates for immobilization. Other methods of immobilization are also possible. Printing of enzymes, layer-by-layer immobilization, encapsulation, and 3D textile structures are a few possibilities. Since this field is very new, few forms of textiles have been explored so far. Other tailored and specially designed textiles (from both natural and synthetic sources) with engineered surfaces and structures can be tested for biocatalyst immobilization. Nanofibers from electrospinning of conductive polymers, conductive coatings, and fillers can also be considered. New effective immobilization techniques on appropriate supports could help improve human life and welfare. More efficient removal of contamination from water bodies and electricity generation from industrial wastewater are some of the prospects in this field.

A heterogeneous bio-Fenton system using immobilized catalysts

The heterogeneous bio-Fenton system described in this thesis is a proof of concept. Where we did not do a detailed parameter study with statistical modeling but we highly recommend one. Endless challenges came up during this work. Long treatment time is one of the challenges that must be resolved before large-scale application. The performance of the system in removing complex pollutants, such as pesticides, antibiotics, and other persistent organic pollutants, needs to be studied in detail. Furthermore, the system depends on favorable reaction conditions; any change in parameters may significantly alter the performance of the system. The influencing factors such as concentration of D-glucose, the concentration of catalysts, temperature, and pH need to be studied thoroughly to determine the mechanism of the proposed system. Another challenge of the system is interference in the catalyst activity by elements other than its substrates, and the ability of reactive species produced in the system to denature the biocatalysts.

The prospects of this new concept are directly related to the development of immobilization of inorganic catalysts and biocatalysts on textiles. Improvements in catalyst loading and stability by tailoring the surface can greatly increase the efficiency of the system. To address the challenges related to the dependence of the system on favorable reaction conditions, a new type of enzyme known as extremozymes can be used. Extremozymes are robust enzymes capable of performing in various extreme environments. To avoid the interference of other elements in catalytic activity, the catalyst can be shielded with an additional membrane, such as Nafion®, which would still allow only the substrates to reach the catalyst. This approach would also protect the catalysts from the reactive species. As a new approach, a bio-electro-Fenton system with the same catalysts can also be explored.

Appendix- Additional publications by the author

During the time of the thesis, the author took part in additional research work to enrich knowledge around the domain. They are not included in the thesis but directly/indirectly related to the focus area. The findings of those works had been released as publications below.

Peer-Reviewed Journal Publications

Additional Publication I

M. N. Morshed, M. A. Miankafshe, N-K Persson, N. Behary and V. A. Nierstrasz; (*2020*) Development of a multifunctional graphene/Fe-loaded polyester textile: robust electrical and catalytic properties; Dalton Transactions, 49, 17281-17300. DOI: 10.1039/D0DT03291C

Summary of additional publication I: This work studied the concept related to the possibility to impart both electrical and catalytic properties on zerovalent iron immobilized flexible dual-functional textiles.

Additional Publication II

J. Vieillard, N. Bouazizi, M. N. Morshed, C. Thomas, D. Florie, B. Radhouane, P. Thébault, O. Lesouhaitier, F. L. Derf, and A. Azzouz; (*2019*) CuO nanosheets modified with amine and thiol grafting for high catalytic and antibacterial activities; ACS Industrial & Engineering Chemistry Research, 58, 24, 10179-10189 DOI: 10.1021/acs.iecr.9b00609

Summary of additional publication II: This work investigated the effect of amine and thiol-rich functional crosslinkers/polymers for immobilization of CuO nanosheets for organic and pathogenic pollutant removal from water.

Additional Publication III

N. Bouazizi, M. N. Morshed, A. El Achari, N. Behary, C. Campagne, J. Vieillard, O. Thoumire and A. Azzouz; (*2018*) Development of new multifunctional filter based nonwovens for organics pollutants reduction and detoxification: High catalytic and antibacterial activities; Chemical Engineering Journal, 356, 702-716; DOI: 10.1016/j.cej.2018.08.166.

Summary of additional publication III: By immobilizing Ag/Cu nanoparticles on tailor-made polyester textile, this study designed a continuous catalytic reduction system for the removal of various colorants, phenolic compounds, and pathogenic bacteria strains from water.

Vita of the author

Full Name   Mohammad Neaz MORSHED
Nationality   Bangladeshi

EDUCATION

2017-2021   Doctor of Engineering Sciences in Textile Material Engineering/ Textile Materials and Mechanics / Textile Engineering
[Erasmus Mundus joint Doctorate Fellowship Program, co-hosting by the University of Lille, ENSAIT/GEMTex (France), University of Boras (Sweden), and Soochow University (China)]

2015 - 2017   Master of Engineering in Textile Engineering
School of Textile Science and Engineering, Wuhan Textile University,
Wuhan (430200), Hubei, China
Recognition: "International student of the year 2017" and First of the class.

2010 – 2014   Bachelor of Science in Textile Engineering
Department of Textile Engineering, School of Science and Engineering
Southeast University, Dhaka (1218), Bangladesh
Recognition: First of the class and best student award.

SCHOLARSHIPS AND AWARDS

2020	Chinese Govt. Scholarship for Doctoral Studies at Soochow University (China)
2017	Erasmus Mundus joint Doctorate Fellowship about SMDTex (European Commission).
2017	College Scholarship for Top International Students-2017, Wuhan Textile University, China.
2016	Hubei Provincial Government Scholarship for Excellent International students (China Scholarship Council, Ministry of Education, China).
2015	Wuhan Textile University President Scholarship 2015 (Master studies, China).
2014	Champion, Textile Talent Hunt 2013 (Multilayered National Competition, Bangladesh).
2011	Merit-based Tuition-waiver Scholarship, Southeast University (Bachelor studies, Bangladesh).

MAJOR RESEARCH PROJECTS

2017-2021   SMDTex project 2017-42: Immobilizing catalysts on textiles for wastewater treatment.
Funder: Education, audiovisual and culture executive agency (EACEA), European Union.

2015-2017   WTU: In-Situ sonosynthesis of nanocrystalline titanium dioxide (TiO_2) on cellulosic substrates.
Funder: Wuhan Textile University & Jiangsu suqian innovative entrepreneurial talent project.

PUBLICATIONS AND PATENTS

As of June 2021, Mohammad Neaz Morshed has published sixteen (16) articles on prestigious peer-reviewed journals as first or co-author with eight (8) communications in international conferences. Publications can be found on the author's digital platforms (www.researchgate.net/profile/Mohammad_Morshed4, www.neazmorshed.se)

References

[1] T. Shimomura, T. Itoh, T. Sumiya, F. Mizukami, M. Ono, Electrochemical biosensor for the detection of formaldehyde based on enzyme immobilization in mesoporous silica materials, Sensors and Actuators B: Chemical, 135 (2008) 268-275.

[2] C. Chao, J. Liu, J. Wang, Y. Zhang, B. Zhang, Y. Zhang, X. Xiang, R. Chen, Surface modification of halloysite nanotubes with dopamine for enzyme immobilization, ACS applied materials & interfaces, 5 (2013) 10559-10564.

[3] T. Kong, Y. Chen, Y. Ye, K. Zhang, Z. Wang, X. Wang, An amperometric glucose biosensor based on the immobilization of glucose oxidase on the ZnO nanotubes, Sensors and Actuators B: Chemical, 138 (2009) 344-350.

[4] M. Moses Phiri, D. Wingrove Mulder, S. Mason, B. Christiaan Vorster, Facile immobilization of glucose oxidase onto gold nanostars with enhanced binding affinity and optimal function, Royal Society open science, 6 (2019) 190205.

[5] M. Rahman, A. Ahammad, J.-H. Jin, S.J. Ahn, J.-J. Lee, A comprehensive review of glucose biosensors based on nanostructured metal-oxides, Sensors, 10 (2010) 4855-4886.

[6] S. Pakapongpan, R.P. Poo-Arporn, Self-assembly of glucose oxidase on reduced graphene oxide-magnetic nanoparticles nanocomposite-based direct electrochemistry for reagentless glucose biosensor, Materials Science and Engineering: C, 76 (2017) 398-405.

[7] M. Abbasi, R. Amiri, A.-K. Bordbar, E. Ranjbakhsh, A.-R. Khosropour, Improvement of the stability and activity of immobilized glucose oxidase on modified iron oxide magnetic nanoparticles, Applied Surface Science, 364 (2016) 752-757.

[8] W.E. Forum, Global Risks 2015, in, Geneva, Switzerland., 2015.

[9] R.N. Carvalho, L. Ceriani, A. Ippolito, T. Lettieri, Development of the first watch list under the environmental quality standards directive, JRC Science Hub, (2015).

[10] C. Bernes, Persistent organic pollutants, Swedish Environmental Protection Agency, Stockholm, (1998) 9-21.

[11] N. Gaur, K. Narasimhulu, Y. PydiSetty, Recent advances in the bio-remediation of persistent organic pollutants and its effect on environment, Journal of cleaner production, 198 (2018) 1602-1631.

[12] M. Cheng, G. Zeng, D. Huang, C. Lai, P. Xu, C. Zhang, Y. Liu, Hydroxyl radicals based advanced oxidation processes (AOPs) for remediation of soils contaminated with organic compounds: a review, Chemical Engineering Journal, 284 (2016) 582-598.

[13] S. Ravi, L. Lonappan, I. Touahar, É. Fonteneau, V.K. Vaidyanathan, H. Cabana, Evaluation of bio-fenton oxidation approach for the remediation of trichloroethylene from aqueous solutions, Journal of Environmental Management, 270 (2020) 110899.

[14] S. Aber, E. Mahmoudikia, A. Karimi, F. Mahdizadeh, Immobilization of glucose oxidase on Fe_3O_4 magnetic nanoparticles and its application in the removal of acid yellow 12, Water, Air, & Soil Pollution, 227 (2016) 93.

[15] A. Karimi, F. Mahdizadeh, M. Eskandarian, Enzymatic in-situ generation of H_2O_2 for decolorization of Acid Blue 113 by fenton process, Chemical Industry and Chemical Engineering Quarterly/CICEQ, 18 (2012) 89-94.

[16] M. Eskandarian, F. Mahdizadeh, L. Ghalamchi, S. Naghavi, Bio-Fenton process for Acid Blue 113 textile azo dye decolorization: characteristics and neural network modeling, Desalination and Water Treatment, 52 (2014) 4990-4998.

[17] A. Karimi, M. Aghbolaghy, A. Khataee, S. Shoa Bargh, Use of enzymatic bio-Fenton as a new approach in decolorization of malachite green, The scientific world journal, 2012 (2012).

[18] V. Elhami, A. Karimi, M. Aghbolaghy, Preparation of heterogeneous bio-Fenton catalyst for decolorization of Malachite Green, Journal of the Taiwan Institute of Chemical Engineers, 56 (2015) 154-159.

[19] J. Wisniak, The history of catalysis. From the beginning to Nobel Prizes, Educación química, 21 (2010) 60-69.

[20] J. Hagen, Industrial catalysis: a practical approach, John Wiley & Sons, 2015.

[21] J.N. Armor, Environmental catalysis, Applied Catalysis B: Environmental, 1 (1992) 221-256.

[22] W.P. Jencks, Catalysis in chemistry and enzymology, Courier Corporation, 1987.

[23] F.E. Osterloh, Inorganic materials as catalysts for photochemical splitting of water, Chemistry of Materials, 20 (2008) 35-54.

[24] A.P. Wight, M.E. Davis, Design and preparation of organic– inorganic hybrid catalysts, Chemical reviews, 102 (2002) 3589-3614.

[25] F. Cozzi, Immobilization of organic catalysts: when, why, and how, Advanced Synthesis & Catalysis, 348 (2006) 1367-1390.

[26] M. Benaglia, A. Puglisi, F. Cozzi, Polymer-supported organic catalysts, Chemical reviews, 103 (2003) 3401-3430.

[27] B. List, Introduction: organocatalysis, in, ACS Publications, 2007.

[28] A.S. Bommarius, B.R. Riebel-Bommarius, Biocatalysis: fundamentals and applications, John Wiley & Sons, 2004.

[29] A.K. Endalew, Y. Kiros, R. Zanzi, Inorganic heterogeneous catalysts for biodiesel production from vegetable oils, Biomass and bioenergy, 35 (2011) 3787-3809.

[30] L. Liu, A. Corma, Metal catalysts for heterogeneous catalysis: from single atoms to nanoclusters and nanoparticles, Chemical reviews, 118 (2018) 4981-5079.

[31] C. Bolm, M. Beller, Transition metals for organic synthesis, Wiley-VCH: Weinheim, 2004.

[32] D.M. Miller, G.R. Buettner, S.D. Aust, Transition metals as catalysts of "autoxidation" reactions, Free Radical Biology and Medicine, 8 (1990) 95-108.

[33] K. Buchholz, V. Kasche, U.T. Bornscheuer, Biocatalysts and enzyme technology, John Wiley & Sons, 2012.

[34] M. Kahoush, Eco-technologies for immobilizing redox enzymes on conductive textiles, for sustainable development, in, Högskolan i Borås, 2019.

[35] K. Tipton, A. McDonald, A brief guide to enzyme nomenclature and classification, in, IUBMB, 2018.

[36] C. Copéret, M. Chabanas, R. Petroff Saint-Arroman, J.M. Basset, Homogeneous and heterogeneous catalysis: bridging the gap through surface organometallic chemistry, Angewandte Chemie International Edition, 42 (2003) 156-181.

[37] S. Bhaduri, D. Mukesh, Homogeneous Catalysis, Wiley Online Library, 2014.

[38] E. Farnetti, R. Di Monte, J. Kašpar, Homogeneous and heterogeneous catalysis, Inorganic and bio-inorganic chemistry, 2 (2009) 50-86.

[39] G. Ertl, H. Knözinger, J. Weitkamp, Handbook of heterogeneous catalysis, Citeseer, 1997.

[40] R.A. Sheldon, Engineering a more sustainable world through catalysis and green chemistry, Journal of The Royal Society Interface, 13 (2016) 20160087.

[41] G.A. Somorjai, Y. Li, Introduction to surface chemistry and catalysis, John Wiley & Sons, 2010.

[42] L. Lai, H. Chun, Heterogeneous Fenton catalytic water treatment technology and mechanism, Progress in Chemistry, 29 (2017) 981.

[43] S. Kobayashi, A. Makino, Enzymatic polymer synthesis: an opportunity for green polymer chemistry, Chemical reviews, 109 (2009) 5288-5353.

[44] M.A.F. Delgove, A.B. Laurent, J.M. Woodley, S.M.A. De Wildeman, K.V. Bernaerts, Y. van der Meer, A prospective life cycle assessment (LCA) of monomer synthesis: comparison of biocatalytic and oxidative chemistry, ChemSusChem, 12 (2019) 1349-1360.

[45] A.A. Homaei, R. Sariri, F. Vianello, R. Stevanato, Enzyme immobilization: an update, Journal of chemical biology, 6 (2013) 185-205.

[46] A.M. Klibanov, Enzyme stabilization by immobilization, Analytical biochemistry, 93 (1979) 1-25.

[47] B. Lothenbach, G. Furrer, R. Schulin, Immobilization of heavy metals by polynuclear aluminium and montmorillonite compounds, Environmental Science & Technology, 31 (1997) 1452-1462.

[48] R. Messing, Immobilized enzymes for industrial reactors, Elsevier, 2012.

[49] Y.J. Weng, R.X. Hou, G.C. Li, J. Wang, N. Huang, H.Q. Liu, Immobilization of bovine serum albumin on TiO2 film via chemisorption of H3PO4 interface and effects on platelets adhesion, Applied surface science, 254 (2008) 2712-2719.

[50] C. Airoldi, E.F.C. Alcântara, Chemisorption of some metal (II) chlorides on silica-immobilized acetylhydrazine, Colloids and surfaces, 39 (1989) 291-302.

[51] S. Bone, A. Alum, J. Markovski, K. Hristovski, E. Bar-Zeev, Y. Kaufman, M. Abbaszadegan, F. Perreault, Physisorption and chemisorption of T4 bacteriophages on amino functionalized silica particles, Journal of colloid and interface science, 532 (2018) 68-76.

[52] X.S. Zhao, X.Y. Bao, W. Guo, F.Y. Lee, Immobilizing catalysts on porous materials, Materials Today, 9 (2006) 32-39.

[53] B. Thangaraj, P.R. Solomon, Immobilization of lipases–A review. Part I: Enzyme immobilization, ChemBioEng Reviews, 6 (2019) 157-166.

[54] M.B. Majewski, A.J. Howarth, P. Li, M.R. Wasielewski, J.T. Hupp, O.K. Farha, Enzyme encapsulation in metal–organic frameworks for applications in catalysis, CrystEngComm, 19 (2017) 4082-4091.

[55] P. Zucca, E. Sanjust, Inorganic materials as supports for covalent enzyme immobilization: methods and mechanisms, Molecules, 19 (2014) 14139-14194.

[56] J. Zdarta, A.S. Meyer, T. Jesionowski, M. Pinelo, A general overview of support materials for enzyme immobilization: characteristics, properties, practical utility, Catalysts, 8 (2018) 92.

[57] D. Moelans, P. Cool, J. Baeyens, E.F. Vansant, Using mesoporous silica materials to immobilise biocatalysis-enzymes, Catalysis Communications, 6 (2005) 307-311.

[58] H.R. Luckarift, J.C. Spain, R.R. Naik, M.O. Stone, Enzyme immobilization in a biomimetic silica support, Nature biotechnology, 22 (2004) 211-213.

[59] Y. Wang, F. Caruso, Mesoporous silica spheres as supports for enzyme immobilization and encapsulation, Chemistry of Materials, 17 (2005) 953-961.

[60] B. Zou, Y. Hu, F. Cui, L. Jiang, D. Yu, H. Huang, Effect of surface modification of low cost mesoporous SiO_2 carriers on the properties of immobilized lipase, Journal of Colloid and interface science, 417 (2014) 210-216.

[61] R. Chrisnasari, Z.G. Wuisan, A. Budhyantoro, R.K. Widi, Glucose oxidase immobilization on TMAH-modified bentonite, Indonesian Journal of Chemistry, 15 (2015) 22-28.

[62] H. Vaghari, H. Jafarizadeh-Malmiri, M. Mohammadlou, A. Berenjian, N. Anarjan, N. Jafari, S. Nasiri, Application of magnetic nanoparticles in smart enzyme immobilization, Biotechnology letters, 38 (2016) 223-233.

[63] S.V. Otari, S.K.S. Patel, S.-Y. Kim, J.R. Haw, V.C. Kalia, I.-W. Kim, J.-K. Lee, Copper ferrite magnetic nanoparticles for the immobilization of enzyme, Indian journal of microbiology, 59 (2019) 105-108.

[64] M. Bilal, Y. Zhao, T. Rasheed, H.M.N. Iqbal, Magnetic nanoparticles as versatile carriers for enzymes immobilization: A review, International journal of biological macromolecules, 120 (2018) 2530-2544.

[65] Y. Wang, Y.L. Hsieh, Immobilization of lipase enzyme in polyvinyl alcohol (PVA) nanofibrous membranes, Journal of Membrane Science, 309 (2008) 73-81.

[66] A. Mohamed, B. Nemeshwaree, M. Brigitte, P. Anne, B. Kalim, D. Pascal, M. Anne-Sophie, F. Rénato, Activity of enzymes immobilized on plasma treated polyester, Journal of Molecular Catalysis B: Enzymatic, 134 (2016) 261-272.

[67] S. Li, S. Zhao, Y. Hou, G. Chen, Y. Chen, Z. Zhang, Polylactic acid (PLA) modified by polyethylene glycol (PEG) for the immobilization of lipase, Applied biochemistry and biotechnology, 190 (2020) 982-996.

[68] J. Zhang, L. Wang, B. Zhang, H. Zhao, U. Kolb, Y. Zhu, L. Liu, Y. Han, G. Wang, C. Wang, Sinter-resistant metal nanoparticle catalysts achieved by immobilization within zeolite crystals via seed-directed growth, Nature Catalysis, 1 (2018) 540-546.

[69] K. Fan, F. Li, L. Wang, Q. Daniel, H. Chen, E. Gabrielsson, J. Sun, L. Sun, Immobilization of a molecular ruthenium catalyst on hematite nanorod arrays for water oxidation with stable photocurrent, ChemSusChem, 8 (2015) 3242-3247.

[70] A. Kumar, G.D. Park, S.K.S. Patel, S. Kondaveeti, S. Otari, M.Z. Anwar, V.C. Kalia, Y. Singh, S.C. Kim, B.-K. Cho, SiO2 microparticles with carbon nanotube-derived mesopores as an efficient support for enzyme immobilization, Chemical Engineering Journal, 359 (2019) 1252-1264.

[71] J. Zhang, F. Zhang, H. Yang, X. Huang, H. Liu, J. Zhang, S. Guo, Graphene oxide as a matrix for enzyme immobilization, Langmuir, 26 (2010) 6083-6085.

[72] V. Esquivel-Peña, J. Bastos-Arrieta, M. Muñoz, L. Mora-Tamez, N.M. Munguía-Acevedo, A.L. Ocampo, J. de Gyves, Metal nanoparticle–carbon nanotubes hybrid catalysts immobilized in a polymeric membrane for the reduction of 4-nitrophenol, SN Applied Sciences, 1 (2019) 1-11.

[73] K. Kiehl, T. Straube, K. Opwis, J.S. Gutmann, Strategies for permanent immobilization of enzymes on textile carriers, Engineering in Life Sciences, 15 (2015) 622-626.

[74] T. Mayer-Gall, J.W. Lee, K. Opwis, B. List, J.S. Gutmann, Textile Catalysts—An unconventional approach towards heterogeneous catalysis, ChemCatChem, 8 (2016) 1428-1436.

[75] M.N. Morshed, N. Behary, N. Bouazizi, G. Jinping, V.A. Nierstrasz, An overview on biocatalysts immobilization on textiles: preparation, progress and application in wastewater treatment, Chemosphere, (2021) 130481.

[76] Y. Gao, Y.B. Truong, P. Cacioli, P. Butler, I.L. Kyratzis, Bioremediation of pesticide contaminated water using an organophosphate degrading enzyme immobilized on nonwoven polyester textiles, Enzyme and Microbial Technology, 54 (2014) 38-44.

[77] M.J. John, R.D. Anandjiwala, Surface modification and preparation techniques for textile materials, in: Surface modification of textiles, Elsevier, 2009, pp. 1-25.

[78] J. Wang, J. Liu, Surface modification of textiles by aqueous solutions, in: Surface modification of textiles, Elsevier, 2009, pp. 269-295.

[79] Q. Wei, Emerging approaches to the surface modification of textiles, Surface Modification of Textiles, (2009) 318-323.

[80] J.I.B. Wilson, Textile surface functionalisation by chemical vapour deposition (CVD), in: Surface Modification of Textiles, Elsevier, 2009, pp. 126-138.

[81] A.C.Q. Silva, A.J.D. Silvestre, C.S.R. Freire, C. Vilela, Modification of textiles for functional applications, in: Fundamentals of Natural Fibres and Textiles, Elsevier, 2021, pp. 303-365.

[82] B. Nabil, C. Christine, V. Julien, A. Abdelkrim, Polyfunctional cotton fabrics with catalytic activity and antibacterial capacity, Chemical Engineering Journal, 351 (2018) 328-339.

[83] B. Nabil, E.-A. Ahmida, C. Christine, V. Julien, A. Abdelkrim, Inorganic-organic-fabrics based polyester/cotton for catalytic reduction of 4-nitrophenol, Journal of Molecular Structure, 1180 (2019) 523-531.

[84] M. Vertommen, V.A. Nierstrasz, M. Van Der Veer, M. Warmoeskerken, Enzymatic surface modification of poly (ethylene terephthalate), Journal of Biotechnology, 120 (2005) 376-386.

[85] M. Kanelli, S. Vasilakos, S. Ladas, E. Symianakis, P. Christakopoulos, E. Topakas, Surface modification of polyamide 6.6 fibers by enzymatic hydrolysis, Process Biochemistry, 59 (2017) 97-103.

[86] V.A. Nierstrasz, Enzyme surface modification of textiles, in: Surface Modification of Textiles, Elsevier, 2009, pp. 139-163.

[87] R.R. Mather, Surface modification of textiles by plasma treatments, in: Surface modification of textiles, Elsevier, 2009, pp. 296-317.

[88] F. Leroux, C. Campagne, A. Perwuelz, L. Gengembre, Atmospheric air plasma treatment of polyester textile materials. Textile structure influence on surface oxidation and silicon resin adhesion, Surface and Coatings Technology, 203 (2009) 3178-3183.

[89] S.N. Iyer, N. Behary, V. Nierstrasz, J. Guan, Glow-in-the-Dark Patterned PET Nonwoven Using Air-Atmospheric Plasma Treatment and Vitamin B2-Derivative (FMN), Sensors, 20 (2020) 6816.

[90] H. Höcker, Plasma treatment of textile fibers, Pure and applied chemistry, 74 (2002) 423-427.

[91] R. Abd Jelil, A review of low-temperature plasma treatment of textile materials, Journal of materials science, 50 (2015) 5913-5943.

[92] R. Morent, N. De Geyter, J. Verschuren, K. De Clerck, P. Kiekens, C. Leys, Non-thermal plasma treatment of textiles, Surface and coatings technology, 202 (2008) 3427-3449.

[93] F. Shi, X. Cui, Catalytic amination for N-alkyl amine synthesis, Academic Press, 2018.

[94] J.M. Fraile, J.I. García, J.A. Mayoral, Recent advances in the immobilization of chiral catalysts containing bis (oxazolines) and related ligands, Coordination Chemistry Reviews, 252 (2008) 624-646.

[95] H. Zhang, H. Zhu, Preparation of Fe-doped TiO_2 nanoparticles immobilized on polyamide fabric, Applied Surface Science, 258 (2012) 10034-10041.

[96] J. Fan, Y. Gao, Nanoparticle-supported catalysts and catalytic reactions–a mini-review, Journal of Experimental Nanoscience, 1 (2006) 457-475.

[97] S. Xiao, S. Wu, M. Shen, R. Guo, Q. Huang, S. Wang, X. Shi, Polyelectrolyte multilayer-assisted immobilization of zero-valent iron nanoparticles onto polymer nanofibers for potential environmental applications, ACS applied materials & interfaces, 1 (2009) 2848-2855.

[98] J. Ren, Y.C. Woo, M. Yao, S. Lim, L.D. Tijing, H.K. Shon, Nanoscale zero-valent iron (nZVI) immobilization onto graphene oxide (GO)-incorporated electrospun polyvinylidene fluoride (PVDF) nanofiber membrane for groundwater remediation via gravity-driven membrane filtration, Science of the total environment, 688 (2019) 787-796.

[99] S. Ogo, Y. Sekine, Recent progress in ethanol steam reforming using non-noble transition metal catalysts: a review, Fuel Processing Technology, 199 (2020) 106238.

[100] V.S. Kosera, T.M. Cruz, E.S. Chaves, E.R.L. Tiburtius, Triclosan degradation by heterogeneous photocatalysis using ZnO immobilized in biopolymer as catalyst, Journal of Photochemistry and Photobiology A: Chemistry, 344 (2017) 184-191.

[101] S.I. Wilkanowicz, N.R. Hollingsworth, K. Saud, U. Kadiyala, R.G. Larson, Immobilization of calcium oxide onto polyacrylonitrile (PAN) fibers as a heterogeneous catalyst for biodiesel production, Fuel Processing Technology, 197 (2020) 106214.

[102] T. Zhang, J. Yu, H. Guo, J. Liu, Q. Liu, D. Song, R. Chen, R. Li, P. Liu, J. Wang, Heterogeneous $CoSe_2$–CoO nanoparticles immobilized into N-doped carbon fibers for efficient overall water splitting, Electrochimica Acta, 356 (2020) 136822.

[103] D. Zhang, T. Xu, C. Li, W. Xu, J. Wang, J. Bai, Synthesis of carbon fibers support graphitic carbon nitride immobilize ZnBr2 catalyst in the catalytic reaction between styrene oxide and CO_2, Journal of CO_2 Utilization, 34 (2019) 716-724.

[104] S.M. Hosseini, M. Ghiaci, S.A. Kulinich, W. Wunderlich, B.H. Monjezi, Y. Ghorbani, H.S. Ghaziaskar, A.J. Koupaei, Au-Pd nanoparticles enfolded in coil-like TiO_2 immobilized on carbon fibers felt as recyclable nanocatalyst for benzene oxidation under mild conditions, Applied Surface Science, 506 (2020) 144644.

[105] L. Wang, H. Mao, Z. Li, C. Wang, D. Gao, Immobilizing Ag/Cu_2O on cotton fabric to enhance visible light photocatalytic activity, New Journal of Chemistry, 44 (2020) 20759-20769.

[106] J. Ran, H. Chen, X. Bai, S. Bi, H. Jiang, G. Cai, D. Cheng, X. Wang, Immobilizing CuO/$BiVO_4$ nanocomposite on PDA-templated cotton fabric for visible light photocatalysis, antimicrobial activity and UV protection, Applied Surface Science, 493 (2019) 1167-1176.

[107] Y. Yao, L. Wang, L. Sun, S. Zhu, Z. Huang, Y. Mao, W. Lu, W. Chen, Efficient removal of dyes using heterogeneous Fenton catalysts based on activated carbon fibers with enhanced activity, Chemical Engineering Science, 101 (2013) 424-431.

[108] M.S. Mia, B. Yan, X. Zhu, T. Xing, G. Chen, Dopamine Grafted Iron-Loaded Waste Silk for Fenton-Like Removal of Toxic Water Pollutants, Polymers, 11 (2019) 2037.

[109] M.N. Morshed, N. Behary, N. Bouazizi, J. Vieillard, J. Guan, F. Le Derf, V. Nierstrasz, Modification of fibrous membrane for organic and pathogenic contaminants removal: from design to application, RSC Advances, 10 (2020) 13155-13173.

[110] X. Zhao, Y. Dong, B. Cheng, W. Kang, Removal of textile dyes from aqueous solution by heterogeneous photo-Fenton reaction using modified PAN nanofiber Fe complex as catalyst, International Journal of Photoenergy, 2013 (2013).

[111] K. Atacan, M. Özacar, M. Özacar, Investigation of antibacterial properties of novel papain immobilized on tannic acid modified Ag/CuFe2O4 magnetic nanoparticles, International journal of biological macromolecules, 109 (2018) 720-731.

[112] S. Datta, L.R. Christena, Y.R.S. Rajaram, Enzyme immobilization: an overview on techniques and support materials, 3 Biotech, 3 (2013) 1-9.

[113] C. Zhang, X.-H. Xing, 2.23 Enzyme Bioreactors, Academic Press, 2011.

[114] A. Dwevedi, 100 years of enzyme immobilization, in: Enzyme Immobilization, Springer, 2016, pp. 1-20.

[115] T.M. Mohamed, S.M.A. El-Souod, E.M. Ali, M.O. El-Badry, M.M. El-Keiy, A.S. Aly, Immobilization and characterization of inulinase from Ulocladium atrum on nonwoven fabrics, Journal of biosciences, 39 (2014) 785-793.

[116] Y. Dai, J. Yao, Y. Song, X. Liu, S. Wang, Y. Yuan, Enhanced performance of immobilized laccase in electrospun fibrous membranes by carbon nanotubes modification and its application for bisphenol A removal from water, Journal of hazardous materials, 317 (2016) 485-493.

[117] J. Niu, J. Xu, Y. Dai, J. Xu, H. Guo, K. Sun, R. Liu, Immobilization of horseradish peroxidase by electrospun fibrous membranes for adsorption and degradation of pentachlorophenol in water, Journal of hazardous materials, 246 (2013) 119-125.

[118] N. Bal, S. Houshyar, Y. Gao, I.L. Kyratzis, R. Padhye, Digital printing of enzymes on textile substrates as functional materials, Journal of Fiber Bioengineering and Informatics, 7 (2014) 595-602.

[119] T. Biswas, J. Yu, V. Nierstrasz, Effective Pretreatment Routes of Polyethylene Terephthalate Fabric for Digital Inkjet Printing of Enzyme, Advanced Materials Interfaces, (2021) 2001882.

[120] J.J. Karimpil, J.S. Melo, S.F. D'Souza, Immobilization of lipase on cotton cloth using the layer-by-layer self-assembly technique, International journal of biological macromolecules, 50 (2012) 300-302.

[121] J. Zhang, X. Huang, L. Zhang, Y. Si, S. Guo, H. Su, J. Liu, Layer-by-layer assembly for immobilizing enzymes in enzymatic biofuel cells, Sustainable Energy & Fuels, 4 (2020) 68-79.

[122] D. Zhao, C. Peng, J. Zhou, Lipase adsorption on different nanomaterials: a multi-scale simulation study, Physical Chemistry Chemical Physics, 17 (2015) 840-850.

[123] S.A. Mohamed, A.S. Aly, T.M. Mohamed, H.A. Salah, Immobilization of horseradish peroxidase on nonwoven polyester fabric coated with chitosan, Applied biochemistry and biotechnology, 144 (2008) 169-179.

[124] M.N. Morshed, N. Behary, N. Bouazizi, J. Guan, G. Chen, V. Nierstrasz, Surface modification of polyester fabric using plasma-dendrimer for robust immobilization of glucose oxidase enzyme, Scientific reports, 9 (2019) 1-16.

[125] J.E. Song, W.S. Song, S.Y. Yeo, H.R. Kim, S.H. Lee, Covalent immobilization of enzyme on aminated woven poly (lactic acid) via ammonia plasma: evaluation of the optimum immobilization conditions, Textile Research Journal, 87 (2017) 1177-1191.

[126] M. Hoarau, S. Badieyan, E.N.G. Marsh, Immobilized enzymes: understanding enzyme–surface interactions at the molecular level, Organic & Biomolecular Chemistry, 15 (2017) 9539-9551.

[127] C. Mateo, J.M. Palomo, M. Fuentes, L. Betancor, V. Grazu, F. López-Gallego, B.C.C. Pessela, A. Hidalgo, G. Fernández-Lorente, R. Fernández-Lafuente, Glyoxyl agarose: a fully inert and hydrophilic support for immobilization and high stabilization of proteins, Enzyme and Microbial Technology, 39 (2006) 274-280.

[128] V.A. Nierstrasz, M. Warmoeskerken, Process engineering and industrial enzyme applications, Woodhead Publishing Ltd, Cambridge, 2003.

[129] M. Kahoush, N. Behary, A. Cayla, B. Mutel, J. Guan, V. Nierstrasz, Surface modification of carbon felt by cold remote plasma for glucose oxidase enzyme immobilization, Applied Surface Science, 476 (2019) 1016-1024.

[130] F. Shakerian, J. Zhao, S.-P. Li, Recent development in the application of immobilized oxidative enzymes for bioremediation of hazardous micropollutants–A review, Chemosphere, 239 (2020) 124716.

[131] M. Defaei, A. Taheri-Kafrani, M. Miroliaei, P. Yaghmaei, Improvement of stability and reusability of α-amylase immobilized on naringin functionalized magnetic nanoparticles: A robust nanobiocatalyst, International journal of biological macromolecules, 113 (2018) 354-360.

[132] C. Singh, A. Goyal, S. Singhal, Nickel-doped cobalt ferrite nanoparticles: efficient catalysts for the reduction of nitroaromatic compounds and photo-oxidative degradation of toxic dyes, Nanoscale, 6 (2014) 7959-7970.

[133] B.M. Hedi, O. Boughzala, D. Dorra, B. Daniel, C.G. Leila, M. Ridha, Textiles dyes as a source of wastewater contamination: screening of the toxicity and treatment methods, Journal of Water Science, 24 (2011) 209-238.

[134] Q.-Q. Zhang, G.-G. Ying, C.-G. Pan, Y.-S. Liu, J.-L. Zhao, Comprehensive evaluation of antibiotics emission and fate in the river basins of China: source analysis, multimedia modeling, and linkage to bacterial resistance, Environmental science & technology, 49 (2015) 6772-6782.

[135] J. Xu, Y. Xu, H. Wang, C. Guo, H. Qiu, Y. He, Y. Zhang, X. Li, W. Meng, Occurrence of antibiotics and antibiotic resistance genes in a sewage treatment plant and its effluent-receiving river, Chemosphere, 119 (2015) 1379-1385.

[136] S.D. Richardson, Water analysis: emerging contaminants and current issues, Analytical chemistry, 81 (2009) 4645-4677.

[137] M.B. Campanha, A.T. Awan, D.N.R. de Sousa, G.M. Grosseli, A.A. Mozeto, P.S. Fadini, A 3-year study on occurrence of emerging contaminants in an urban stream of São Paulo State of Southeast Brazil, Environmental Science and Pollution Research, 22 (2015) 7936-7947.

[138] C. Macci, E. Peruzzi, S. Doni, R. Iannelli, G. Masciandaro, Ornamental plants for micropollutant removal in wetland systems, Environmental Science and Pollution Research, 22 (2015) 2406-2415.

[139] C. Yan, M. Nie, Y. Yang, J. Zhou, M. Liu, M. Baalousha, J.R. Lead, Effect of colloids on the occurrence, distribution and photolysis of emerging organic contaminants in wastewaters, Journal of hazardous materials, 299 (2015) 241-248.

[140] P. Khurana, S. Thatai, D. Kumar, Destruction of recalcitrant nanomaterials contaminants in industrial wastewater, in: Emerging and Nanomaterial Contaminants in Wastewater, Elsevier, 2019, pp. 137-158.

[141] J. Hoigné, Inter-calibration of OH radical sources and water quality parameters, Water Science and Technology, 35 (1997) 1-8.

[142] W.H. Glaze, J.-W. Kang, D.H. Chapin, The chemistry of water treatment processes involving ozone, hydrogen peroxide and ultraviolet radiation, (1987).

[143] T.H. Pham, H.M. Bui, T.X. Bui, Advanced oxidation processes for the removal of pesticides, in: Current Developments in Biotechnology and Bioengineering, Elsevier, 2020, pp. 309-330.

[144] D.G. Rao, R. Senthilkumar, J.A. Byrne, S. Feroz, Wastewater treatment: advanced processes and technologies, CRC Press, 2012.

[145] G. Tezcanli-Güyer, N.H. Ince, Individual and combined effects of ultrasound, ozone and UV irradiation: a case study with textile dyes, Ultrasonics, 42 (2004) 603-609.

[146] Z. Liu, S. Hosseinzadeh, N. Wardenier, Y. Verheust, M. Chys, S.V. Hulle, Combining ozone with UV and H_2O_2 for the degradation of micropollutants from different origins: lab-scale analysis and optimization, Environmental technology, 40 (2019) 3773-3782.

[147] M. Umar, H.A. Aziz, Photocatalytic degradation of organic pollutants in water, Organic pollutants-monitoring, risk and treatment, 8 (2013) 196-197.

[148] O.Ö. Söğüt, M. Akgün, Treatment of dyehouse waste-water by supercritical water oxidation: a case study, Journal of Chemical Technology & Biotechnology, 85 (2010) 640-647.

[149] C. Jiang, S. Pang, F. Ouyang, J. Ma, J. Jiang, A new insight into Fenton and Fenton-like processes for water treatment, Journal of hazardous materials, 174 (2010) 813-817.

[150] J. Wang, H. Chen, Catalytic ozonation for water and wastewater treatment: recent advances and perspective, Science of the Total Environment, 704 (2020) 135249.

[151] Z. Zhang, Y. Xu, X. Ma, F. Li, D. Liu, Z. Chen, F. Zhang, D.D. Dionysiou, Microwave degradation of methyl orange dye in aqueous solution in the presence of nano-TiO2-supported activated carbon (supported-TiO_2/AC/MW), Journal of hazardous materials, 209 (2012) 271-277.

[152] L. Sanchez-Prado, R. Barro, C. Garcia-Jares, M. Llompart, M. Lores, C. Petrakis, N. Kalogerakis, D. Mantzavinos, E. Psillakis, Sonochemical degradation of triclosan in water and wastewater, Ultrasonics sonochemistry, 15 (2008) 689-694.

[153] L. Zhou, H. Cao, C. Descorme, Y. Xie, Phenolic compounds removal by wet air oxidation based processes, Frontiers of Environmental Science & Engineering, 12 (2018) 1-20.

[154] D. Koushik, S.S. Gupta, S.M. Maliyekkal, T. Pradeep, Rapid dehalogenation of pesticides and organics at the interface of reduced graphene oxide–silver nanocomposite, Journal of hazardous materials, 308 (2016) 192-198.

[155] K. Sahu, J. Singh, S. Mohapatra, Catalytic reduction of 4-nitrophenol and photocatalytic degradation of organic pollutants in water by copper oxide nanosheets, Optical Materials, 93 (2019) 58-69.

[156] J.T. Chacko, K. Subramaniam, Enzymatic degradation of azo dyes-a review, International Journal of Environmental Sciences, 1 (2011) 1250.

[157] A.H. Alneyadi, M.A. Rauf, S.S. Ashraf, Oxidoreductases for the remediation of organic pollutants in water–a critical review, Critical reviews in biotechnology, 38 (2018) 971-988.

[158] M. Alcalde, M. Ferrer, F.J. Plou, A. Ballesteros, Environmental biocatalysis: from remediation with enzymes to novel green processes, TRENDS in Biotechnology, 24 (2006) 281-287.

[159] T. Chiong, S.Y. Lau, Z.H. Lek, B.Y. Koh, M.K. Danquah, Enzymatic treatment of methyl orange dye in synthetic wastewater by plant-based peroxidase enzymes, Journal of environmental chemical engineering, 4 (2016) 2500-2509.

[160] L. Lonappan, Y. Liu, T. Rouissi, F. Pourcel, S.K. Brar, M. Verma, R.Y. Surampalli, Covalent immobilization of laccase on citric acid functionalized micro-biochars derived from different feedstock and removal of diclofenac, Chemical Engineering Journal, 351 (2018) 985-994.

[161] C. Barrios-Estrada, M. de Jesús Rostro-Alanis, A.L. Parra, M.-P. Belleville, J. Sanchez-Marcano, H.M.N. Iqbal, R. Parra-Saldívar, Potentialities of active membranes with immobilized laccase for Bisphenol A degradation, International journal of biological macromolecules, 108 (2018) 837-844.

[162] B.C. Kim, E. Jeong, E. Kim, S.W. Hong, Bio-organic–inorganic hybrid photocatalyst, TiO_2 and glucose oxidase composite for enhancing antibacterial performance in aqueous environments, Applied Catalysis B: Environmental, 242 (2019) 194-201.

[163] M. Naghdi, M. Taheran, S.K. Brar, A. Kermanshahi-Pour, M. Verma, R.Y. Surampalli, Removal of pharmaceutical compounds in water and wastewater using fungal oxidoreductase enzymes, Environmental pollution, 234 (2018) 190-213.

[164] L.Y. Jun, L.S. Yon, N.M. Mubarak, C.H. Bing, S. Pan, M.K. Danquah, E.C. Abdullah, M. Khalid, An overview of immobilized enzyme technologies for dye and phenolic removal from wastewater, Journal of Environmental Chemical Engineering, 7 (2019) 102961.

[165] H.J.H. Fenton, LXXIII.—Oxidation of tartaric acid in presence of iron, Journal of the Chemical Society, Transactions, 65 (1894) 899-910.

[166] R. Vasquez-Medrano, D. Prato-Garcia, M. Vedrenne, Ferrioxalate-Mediated Processes, in: Advanced Oxidation Processes for Waste Water Treatment, Elsevier, 2018, pp. 89-113.

[167] R. Andreozzi, V. Caprio, A. Insola, R. Marotta, Advanced oxidation processes (AOP) for water purification and recovery, Catalysis today, 53 (1999) 51-59.

[168] E. Neyens, J. Baeyens, A review of classic Fenton's peroxidation as an advanced oxidation technique, Journal of Hazardous materials, 98 (2003) 33-50.

[169] M. Kahoush, N. Behary, A. Cayla, V. Nierstrasz, Bio-Fenton and Bio-electro-Fenton as sustainable methods for degrading organic pollutants in wastewater, Process Biochemistry, 64 (2018) 237-247.

[170] R. Ameta, A.K. Chohadia, A. Jain, P.B. Punjabi, Fenton and photo-fenton processes, in: Advanced Oxidation Processes for Waste Water Treatment, Elsevier, 2018, pp. 49-87.

[171] R. Liu, H.M. Chiu, C.-S. Shiau, R.Y.-L. Yeh, Y.-T. Hung, Degradation and sludge production of textile dyes by Fenton and photo-Fenton processes, Dyes and Pigments, 73 (2007) 1-6.

[172] A. Morone, P. Mulay, S.P. Kamble, Removal of pharmaceutical and personal care products from wastewater using advanced materials, in: Pharmaceuticals and Personal Care Products: Waste Management and Treatment Technology, Elsevier, 2019, pp. 173-212.

[173] F.J. Rivas, F.J. Beltran, J. Frades, P. Buxeda, Oxidation of p-hydroxybenzoic acid by Fenton's reagent, Water research, 35 (2001) 387-396.

[174] B. Iurascu, I. Siminiceanu, D. Vione, M.A. Vicente, A. Gil, Phenol degradation in water through a heterogeneous photo-Fenton process catalyzed by Fe-treated laponite, Water research, 43 (2009) 1313-1322.

[175] W.Z. Tang, R.Z. Chen, Decolorization kinetics and mechanisms of commercial dyes by H2O2/iron powder system, Chemosphere, 32 (1996) 947-958.

[176] L. Xu, J. Wang, A heterogeneous Fenton-like system with nanoparticulate zero-valent iron for removal of 4-chloro-3-methyl phenol, Journal of hazardous materials, 186 (2011) 256-264.

[177] K. Choi, W. Lee, Enhanced degradation of trichloroethylene in nano-scale zero-valent iron Fenton system with Cu (II), Journal of Hazardous materials, 211 (2012) 146-153.

[178] M.I. Litter, M. Slodowicz, An overview on heterogeneous Fenton and photoFenton reactions using zerovalent iron materials, Journal of Advanced Oxidation Technologies, 20 (2017).

[179] A. Babuponnusami, K. Muthukumar, Removal of phenol by heterogenous photo electro Fenton-like process using nano-zero valent iron, Separation and Purification Technology, 98 (2012) 130-135.

[180] J. Prousek, E. Palacková, S. Priesolová, L. Marková, A. Alevová, Fenton-and Fenton-Like AOPs for Wastewater Treatment: From Laboratory-To-Plant-Scale Application, Separation Science and Technology, 42 (2007) 1505-1520.

[181] H. Barndõk, L. Blanco, D. Hermosilla, Á. Blanco, Heterogeneous photo-Fenton processes using zero valent iron microspheres for the treatment of wastewaters contaminated with 1, 4-dioxane, Chemical Engineering Journal, 284 (2016) 112-121.

[182] J.A. Bergendahl, T.P. Thies, Fenton's oxidation of MTBE with zero-valent iron, Water research, 38 (2004) 327-334.

[183] Q. Huang, X. Shi, R.A. Pinto, E.J. Petersen, W.J. Weber Jr, Tunable synthesis and immobilization of zero-valent iron nanoparticles for environmental applications, Environmental science & technology, 42 (2008) 8884-8889.

[184] S. Xiao, M. Shen, R. Guo, S. Wang, X. Shi, Immobilization of zerovalent iron nanoparticles into electrospun polymer nanofibers: synthesis, characterization, and potential environmental applications, The Journal of Physical Chemistry C, 113 (2009) 18062-18068.

[185] C.-H. Feng, F.-B. Li, H.-J. Mai, X.-Z. Li, Bio-electro-Fenton process driven by microbial fuel cell for wastewater treatment, Environmental science & technology, 44 (2010) 1875-1880.

[186] A.G.A. SÁ, A.C. de Meneses, P.H.H. de Araújo, D. de Oliveira, A review on enzymatic synthesis of aromatic esters used as flavor ingredients for food, cosmetics and pharmaceuticals industries, Trends in Food Science & Technology, 69 (2017) 95-105.

[187] A. Sassolas, L.J. Blum, B.D. Leca-Bouvier, Immobilization strategies to develop enzymatic biosensors, Biotechnology advances, 30 (2012) 489-511.

[188] R.A. Sheldon, Enzyme immobilization: the quest for optimum performance, Advanced Synthesis & Catalysis, 349 (2007) 1289-1307.

[189] Z. Temoçin, M. Inal, M. Gökgöz, M. Yiğitoğlu, Immobilization of horseradish peroxidase on electrospun poly (vinyl alcohol)–polyacrylamide blend nanofiber membrane and its use in the conversion of phenol, Polymer Bulletin, 75 (2018) 1843-1865.

[190] V. Aggarwal, C.S. Pundir, Rational design of nanoparticle platforms for "cutting-the-fat": Covalent immobilization of lipase, glycerol kinase, and glycerol-3-phosphate oxidase on metal nanoparticles, in: Methods in Enzymology, Elsevier, 2016, pp. 197-223.

[191] L. Cao, Immobilised enzymes: science or art?, Current opinion in chemical biology, 9 (2005) 217-226.

[192] M. Hu, Y. Liu, Z. Yao, L. Ma, X. Wang, Catalytic reduction for water treatment, Frontiers of Environmental Science & Engineering, 12 (2018) 1-18.

[193] N. Bouazizi, J. Vieillard, R. Bargougui, N. Couvrat, O. Thoumire, S. Morin, G. Ladam, N. Mofaddel, N. Brun, A. Azzouz, Entrapment and stabilization of iron nanoparticles within APTES modified graphene oxide sheets for catalytic activity improvement, Journal of Alloys and Compounds, 771 (2019) 1090-1102.

[194] N. Bouazizi, C. Campagne, J. Vieillard, A. Azzouz, Copper oxide coated polyester fabrics with enhanced catalytic properties towards the reduction of 4-nitrophenol, Journal of Materials Science: Materials in Electronics, 29 (2018) 10802-10813.

[195] M. Aazza, H. Ahlafi, H. Moussout, C. Mounir, A. Fadel, A. Addad, Catalytic reduction of nitro-phenolic compounds over Ag, Ni and Co nanoparticles catalysts supported on γ-Al_2O_3, Journal of Environmental Chemical Engineering, 8 (2020) 103707.

[196] P.M. Reddy, A.V.S.S. Prasad, R. Rohini, V. Ravinder, Catalytic reduction of pralidoxime in pharmaceuticals by macrocyclic Ni (II) compounds derived from orthophthalaldehyde, Spectrochimica Acta Part A: Molecular and Biomolecular Spectroscopy, 70 (2008) 704-712.

[197] L. Ge, M. Zhang, R. Wang, N. Li, L. Zhang, S. Liu, T. Jiao, Fabrication of CS/GA/RGO/Pd composite hydrogels for highly efficient catalytic reduction of organic pollutants, RSC Advances, 10 (2020) 15091-15097.

[198] M. Ismail, M.I. Khan, S.A. Khan, M. Qayum, M.A. Khan, Y. Anwar, K. Akhtar, A.M. Asiri, S.B. Khan, Green synthesis of antibacterial bimetallic Ag–Cu nanoparticles for catalytic reduction of persistent organic pollutants, Journal of Materials Science: Materials in Electronics, 29 (2018) 20840-20855.

[199] M.I. Din, R. Khalid, Z. Hussain, T. Hussain, A. Mujahid, J. Najeeb, F. Izhar, Nanocatalytic assemblies for catalytic reduction of nitrophenols: a critical review, Critical reviews in analytical chemistry, 50 (2020) 322-338.

[200] V.K. Gupta, N. Atar, M.L. Yola, Z. Üstündağ, L. Uzun, A novel magnetic Fe@ Au core–shell nanoparticles anchored graphene oxide recyclable nanocatalyst for the reduction of nitrophenol compounds, Water research, 48 (2014) 210-217.

[201] S.R. Thawarkar, B. Thombare, B.S. Munde, N.D. Khupse, Kinetic investigation for the catalytic reduction of nitrophenol using ionic liquid stabilized gold nanoparticles, RSC advances, 8 (2018) 38384-38390.

[202] B. Liu, S. Yan, A. Zhang, Z. Song, Q. Sun, B. Huo, W. Yang, C.J. Barrow, J. Liu, Insight into catalytic mechanisms for the reduction of nitrophenol via heterojunctions of gold nanoclusters on 2D boron nitride nanosheets, ChemNanoMat, 5 (2019) 784-791.

[203] S. Shoabargh, A. Karimi, G. Dehghan, A. Khataee, A hybrid photocatalytic and enzymatic process using glucose oxidase immobilized on TiO$_2$/polyurethane for removal of a dye, Journal of Industrial and Engineering Chemistry, 20 (2014) 3150-3156.

[204] P. Abdi, A. Farzi, A. Karimi, Application of a hybrid enzymatic and photo-fenton process for investigation of azo dye decolorization on TiO$_2$/metal-foam catalyst, Journal of the Taiwan Institute of Chemical Engineers, 71 (2017) 137-144.

[205] Q. Chen, F. Ji, T. Liu, P. Yan, W. Guan, X. Xu, Synergistic effect of bifunctional Co–TiO$_2$ catalyst on degradation of Rhodamine B: Fenton-photo hybrid process, Chemical engineering journal, 229 (2013) 57-65.

[206] S. Mozia, A.W. Morawski, M. Toyoda, T. Tsumura, Effect of process parameters on photodegradation of Acid Yellow 36 in a hybrid photocatalysis–membrane distillation system, Chemical Engineering Journal, 150 (2009) 152-159.

[207] J. Zhang, L. Wang, G. Zhang, Z. Wang, L. Xu, Z. Fan, Influence of azo dye-TiO$_2$ interactions on the filtration performance in a hybrid photocatalysis/ultrafiltration process, Journal of colloid and interface science, 389 (2013) 273-283.

[208] S. Zhong, Y. Xi, S. Wu, Q. Liu, L. Zhao, S. Bai, Hybrid cocatalysts in semiconductor-based photocatalysis and photoelectrocatalysis, Journal of Materials Chemistry A, 8 (2020) 14863-14894.

[209] K. Kabra, R. Chaudhary, R.L. Sawhney, Treatment of hazardous organic and inorganic compounds through aqueous-phase photocatalysis: a review, Industrial & engineering chemistry research, 43 (2004) 7683-7696.

[210] J.Y. Huh, J. Lee, S.Z.A. Bukhari, J.-H. Ha, I.-H. Song, Development of TiO$_2$-coated YSZ/silica nanofiber membranes with excellent photocatalytic degradation ability for water purification, Scientific reports, 10 (2020) 1-12.

[211] X. Liu, R. Tang, Q. He, X. Liao, B. Shi, Fe (III)-loaded collagen fiber as a heterogeneous catalyst for the photo-assisted decomposition of Malachite Green, Journal of hazardous materials, 174 (2010) 687-693.

[212] M. Dehghani, H. Nadeem, V. Singh Raghuwanshi, H. Mahdavi, M.M. Banaszak Holl, W. Batchelor, ZnO/cellulose nanofiber composites for sustainable sunlight-driven dye degradation, ACS Applied Nano Materials, 3 (2020) 10284-10295.

[213] M. Hua, S. Zhang, B. Pan, W. Zhang, L. Lv, Q. Zhang, Heavy metal removal from water/wastewater by nanosized metal oxides: a review, Journal of hazardous materials, 211 (2012) 317-331.

[214] M. Mondal, M. Dutta, S. De, A novel ultrafiltration grade nickel iron oxide doped hollow fiber mixed matrix membrane: spinning, characterization and application in heavy metal removal, Separation and Purification Technology, 188 (2017) 155-166.

[215] S. Xiao, H. Ma, M. Shen, S. Wang, Q. Huang, X. Shi, Excellent copper (II) removal using zero-valent iron nanoparticle-immobilized hybrid electrospun polymer nanofibrous mats, Colloids and Surfaces A: Physicochemical and Engineering Aspects, 381 (2011) 48-54.

[216] B. Barrocas, T.J. Entradas, C.D. Nunes, O.C. Monteiro, Titanate nanofibers sensitized with ZnS and Ag2S nanoparticles as novel photocatalysts for phenol removal, Applied Catalysis B: Environmental, 218 (2017) 709-720.

[217] Y. Wang, H. Tian, Y. Yu, C. Hu, Enhanced catalytic activity of α-FeOOH-rGO supported on active carbon fiber (ACF) for degradation of phenol and quinolone in the solar-Fenton system, Chemosphere, 208 (2018) 931-941.

[218] S. Fakhravar, M. Farhadian, S. Tangestaninejad, Excellent performance of a novel dual Z-scheme Cu2S/Ag2S/BiVO4 heterostructure in metronidazole degradation in batch and continuous systems: immobilization of catalytic particles on α-Al2O3 fiber, Applied surface science, 505 (2020) 144599.

[219] H. Karimnezhad, A.H. Navarchian, T.T. Gheinani, S. Zinadini, Amoxicillin removal by Fe-based nanoparticles immobilized on polyacrylonitrile membrane: Effects of input parameters and optimization by response surface methodology, Chemical Engineering and Processing-Process Intensification, 147 (2020) 107785.

[220] Y. Wang, Y. Fang, W. Lu, N. Li, W. Chen, Oxidative removal of sulfa antibiotics by introduction of activated carbon fiber to enhance the catalytic activity of iron phthalocyanine, Microporous and Mesoporous Materials, 261 (2018) 98-104.

[221] L. Paredes, S. Murgolo, H. Dzinun, M.H.D. Othman, A.F. Ismail, M. Carballa, G. Mascolo, Application of immobilized TiO2 on PVDF dual layer hollow fibre membrane to improve the photocatalytic removal of pharmaceuticals in different water matrices, Applied Catalysis B: Environmental, 240 (2019) 9-18.

[222] M.J. Soberman, R.R. Farnood, S. Tabe, Functionalized powdered activated carbon electrospun nanofiber membranes for adsorption of micropollutants, Separation and Purification Technology, 253 (2020) 117461.

[223] L. Yuan, Z.R. Tang, Y.J. Xu, Photocatalytic Abatement of Emerging Micropollutants in Water and Wastewater, Heterogeneous Catalysts: Advanced Design, Characterization and Applications, 2 (2021) 671-684.

[224] F. Ali, S.B. Khan, T. Kamal, Y. Anwar, K.A. Alamry, A.M. Asiri, Bactericidal and catalytic performance of green nanocomposite based-on chitosan/carbon black fiber supported monometallic and bimetallic nanoparticles, Chemosphere, 188 (2017) 588-598.

[225] F. Ali, S.B. Khan, T. Kamal, Y. Anwar, K.A. Alamry, A.M. Asiri, Anti-bacterial chitosan/zinc phthalocyanine fibers supported metallic and bimetallic nanoparticles for the removal of organic pollutants, Carbohydrate polymers, 173 (2017) 676-689.

[226] H. Deb, M.N. Morshed, S. Xiao, S. Al Azad, Z. Cai, A. Ahmed, Design and development of TiO_2-Fe^0 nanoparticle-immobilized nanofibrous mat for photocatalytic degradation of hazardous water pollutants, Journal of Materials Science: Materials in Electronics, 30 (2019) 4842-4854.

[227] B.K. Nandi, A. Goswami, M.K. Purkait, Adsorption characteristics of brilliant green dye on kaolin, Journal of hazardous materials, 161 (2009) 387-395.

[228] M. Taheran, M. Naghdi, S.K. Brar, E.J. Knystautas, M. Verma, R.Y. Surampalli, Covalent immobilization of laccase onto nanofibrous membrane for degradation of pharmaceutical residues in water, ACS Sustainable Chemistry & Engineering, 5 (2017) 10430-10438.

[229] R. Xu, J. Cui, R. Tang, F. Li, B. Zhang, Removal of 2, 4, 6-trichlorophenol by laccase immobilized on nano-copper incorporated electrospun fibrous membrane-high efficiency, stability and reusability, Chemical Engineering Journal, 326 (2017) 647-655.

[230] R. Xu, Y. Si, X. Wu, F. Li, B. Zhang, Triclosan removal by laccase immobilized on mesoporous nanofibers: strong adsorption and efficient degradation, Chemical Engineering Journal, 255 (2014) 63-70.

[231] Q. Wang, J. Cui, G. Li, J. Zhang, D. Li, F. Huang, Q. Wei, Laccase immobilized on a PAN/adsorbents composite nanofibrous membrane for catechol treatment by a biocatalysis/adsorption process, Molecules, 19 (2014) 3376-3388.

[232] M. Taheran, M. Naghdi, S.K. Brar, E.J. Knystautas, M. Verma, R.Y. Surampalli, Degradation of chlortetracycline using immobilized laccase on Polyacrylonitrile-biochar composite nanofibrous membrane, Science of The Total Environment, 605 (2017) 315-321.

[233] J. Zdarta, K. Jankowska, M. Wyszowska, E. Kijeńska-Gawrońska, A. Zgoła-Grześkowiak, M. Pinelo, A.S. Meyer, D. Moszyński, T. Jesionowski, Robust biodegradation of naproxen and diclofenac by laccase immobilized using electrospun nanofibers with enhanced stability and reusability, Materials Science and Engineering: C, 103 (2019) 109789.

[234] R. Xu, Y. Si, F. Li, B. Zhang, Enzymatic removal of paracetamol from aqueous phase: horseradish peroxidase immobilized on nanofibrous membranes, Environmental Science and Pollution Research, 22 (2015) 3838-3846.

[235] R.O. Cristóvão, A.P.M. Tavares, A.I. Brígida, J.M. Loureiro, R.A.R. Boaventura, E.A. Macedo, M.A.Z. Coelho, Immobilization of commercial laccase onto green coconut fiber by adsorption and its application for reactive textile dyes degradation, Journal of Molecular Catalysis B: Enzymatic, 72 (2011) 6-12.

[236] M. Arslan, Immobilization horseradish peroxidase on amine-functionalized glycidyl methacrylate-g-poly (ethylene terephthalate) fibers for use in azo dye decolorization, Polymer bulletin, 66 (2011) 865-879.

[237] R. Xu, C. Chi, F. Li, B. Zhang, Laccase–polyacrylonitrile nanofibrous membrane: highly immobilized, stable, reusable, and efficacious for 2, 4, 6-trichlorophenol removal, ACS applied materials & interfaces, 5 (2013) 12554-12560.

[238] Y. Dai, J. Yao, Y. Song, S. Wang, Y. Yuan, Enhanced adsorption and degradation of phenolic pollutants in water by carbon nanotube modified laccase-carrying electrospun fibrous membranes, Environmental Science: Nano, 3 (2016) 857-868.

[239] J. Zdarta, M. Staszak, K. Jankowska, K. Kaźmierczak, O. Degórska, L.N. Nguyen, E. Kijeńska-Gawrońska, M. Pinelo, T. Jesionowski, The response surface methodology for optimization of tyrosinase immobilization onto electrospun polycaprolactone–chitosan fibers for use in bisphenol A removal, International Journal of Biological Macromolecules, 165 (2020) 2049-2059.

[240] P.A. Frey, G.H. Reed, The ubiquity of iron, in, ACS Publications, 2012.

[241] W. Xiang, B. Zhang, T. Zhou, X. Wu, J. Mao, An insight in magnetic field enhanced zero-valent iron/H_2O_2 Fenton-like systems: Critical role and evolution of the pristine iron oxides layer, Scientific reports, 6 (2016) 1-11.

[242] C.-B. Wang, W.-x. Zhang, Synthesizing nanoscale iron particles for rapid and complete dechlorination of TCE and PCBs, Environmental science & technology, 31 (1997) 2154-2156.

[243] J.T. Nurmi, P.G. Tratnyek, V. Sarathy, D.R. Baer, J.E. Amonette, K. Pecher, C. Wang, J.C. Linehan, D.W. Matson, R.L. Penn, Characterization and properties of metallic iron nanoparticles: spectroscopy, electrochemistry, and kinetics, Environmental science & technology, 39 (2005) 1221-1230.

[244] Y. Zhang, Y. Su, X. Zhou, C. Dai, A.A. Keller, A new insight on the core–shell structure of zerovalent iron nanoparticles and its application for Pb (II) sequestration, Journal of Hazardous Materials, 263 (2013) 685-693.

[245] Y. Mu, F. Jia, Z. Ai, L. Zhang, Iron oxide shell mediated environmental remediation properties of nano zero-valent iron, Environmental Science: Nano, 4 (2017) 27-45.

[246] M. Minella, E. Sappa, K. Hanna, F. Barsotti, V. Maurino, C. Minero, D. Vione, Considerable Fenton and photo-Fenton reactivity of passivated zero-valent iron, Rsc Advances, 6 (2016) 86752-86761.

[247] X.-q. Li, D.W. Elliott, W.-x. Zhang, Zero-valent iron nanoparticles for abatement of environmental pollutants: materials and engineering aspects, Critical reviews in solid state and materials sciences, 31 (2006) 111-122.

[248] J.E. Martin, A.A. Herzing, W. Yan, X.-q. Li, B.E. Koel, C.J. Kiely, W.-x. Zhang, Determination of the oxide layer thickness in core– shell zerovalent iron nanoparticles, Langmuir, 24 (2008) 4329-4334.

[249] Y. Wu, C.-Y. Guan, N. Griswold, L.-y. Hou, X. Fang, A. Hu, Z.-q. Hu, C.-P. Yu, Zero-valent iron-based technologies for removal of heavy metal (loid) s and organic pollutants from the aquatic environment: Recent advances and perspectives, Journal of Cleaner Production, (2020) 123478.

[250] C.M. Wong, K.H. Wong, X.D. Chen, Glucose oxidase: natural occurrence, function, properties and industrial applications, Applied microbiology and biotechnology, 78 (2008) 927-938.

[251] S.V. Bhat, B.R. Swathi, M. Rosy, M. Govindappa, Isolation and charecterization of glucose oxidase (GOD) from Aspergillus flavus and Penicillium sp, International Journal of Current Microbiology and Applied Sciences, 2 (2013) 153-161.

[252] T. Tu, Y. Wang, H. Huang, Y. Wang, X. Jiang, Z. Wang, B. Yao, H. Luo, Improving the thermostability and catalytic efficiency of glucose oxidase from Aspergillus niger by molecular evolution, Food chemistry, 281 (2019) 163-170.

[253] R. Wilson, A.P.F. Turner, Glucose oxidase: an ideal enzyme, Biosensors and Bioelectronics, 7 (1992) 165-185.

[254] S.B. Bankar, M.V. Bule, R.S. Singhal, L. Ananthanarayan, Glucose oxidase—an overview, Biotechnology advances, 27 (2009) 489-501.

[255] J.D. Newman, A.P.F. Turner, Home blood glucose biosensors: a commercial perspective, Biosensors and bioelectronics, 20 (2005) 2435-2453.

[256] Y. Liu, M. Wang, F. Zhao, Z. Xu, S. Dong, The direct electron transfer of glucose oxidase and glucose biosensor based on carbon nanotubes/chitosan matrix, Biosensors and Bioelectronics, 21 (2005) 984-988.

[257] C. Chen, Q. Xie, D. Yang, H. Xiao, Y. Fu, Y. Tan, S. Yao, Recent advances in electrochemical glucose biosensors: a review, Rsc Advances, 3 (2013) 4473-4491.

[258] A.S. Meyer, A. Isaksen, Application of enzymes as food antioxidants, Trends in Food Science & Technology, 6 (1995) 300-304.

[259] Y. Wang, Y. Wang, H. Xu, X. Mei, L. Gong, B. Wang, W. Li, S. Jiang, Direct-fed glucose oxidase and its combination with B. amyloliquefaciens SC06 on growth performance, meat quality, intestinal barrier, antioxidative status, and immunity of yellow-feathered broilers, Poultry science, 97 (2018) 3540-3549.

[260] M. Tiina, M. Sandholm, Antibacterial effect of the glucose oxidase-glucose system on food-poisoning organisms, International Journal of Food Microbiology, 8 (1989) 165-174.

[261] M. Jaffe, A.J. Easts, X. Feng, Polyester fibers, in: Thermal Analysis of Textiles and Fibers, Elsevier, 2020, pp. 133-149.

[262] L. Zhang, H. Li, X. Lai, T. Gao, J. Yang, X. Zeng, Thiolated graphene@ polyester fabric-based multilayer piezoresistive pressure sensors for detecting human motion, ACS applied materials & interfaces, 10 (2018) 41784-41792.

[263] X. Ren, H.B. Kocer, L. Kou, S.D. Worley, R.M. Broughton, Y.M. Tzou, T.S. Huang, Antimicrobial polyester, Journal of applied polymer science, 109 (2008) 2756-2761.

[264] S. Kovačević, D. Ujević, Seams in car seat coverings: properties and performance, in: Joining Textiles, Elsevier, 2013, pp. 478-506.

[265] A. Pourmohammadi, Nonwoven materials and joining techniques, in: Joining Textiles, Elsevier, 2013, pp. 565-581.

[266] R.H. Gong, Developments in 3D nonwovens, in: Advances in 3D Textiles, Elsevier, 2015, pp. 183-203.

[267] P.A. Smith, Technical fabric structures–3. Nonwoven fabrics, Handbook of technical textiles, 12 (2000) 130.

[268] W. Albrecht, H. Fuchs, W. Kittelmann, Nonwoven fabrics: raw materials, manufacture, applications, characteristics, testing processes, John Wiley & Sons, 2006.

[269] J. Oldrich, C.W. Larry, Non-woven Textiles, in, Carolina Academic Press, Durham, North Carolina, USA, 1999.

[270] R. Krčma, Manual of nonwovens, Textile Trade Press, 1971.

[271] S.J. Russell, Handbook of nonwovens, Woodhead Publishing, 2006.

[272] A. Turbak, T. Vigo, Nonwovens: an advanced tutorial, na, 1989.

[273] T. Karthik, R. Rathinamoorthy, Nonwovens: process, structure, properties and applications, WPI Publishing, 2017.

[274] N.M. Coutinho, M.R. Silveira, L.M. Fernandes, J. Moraes, T.C. Pimentel, M.Q. Freitas, M.C. Silva, R.S.L. Raices, C.S. Ranadheera, F.O. Borges, Processing chocolate milk drink by low-pressure cold plasma technology, Food chemistry, 278 (2019) 276-283.

[275] S.K. Pankaj, K.M. Keener, Cold plasma: Background, applications and current trends, Current Opinion in Food Science, 16 (2017) 49-52.

[276] A.C. Perinotto, L. Caseli, C.O. Hayasaka, A. Riul Jr, O.N. Oliveira Jr, V. Zucolotto, Dendrimer-assisted immobilization of alcohol dehydrogenase in nanostructured films for biosensing: Ethanol detection using electrical capacitance measurements, Thin Solid Films, 516 (2008) 9002-9005.

[277] L. Xu, Y. Zhu, L. Tang, X. Yang, C. Li, Biosensor Based on Self-Assembling Glucose Oxidase and Dendrimer-Encapsulated Pt Nanoparticles on Carbon Nanotubes for Glucose Detection, Electroanalysis: An International Journal Devoted to Fundamental and Practical Aspects of Electroanalysis, 19 (2007) 717-722.

[278] S. Wang, P. Su, E. Hongjun, Y. Yang, Polyamidoamine dendrimer as a spacer for the immobilization of glucose oxidase in capillary enzyme microreactor, Analytical biochemistry, 405 (2010) 230-235.

[279] L. Svobodova, M. Šnejdárková, T. Hianik, Properties of glucose biosensors based on dendrimer layers. Effect of enzyme immobilization, Analytical and bioanalytical chemistry, 373 (2002) 735-741.

[280] D. Wan, C. Yan, Y. Liu, K. Zhu, Q. Zhang, A novel mesoporous nanocarrier: Integrating hollow magnetic fibrous silica with PAMAM into a single nanocomposite for enzyme immobilization, Microporous and Mesoporous Materials, 280 (2019) 46-56.

[281] J. Jiang, Y. Yu, L. Wang, J. Li, J. Ling, Y. Li, G. Duan, Enzyme immobilized on polyamidoamine-coated magnetic microspheres for α-glucosidase inhibitors screening from Radix Paeoniae Rubra extracts accompanied with molecular modeling, Talanta, 195 (2019) 127-136.

[282] M.N. Morshed, N. Bouazizi, N. Behary, J. Guan, V. Nierstrasz, Stabilization of zero valent iron (Fe^0) on plasma/dendrimer functionalized polyester fabrics for Fenton-like removal of hazardous water pollutant, Chemical Engineering Journal, (2019).

[283] F. Leroux, A. Perwuelz, C. Campagne, N. Behary, Atmospheric air-plasma treatments of polyester textile structures, Journal of adhesion science and technology, 20 (2006) 939-957.

[284] D. Ning, H. Zhang, J. Zheng, Electrochemical sensor for sensitive determination of nitrite based on the PAMAM dendrimer-stabilized silver nanoparticles, Journal of Electroanalytical Chemistry, 717 (2014) 29-33.

[285] R. Esfand, D.A. Tomalia, Poly (amidoamine)(PAMAM) dendrimers: from biomimicry to drug delivery and biomedical applications, Drug discovery today, 6 (2001) 427-436.

[286] B. Nabil, N.M. Mohammad, N. Behary, C. Christine, V. Julien, O. Thoumire, A. Abdelkrim, Development of New Multifunctional Filter Based Nonwovens for Organics Pollutants Reduction and Detoxification: High Catalytic and Antibacterial activities, Chemical Engineering Journal, (2018).

[287] M.N.V.R. Kumar, A review of chitin and chitosan applications, Reactive and functional polymers, 46 (2000) 1-27.

[288] G. Höhne, W.F. Hemminger, H.J. Flammersheim, Differential scanning calorimetry, Springer Science & Business Media, 2013.

[289] H. Deb, S. Xiao, M.N. Morshed, S. Al Azad, Immobilization of Cationic Titanium Dioxide (TiO$_2^+$) on Electrospun Nanofibrous Mat: Synthesis, Characterization, and Potential Environmental Application, Fibers and Polymers, 19 (2018) 1715-1725.

[290] B. Nabil, M.N. Morshed, B. Nemeshwaree, C. Christine, V. Julien, T. Olivier, A. Abdelkrim, Development of new multifunctional filter based nonwovens for organics pollutants reduction and detoxification: High catalytic and antibacterial activities, Chemical Engineering Journal, 356 (2019) 702-716.

[291] Z. Hai, N. El Kolli, D.B. Uribe, P. Beaunier, M. José-Yacaman, J. Vigneron, A. Etcheberry, S. Sorgues, C. Colbeau-Justin, J. Chen, Modification of TiO 2 by bimetallic Au–Cu nanoparticles for wastewater treatment, Journal of Materials Chemistry A, 1 (2013) 10829-10835.

[292] R. Yamaguchi, S. Kurosu, M. Suzuki, Y. Kawase, Hydroxyl radical generation by zero-valent iron/Cu (ZVI/Cu) bimetallic catalyst in wastewater treatment: Heterogeneous Fenton/Fenton-like reactions by Fenton reagents formed in-situ under oxic conditions, Chemical Engineering Journal, 334 (2018) 1537-1549.

[293] W. Xue, D. Huang, G. Zeng, J. Wan, M. Cheng, C. Zhang, C. Hu, J. Li, Performance and toxicity assessment of nanoscale zero valent iron particles in the remediation of contaminated soil: a review, Chemosphere, 210 (2018) 1145-1156.

[294] G. Vilardi, L. Di Palma, N. Verdone, On the critical use of zero valent iron nanoparticles and Fenton processes for the treatment of tannery wastewater, Journal of Water Process Engineering, 22 (2018) 109-122.

[295] M. Raji, S.A. Mirbagheri, F. Ye, J. Dutta, Nano zero-valent iron on activated carbon cloth support as Fenton-like catalyst for efficient color and COD removal from melanoidin wastewater, Chemosphere, 263 (2021) 127945.

[296] V. Takke, N. Behary, A. Perwuelz, C. Campagne, Studies on the atmospheric air–plasma treatment of PET (polyethylene terephtalate) woven fabrics: effect of process parameters and of aging, Journal of applied polymer science, 114 (2009) 348-357.

[297] T. Saito, K. Matsushige, K. Tanaka, Chemical treatment and modification of multi-walled carbon nanotubes, Physica B: Condensed Matter, 323 (2002) 280-283.

[298] J. Coates, Interpretation of infrared spectra, a practical approach, Encyclopedia of analytical chemistry: applications, theory and instrumentation, (2006).

[299] M. Tammer, G. Sokrates: Infrared and Raman characteristic group frequencies: tables and charts, in, Springer, 2004.

[300] J. Sun, L. Yao, Z. Gao, S. Peng, C. Wang, Y. Qiu, Surface modification of PET films by atmospheric pressure plasma-induced acrylic acid inverse emulsion graft polymerization, Surface and Coatings Technology, 204 (2010) 4101-4106.

[301] Z. Fang, X. Wang, R. Shao, Y. Qiu, K. Edmund, The effect of discharge power density on polyethylene terephthalate film surface modification by dielectric barrier discharge in atmospheric air, Journal of Electrostatics, 69 (2011) 60-66.

[302] H. Dave, L. Ledwani, N. Chandwani, P. Kikani, B. Desai, S.K. Nema, Surface modification of polyester fabric by non-thermal plasma treatment and its effect on coloration using natural dye, Journal of Polymer Materials, 30 (2013) 291-304.

[303] B. Chieng, N. Ibrahim, W. Yunus, M. Hussein, Poly (lactic acid)/poly (ethylene glycol) polymer nanocomposites: effects of graphene nanoplatelets, Polymers, 6 (2014) 93-104.

[304] W. Yan, A.A. Herzing, C.J. Kiely, W.-x. Zhang, Nanoscale zero-valent iron (nZVI): aspects of the core-shell structure and reactions with inorganic species in water, Journal of Contaminant Hydrology, 118 (2010) 96-104.

[305] V.S. Myers, M.G. Weir, E.V. Carino, D.F. Yancey, S. Pande, R.M. Crooks, Dendrimer-encapsulated nanoparticles: new synthetic and characterization methods and catalytic applications, Chemical Science, 2 (2011) 1632-1646.

[306] Y.-P. Sun, X.-q. Li, J. Cao, W.-x. Zhang, H.P. Wang, Characterization of zero-valent iron nanoparticles, Advances in colloid and interface science, 120 (2006) 47-56.

[307] Y. Wu, S. Zeng, F. Wang, M. Megharaj, R. Naidu, Z. Chen, Heterogeneous Fenton-like oxidation of malachite green by iron-based nanoparticles synthesized by tea extract as a catalyst, Separation and Purification technology, 154 (2015) 161-167.

[308] L.B. Vilhelmsen, K.S. Walton, D.S. Sholl, Structure and mobility of metal clusters in MOFs: Au, Pd, and AuPd clusters in MOF-74, Journal of the American Chemical Society, 134 (2012) 12807-12816.

[309] A.K. Srivastav, D. Roy, Acute toxicity of malachite green (Triarylmethane dye) and pyceze (Bronopol) on carbohydrate metabolism in the freshwater fish Heteropneustes fossilis (Bloch.), (2018).

[310] N. Bouazizi, J. Vieillard, R. Bargougui, N. Couvrat, O. Thoumire, S. Morin, G. Ladam, N. Mofaddel, N. Brun, A. Azzouz, Entrapment and stability of iron nanoparticles within APTES modified graphene oxide sheets with improved catalytic activity, Journal of Alloys and Compounds, (2018).

[311] J. Deng, H. Dong, C. Zhang, Z. Jiang, Y. Cheng, K. Hou, L. Zhang, C. Fan, Nanoscale zero-valent iron/biochar composite as an activator for Fenton-like removal of sulfamethazine, Separation and Purification Technology, 202 (2018) 130-137.

[312] H.-J. Kim, T. Phenrat, R.D. Tilton, G.V. Lowry, Fe^0 nanoparticles remain mobile in porous media after aging due to slow desorption of polymeric surface modifiers, Environmental science & technology, 43 (2009) 3824-3830.

[313] Y. Zhou, B. Gao, A.R. Zimmerman, H. Chen, M. Zhang, X. Cao, Biochar-supported zerovalent iron for removal of various contaminants from aqueous solutions, Bioresource technology, 152 (2014) 538-542.

[314] S.K. Ghosh, M. Mandal, S. Kundu, S. Nath, T. Pal, Bimetallic Pt–Ni nanoparticles can catalyze reduction of aromatic nitro compounds by sodium borohydride in aqueous solution, Applied Catalysis A: General, 268 (2004) 61-66.

[315] S. Xiao, X. Luo, Q. Peng, H. Deb, Effective removal of calcium ions from simulated hard water using electrospun polyelectrolyte nanofibrous mats, Fibers and Polymers, 17 (2016) 1428-1437.

[316] R.G. Zepp, B.C. Faust, J. Hoigne, Hydroxyl radical formation in aqueous reactions (pH 3-8) of iron (II) with hydrogen peroxide: the photo-Fenton reaction, Environmental Science & Technology, 26 (1992) 313-319.

[317] M. Turabik, U.B. Simsek, Effect of synthesis parameters on the particle size of the zero valent iron particles, Inorganic and nano-metal chemistry, 47 (2017) 1033-1043.

[318] C. Riccardi, R. Barni, E. Selli, G. Mazzone, M.R. Massafra, B. Marcandalli, G. Poletti, Surface modification of poly (ethylene terephthalate) fibers induced by radio frequency air plasma treatment, Applied surface science, 211 (2003) 386-397.

[319] M.R. Sanchis, V. Blanes, M. Blanes, D. Garcia, R. Balart, Surface modification of low density polyethylene (LDPE) film by low pressure O2 plasma treatment, European Polymer Journal, 42 (2006) 1558-1568.

[320] V. Takke, N. Behary, A. Perwuelz, C. Campagne, Surface and adhesion properties of poly (ethylene glycol) on polyester (polyethylene terephthalate) fabric surface: Effect of air-atmospheric plasma treatment, Journal of Applied Polymer Science, 122 (2011) 2621-2629.

[321] R. Mukherjee, R. Kumar, A. Sinha, Y. Lama, A.K. Saha, A review on synthesis, characterization, and applications of nano zero valent iron (nZVI) for environmental remediation, Critical reviews in environmental science and technology, 46 (2016) 443-466.

[322] H.-L. Lien, W.-x. Zhang, Nanoscale iron particles for complete reduction of chlorinated ethenes, Colloids and Surfaces A: Physicochemical and Engineering Aspects, 191 (2001) 97-105.

[323] J. Rowley, N.H. Abu-Zahra, Synthesis and characterization of polyethersulfone membranes impregnated with (3-aminopropyltriethoxysilane) APTES-Fe$_3$O$_4$ nanoparticles for As (V) removal from water, Journal of Environmental Chemical Engineering, 7 (2019) 102875.

[324] R. Zanella, E.V. Basiuk, P. Santiago, V.A. Basiuk, E. Mireles, I. Puente-Lee, J.M. Saniger, Deposition of gold nanoparticles onto thiol-functionalized multiwalled carbon nanotubes, The Journal of Physical Chemistry B, 109 (2005) 16290-16295.

[325] M.-A. Neouze, U. Schubert, Surface modification and functionalization of metal and metal oxide nanoparticles by organic ligands, Monatshefte für Chemie-Chemical Monthly, 139 (2008) 183-195.

[326] C.L. Mazzitelli, J.S. Brodbelt, Investigation of silver binding to polyamidoamine (PAMAM) dendrimers by ESI tandem mass spectrometry, Journal of the American Society for Mass Spectrometry, 17 (2006) 676-684.

[327] R.M. Crooks, B.I. Lemon, L. Sun, L.K. Yeung, M. Zhao, Dendrimer-encapsulated metals and semiconductors: synthesis, characterization, and applications, Dendrimers III, (2001) 81-135.

[328] H.N. Patel, P.M. Patel, Dendrimer applications—A review, Int J Pharm Bio Sci, 4 (2013) 454-463.

[329] V.P. Kothavale, V.D. Chavan, S.C. Sahoo, P. Kollu, T.D. Dongale, P.S. Patil, P.B. Patil, Removal of Cu (II) from aqueous solution using APTES-GA modified magnetic iron oxide nanoparticles: kinetic and isotherm study, Materials Research Express, 6 (2019) 106103.

[330] S. Tiwari, M. Sharma, S. Panier, B. Mutel, P. Mitschang, J. Bijwe, Influence of cold remote nitrogen oxygen plasma treatment on carbon fabric and its composites with specialty polymers, Journal of Materials Science, 46 (2011) 964-974.

[331] D. Shao, Q. Wei, Microwave-Assisted Rapid Preparation of Nano-ZnO/Ag Composite Functionalized Polyester Nonwoven Membrane for Improving Its UV Shielding and Antibacterial Properties, Materials, 11 (2018) 1412.

[332] X. Wang, Y. Gao, W. Wang, A. Qin, J.Z. Sun, B.Z. Tang, Different amine-functionalized poly (diphenylsubstituted acetylenes) from the same precursor, Polymer Chemistry, 7 (2016) 5312-5321.

[333] A. Singh, A. Guleria, A. Kunwar, S. Neogy, M.C. Rath, Highly facile and rapid one-pot synthetic protocol for the formation of Se nanoparticles at ambient conditions with controlled phase and morphology: role of starch and cytotoxic studies, Materials Research Express, 6 (2018) 015029.

[334] J. Wei, M.S. Saharudin, T. Vo, F. Inam, N, N-Dimethylformamide (DMF) usage in epoxy/graphene nanocomposites: problems associated with reaggregation, Polymers, 9 (2017) 193.

[335] W. Liu, Q. Yang, Z. Yang, W. Wang, Adsorption of 2, 4-D on magnetic graphene and mechanism study, Colloids and Surfaces A: Physicochemical and Engineering Aspects, 509 (2016) 367-375.

[336] Z. Hasan, N.A. Khan, S.H. Jhung, Adsorptive removal of diclofenac sodium from water with Zr-based metal–organic frameworks, Chemical Engineering Journal, 284 (2016) 1406-1413.

[337] M. Kahoush, N. Behary, A. Cayla, B. Mutel, J. Guan, V. Nierstrasz, Surface modification of carbon felt by cold remote plasma for glucose oxidase enzyme immobilization, Applied Surface Science, (2019).

[338] X. Ye, X. Qin, X. Yan, J. Guo, L. Huang, D. Chen, T. Wu, Q. Shi, S. Tan, X. Cai, π–π conjugations improve the long-term antibacterial properties of graphene oxide/quaternary ammonium salt nanocomposites, Chemical Engineering Journal, 304 (2016) 873-881.

[339] K. Matsuyama, M. Motomura, T. Kato, T. Okuyama, H. Muto, Catalytically active Pt nanoparticles immobilized inside the pores of metal organic framework using supercritical CO$_2$ solutions, Microporous and Mesoporous Materials, 225 (2016) 26-32.

[340] N. Horzum, M.M. Demir, M. Nairat, T. Shahwan, Chitosan fiber-supported zero-valent iron nanoparticles as a novel sorbent for sequestration of inorganic arsenic, RSC Advances, 3 (2013) 7828-7837.

[341] H. Yan, H. Wu, K. Li, Y. Wang, X. Tao, H. Yang, A. Li, R. Cheng, Influence of the surface structure of graphene oxide on the adsorption of aromatic organic compounds from water, ACS applied materials & interfaces, 7 (2015) 6690-6697.

[342] A. Mittal, J. Mittal, A. Malviya, D. Kaur, V.K. Gupta, Adsorption of hazardous dye crystal violet from wastewater by waste materials, Journal of Colloid and Interface Science, 343 (2010) 463-473.

[343] M. Li, Q. Gao, T. Wang, Y.-S. Gong, B. Han, K.-S. Xia, C.-G. Zhou, Solvothermal synthesis of MnxFe$_3$– xO$_4$ nanoparticles with interesting physicochemical characteristics and good catalytic degradation activity, Materials & Design, 97 (2016) 341-348.

[344] R.E. Palma-Goyes, F.L. Guzmán-Duque, G. Peñuela, I. González, J.L. Nava, R.A. Torres-Palma, Electrochemical degradation of crystal violet with BDD electrodes: Effect of electrochemical parameters and identification of organic by-products, Chemosphere, 81 (2010) 26-32.

[345] H. Zhang, J. Wu, Z. Wang, D. Zhang, Electrochemical oxidation of Crystal Violet in the presence of hydrogen peroxide, Journal of Chemical Technology & Biotechnology, 85 (2010) 1436-1444.

[346] F. Guzman-Duque, C. Pétrier, C. Pulgarin, G. Peñuela, R.A. Torres-Palma, Effects of sonochemical parameters and inorganic ions during the sonochemical degradation of crystal violet in water, Ultrasonics sonochemistry, 18 (2011) 440-446.

[347] J. Liu, Y. Du, W. Sun, Q. Chang, C. Peng, Preparation of new adsorbent-supported Fe/Ni particles for the removal of crystal violet and methylene blue by a heterogeneous Fenton-like reaction, RSC advances, 9 (2019) 22513-22522.

[348] A. Elhalil, H. Tounsadi, R. Elmoubarki, F. Mahjoubi, M. Farnane, M. Sadiq, M. Abdennouri, S. Qourzal, N. Barka, Factorial experimental design for the optimization of catalytic degradation of malachite green dye in aqueous solution by Fenton process, Water Resources and Industry, 15 (2016) 41-48.

[349] C.K. Duesterberg, T.D. Waite, Process optimization of Fenton oxidation using kinetic modeling, Environmental science & technology, 40 (2006) 4189-4195.

[350] J.J. Pignatello, E. Oliveros, A. MacKay, Advanced oxidation processes for organic contaminant destruction based on the Fenton reaction and related chemistry, Critical reviews in environmental science and technology, 36 (2006) 1-84.

[351] J. Hu, P. Zhang, W. An, L. Liu, Y. Liang, W. Cui, In-situ Fe-doped g-C_3N_4 heterogeneous catalyst via photocatalysis-Fenton reaction with enriched photocatalytic performance for removal of complex wastewater, Applied Catalysis B: Environmental, 245 (2019) 130-142.

[352] R.G. Miller Jr, Beyond ANOVA: basics of applied statistics, CRC press, 1997.

[353] L. St, S. Wold, Analysis of variance (ANOVA), Chemometrics and intelligent laboratory systems, 6 (1989) 259-272.

[354] B. Lodha, S. Chaudhari, Optimization of Fenton-biological treatment scheme for the treatment of aqueous dye solutions, Journal of Hazardous Materials, 148 (2007) 459-466.

[355] X. Zhu, J. Tian, R. Liu, L. Chen, Optimization of Fenton and electro-Fenton oxidation of biologically treated coking wastewater using response surface methodology, Separation and Purification Technology, 81 (2011) 444-450.

[356] I. Arslan-Alaton, A.B. Yalabik, T. Olmez-Hanci, Development of experimental design models to predict Photo-Fenton oxidation of a commercially important naphthalene sulfonate and its organic carbon content, Chemical Engineering Journal, 165 (2010) 597-606.

[357] S. Saha, A. Pal, S. Kundu, S. Basu, T. Pal, Photochemical green synthesis of calcium-alginate-stabilized Ag and Au nanoparticles and their catalytic application to 4-nitrophenol reduction, Langmuir, 26 (2009) 2885-2893.

[358] S. Mondal, U. Rana, R.R. Bhattacharjee, S. Malik, One pot green synthesis of polyaniline coated gold nanorods and its applications, RSC Advances, 4 (2014) 57282-57289.

[359] M. Ma, Y. Yang, W. Li, R. Feng, Z. Li, P. Lyu, Y. Ma, Gold nanoparticles supported by amino groups on the surface of magnetite microspheres for the catalytic reduction of 4-nitrophenol, Journal of Materials Science, 54 (2019) 323-334.

[360] S. Wunder, F. Polzer, Y. Lu, Y. Mei, M. Ballauff, Kinetic analysis of catalytic reduction of 4-nitrophenol by metallic nanoparticles immobilized in spherical polyelectrolyte brushes, The Journal of Physical Chemistry C, 114 (2010) 8814-8820.

[361] M. Orhan, D. Kut, C. Gunesoglu, Improving the antibacterial activity of cotton fabrics finished with triclosan by the use of 1, 2, 3, 4-butanetetracarboxylic acid and citric acid, Journal of Applied Polymer Science, 111 (2009) 1344-1352.

[362] E. Pinho, L. Magalhães, M. Henriques, R. Oliveira, Antimicrobial activity assessment of textiles: standard methods comparison, Annals of microbiology, 61 (2011) 493-498.

[363] S. Saqib, M.F. Hussain Munis, W. Zaman, F. Ullah, S.N. Shah, A. Ayaz, M. Farooq, S. Bahadur, Synthesis, characterization and use of iron oxide nano particles for antibacterial activity, Microscopy research and technique, (2018).

[364] V.T. Trang, N.X. Dinh, H. Lan, T.Q. Huy, P.A. Tuan, V.N. Phan, A.-T. Le, APTES Functionalized Iron Oxide–Silver Magnetic Hetero-Nanocomposites for Selective Capture and Rapid Removal of Salmonella enteritidis from Aqueous Solution, Journal of Electronic Materials, 47 (2018) 2851-2860.

[365] C. Lee, J.Y. Kim, W.I. Lee, K.L. Nelson, J. Yoon, D.L. Sedlak, Bactericidal effect of zero-valent iron nanoparticles on Escherichia coli, Environmental science & technology, 42 (2008) 4927-4933.

[366] X. Chen, Q. Zhou, Y. Zhang, J. Zhao, B. Yan, S. Tang, T. Xing, G. Chen, Fabrication of superhydrophobic cotton fabric based on reaction of thiol-ene click chemistry, Colloids and Surfaces A: Physicochemical and Engineering Aspects, 586 (2020) 124175.

[367] A. Monzavi, M. Montazer, R.M.A. Malek, A novel polyester fabric treated with nanoclay/nano TiO$_2$/PAMAM for discoloration of reactive red 4 from aqueous solution under UVA irradiation, Journal of Polymers and the Environment, 25 (2017) 1321-1334.

[368] T. Salem, F. Simon, A.A. El-Sayed, M. Salama, Plasma-assisted surface modification of polyester fabric for developing halochromic properties, Fibers and Polymers, 18 (2017) 731-740.

[369] Q. Zhao, L.Y.L. Wu, H. Huang, Y. Liu, Ambient-curable superhydrophobic fabric coating prepared by water-based non-fluorinated formulation, Materials & Design, 92 (2016) 541-545.

[370] R. Duan, Y. Dong, Q. Zhang, Characteristics of aggregate size distribution of nanoscale zero-valent iron in aqueous suspensions and its effect on transport process in porous media, Water, 10 (2018) 670.

[371] A. Azzouz, S. Nousir, N. Bouazizi, R. Roy, Metal–inorganic–organic matrices as efficient sorbents for hydrogen storage, ChemSusChem, 8 (2015) 800-803.

[372] B. Kakavandi, A. Takdastan, S. Pourfadakari, M. Ahmadmoazzam, S. Jorfi, Heterogeneous catalytic degradation of organic compounds using nanoscale zero-valent iron supported on kaolinite: Mechanism, kinetic and feasibility studies, Journal of the Taiwan Institute of Chemical Engineers, 96 (2019) 329-340.

[373] F. Fu, D.D. Dionysiou, H. Liu, The use of zero-valent iron for groundwater remediation and wastewater treatment: a review, Journal of hazardous materials, 267 (2014) 194-205.

[374] M. Stefaniuk, P. Oleszczuk, Y.S. Ok, Review on nano zerovalent iron (nZVI): from synthesis to environmental applications, Chemical Engineering Journal, 287 (2016) 618-632.

[375] K.V.G. Ravikumar, S. Dubey, N. Chandrasekaran, A. Mukherjee, Scale-up synthesis of zero-valent iron nanoparticles and their applications for synergistic degradation of pollutants with sodium borohydride, Journal of Molecular Liquids, 224 (2016) 589-598.

[376] A. Boveris, N. Oshino, B. Chance, The cellular production of hydrogen peroxide, Biochemical Journal, 128 (1972) 617-630.

[377] G.F. Bickerstaff, Immobilization of enzymes and cells, in: Immobilization of enzymes and cells, Springer, 1997, pp. 1-11.

[378] P.N. Bartlett, J.M. Cooper, A review of the immobilization of enzymes in electropolymerized films, Journal of Electroanalytical Chemistry, 362 (1993) 1-12.

[379] N. Miletić, A. Nastasović, K. Loos, Immobilization of biocatalysts for enzymatic polymerizations: possibilities, advantages, applications, Bioresource Technology, 115 (2012) 126-135.

[380] C. Horvath, J.-M. Engasser, Pellicular heterogeneous catalysts. A theoretical study of the advantages of shell structured immobilized enzyme particles, Industrial & Engineering Chemistry Fundamentals, 12 (1973) 229-235.

[381] Y.C. Yee, R. Hashim, A.R.M. Yahya, Y. Bustami, Colorimetric Analysis of Glucose Oxidase-Magnetic Cellulose Nanocrystals (CNCs) for Glucose Detection, Sensors, 19 (2019) 2511.

[382] B.K. Shrestha, R. Ahmad, H.M. Mousa, I.-G. Kim, J.I. Kim, M.P. Neupane, C.H. Park, C.S. Kim, High-performance glucose biosensor based on chitosan-glucose oxidase immobilized polypyrrole/Nafion/functionalized multi-walled carbon nanotubes bio-nanohybrid film, Journal of colloid and interface science, 482 (2016) 39-47.

[383] K. Hyun, S.W. Han, W.-G. Koh, Y. Kwon, Direct electrochemistry of glucose oxidase immobilized on carbon nanotube for improving glucose sensing, International journal of hydrogen energy, 40 (2015) 2199-2206.

[384] M. Kahoush, A. Cayla, B. Mutel, J. Guan, V. Nierstrasz, N. Behary, Influence of remote plasma on PEDOT:PSS–coated carbon felt for improved activity of glucose oxidase, Journal of Applied Polymer Science, (2019).

[385] J. Dave, R. Kumar, H.C. Srivastava, Studies on modification of polyester fabrics I: Alkaline hydrolysis, Journal of Applied Polymer Science, 33 (1987) 455-477.

[386] Y.-P. Jiao, F.-Z. Cui, Surface modification of polyester biomaterials for tissue engineering, Biomedical Materials, 2 (2007) R24.

[387] C. He, Z. Gu, Studies on acrylic acid–grafted polyester fabrics by electron beam preirradiation method. I. Effects of process parameters on graft ratio and characterization of grafting products, Journal of Applied Polymer Science, 89 (2003) 3931-3938.

[388] A. Vesel, I. Junkar, U. Cvelbar, J. Kovac, M. Mozetic, Surface modification of polyester by oxygen-and nitrogen-plasma treatment, Surface and Interface Analysis: An International Journal devoted to the development and application of techniques for the analysis of surfaces, interfaces and thin films, 40 (2008) 1444-1453.

[389] P. Chevallier, M. Castonguay, S. Turgeon, N. Dubrulle, D. Mantovani, P.H. McBreen, J.C. Wittmann, G. Laroche, Ammonia RF– plasma on PTFE surfaces: Chemical characterization of the species created on the surface by vapor– phase chemical derivatization, The Journal of Physical Chemistry B, 105 (2001) 12490-12497.

[390] A.M. Wrobel, M. Kryszewski, W. Rakowski, M. Okoniewski, Z. Kubacki, Effect of plasma treatment on surface structure and properties of polyester fabric, Polymer, 19 (1978) 908-912.

[391] B. Klajnert, M. Bryszewska, Dendrimers: properties and applications, Acta biochimica polonica, 48 (2001) 199-208.

[392] B. Mutel, O. Dessaux, P. Goudmand, L. Gengernbre, J. Grimblot, Energy consumption and kinetic evolution of nitrogen fixation on polyethlene terephthalate by remote nitrogen plasma: XPS study, Surface and interface analysis, 20 (1993) 283-289.

[393] D. Eyre, [7] Collagen cross-linking amino acids, in: Methods in enzymology, Elsevier, 1987, pp. 115-139.

[394] S.G. Padilla-Martínez, L. Martínez-Jothar, J.G. Sampedro, F. Tristan, E. Pérez, Enhanced thermal stability and pH behavior of glucose oxidase on electrostatic interaction with polyethylenimine, International journal of biological macromolecules, 75 (2015) 453-459.

[395] E.P. Golikova, N.V. Lakina, O.V. Grebennikova, V.G. Matveeva, E.M. Sulman, A study of biocatalysts based on glucose oxidase, Faraday discussions, 202 (2017) 303-314.

[396] J.W. Parker, C.S. Schwartz, Modeling the kinetics of immobilized glucose oxidase, Biotechnology and bioengineering, 30 (1987) 724-735.

[397] C. Lei, Y. Shin, J. Liu, E.J. Ackerman, Entrapping enzyme in a functionalized nanoporous support, Journal of the American Chemical Society, 124 (2002) 11242-11243.

[398] X. Zhang, R.-F. Guan, D.-Q. Wu, K.-Y. Chan, Enzyme immobilization on amino-functionalized mesostructured cellular foam surfaces, characterization and catalytic properties, Journal of Molecular Catalysis B: Enzymatic, 33 (2005) 43-50.

[399] P.A. Frey, A.D. Hegeman, Enzymatic reaction mechanisms, Oxford University Press, 2007.

[400] K. Mullis, F. Faloona, S. Scharf, R.K. Saiki, G.T. Horn, H. Erlich, Specific enzymatic amplification of DNA in vitro: the polymerase chain reaction, in: Cold Spring Harbor symposia on quantitative biology, Cold Spring Harbor Laboratory Press, 1986, pp. 263-273.

[401] D.M. Roundhill, Transition metal and enzyme catalyzed reactions involving reactions with ammonia and amines, Chemical reviews, 92 (1992) 1-27.

[402] T. Ramanathan, F.T. Fisher, R.S. Ruoff, L.C. Brinson, Amino-functionalized carbon nanotubes for binding to polymers and biological systems, Chemistry of Materials, 17 (2005) 1290-1295.

[403] F. Bergel, K.R. Harrap, A.M. Scott, 205. Interaction between carbonyl groups and biologically essential substituents. Part IV. An enzyme model system for cysteine desulphydrase, Journal of the Chemical Society (Resumed), (1962) 1101-1112.

[404] C.-H. Kuo, Y.-C. Liu, C.-M.J. Chang, J.-H. Chen, C. Chang, C.-J. Shieh, Optimum conditions for lipase immobilization on chitosan-coated Fe3O4 nanoparticles, Carbohydrate Polymers, 87 (2012) 2538-2545.

[405] M.L. Verma, S. Kumar, A. Das, J.S. Randhawa, M. Chamundeeswari, Chitin and chitosan-based support materials for enzyme immobilization and biotechnological applications, Environmental Chemistry Letters, (2020) 1-9.

[406] U.D. Kamaci, A. Peksel, Fabrication of PVA-chitosan-based nanofibers for phytase immobilization to enhance enzymatic activity, International Journal of Biological Macromolecules, (2020).

[407] N.S. Rios, S. Arana-Peña, C. Mendez-Sanchez, Y. Lokha, V. Cortes-Corberan, L.R.B. Gonçalves, R. Fernandez-Lafuente, Increasing the enzyme loading capacity of porous supports by a layer-by-layer immobilization strategy using PEI as glue, Catalysts, 9 (2019) 576.

[408] J.J. Virgen-Ortíz, J.C.S. dos Santos, Á. Berenguer-Murcia, O. Barbosa, R.C. Rodrigues, R. Fernandez-Lafuente, Polyethylenimine: a very useful ionic polymer in the design of immobilized enzyme biocatalysts, Journal of Materials Chemistry B, 5 (2017) 7461-7490.

[409] R. Wu, L. Liu, Magnetic Cellulose Beads as Support for Enzyme Immobilization Using Polyelectrolytes through Electrostatic Adsorption, BioResources, 15 (2020) 3190-3200.

[410] Z. Changani, A. Razmjou, A. Taheri-Kafrani, M. Asadnia, Domino P-µMB: A New Approach for the Sequential Immobilization of Enzymes Using Polydopamine/Polyethyleneimine Chemistry and Microfabrication, Advanced Materials Interfaces, (2020) 1901864.

[411] M.N. Morshed, N. Bouazizi, N. Behary, J. Guan, V. Nierstrasz, Stabilization of zero valent iron (Fe^0) on plasma/dendrimer functionalized polyester fabrics for Fenton-like removal of hazardous water pollutants, Chemical Engineering Journal, 374 (2019) 658-673.

[412] J. Rahel, M. Černák, I. Hudec, M. Štefečka, M. Kando, I. Chodák, Surface modification of polyester monofilaments by atmospheric-pressure nitrogen plasma, Plasmas and polymers, 5 (2000) 119-127.

[413] S. Mani, R.N. Bharagava, Exposure to crystal violet, its toxic, genotoxic and carcinogenic effects on environment and its degradation and detoxification for environmental safety, in: Reviews of Environmental Contamination and Toxicology Volume 237, Springer, 2016, pp. 71-104.

[414] W. Au, S. Pathak, C.J. Collie, T.C. Hsu, Cytogenetic toxicity of gentian violet and crystal violet on mammalian cells in vitro, Mutation Research/Genetic Toxicology, 58 (1978) 269-276.

[415] G.K. Cheruiyot, W.C. Wanyonyi, K.J. Joyce, E.N. Maina, Adsorption of Toxic Crystal Violet Dye Using Coffee Husks: Equilibrium, Kinetics and Thermodynamics Study, Scientific African, (2019) e00116.

[416] K. Kwasniewska, Biodegradation of crystal violet (hexamethyl-p-rosaniline chloride) by oxidative red yeasts, Bulletin of environmental contamination and toxicology, 34 (1985) 323-330.

[417] K. Mohanty, J.T. Naidu, B.C. Meikap, M.N. Biswas, Removal of crystal violet from wastewater by activated carbons prepared from rice husk, Industrial & engineering chemistry research, 45 (2006) 5165-5171.

[418] H.-J. Fan, S.-T. Huang, W.-H. Chung, J.-L. Jan, W.-Y. Lin, C.-C. Chen, Degradation pathways of crystal violet by Fenton and Fenton-like systems: condition optimization and intermediate separation and identification, Journal of hazardous materials, 171 (2009) 1032-1044.

[419] I. Sirés, E. Guivarch, N. Oturan, M.A. Oturan, Efficient removal of triphenylmethane dyes from aqueous medium by in situ electrogenerated Fenton's reagent at carbon-felt cathode, Chemosphere, 72 (2008) 592-600.

[420] B. Yang, Z. Tian, L. Zhang, Y. Guo, S. Yan, Enhanced heterogeneous Fenton degradation of Methylene Blue by nanoscale zero valent iron (nZVI) assembled on magnetic Fe3O4/reduced graphene oxide, Journal of Water Process Engineering, 5 (2015) 101-111.

[421] Y. Segura, F. Martínez, J.A. Melero, Effective pharmaceutical wastewater degradation by Fenton oxidation with zero-valent iron, Applied Catalysis B: Environmental, 136 (2013) 64-69.

[422] S. Zha, Y. Cheng, Y. Gao, Z. Chen, M. Megharaj, R. Naidu, Nanoscale zero-valent iron as a catalyst for heterogeneous Fenton oxidation of amoxicillin, Chemical Engineering Journal, 255 (2014) 141-148.

[423] Y. Segura, F. Martínez, J.A. Melero, J.L.G. Fierro, Zero valent iron (ZVI) mediated Fenton degradation of industrial wastewater: Treatment performance and characterization of final composites, Chemical Engineering Journal, 269 (2015) 298-305.

[424] A. Babuponnusami, K. Muthukumar, Treatment of phenol-containing wastewater by photoelectro-Fenton method using supported nanoscale zero-valent iron, Environmental Science and Pollution Research, 20 (2013) 1596-1605.

[425] T. Phenrat, G.V. Lowry, P. Babakhani, Nanoscale zerovalent iron (NZVI) for environmental decontamination: a brief history of 20 years of research and field-scale application, Nanoscale Zerovalent Iron Particles for Environmental Restoration, (2019) 1-43.

[426] T. Pasinszki, M. Krebsz, Synthesis and application of zero-valent iron nanoparticles in water treatment, environmental remediation, catalysis, and their biological effects, Nanomaterials, 10 (2020) 917.

[427] S.J. Benkovic, S. Hammes-Schiffer, A perspective on enzyme catalysis, Science, 301 (2003) 1196-1202.

[428] H. Haslaniza, M.Y. Maskat, W.M. Wan Aida, S. Mamot, The effects of enzyme concentration, temperature and incubation time on nitrogen content and degree of hydrolysis of protein precipitate from cockle (Anadara granosa) meat wash water, International Food Research Journal, 17 (2010) 147-152.

[429] T.C. Bruice, S.J. Benkovic, Chemical basis for enzyme catalysis, Biochemistry, 39 (2000) 6267-6274.

[430] A. Babuponnusami, K. Muthukumar, A review on Fenton and improvements to the Fenton process for wastewater treatment, Journal of Environmental Chemical Engineering, 2 (2014) 557-572.

[431] B.H. Hameed, T.W. Lee, Degradation of malachite green in aqueous solution by Fenton process, Journal of hazardous materials, 164 (2009) 468-472.

[432] J.A. Zazo, G. Pliego, S. Blasco, J.A. Casas, J.J. Rodriguez, Intensification of the Fenton process by increasing the temperature, Industrial & Engineering Chemistry Research, 50 (2011) 866-870.

[433] A.R. Ribeiro, O.C. Nunes, M.F.R. Pereira, A.M.T. Silva, An overview on the advanced oxidation processes applied for the treatment of water pollutants defined in the recently launched Directive 2013/39/EU, Environment international, 75 (2015) 33-51.

[434] N. Wang, T. Zheng, G. Zhang, P. Wang, A review on Fenton-like processes for organic wastewater treatment, Journal of Environmental Chemical Engineering, 4 (2016) 762-787.

[435] S.C. Ameta, R. Ameta, Advanced oxidation processes for wastewater treatment: emerging green chemical technology, Academic press, 2018.

[436] İ.H. Boyacı, A new approach for determination of enzyme kinetic constants using response surface methodology, Biochemical Engineering Journal, 25 (2005) 55-62.